

**Development of capillary based separation
techniques for the separation of proteins
equilibrated using hexapeptide ligand libraries**

Dissertation

der Mathematisch-Naturwissenschaftlichen Fakultät
der Eberhard Karls Universität Tübingen
zur Erlangung des Grades eines
Doktors der Naturwissenschaften
(Dr. rer. nat.)

vorgelegt von
Martin Meixner
aus Herrenberg

Tübingen
2019

Gedruckt mit Genehmigung der Mathematisch-Naturwissenschaftlichen Fakultät der
Eberhard Karls Universität Tübingen.

Tag der mündlichen Qualifikation:

08.07.2019

Dekan:

Prof. Dr. Wolfgang Rosenstiel

1. Berichterstatter:

Prof. Dr. Carolin Huhn

2. Berichterstatter:

Prof. Dr. Günter Gauglitz

Für meine Mutter.

Danksagung

Diese Arbeit wurde im Zeitraum zwischen Januar 2016 und Januar 2019 angefertigt. An dieser Stelle danke ich all denen, die mich während meiner Doktorarbeit fachlich und moralisch unterstützt haben. Hierzu gehören natürlich meine Familie, allen voran meine Mutter, die mich schon immer unterstützt und mir gut zugeredet hat. Selbstverständlich nicht durch unqualifizierte Kommentare und Bemerkungen, wer meine Mutter kennt weiß, dass das wider ihrer Natur ist. Ein riesiger Dank gilt meiner Freundin Anne, die mir Freiräume ließ, damit ich mich in Sachen hineinsteigern konnte, mich aber auch bremste, wenn ich es nicht mehr sollte und konnte.

Natürlich auch den AKs Huhn und Gauglitz, sowie allen ehemaligen Mitgliedern aus beiden AKs, mit denen ich zusammenarbeiten durfte. Danke, dass ihr eine tolle Arbeitsatmosphäre geschaffen habt, wodurch ich gerne zur Arbeit gegangen bin. Nicht zu vergessen sind natürlich auch die stets niveaувollen Gespräche – natürlich nur auf fachlicher Ebene, was sonst? - bei Mittags- und Kaffeepausen und auch abends bei ~~Bier und Wein~~ einem Grüntee. Ein besonderer Dank an meinen Kollegen Benjamin Rudisch, welcher mir moralisch und fachlich eine Stütze war, und sei es nur, um meine Gedanken laut auszuformulieren, rück zu versichern oder neuen Input zu geben. Auch und vor allem danke ich meiner Chefin Carolin Huhn, die mich trotz Schwangerschaft, Elternzeit und Krankheit forderte und förderte und trotz allem Zeiträume geschaffen hat um mit mir über die spannenden Themen meiner Doktorarbeit zu diskutieren.

Dank geht auch an Dr. Sebastian Hörber, Dr. Christoph Hoffman, Dr. Lisa Kappler aus dem Uniklinikum, welche mir bei der Blutentnahme (die mir signifikant weniger Spaß gemacht hat als dir, Sebastian 😊), Fragen zu Blutproteinen und der Durchführung und Interpretation von SDS-PAGE geholfen haben.

Vielen Dank auch an die Gruppe von Prof. Hermann A. Mayer, besonders an Thomasz Mistal, Dennis M. Meisel and Farhad Jafarli, die mich während der Kapillarbeschichtungen mit SPS-getrockneten Lösungsmitteln versorgt haben, für Diskussionen und Fragen zur Verfügung standen und sogar Zeit gefunden haben, sich mit mir an eine in dieser Arbeit nicht gezeigte Partikelsynthese zu wagen.

Meinem Kooperationspartner Dr. Pavel Karásek danke ich für seine Ideen, sein Engagement und seine erstklassige Leistung bei der Synthese und SEM-Charakterisierung der geätzten Kapillaren. Frau Nadler danke ich für die tollen Gespräche und den Input bei der Vorbereitung der Proben und bei der Durchführung der Messungen.

Ein Dank gilt auch denen, die mich bei dieser Arbeit durch Praktika und Bachelorarbeiten unterstützt haben, namentlich Sandra Köhn, Ronja Jordan, Jacqueline Kieler, Jasmin Strohmeier, Xinyue Fu, Feiyang Li, Jacqueline Händel und Biwen Wang.

Erklärung nach § 6 Abs. 2 der PromO der Naturwissenschaftlichen Fakultät

Research questions and all experiments were designed by Martin Meixner, aided by his supervisor. Experiments were conducted by him, sometimes including students under his supervision as indicated for the chapters below. Specialized measurements like SEM measurements were conducted in cooperation with the instrument scientists. Capillary preconditioning was made by cooperation partners (see below) after joint discussion of the common project. With rare exception, data analysis and interpretation together with literature work was conducted by Martin Meixner and discussed with cooperation partners and supervisor, where applicable. Writing and summarizing the results was his duty. Details for the specific chapters are given below, where relevant:

Chapter 2: Investigation of temperature and additive influences on SDS-CE part 1: A set of modifications for either fast or high resolving separations using PEO with a single molecular weight only

General idea:

The idea and experimental designs for the systematic investigation of alkanols as additives and temperature on a separation system utilizing PEO came from Martin Meixner. Literature research was entirely conducted by Martin Meixner.

Experimental laboratory work:

Early phase experiments, which were shown here only in parts, contained the development of cleaning, preconditioning and detection protocols as well as enrichment plugs. These experiments conducted by Martin Meixner summarize to a participation of approx. 20 %. Most work was conducted under Martin Meixner's supervision during internships and a bachelor thesis by Xinyue Fu (30 %, 6 week internship), Jacqueline Händel (30 %, 6 week bachelor thesis) and Biwen Wang (20 %, 3 week internship).

Evaluation and interpretation of experimental results:

Data treatment and analysis were developed by Martin Meixner and conducted either by him (80 %) or under his supervision by various interns (Jacqueline Händel, Xinyue Fu, Biwen Wang). Carolin Huhn gave valuable input by proposing the investigation of sieving mechanism.

Writing:

Writing was entirely done by Martin Meixner. The layout of each graph in this whole work was influenced by the bachelor thesis of Jacqueline Händel.

Chapter 3: Investigation of temperature and additive on SDS-CE part 2: mechanistic investigation of the influence of alkanols and temperature on the sieving mechanism via interaction with SDS-protein-agglomerates and sieving polymer

General idea:

Prof. Carolin Huhn gave valuable input by proposing the investigation of sieving mechanism. Literature research was conducted by Martin Meixner.

Experimental laboratory work:

Some measurements were conducted by Xinyue Fu and Jacqueline Händel during their internships at about equal portions under supervision of Martin Meixner.

Evaluation and interpretation of experimental results:

Data manipulations were developed and conducted by Martin Meixner.

Writing:

Writing was entirely done by Martin Meixner.

Chapter 4: Novel approach for the synthesis of a covalently bound, highly polar and pH-persistent N-acryloylamido ethoxyethanol capillary coating for capillary electrophoresis-mass spectrometry. Part 1: strategy, performance and stability

General idea:

Papers presenting AAEE as coating material were supplied by Prof. Carolin Huhn. The immobilization of alkene groups on the silica surface via preliminary hydration step using LiAlH_4 was found and suggested by Martin Meixner.

Experimental laboratory work:

Experimental laboratory work for capillary preparation was entirely investigated by Martin Meixner. Preliminary experiments (not shown in this work) were conducted under supervision during an internship and a bachelor thesis by interns (Ronja Jordan (6 week internship), Jasmin Strohmeier (6 week bachelor thesis) and Jacqueline Kienzle (6 week internship)) and are evaluated as 10 %.

Experiments considering the investigation of polyamines in fish eggs were entirely designed by Dr. Martin Pattky and conducted under his supervision by Sarah Köhn (6 week internship). AAEE capillaries necessary were provided by Martin Meixner who aided in data interpretation.

Evaluation and interpretation of experimental results:

Evaluation and interpretation of experimental results of each topic except the analysis polyamines in fish eggs was fully done by Martin Meixner. The evaluation and interpretation of the experiments considering polyamines in fish eggs was done by Dr. Martin Pattky and Sarah Köhn.

Writing:

Writing was entirely done by Martin Meixner.

Chapter 5: Novel approach for the synthesis of a covalently bound, highly polar and pH-persistent N-acryloylamido ethoxyethanol capillary coating for capillary electrophoresis-mass spectrometry. Part 2: Etching with supercritical water as capillary pretreatment for coatings covalently coupled via Si-C bonds after Si-H surface reaction

General idea:

The general idea to use etched capillaries for capillary coatings was discussed with Dr. Pavel Karásek during a conference. The experimental design was entirely developed by Martin Meixner including several iteration cycles.

Experimental laboratory work:

The etching procedures for capillaries with 50 µm internal diameter (publications so far with larger inner bore capillaries) were entirely developed by Dr. Pavel Karásek. Etching of capillaries and SEM measurements were conducted by Dr. Pavel Karásek. Coating experiments and CE-MS experiments were made by Martin Meixner (100 %). EDX-measurements were conducted by Elke Nader and Martin Meixner.

Evaluation and interpretation of experimental results:

Evaluation of coating procedure via CE-MS and μ_{EOF} was entirely conducted by Martin Meixner. Interpretation of SEM with regard to coating synthesis was done by Martin Meixner and Dr. Pavel Karásek in equal portions. Results were compiled and summarized by Martin Meixner

Writing:

Writing was entirely done by Martin Meixner.

Chapter 6: Step-wise equilibration of protein samples using hexapeptide ligand libraries. Optimization of the elution and purification protocols to enable reloading

General idea:

The idea of consecutive equilibration of protein samples via HLLs using cut off-filters for sample purification came from Prof. Carolin Huhn. The idea to investigate various elution solutions, elution and washing protocols as well as measurement techniques came from Martin Meixner and Prof. Carolin Huhn. These developments were done in close collaboration, a distinction in percent-per-person is thereby hardly possible.

Experimental laboratory work:

Experimental and laboratory work was entirely conducted by Martin Meixner.

Evaluation and interpretation of experimental results:

Evaluation and interpretation of results was conducted by Martin Meixner in consultation with Prof. Carolin Huhn.

Writing:

Writing was entirely done by Martin Meixner.

Chapter 7: Fast CE-MS-based screening method for the determination of pI-values of cyclic peptides of very low solubility in water

General idea:

The general idea to conduct CE-MS measurements with citric acid as BGE came from Martin Meixner.

Experimental laboratory work:

The preparation, purification and lyophilization of LugduninA was entirely done by Dr. Martin Konnerth, Dr. Nadine Schilling and Sebastian Wirtz. CE-MS experiments were conducted by Martin Meixner.

Evaluation and interpretation of experimental results:

Evaluation of measurement data was conducted by Martin Meixner while consulting Dr. Nadine Schilling and Sebastian Wirtz for structural issues of the molecules. Martin Meixner corresponded as central organizer of the experiments for pI-investigation with a participation of 90 %.

Writing:

Writing of this chapter was done entirely by Martin Meixner.

Table of content

Danksagung	i
Erklärung nach § 6 Abs. 2 der PromO der Naturwissenschaftlichen Fakultät.....	ii
Table of content	vi
Abstract (English).....	1
Abstract (Deutsch).....	3
1. Motivation	5
2. Investigation of temperature and additive influences on SDS-CE part 1: A set of modifications for either fast or high resolving separations using PEO with a single molecular weight only	7
2.1. Abstract	7
2.2. Introduction and motivation	8
2.3. Materials and methods	10
2.3.1. Chemicals.....	10
2.3.2. Buffer and sieving polymer solution preparation	10
2.3.3. Instrumentation and separation parameters.....	10
2.3.4. Sample preparation	11
2.3.5. Data processing	11
2.4. Results	13
2.4.1. Influences of alkanols in the sieving medium	13
2.4.2. Influence of cassette temperature.....	24
2.4.3. Variation of the detection aperture	25
2.4.4. Combined influence of temperature and additive at 14 % aperture size	27
2.4.5. Aspects of sample injection.....	29
2.5. Discussion	33
2.5.1. The influence of alkanols and temperature on the separation.....	33
2.5.2. Influence of detection and injections parameters on the separation.....	34
2.6. Conclusion and outlook.....	34
3. Investigation of temperature and additive on SDS-CE part 2: mechanistic investigation of the influence of alkanols and temperature on the sieving mechanism via interaction with SDS-protein-agglomerates and sieving polymer	36
3.1. Abstract	36
3.2. Introduction and motivation	37
3.3. Materials and methods	38

TABLE OF CONTENT

3.3.1.	Chemicals.....	38
3.3.2.	Buffer and sieving polymer solution preparation	38
3.3.3.	Instrumentation and separation parameters.....	38
3.3.4.	Sample preparation.....	38
3.3.5.	Data processing	38
3.4.	Results	39
3.4.1.	Intermediate precision	39
3.4.2.	Separation performance – Linearity of the mass scale	40
3.4.3.	Ogston- and Reptation-sieving.....	41
3.4.4.	Influence of cassette temperature.....	43
3.5.	Discussion.....	45
3.5.1.	The non-linearity of mass determination as an intrinsic property of sieving mechanisms.....	45
3.5.2.	Preliminary remarks about the addition of alkanols to the sieving medium and the influence of temperature.....	47
3.6.	Conclusion and outlook.....	54
4.	Novel approach for the synthesis of a covalently bound, highly polar and pH-persistent <i>N</i> -acryloylamido ethoxyethanol capillary coating for capillary electrophoresis-mass spectrometry part 1: strategy, performance and stability	55
4.1.	Abstract	55
4.2.	Introduction and motivation	56
4.3.	Materials and methods	59
4.3.1.	Instrumentation and methods	59
4.3.2.	Chemicals.....	60
4.3.3.	Preparation of tryptically digested BSA and PBS.....	60
4.3.4.	Preparation of fish egg samples	61
4.3.5.	Preparation of serum samples and extraction of protein signals	61
4.3.6.	Capillary coating	61
4.4.	Results	64
4.4.1.	Reproducibility of capillary coatings	65
4.4.2.	Stability towards harsh rinsing conditions	69
4.4.3.	Application of AAEE-coated capillaries to complex samples	72
4.5.	Discussion.....	75
4.5.1.	Novelties in preparation procedure.....	75

TABLE OF CONTENT

4.5.2.	Reproducibility and stability of prepared capillaries.....	75
4.5.3.	Stability of capillary surfaces due to preparation via Si-H-route	76
4.5.4.	Application of coated capillaries for complicated separations	76
4.6.	Conclusion and outlook.....	77
5.	Novel approach for the synthesis of a covalently bound, highly polar and pH-persistent <i>N</i> -acryloylamido ethoxyethanol capillary coating for capillary electrophoresis-mass spectrometry part 2: Etching with supercritical water as capillary pretreatment	79
5.1.	Abstract	79
5.2.	Introduction and motivation	80
5.3.	Materials and methods	81
5.3.1.	Instrumentation.....	81
5.3.2.	Chemicals.....	82
5.3.3.	Preparation of tryptically digested BSA.....	83
5.3.4.	Capillary coating	83
5.4.	Results	84
5.4.1.	SEM-investigation.....	84
5.4.2.	Electroosmotic mobilities	95
5.4.3.	CE-MS	96
5.5.	Discussion	99
5.5.1.	Etched surfaces during coating procedure.....	99
5.5.2.	Advantages of preconditioning with supercritical water	99
5.5.3.	Co-existence of aluminate layer and Si-H-groups	100
5.6.	Conclusion and outlook.....	101
6.	Step-wise equilibration of protein samples using hexapeptide ligand libraries. Optimization of the elution and purification protocols to enable reloading.....	102
6.1.	Abstract	102
6.2.	Introduction and motivation	103
6.3.	Materials and methods	106
6.3.1.	Instrumentation.....	106
6.3.2.	Chemicals.....	106
6.3.3.	Preparation of sample, HLL elution solutions and PBS	107
6.3.4.	Preparation and application of HLLs and protein cleanup with 10 kDa cut-off-filters.....	109
6.3.5.	Sodium dodecyl sulfate polyacrylamide gel electrophoresis (SDS-PAGE).....	109

TABLE OF CONTENT

6.3.6.	Sodium dodecyl sulfate capillary electrophoresis.....	110
6.4.	Results	111
6.4.1.	Quantification of proteins by CE-MS.....	111
6.4.2.	Compatibility with eluate composition	111
6.4.3.	Protein purification and recovery from cut-off-filters	114
6.4.4.	Investigation of elution protocols for one-fold HLL equilibration.....	120
6.4.5.	Consecutive equilibration.....	123
6.4.6.	Reproducibility and ruggedness of 1-fold equilibration.....	124
6.4.7.	Pre-equilibration of HLLs	127
6.4.8.	Intra-protein equilibration	128
6.4.9.	Application to serum samples and method comparison to SDS-PAGE	130
6.5.	Discussion	134
6.5.1.	Quantification via CE-MS and compatibility with sample composition and excess co-migrating protein.....	134
6.5.2.	Applicability of cut-off-filters for protein purification to re-establish binding conditions	134
6.5.3.	Performance of HLL protein equilibration	136
6.6.	Summary and outlook	140
6.7.	Supporting information	141
7.	Fast CE-MS-based screening method for the determination of pI-values of cyclic peptides of very low solubility in water.....	148
7.1.	Abstract	148
7.2.	Introduction and motivation	149
7.3.	Strategy	150
7.4.	Materials and Methods	152
7.4.1.	Instrumentation	152
7.4.2.	Chemicals.....	152
7.4.3.	Preparation of samples and background electrolytes	152
7.4.4.	Sequential sample injection and electrophoretic conditions.....	153
7.5.	Results	154
7.5.1.	pI-determination of amino acids and reference substances	154
7.5.2.	pI-determination of Lugdunin A.....	155
7.6.	Discussion	158
7.6.1.	Suitability of the method for pI-value determination.....	158

TABLE OF CONTENT

7.6.2.	Transformation of of Lugdunin A: Closed condensation- and open hydrolyzation-product of Lugunin A	158
7.7.	Supporting Information	161
7.7.1.	Electropherograms of Lugdunin A.....	161
7.7.2.	pI-determination for all investigated compounds	162
8.	Conclusion	164
9.	Literature	166

Abstract (English)

Challenges in research areas such as chemistry, medicine, environmental toxicology and biology require the analysis of complex samples. Fast analysis of these samples using separation techniques with spectrometric or spectroscopic detection is common. Most often, chromatographic separation techniques such as gas and liquid chromatography coupled to mass spectrometry are chosen. These techniques, however, often reach their limits when highly charged analytes are investigated. Here, electromigrative separation techniques with their orthogonal separation mechanism are an attractive alternative.

A very promising electrophoretic separation technique, which is primarily used during this work, is capillary electrophoresis (CE). One of the greatest challenges using this technique lies in the separation of biological samples, since analytes such as polyamines, peptides and proteins interact with and adsorb on the surface of “*bare fused silica*”-capillaries which impairs reproducibility. Without efficient suppression of these interactions, separation efficiency and run-to-run reproducibility suffer. A good way to suppress these detrimental interactions of analytes with the capillary surface is to modify the surface using of dynamic, statically adsorbed or covalently bound capillary coatings.

In this work, I present approaches for the reproducible separation of polyamines, peptides and proteins:

1) In Chapter 2, the use of poly ethylene oxide as dynamic coating in SDS-CE enables the size-based separation of proteins up to a weight of 100 kDa. Advantages of this technique over classic gel-based SDS-PAGE are separation times of about 20 min and direct quantification via on-line UV-detection without the need of preliminary labeling or subsequent dyeing. Separation times were reduced to 5 min by short-end-injection and modification of the aperture for UV-detection. The presented separation system offers outstanding matrix tolerance: even complex samples such as serum were successfully separated without additional processing. Increased separation performance and efficiency were aspired by the addition of alkanols to the BGE, variation of temperature and the use of enrichment plugs in the capillary. Therein, especially the use of 2-propanol in the BGE proves fruitful regarding separation efficiency in the mass range up to 40 kDa. In Chapter 3 I will interpret my results with an extensive literature search to show, that the observed increase in separation efficiency is linked to a change of the separation mechanism from Reptation- to Ogston-sieving.

2) In Chapter 4, I proudly present, that I achieved CE-separation with MS-hyphenation not only for small polyamines and peptides, but also of large, non-digested proteins. This was possible using a single capillary coating only based on *N*-acryloylamido ethoxyethanol (AAEE). This highly polar and covalently bound capillary coating offers enjoyably high reproducibly and stability, the latter enabling operating times of 100 h, even when complex samples such as human serum and polyamines in fish eggs were analyzed. In Chapter 5 a novel and parallelized approach for the synthesis of this capillary coating is presented. SEM-measurements of the capillary surface between reaction steps forced me to postulate a novel reaction-mechanism for the formation of the coated surface. Additionally, I present, that pre-conditioning of capillaries with hypercritical water can result in higher reproducibility of capillary-to-capillary performance and reduced synthesis time.

ABSTRACT (ENGLISH)

In Chapter 6 I will show that the presented separation techniques are excellent for the separation and detection of proteins equilibrated using hexapeptide ligand libraries (HLL). A novel approach for the consecutive equilibration of small sample volumes, which enables a deep insight into the proteome, is critically discussed. Challenges intrinsic to the solid phase extraction of proteins using HLLs are traced back to irreversible binding sites on HLLs. To tackle this issue, different elution and pre-equilibration protocols are designed and investigated. To re-establish binding conditions in consecutive equilibration, which is consecutive equilibration, different protocols for the processing of eluates from HLLs using 10 kDa cut-off filters are presented. Aspects that critically impair yields and recovery rates come to the fore and improved protocols are presented.

A further project focused on CE-MS-based pI-value determination of a hardly soluble, cyclic and antibiotic peptide (Chapter 7). Detection of this peptide was not possible using AAEE-coated capillaries. This problem was overcome by using non-coated capillaries and BGEs containing small amounts of citric acid, which functions not only as buffer but also as a dynamic capillary coating. To confirm the determined pI-values, a novel and time-saving approach for the sequential injection of amino acid reference substances was developed.

Abstract (Deutsch)

Fragestellungen in der Chemie aber auch in vielen anderen Disziplinen wie der Medizin, Umwelttoxikologie und Biologie, erfordern die Untersuchung von teilweise sehr komplexen Stoffgemischen. Eine schnelle Untersuchung von komplexen Proben ist mittels Trenntechniken, gefolgt von spektroskopischer oder spektrometrischer Detektion möglich. Zu den am weitesten verbreiteten Techniken gehören hierbei chromatographische Methoden wie die Gas- und Flüssigchromatographie, häufig gekoppelt mit Massenspektrometrie. Geraten diese chromatographischen Techniken an ihre Grenzen, beispielsweise bei hoch geladenen Stoffen, so bietet sich der Einsatz von elektromigrativen Trenntechniken an, da diese einen orthogonalen Trennmechanismus besitzen.

Die Kapillarelektrophorese (engl.: capillary electrophoresis, CE), mit welcher sich diese Arbeit befasst, zählt zu den elektromigrativen Trenntechniken. Eine große Herausforderung dieser Technik besteht u.a. in der geringen Reproduzierbarkeit bei der Analytik von Biomolekülen, welche sich auf die Verwendung von „bare fused silica“-Kapillaren und deren Wechselwirkung mit den Analyten zurückführen lässt. Wird diese Wechselwirkung nicht effizient unterdrückt, so sinkt die Trenneffizienz innerhalb und die Wiederholbarkeit zwischen Trennungen. Durch die Verwendung von dynamischen, statisch adsorbierten oder kovalent gebundenen Kapillarbeschichtungen kann diese Wechselwirkung effizient unterdrückt werden.

In dieser Arbeit werden mehrere Möglichkeiten zur reproduzierbaren Trennung von Polyaminen, Peptiden und Proteinen vorgestellt:

1) In Kapitel 2 wird durch die Verwendung von Polyethylenoxid als dynamische Beschichtung und Siebmatrix in der SDS-CE die größenbasierte Trennung von Proteinen bis zu einer Masse von 100 kDa erreicht. Ein Vorteil gegenüber klassischen gelbasierten Verfahren wie SDS-PAGE ist hierbei, dass Proben innerhalb von 20 min getrennt und durch on-column UV-Detektion quantifiziert werden können, ohne vor- oder nachträgliches Anfärben oder Derivatisieren. Durch eine selbst entworfene Modifikation der Trennapparatur und Injektion vom kurzen Ende der Kapillare konnte diese Trennzeit für ein schnelles Screening auf 5 Minuten reduziert werden. Das vorgestellte Trennsystem zeichnet sich durch eine hohe Matrixtoleranz aus; selbst Proben wie menschliches Serum können ohne Aufarbeitung injiziert werden. Eine Verbesserung der Auflösung und Trenneffizienz wurde durch die Verwendung von verschiedenen Alkoholen im Hintergrundelektrolyten, die Variation der Trenntemperatur und die Etablierung von Anreicherungszonen in der Kapillare angestrebt. Hierbei zeigte vor allem die Verwendung von 2-Propanol im Hintergrundelektrolyten eine erhöhte Trenneffizienz im Massenbereich bis ca. 40 kDa. In Kapitel 3 wird anhand der eigenen Ergebnisse und durch ausführliche Literaturarbeit gezeigt, dass diese Verbesserung der Auflösung durch eine Verschiebung des Trennmechanismus von Reptation- zu Ogstonseven ermöglicht wird.

2) Durch die Verwendung einer sehr polaren kovalenten Kapillarbeschichtung, dem *N*-Acryloylamido-ethoxyethanol (AAEE), lässt sich die kapillarelektrophoretische Trennung von kleinen Polyaminen und Peptiden, aber auch großen und unverdauten Proteinen, bei gleichzeitiger massenspektrometrischer Detektion erreichen. Dies wird in Kapitel 4 vorgestellt. Erfreulich hohe Einsatzzeiten von ca. 100 h und gute Wiederholbarkeiten werden sogar bei der Untersuchung von menschlichem Serum oder Polyaminen in Fischeiern beobachtet. In Kapitel 5 werden ein neuer und

parallelisierter Ansatz zur Kapillarsynthese sowie ein koexistenter und durch SEM-Aufnahmen postulierter Reaktionsmechanismus vorgestellt. Zusätzlich wird ein Ansatz zur Vorbehandlung der Kapillaren durch die Verwendung von überkritischem Wasser vorgeschlagen, welcher ersten Versuchen nach zu einer höheren Reproduzierbarkeit der Beschichtung und einer beschleunigten Synthese führen kann.

In Kapitel 6 werden die vorgestellten Analysetechniken werden für die Bestimmung von Proteinen in mittels Hexapeptidligandenbibliotheken angereicherten Proben verwendet. Ein Ansatz zur mehrfachen Anreicherung, der einen tiefen Blick ins Proteom erlauben soll, wird kritisch bewertet. Herausforderungen in der Festphasenanreicherung werden auf irreversible Bindungsstellen zurückgeführt. In diesem Zusammenhang werden verschiedene Elutions- und Pre-Äquilibrationsprotokolle untersucht. Für die erfolgreiche Wiederbeladung, welche einen tieferen Blick ins Proteom erlaubt, werden verschiedene Protokolle zur Aufarbeitung des Eluats mittels 10 kDa-Cut-off-Filtern vorgestellt. Kritische Aspekte, welche die Ausbeuten beeinträchtigen, werden beleuchtet und Lösungswege aufgezeigt.

In Kapitel 7 wird die MS-basierte pI-Wertbestimmung eines schwerlöslichen zyklischen Peptidantibiotikums vorgestellt. Dieses konnte mit AAEE-beschichteten Kapillaren nicht erfasst werden. Diese Herausforderung konnte durch die Verwendung unbeschichteter Kapillaren und geringen Mengen Zitronensäure im Hintergrundelektrolyt, welche als dynamische Beschichtung fungiert, umgangen werden. Zur Absicherung der bestimmten pI-Werte mit Aminosäurestandards wurde ein neuer und zeitsparender Ansatz der sequentiellen Injektion entwickelt.

1. Motivation

Proteomics research is a topic of high interest since it promises a better understanding of biological processes. Especially, advances in the search for novel biomarkers for early-stage diagnostics of various diseases such as cancer, Alzheimer's disease and others are desirable¹⁻¹². Due to both the high physicochemical variability of biomarkers as well as their extremely low concentrations, the development of specific antibody tests for every disease is an endless approach. Non-specific screening techniques such as 2D-electrophoresis¹³ or nanoLC-MS¹⁴—often even combinations of both¹⁴—are state-of-the-art, yet cumbersome and time-consuming approaches. Considering the goal of an easy routine analysis in clinical diagnostics, there is a demand for a fast, automatized and easily applicable analysis technique. Capillary electrophoresis gives the possibility to meet all these demands. By choosing either UV or MS detection, methods with a focus on either cost-efficiency or the amount of obtainable information can be made. One of the greatest challenges for these methods is protein adsorption on capillary surfaces, which can be tackled by the functionalization of capillary surfaces either via dynamic, statically adsorbed or covalently bound coatings. For CE-MS, covalently bound and for CE-UV, dynamic coatings that also function as sieving polymer in the mode of SDS-CE, are promising. Therefore, one aim of this thesis was to develop a covalently bound and stable coating for CE-MS analysis of both intact and digested proteins. Another aim was to find an easy yet reliable SDS-CE measurement system using commercially available chemicals. For both techniques, high reproducibility, good separation performance, the possibility quantification via external calibration and high matrix tolerance were desired, to make them applicable for fast proteomics research.

Another challenge in the search for biomarkers is the high concentration range of proteins in easily accessible body fluids, such as blood. Here, a concentration range between 10^{10} to 10^{12} is postulated¹⁵⁻¹⁷. No measurement technique is apt to cover this large concentration range, therefore appropriate sample preparation techniques for the depletion of highly concentrated proteins¹⁸ or enrichment of low concentrated proteins are required. An extraordinary tool for the simultaneous depletion of high-abundant and enrichment of low-abundant proteins are hexapeptide ligand libraries (HLLs). Ideally speaking, HLLs provide numerous different binding sites due to the various amino acid sequences in the hexapeptides. Each protein can find appropriate ligands, but low concentrated proteins—which are likely to be of interest as biomarkers—will be caught quantitatively. The absolute number of binding sites for high-abundant proteins does not match the number of proteins in solution, therefore overloading conditions are present leading to their depletion upon washing. In contrast, low-abundant proteins bind quantitatively. After elution of surface-bound proteins in a volume smaller than the initial sample, equilibration of protein concentrations is observed.

A limitation of this technique is, that equilibration rates higher than 1:50 are only obtained using large sample volumes¹⁹, which is a no-deal for clinical diagnosis. To illustrate this problem: for an equilibration rate of 1:50, 1 mL of serum is required. For a deeper look inside the proteome, e.g. by using an equilibration rate of only 10^5 —which would reduce the protein concentration range in blood by a factor of two—2 L of serum would have to be loaded on a very small amount of HLL beads.

To enable high equilibration efficiencies, I aimed to develop consecutive equilibration via HLLs. The main idea is to start with the equilibration of a relatively small protein sample on a fixed amount of

MOTIVATION

HLLs, eluting this fraction and depleting it from elution agents to gain rebinding conditions. Then, binding of this “cleaned” protein-sample on a new but smaller HLL-fraction is possible under overloading conditions to again deplete high-abundant and enrich low-abundant proteins. Even third or fourth equilibration steps may be possible. With this cumbersome process, a deep insight into the proteome using only small sample volumes is possible.

In this thesis I want to show that the combination of consecutive HLL-equilibration with rapid and automated CE-separation can give rise to an overall methodology offering the possibility to gain higher understanding of the proteome. The low sample volumes required and the high automatability can even allow its application in routine clinical diagnostics.

2. Investigation of temperature and additive influences on SDS-CE part 1: A set of modifications for either fast or high resolving separations using PEO with a single molecular weight only

2.1. Abstract

SDS-CE methods are often applied in pharmaceutical laboratories to control the quality of biopharmaceuticals such as proteins or antibodies. Usually, commercially available kits are used for separation, which are mostly fit for purpose but do not allow versatile alteration or fine-tuning of separation conditions, which may be necessary especially when investigating degradation products or isoforms of similar molecular weight.

I here present a versatile separation medium for SDS-CE measurements, which consists of commercially available components. Fine-tuning of separations is possible by instrumental aspects (short-end-injection, detection aperture) or chemical aspects (addition of organic solvents) to reach either a fast screening or in-depth characterization of a sample at high resolution. Parameters varied for the development were: addition of various alkanols, separation temperature, sample composition, enrichment plug composition, detection aperture and combinations thereof. Separation performance was judged via separation efficiency, resolution of proteins and their micro-heterogeneity, peak capacity and stability of the separation medium via intermediate precision. Significant improvements in separation efficiency and high repeatability were achieved by the addition of 2-propanol, even the separation of protein isoforms and impurities, not detectable via SDS-PAGE, was observed. Relative quantification of sample constituents is possible in the sub-nanomolar range.

2.2. Introduction and motivation

The first successful production of monoclonal antibodies (mAbs) via hybridoma cells by Milstein and Köhler forms a milestone in clinical therapy²⁰ and was honored with the Nobel Prize in Medicine in 1974. Further progression of the technology led to chimerization and antibody humanization by Morrison *et al.*²¹ and Jones *et al.*²². Since the late 1990s, mAbs are commercially available. Since then, the variety of antibody structures considerably extended, giving rise to the approval of more than 30 different immunoglobulins (IgGs) by 2010²³. The interest in biopharmaceuticals such as mAbs is associated with their high target specificity and activity compared to conventional small-molecular drugs, leading to fewer adverse effects^{24, 25}.

It is not surprising that, as for any chemical or biochemical compound, impurities and structural modifications occur during production, purification or storage. For mAbs, the most important changes are deamidation, oxidation and variation in *N*-glycosylation²⁶. These structural modifications generate undesired mAb heterogeneity and lead to altered biological activity up to immunogenicity²⁷⁻²⁹. Therefore, appropriate analytical techniques are required for research and development (R&D) as well as quality control (QC). Enzyme-linked immunosorbent assays (ELISA), often associated with mAbs, are not suitable for this task due to high cross-sensitivities and lack of structural information about impurities³⁰. The challenges of mAb characterization add to the high development and production costs for each mAb.

Currently, analytical techniques for R&D include hyphenated liquid chromatography (LC) and mass spectrometry (MS) for quantification of mAbs and isoforms, since LODs similar to ELISA are accessible³¹. LC-MS/MS³¹, ion-exchange chromatography (IEC) followed by off-line MALDI-TOF²⁹, affinity-capturing of diverse glycosylation sites via lectin columns^{32, 33} or beads³⁴, are often applied. The detailed information obtained gives a profound understanding of the origin and nature of by-products and mAb heterogeneity.

For quality control of biopharmaceuticals, electromigrative separation techniques are often an attractive alternative to chromatographic techniques. Here, state-of-the-art is sodium dodecyl sulfate polyacrylamide gel electrophoresis (SDS-PAGE³⁵). SDS-PAGE evolved to its full potential within the last 50 years since its first publication³⁶ and became indispensable in various research fields. One of the advantages of SDS-PAGE is the large number of available detection techniques, among them highly selective combinations of antibody-based detection after Western and Southern blotting^{37, 38}, post-run mass spectrometry^{39, 40} or prior separation by isoelectric focusing (IEF)^{41, 42} in a 2nd dimension^{43, 44}. For a more precise quantification of protein samples, laborious differential gel electrophoresis (DIGE) followed by in-gel digestion and MS-detection¹⁴ may be used. However, the high automation reached in the human genome project with size-based DNA sieving has not yet been achieved. A similar technological innovation would allow for faster, highly automatable yet still reliable proteomic techniques for quality control of biopharmaceuticals. Likewise, a fast screening method with a very low consumption of sample and minimal manual work would be of interest as an alternative to SDS-PAGE.

Replacing SDS-PAGE by a chip- or capillary-based format using sodium dodecyl sulfate capillary electrophoresis (SDS-CE)^{35, 45-48}, offers the potential for rapid, precise, repeatable and automated analysis including direct quantification, e.g. for mAbs. These advantages derive from (i) 10-100 times higher field strengths compared to slab-gel formats, which can be applied without deleterious

Joule heating due to miniaturization. Shorter separation times and higher separation efficiencies are achieved, since no convective mixing of separated zones takes place. (ii) Because of the anti-convective nature of capillary-based methods, entangled polymers are used as sieving matrices. The latter can be replaced after each run, so fresh sieving matrix is present for each run, increasing reproducibility. (iii) The utilization of ready-to-use polymerized sieving matrices makes the use of toxic acrylamide obsolete. (iv) Automated and unsupervised measurements⁴⁹ as well as (v) direct detection and quantification are possible, thus reducing manual workload for staining methods and chemical consumption. (vi) For sample injection, 5 μ L solutions are sufficient for standard equipment (in order to fully immerse the capillary in the injection solution for a nL injection), which may be further lowered to less than 100 nL by specialized injection techniques⁵⁰. Absolute protein amounts in the low ng- or high fmol-range, are expected to be accessible via routine SDS-CE-UV. (vii) Furthermore, quantitative precision is improved due to direct on-column UV or fluorescence⁵¹ detection (instead of common grayscale interpretation in the slab-gel format). (viii) Lately, even hyphenation of SDS-CE with MS was realized, including on-line depletion of non-volatile SDS⁵². (ix) Principally, devices for parallel separation in up to 96 capillaries are commercially available, giving rise to a high-throughput analytical technique⁵³. These setups are established for DNA analysis, but so far, they have not yet been applied to SDS-CE.

Today, capillary based separation techniques are prominently applied for routine analysis using optical detection methods such as direct and indirect UV detection^{54, 55}, laser-induced fluorescence (LIF) of labeled⁵⁶ and non-labeled proteins⁵¹ as well as glycans⁵⁷. In addition, hyphenation of capillary based separations with mass spectrometry is a promising technique for peptide⁵⁸⁻⁶⁰, glycopeptide^{56, 61} and glycan^{13, 62} analysis, supporting method transfer from QC to R&D. For the QC of biopharmaceuticals SDS-CE using commercial kits is increasingly applied⁶³. The downside of the kit systems is that methodological and fundamental research on SDS-CE, prominent in the 1990s is hardly conducted today. Several optimization approaches were published, including alteration of sieving polymers⁶⁴⁻⁷⁰, temperature⁷¹, BGE composition with respect to either ionic species^{72, 73} or organic additives^{72, 74, 75}, capillary coatings^{64, 67, 71, 76} and surfactants other than SDS⁷⁷. One outstanding methodological publication by Kaneta *et al.*⁵¹ caught my attention, where self-coating PEO ($M_r = 600$ kDa) was used as a simple sieving matrix available as a bulk chemical in non-coated capillaries.

I further improved this separation system varying type and concentration of organic solvent additives, sample composition, size of the detection window and implementing an enrichment-plug. Separation performance was judged based on separation efficiency, resolution and repeatability. The influence of chain length, branching, $\log(P_{ow})$ -value and number of hydroxyl groups was regarded in this study. Based on results from MEKC⁷⁸, I investigated the influence of linear mono- (methanol to heptanol) and poly-alkanols (2-propanol and the C2 and C3 poly-alkanols ethylene glycol, propylene glycol and glycerol). I demonstrate that both very fast separations (5 min) with limited resolution but also separations with high selectivity and resolution (30 min) are possible with a basic buffer system and sieving matrix, only varying the additive type and concentration.

2.3. Materials and methods

2.3.1. Chemicals

Lysozyme (chicken egg white, $M_r = 14.4$ kDa, **1**), myoglobin (equine heart, $M_r = 16.951$ kDa, **2**), β -lactoglobulin (bovine milk, $M_r = 18.4$ kDa, **3**), carbonic anhydrase (bovine erythrocytes, $M_r = 29$ kDa, **4**), ovalbumin (chicken egg white, $M_r = 42.8$ kDa, **5**), bovine serum albumin (BSA, bovine serum, $M_r = 66.463$ kDa, **6**), phosphorylase B (rabbit muscle, $M_r = 97.412$ kDa, **7**), sodium dodecyl sulfate (SDS, 98,5 %), methanol (HPLC grade), ethanol (reagent grade), isopropanol (LC-MS grade), 1-butanol (reagent grade), 1-pentanol (reagent grade), polyethylene oxide ($M_r = 600$ kDa) were purchased from Sigma-Aldrich (Steinheim, Germany). 1-propanol (reagent grade) was purchased from BASF SE (Ludwigshafen, Germany). Tris(hydroxymethyl)aminomethane (Tris), 1-hexanol (reagent grade), n-heptanol (reagent grade), sodium hydroxide solution (NaOH, 30%, suprapur), 2-mercaptoethanol (≥ 99.9 %), were delivered by Merck (Darmstadt, Germany). n-Butanol (reagent grade) and hydrochloric acid (HCl, 32 %, analytical grade) were purchased from VWR (Darmstadt, Germany). *N*-Cyclohexyltaurine (CHES) was obtained from Alfa Aesar (Karlsruhe, Germany). Deionized water was prepared using an ELGA-Veolia PURELAB Classic system (Celle, Germany).

2.3.2. Buffer and sieving polymer solution preparation

Background electrolyte (BGE) solutions contained 100 mmol/L Tris-CHES, 0.1 % SDS⁵¹, as well as additives. BGEs were used no longer than 5 days after preparation. Sieving solutions containing polymer were prepared by the following standard procedure: 20 mg (equals 2.0 %) PEO were dissolved in 1 mL BGE in a sealed vial at 40 °C while stirring for 2 h. For polymer sieving solutions with BGEs containing poly-alkanols, heating to 80 °C was chosen, see Table 1 for further details. For 2-propanol, both temperatures were investigated. Therefore, the basic separation medium for SDS-CE was 2.0 % PEO, 100 mmol/L Tris-CHES and 0.1 % (3.5 mmol/L) SDS at pH 8.9. Protein stock solutions were dissolved in 30 mmol/L aqueous ammonium acetate, pH 6.8 at a concentration of 10 g/L (1 %) and stored at -20 °C. No degradation upon storage was visible in SDS-CE experiments.

2.3.3. Instrumentation and separation parameters

For CE analysis, an Agilent 7100 CE system (Agilent, Waldbronn, Germany) with UV-detection was used. Detection was performed at a wavelength of 210 \pm 5 nm and 280 \pm 5 nm with 360 \pm 50 nm for reference. Detection at 280 nm was used for the identification of protein species and at 210 nm for quantification due to higher sensitivity. Fused silica capillaries were purchased from Polymicro Technologies (Kehl, Germany). All measurements were conducted in capillaries with a length of 35.0 cm, an effective length of 27.5 cm, an inner diameter of 100 μ m and an outer diameter of 360 μ m. A detection window of 0.2 cm in length was made by carefully burning off the outer capillary polyimide coating, followed by polishing with a wet paper tissue to remove debris. For run series with different additives, capillaries were changed daily and electrodes as well as pre-punchers were thoroughly cleaned between series of measurements to prevent polymer segregation and capillary clogging. Prior to every measurement, the freshly cut capillary was coated by rinsing the capillary with a solution of 2.0 % PEO in BGE without additives at 1 bar for 10 min. To control the integrity of the capillary used, one standard measurement was performed at 25 °C with a separation medium void of organic solvents.

Measurements were performed as follows: rinsing the capillary with 0.1 mol/L NaOH, 0.1 mol/L HCl and water for 1 min at 1 bar each, followed by rinsing with BGE with sieving matrix of interest for 3 min at 1 bar. These rinsing steps were also conducted in-between runs. Excessive polymer sticking to the capillary and electrodes was removed by dipping both capillary ends into water. The sample was injected electrokinetically for 5 s at -10 kV followed by the separation at -8.20 kV (-234 V/cm) for 20 – 45 min. The run time depended on temperature and additive in the separation medium. Measurements were commonly carried out at 25 °C. The influence of temperature was investigated for separation media void of organic solvents in the range of 10 °C to 50 °C with an increment of 5 °C. Measurements were conducted in triplicate. The dependence of resolution and migration times on additive concentration was investigated within one day for each additive.

2.3.4. Sample preparation

A protein stock solution was freshly prepared prior to the first sample preparation at a total protein concentration of 10.0 g/L by mixing solutions of lysozyme, myoglobin, β -lactoglobulin, carbonic anhydrase, ovalbumin, BSA, phosphorylase B in a ratio of 1:1:1:2:3:4.5:7 to obtain similar molar protein concentrations. The final overall protein concentration was 4.15 g/L, which equals a concentration of 11.6-15.3 nmol/L for each protein. Detailed information can be found in Table 1.

The sample injection solution for SDS-CE was prepared by mixing 78.0 μ L of this protein mixture with 109.8 μ L of a solution containing 1.0 % SDS, 5.0 % 2-mercaptoethanol and 100 mmol/L Tris-CHES at pH 8.9 to obtain an SDS:protein ratio of 1.4. This sample injection solution was incubated at 100 °C for 15 min. Aliquots of approx. 20 μ L were stored at -20 °C until use. Protein injection solutions were used for over 100 measurements each, until degradation became visible.

Table 1: Overall concentrations of proteins in the sample injection solution for SDS-CE.

	lysozyme	myoglo- bin	β -lacto- globulin	carbonic anhydrase	ovalbu- min	BSA	phospho- rylase B
M_r (kDa)	14.4	16.951	18.4	29	42.8	66.463	97.412
c (g/L) ^A	0.21	0.21	0.21	0.43	0.64	0.96	1.49
c (nmol/L) ^B	14.8	12.1	11.6	13.7	14.9	14.4	15.3

A: Total protein concentration in grams per liter. B: Concentration of protein in nanomoles per liter.

2.3.5. Data processing

Conversion of .ch data format from Agilent's OpenLAB to .csv was achieved using the free software UniChrom (NAS Ltd., Minsk, Belarus), prior to the import to Origin 9.1 (Additive, Friedrichsdorf, Germany) for further data processing. Baseline subtractions were performed semi-automatically by using the first and second derivative of the graph. In addition, minor manual adjustments of baseline-subtraction points were necessary. In Figure 1, an example for an electropherogram prior to (Trace 2) and after (Trace 3) baseline-subtraction is shown. A typical increase of the baseline within the first 6 minutes of the measurement as well as peaks a-f (presumably system peaks) can be seen, even for blank measurements (Trace 1). The baseline-subtracted electropherograms were used for manual peak fitting, using a bi-Gaussian model⁷⁹ to account for peak-tailing frequently observed in SDS-CE⁸⁰. Depending on the resolution 7-12 peaks were identified, some of them can be ascribed to protein isoforms of unknown composition. Their respective peak-widths and migration times were taken into consideration for the investigation of separation performance.

Therefore, the following parameters were used: (i) intermediate precision of migration times, (ii) in- and decrease of the migration time window given as the time span between first and last protein peak (that is of lysozyme and phosphorylase B), (iii) resolution, calculated using migration times and peak-widths obtained via the bi-Gaussian fit (see Figure 1); and (iv) the peak capacity, which was estimated via Equation (2) for the model proteins.

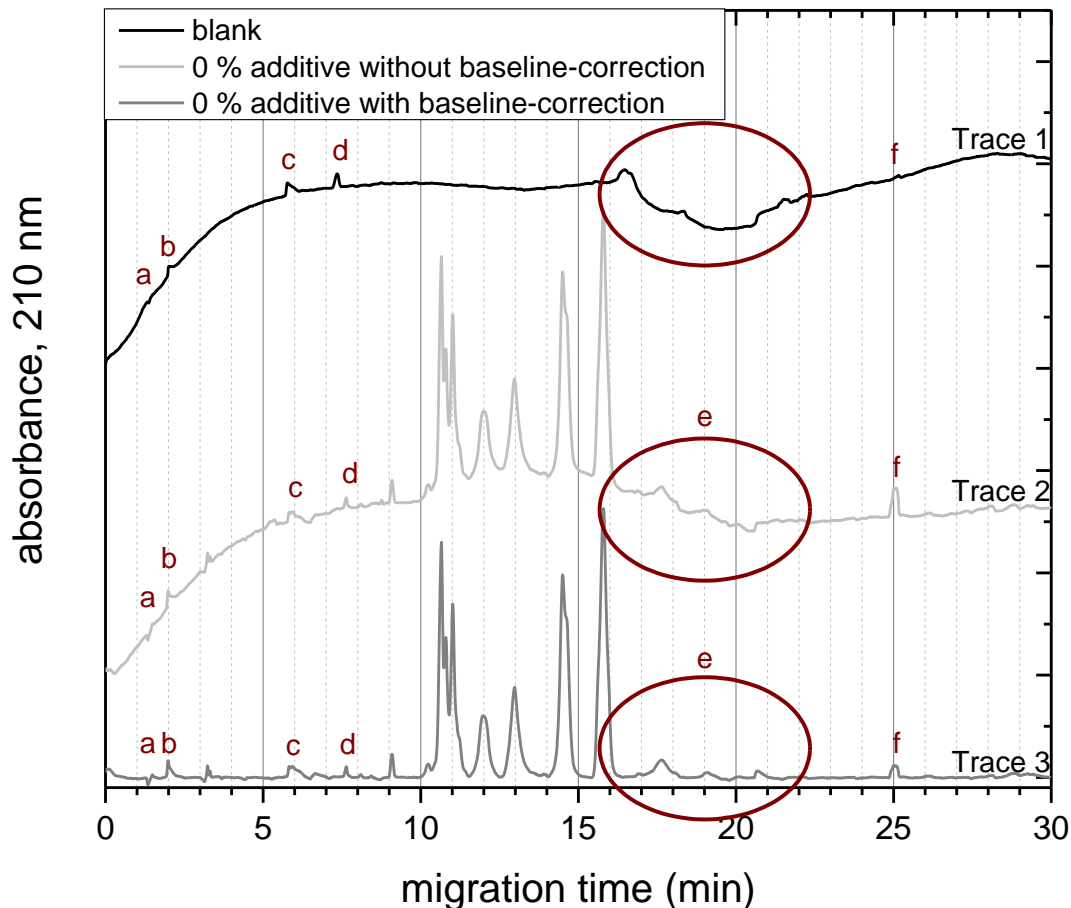


Figure 1: Electropherograms recorded at 210 nm, utilizing 0 % additive and 2.0 % PEO, separation conditions, BGE and sample as noted in Section 2.3.3 and 2.3.4. Trace 1: Electropherogram of a blank measurement. Trace 2: electropherogram of a measurement using the standard-protein mixture as sample. Trace 3: the electropherogram of Trace 2 after baseline-subtraction. The letters a-e indicate impurities and system peaks, originating from buffer-components and f indicates 2-mercaptoethanol. Notice the circled time segment e, which exhibits a dip of the baseline over several minutes as well as 4 signals.

2.4. Results

Based on results from MEKC⁷⁸ I investigated the influence of linear alkanols and temperature on separation efficiency (via resolution, migration time window and peak capacity) and repeatability (via $RSD(t_{mig})$). Members of the homologous series of alkanols (methanol to heptanol) were added at concentrations between 0 % and 10 % (volume per volume). In addition, branched 2-propanol and the C2 and C3 poly-alkanols ethylene glycol, propylene glycol and glycerol at concentrations between 0 % and 20 % were considered to study the influence of polarity (using the partition coefficient between octanol and water (P_{ow}) as overall parameter for chain length and number of hydroxyl groups) and viscosity.

Viscosities and $\log(P_{ow})$ -values are summarized in Table 2. Furthermore, investigated concentrations and respective changes in t_{mig} for the lightest protein lysozyme can be found in Table 2. The temperature was varied between 10 °C and 50 °C. Lower temperatures were not accessible due to restrictions of the cooling system, higher temperatures led to instable separation conditions.

In the following, I will present and discuss the results for ethylene glycol as well as for 1- and 2-propanol in detail as the effects observed here are representative also for other additives. Further results are summarized later on. For 2-propanol, the effect of temperature during dissolution of PEO is presented.

2.4.1. Influences of alkanols in the sieving medium

2.4.1.1. Changes of migration time

In general, increasing the amount of alkanol in the separation medium is accompanied by an almost linear increase in migration times (t_{mig}) of the proteins as can be seen in Figure 2 A for ethylene glycol and in Figure 3 A and B for 1-propanol and 2-propanol, respectively. This effect was observed for each alkanol, indicated in Table 2 by Δt_{mig} for lysozyme as the first migrating protein. Δt_{mig} is the difference between t_{mig} at a given additive concentration to the migration time at the next lower concentration level. For polar alkanols (methanol, ethanol, 1-propanol, ethylene glycol and glycerol) a steeper increase in t_{mig} is observed at a certain alkanol concentration, as indicated in Table 2 by the bold values. This observation was not made for non-polar alkanols (2-propanol, 1-butanol, 1-pentanol, 1-hexanol) and propylene glycol. A further increase of alkanol concentration commonly led to electropherograms void of protein signals within 60 minutes, higher additive concentrations were not investigated.

Additional observations were made for: (i) 1-propanol and ethanol, where separation conditions with alkanol concentrations up to their respective upper limit led to a decrease in t_{mig} prior to electropherograms void of protein signals. This decrease in t_{mig} was accompanied by strong peak-broadening. (ii) Using 2-propanol with PEO dissolved at 40 °C, two concentrations evoking strong increases in t_{mig} were observed. The first step was at a concentration of 2.0 % 2-propanol, followed by a decrease in t_{mig} at 3.0 % and followed again by a strong increase at 4 %. Electropherograms void of protein signals were obtained at > 6.0 % 2-propanol. (iii) For glycerol, a gap in the concentration range was found: For yet unknown reasons, separations with 15.0 % glycerol additive led to electropherograms without protein signals. Yet, the addition of 5.0 %, 10.0 % and 20.0 % glycerol was successful, including a strong increase of migration times at 20.0 %.

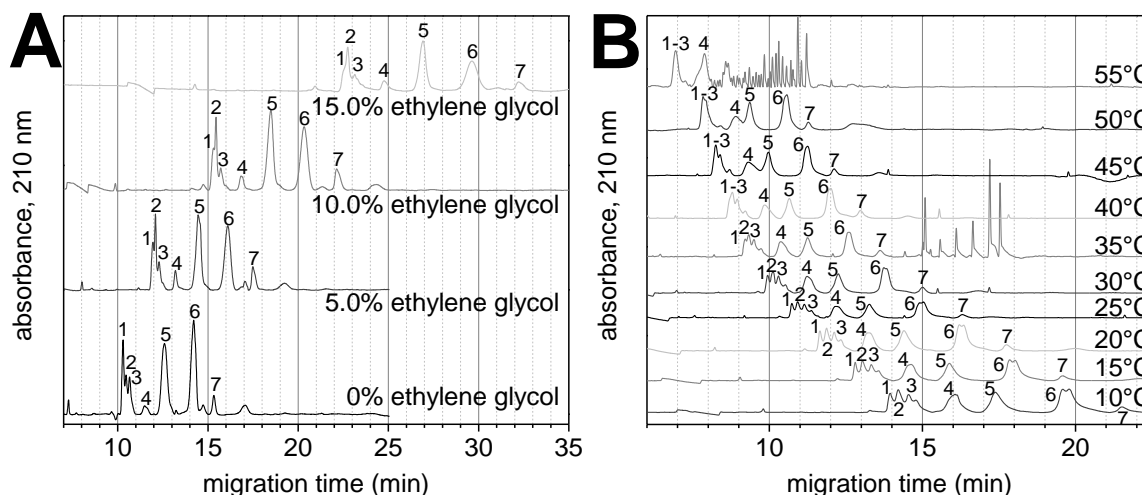


Figure 2: A: Influence of ethylene glycol on an SDS-CE separation. Separation and measurement conditions see Figure 1. BGE was modified by addition of ethylene glycol and contains 100 mmol/L Tris-CHES and 0.1 % SDS at each concentration of ethylene glycol, for further information see Section 2.3.2. A steady increase in t_{mig} for 0 %-10.0 % ethylene glycol is observed, followed by a strong increase at 15.0 %. Electropherograms were void of protein signals for a BGE with 20 %. B: Influence of temperature on the separation without additive. The measurements conducted at 25 °C in a separation medium void of additive are taken as reference. An increase in t_{mig} with decreasing temperature can be observed. Electropherograms of separations conducted at 35 °C show spikes presumably due to Joule heating. All measurement sequences were conducted on a separate, freshly cut capillary using the separation conditions stated in Section 2.3.3, the presented electropherograms are baseline-corrected.

Alkanol specific useful concentration ranges determined in this work correlate well with $\log(P_{\text{ow}})$ -values (see Table 2): polar (nonpolar) alkanols offer widest (smallest) concentration ranges. E.g. glycerol has the lowest $\log P_{\text{ow}}$ -value and is the only alkanol that was successfully applied at concentrations up to 20.0 %. In contrast, separations with 1-heptanol (highest $\log(P_{\text{ow}})$) were not successful even at a concentration of 0.5 %.

Table 2: Overview of the investigated alkanols at various concentrations is given with octanol-water coefficients $\log(P_{\text{ow}})$ and viscosities η . For each concentration of alkanol c , migration time change of lysozyme $\Delta t_{\text{mig},1}$ with respect to the next lower concentration as well as the number of peaks N observed for the low mass range (lysozyme (1), myoglobin (2) and β -lactoglobulin (3), N_{1-3}) and BSA (6, N_6), are presented. Unexpectedly high values of Δt_{mig} are accentuated by bold numbers.

alkanol	$\log(P_{\text{ow}})$	η^c ($\text{kg m}^{-1} \text{s}^{-1}$)	c^d (%)	$\Delta t_{\text{mig},1}^e$ (min)	N_{1-3}^f	N_6^g
methanol	-0.66 ^a	0.6	2.5	0.0	4	2
			5.0	0.8	5	1
			7.5	5.9	4	1
			10.0	0.2	4	1
ethanol ^h	-0.32 ^a	1.2	2.5	0.5	4	1
			5.0	1.5	5	1
			7.5	2.5	4	1
			10.0	9.5	3	1
			12.5	-10.2	3	1

INVESTIGATION OF TEMPERATURE AND ADDITIVE INFLUENCES ON SDS-CE PART 1: A SET OF MODIFICATIONS FOR
EITHER FAST OR HIGH RESOLVING SEPARATIONS USING PEO WITH A SINGLE MOLECULAR WEIGHT ONLY

1-propanol ^h	0.25 ^b	2.3	1.0	0.7	4	1
			2.0	0.6	4	1
			3.0	0.8	4	1
			4.0	2.6	3	1
			5.0	-3.0	3	1
2-propanol, dissolved at 40 °C	0.05 ^{b,k}	2.2	1.0	0.5	4	1
			2.0	2.3	4	1
			3.0	-1.5	4	1
			4.0	9.4	3	1
			5.0	2.1	3	1
2-propanol, dissolved at 80 °C	0.05 ^{b,k}	2.2	5.0	4.8	4	2
			10.0	3.4	6	2
1-butanol	0.83 ^a	2.9	1.0	0.4	4	2
			2.0	0.8	2	2
			3.0	0.2	1	2
			4.0	1.0	2	2
1-pentanol	1.40 ^a	3.7	0.5	0.4	3	1
			1.0	0.6	1	1
			1.5	0.5	2	1
1-hexanol	3.1 ^b	5.9	0.5	2.2	1	2
			1.0	13.2	2	2
1-heptanol	2.62 ^b	7.4	0.5	-	0	0
ethylene glycol	-1.36 ^{b,k}	21.0	5.0	1.6	3	1
			10.0	3.1	3	1
			15.0	12.4	2	1
propylene glycol	-1.07 ^{b,k}	60.5	5.0	1.5	1	1
			10.0	3.9	2	1
			15.0	5.0	2	1
glycerol ⁱ	-1.76 ^{b,k}	1480	5.0	1.9	3	1
			10.0	2.6	3	1
			15.0	-	0	0
			20.0	18.7	2	1

^aData from Leo *et al.*⁸¹ and ^bmanufacturer. ^cViscosity of pure alkanol at 25 °C, according to safety data sheet.
^dInvestigated concentration levels. ^eIncreases of t_{mig} observed for the first protein (lysozyme), determined by

subtraction of t_{mig} determined for the next lower concentration. The first value was obtained by comparison to the measurement with 0.0 % alkanol. Values for the step change in migration times are indicated in bold. ^fNumber of peaks determined in the low mass range (lysozyme N₁, myoglobin N₂ and β -lactoglobulin N₃, <20 kDa) observed at each concentration level (only peaks with sufficient resolution and clear maximum were included). For 0.0 % additive, the replicates were measured in triplicates. ^gNumber of peaks determined for BSA (protein 6) for each alkanol and concentration level. ^h1-propanol and ethanol are the only investigated additives giving decreasing t_{mig} at a certain alkanol concentration. ⁱGlycerol is the only investigated additive leading to a successful separation above the concentration noted in ^e. ^kPolymer sieving solutions containing these alkanols were heated to 80 °C to accelerate dissolution.

2.4.1.1. Separation performance – resolution and protein micro-heterogeneity

During this work, electropherograms often revealed more than 7 protein signals. These may stem from proteins' micro-heterogeneity, such as different posttranslational modifications (e.g. glycosylation⁸²), oxidation processes, deamidation events or differences in the amino acid sequences. Likewise, impurities may be present (see also Section 2.5). The (partial) separation of micro-heterogeneities was mainly observed for the 3 lightest proteins lysozyme (**1**), myoglobin (**2**) and β -lactoglobulin (**3**) and for BSA (**6**). To facilitate discussion, the investigated proteins were divided into 3 classes as indicated in Table 3.

Table 3: Protein classes depending on their molecular mass with the peak pairs considered for the calculation of resolution.

class	mass range	proteins ^a	resolution
low mass range	<20 kDa	1-3	1&2; 2&3
medium mass range	>20 kDa; <60 kDa	4-5	3&4; 4&5
high mass range	>60 kDa	6-7	5&6; 6&7

^aProteins, abbreviated by numbers according to Section 2.3.1.

Four effects on the separation of isoforms/impurities were observed upon addition of alkanols to the separation medium: (i) the overall separation selectivity and resolution of the separation decreased, which can be seen in Figure 2 A for ethylene glycol and in Figure 3 A for 1-propanol at a concentration ≥ 2.0 %. This was also observed for methanol (≥ 7.5 %), ethanol (≥ 5.0 %) and for 1-pentanol and propylene glycol (≥ 5.0 %). (ii) In case of 1-butanol, the selectivity increased only for proteins of high molecular mass (**6**), while the selectivity for light proteins (**1-3**) decreased. (iii) The addition of methanol (≤ 5.0 %), ethanol (2.5 %) and glycerol (≥ 5.0 %) increased the selectivity only for Proteins **1-3** while it decreased for BSA **6**. (iv) An increase in both the selectivity of **1-3** as well as **6**, was observed adding 2-propanol after dissolution of PEO in BGE at 80 °C only (see Figure 3 B).

Exemplarily, a comparison of the separations with 1-propanol (0.0 - 5.0 %) and 2-propanol at both dissolving-temperatures (0.0 – 5.0 % for 40 °C and 0.0 – 10.0 % for 80 °C) is given in Figure 3. Separation performance is best compared on a qualitative level via the enlargements of the migration time region for the small proteins (**1-3**) and BSA (**6**). The close-ups were plotted with like scales for x- and y-axis and with the mean migration time of the signals centered. Four partially resolved signals for the light proteins can be observed without solvent additive. Upon addition of 1-propanol to the separation medium, resolution is lowered, mainly due to a loss in separation efficiency. For BSA **6**, even low amounts of 1-propanol added to the separation medium seem to prevent the separation of the 2 isoforms due to band broadening. The addition of 1.0 – 3.0 % 2-propanol with PEO dissolved at 40 °C led to a similar but smaller decrease in separation

performance than observed for 1-propanol. When using 4.0 % and 5.0 % 2-propanol, separation performance decreases drastically as peak widths almost double.

For 2-propanol with PEO dissolved at 80 °C, completely different results were obtained (see Figure 3 C). Upon addition of 2-propanol to the separation medium, the resolution between isoforms of the light protein fraction increased. Selectivity changes occur, too. In the close-ups for proteins **1-3** it can be seen that the number of peaks increases from four at 0.0 % 2-propanol to six or seven peaks at 10.0 % 2-propanol. The resolution between the two isoforms of BSA **6** increased at higher 2-propanol concentrations in the separation medium, too.

For a quantitative approach, the resolution between two consecutive protein peak-pairs was calculated for each set of measurements with different alkanols. The peak-fitting procedure was described in Section 2.3.5. Results are presented in Figure 4. The inter-run standard deviations of 3 consecutive runs was calculated, considering t_{mig} and FWHM to reveal error bars. It is worth noting that there were differences comparing electropherograms with 0.0 % 1-propanol and 0.0 % 2-propanol at both dissolving temperatures. This is due to the fact that two different capillaries, samples and polymer solutions were used on different days for each sequence. I assume that these differences, evident in Figure 3, are mainly due to the sample composition and protein purity. This assumption is corroborated by the differences in intensities obtained for the protein signals **4** and **7**. Therefore, changes in resolution were directly compared only within measurement series. Using this approach, inter-day differences can be neglected and changes in resolution can be linked to changes in separation conditions only.

When protein micro-heterogeneity was visible in the electropherograms, the signals of highest intensity were assigned to proteins. Resolutions determined for Pairs 1&2 and 2&3 (see Table 3) were always significantly lower than those of the other four peak-pairs due to the small mass differences between the corresponding proteins.

INVESTIGATION OF TEMPERATURE AND ADDITIVE INFLUENCES ON SDS-CE PART 1: A SET OF MODIFICATIONS FOR EITHER FAST OR HIGH RESOLVING SEPARATIONS USING PEO WITH A SINGLE MOLECULAR WEIGHT ONLY

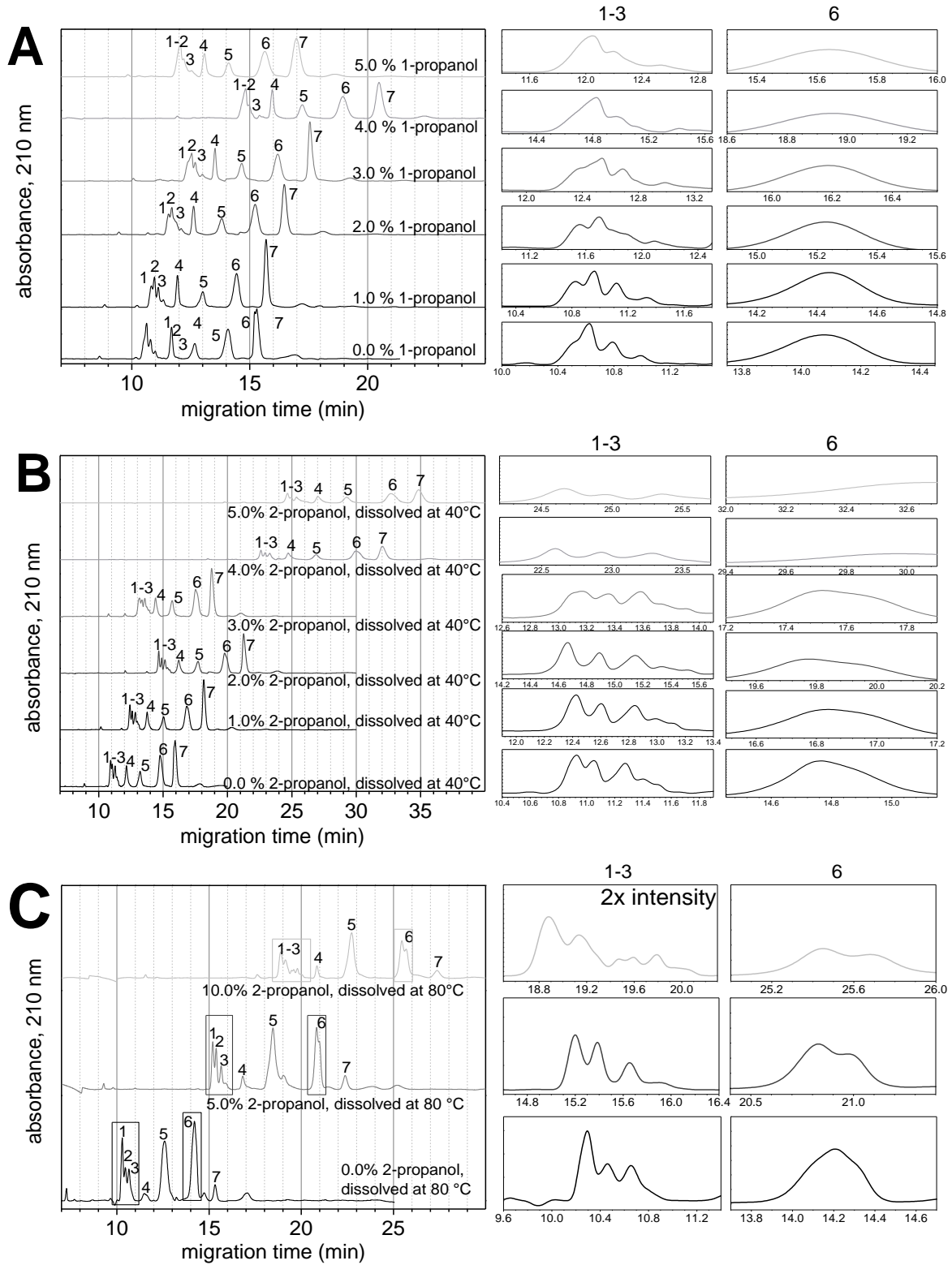


Figure 3: Electropherograms obtained for the addition of alkanols to the BGE: A: 1-propanol, dissolving PEO at 40 °C, B: 2-propanol, dissolving PEO at 40 °C, C: 2-propanol, dissolving PEO at 80 °C. Concentrations of alkanols are given in the figure. Measurement conditions are described in Figure 1 and Section 2.3. All electropherograms were baseline-corrected. The electropherograms on the right side, marked with 1-3 and 6, represent close-ups of the first 3 proteins (lysozyme, myoglobin, β -lactoglobulin) and of BSA.

INVESTIGATION OF TEMPERATURE AND ADDITIVE INFLUENCES ON SDS-CE PART 1: A SET OF MODIFICATIONS FOR EITHER FAST OR HIGH RESOLVING SEPARATIONS USING PEO WITH A SINGLE MOLECULAR WEIGHT ONLY

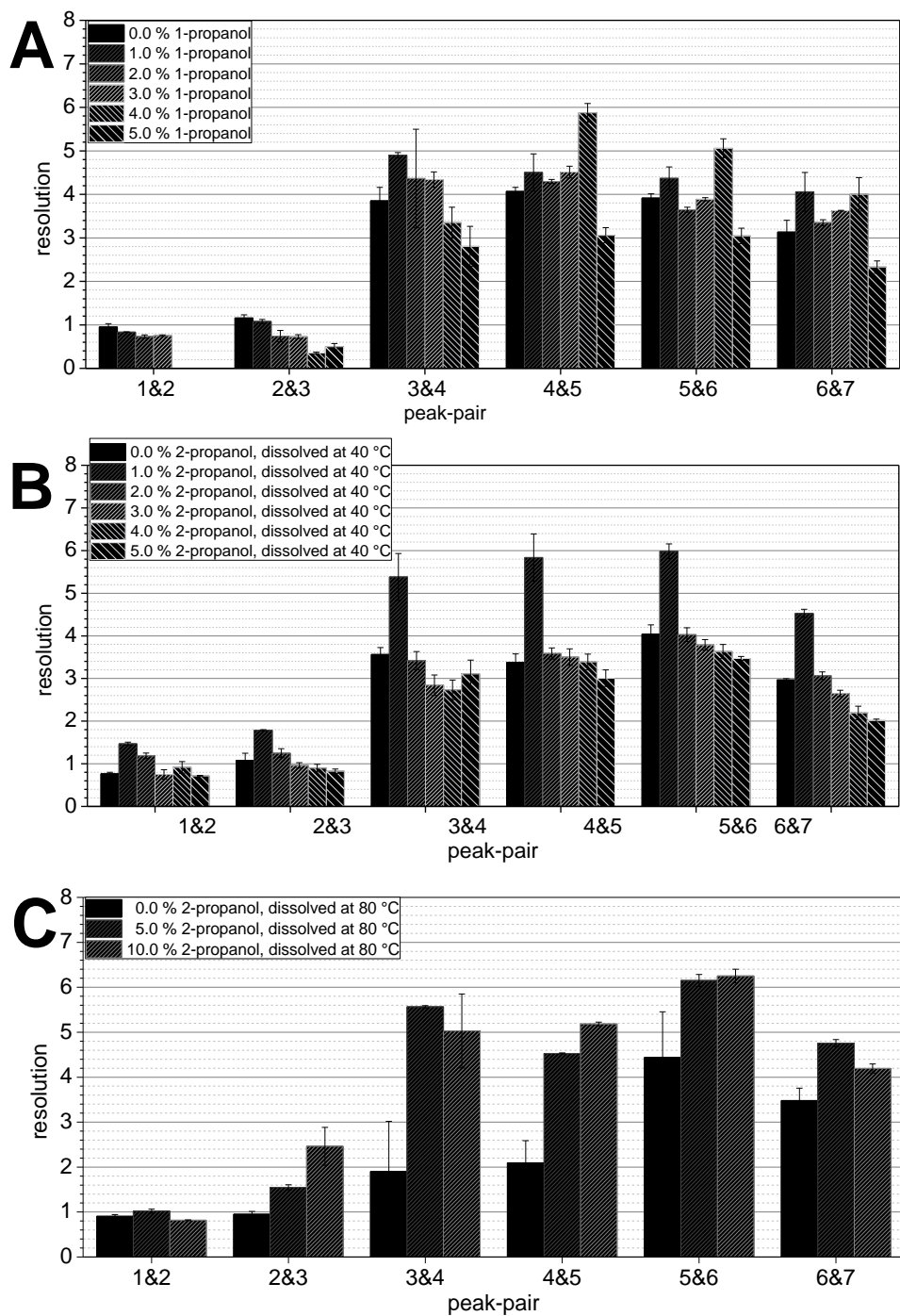


Figure 4: Resolution for peak-pairs (see Table 3). Representative results are shown for A: 1-propanol, dissolving PEO at 40 °C, B: 2-propanol, dissolving PEO at 40 °C, C: 2-propanol, dissolving PEO at 80 °C. Additive concentration levels are given in the figure. Resolutions for Pair 1&2 (Table 3) at 4.0 % and 5.0 % 1-propanol were set to 0 due to comigration. Measurements for each alkanol were conducted in triplicates within the same day.

Overall, for 1-propanol (PEO dissolved at 40 °C) only small changes in resolution were observed. At 1.0 % 1-propanol, Pairs 3&4 and 6&7 show an increase in resolution by 30 % compared to separations in separation media void of 1-propanol. At higher solvent concentration the resolution diminishes again with the exception of separations in 4.0 % 1-propanol. Using a BGE with 2-propanol and dissolving PEO at 40 °C gave a strong increase in separation performance for 1.0 %

only and over the whole mass range. Decreasing but still good separation performance was maintained for the low mass range at each utilized concentration level.

When dissolving PEO at 80 °C in a BGE with 2-propanol, a significant increase in resolution over the whole investigated concentration range was observed. For proteins of low molecular mass, specifically Pairs 1&2 and 2&3, improvement in resolution was about 15-65 %. One outstanding observation herein is the surprisingly high increase in resolution by about 160 % found for Pair 2&3 at 10.0 % 2-propanol concentration, see Figure 3 B. Resolution enhancement included both selectivity changes and improvement of separation efficiency. For Pairs 3&4 as well as 4&5 a strong increase in resolution by 165-195 % and 115-150 % was observed. The increase in resolution was somewhat lower for Pairs 5&6 and 6&7 (20-40 %). Overall, the increase in separation performance was comparable to the one observed for 1.0 % 2-propanol addition. It is worth noting, that a decrease in separation performance mainly occurred for the medium and high mass range. I thereby conclude that the influence of alkanols on the resolution depends on the molecular mass of the separated proteins.

2.4.1.2. Quantification of changes in separation performance

For a more quantitative approach, the resolution between two consecutive protein peak-pairs (see Table 3) was calculated for each set of measurements with different alkanols. The peak-fitting procedure was described in Section 2.3.5. The resolution between peak pairs are presented in Figure 4. Error bars were calculated via inter-run standard deviations of 3 consecutive runs, considering t_{mig} and FWHM.

I compared the resolutions determined from each measurement (R_i) with the resolution of the respective measurement conducted with 0.0 % alkanol of the same day ($R_{0.0\%}$) to minimize the influence of inter-day variations. Thus, the relative resolution ($r_{\%}$) as determined in Equation (1) was used. Therein, $r_{\%}$ -values of 0 % indicate, that no change in resolution was present. Positive (negative) $r_{\%}$ -values indicate increasing (decreasing) resolution compared to the measurement void of alkanol. An $r_{\%}$ -value of -100 % is the lowest obtainable value and indicates that no separation was present. To reduce the amount of data, these $r_{\%}$ -values were first calculated by Equation (1) for each peak-pair and then averaged for proteins of the low, medium and high mass range. The results are presented in Figure 5 A (low mass range), B (medium mass range) and C (high mass range).

$$r_{\%} = \frac{R_i - R_{0.0\%}}{R_{0.0\%}} \cdot 100\% \quad (1)$$

For the low mass range (Figure 5 A), **a decrease** in $r_{\%}$ was found for 2.5 % methanol, 15.0 % ethylene glycol, 20.0 % glycerol as well as for 1-propanol, 1-butanol, 1-pentanol and propylene glycol at each investigated concentration level. **An increase** in $r_{\%}$ is visible for methanol at concentrations of 5.0 % and above, for each investigated concentration of ethanol with highest $r_{\%}$ at its lowest concentration and decreasing $r_{\%}$ with increasing concentration, for 5.0 % and 10.0 % ethylene glycol, glycerol and 2-propanol (dissolving PEO at 80 °C). For 2-propanol (dissolving PEO at 40 °C) highest $r_{\%}$ was found at 1.0 % additive. The value further decreased at higher concentrations, reaching $r_{\%} \approx 0\%$. This observation is comparable the one made for ethanol. For 1-butanol neither an increase nor a decrease in relative resolution was observed. All observations are in good

accordance with the qualitative results for the separation of micro-heterogeneities in the low mass range presented in Table 2.

Different observations were made for the medium mass range, presented in Figure 5 B. **A decrease** in $r_{\%}$ was observed for the following alkanols: Ethanol at every concentration except 5.0 %, 1-propanol at 5.0 % only, 1-pentanol at 1.5 % only and methanol and 1-butanol at each investigated concentration. **An increase** was observed for 5.0 % ethanol, 1.0-4.0 % 1-propanol, 0.5 and 1.0 % 1-pentanol as well as 2-propanol (dissolving PEO at 80 °C), ethylene glycol, propylene glycol and glycerol at every investigated concentration. For 2-propanol (dissolving PEO at 40 °C) highest $r_{\%}$ was at 1.0 % additive concentration, and a decrease to $r_{\%} \sim 0$ % to higher concentration levels. In contrast to the low mass range, beneficial instead of detrimental effects were observed for the polyalkanol propylene glycol as well as the non-polar alkanols 1-propanol and 1-pentanol. For the small and polar alkanols methanol and ethanol, a decrease in separation selectivity was observed.

Compared to the other two mass ranges, the changes in resolution determined for the high mass range were small. **Decreases** in resolution were found for: 7.5 and 10.0 % methanol, 5.0-10.0 % ethanol and 5.0 % 1-propanol as well as for 1-butanol, 1-pentanol, ethylene glycol, propylene glycol and glycerol at every investigated concentration. **Increases** were found for: 2.5-5.0 % methanol, 2.5 % ethanol, 1.0-4.0 % 1-propanol and 2-propanol (dissolving PEO at 80 °C) at every investigated concentration. The increase in relative resolution for methanol and ethanol as well as for 2.0 and 3.0 % 1-propanol were small and below 10 %. Overall, beneficial effects on the separation of the high mass range proteins were mostly observed for the rather polar 1- and 2-propanol (dissolving PEO at 80 °C) as well as methanol and ethanol. For 2-propanol (dissolving PEO at 40 °C), the highest $r_{\%}$ -values were found at 1.0 % additive concentration. They decreased upon further addition of 2-propanol, similar to the observations made for the medium mass range. Non-polar alkanols as well as poly-alkanols exhibit rather detrimental effects on the resolution.

INVESTIGATION OF TEMPERATURE AND ADDITIVE INFLUENCES ON SDS-CE PART 1: A SET OF MODIFICATIONS FOR EITHER FAST OR HIGH RESOLVING SEPARATIONS USING PEO WITH A SINGLE MOLECULAR WEIGHT ONLY

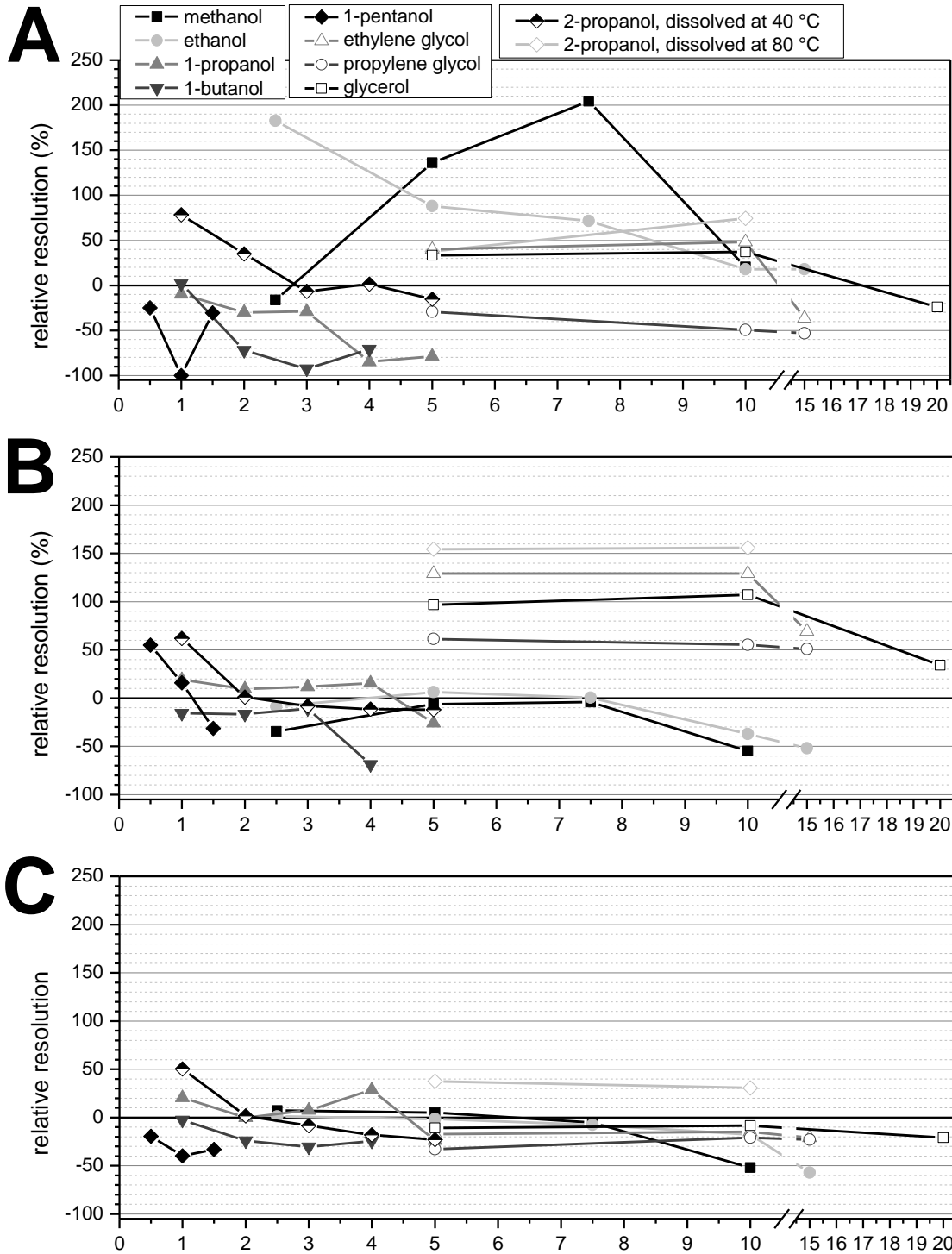


Figure 5: Relative resolutions $r\%$ calculated for A: low, B: medium, C: high mass range. All alcohols investigated are included. An increase in resolution correlated with positive $r\%$ -values. At $r\%$ -values of -100 % no separation of protein occurs.

2.4.1.3. Intermediate precision

Repeatability of migration times was investigated for each protein at each investigated temperature and alkanol concentration using 3 consecutive runs. For separation media void of additive, $RSD(t_{mig})$ was approx. 3 %. The addition of alkanol resulted in $RSD(t_{mig})$ below 5 % and often even lower 3 %, which is an acceptable intermediate precision for this separation medium. A more detailed discussion is presented in Chapter 3.

2.4.1.4. Migration time window and peak capacity

Adapting the definitions of Benedek *et al.*⁸³, I here use the term migration time window to describe the differences in t_{mig} between the slowest migrating protein ($t_{mig,7}$, phosphorylase B) and the fastest migrating protein ($t_{mig,1}$, lysozyme). Addition of alkanols always increased the migration time window, albeit to a different extent, see e.g. Figure 6 A.

In Figure 6 A and Figure 6 B the migration time windows for the different investigated alkanols are presented. For the homologous series of n-alkanols, it can be deduced from Figure 6 A that only methanol and ethanol, the alkanols with the smallest carbohydrate chain and the smallest $\log(P_{ow})$, evoke an increase of the migration time window with increasing concentration of alkanol in the BGE. For ethanol strong run-to-run-variations in t_{mig} were observed at a concentration of 10.0 % and a collapse of the sieving effects at 12.5 % ethanol additive. I presume that the high organic content strongly interferes with the micelle formation and SDS-protein interaction. For 1-propanol, 1-butanol and 1-pentanol almost no change in the size of the migration time window was observed. For the poly-alkanols and 2-propanol the migration time window was enlarged (Figure 6 B). The increase of the migration time window for polyalkanol additives was in the order glycerol (20.0 % in separation medium) > ethylene glycol (15.0 %) \approx propylene glycol (5.0 % and 10.0 %). For the less polar propylene glycol, increasing concentrations lead to a collapse of the sieving mechanism. Interestingly, 2-propanol gave larger migration time windows for 4.0 % and 5.0 % (approx. 9.6 min and 10.2 min, respectively) when dissolving PEO at 40 °C. When dissolving PEO at 80 °C, the migration time window was 7.1 min and 8.3 min for 5.0 % and 10.0 %.

As mentioned, an increase in alkanol content either led to peak sharpening due to separation of isoforms or to peak broadening for yet unknown reasons. To combine both effects, the peak capacity was calculated according to Equation (2), which is helpful to depict the overall separation performance. Error bars are calculated by the Gaussian error propagation.

$$P = \frac{t_{mig,7} - t_{mig,1}}{\frac{1}{7} \sum_{i=1}^7 w_{0.5,i}} \quad (2)$$

The numerator in this ratio is the migration time window discussed earlier and the denominator is the peak width at half height (either known as $w_{0.5}$ or FWHM) discussed in Section 2.4.1.2. By taking the peak capacity into account, the performance of a separation can be described better, since peak widths and resolutions can in- or decrease with increasing alkanol concentration. In Figure 6 C the peak capacities of the homologous series of n-alkanols are presented. It can be seen, that methanol and ethanol both offer an increase in the migration time window, but only separation with 2.5 % ethanol and at 5.0 % and 7.5 % methanol revealed an increase in peak capacity compared to the separation medium without additive. From Figure 6 B it can be seen that, except for 2-propanol (dissolving PEO at 80 °C), all alkanols exhibit peak-capacities lower than those obtained for a separation medium without alkanol. In contrast, separation using 2-propanol (dissolving PEO at

INVESTIGATION OF TEMPERATURE AND ADDITIVE INFLUENCES ON SDS-CE PART 1: A SET OF MODIFICATIONS FOR EITHER FAST OR HIGH RESOLVING SEPARATIONS USING PEO WITH A SINGLE MOLECULAR WEIGHT ONLY

80 °C) exhibits a peak capacity not only superior to those using methanol and ethanol, but almost 50 % higher than the reference separation using no alkanol additive. Based on the observed negative influence of long-chain and non-polar n-alkanols and the differences between glycerol and propylene glycol I suggest that the polarity of the alkanol additive strongly contributes to the separation system stability.

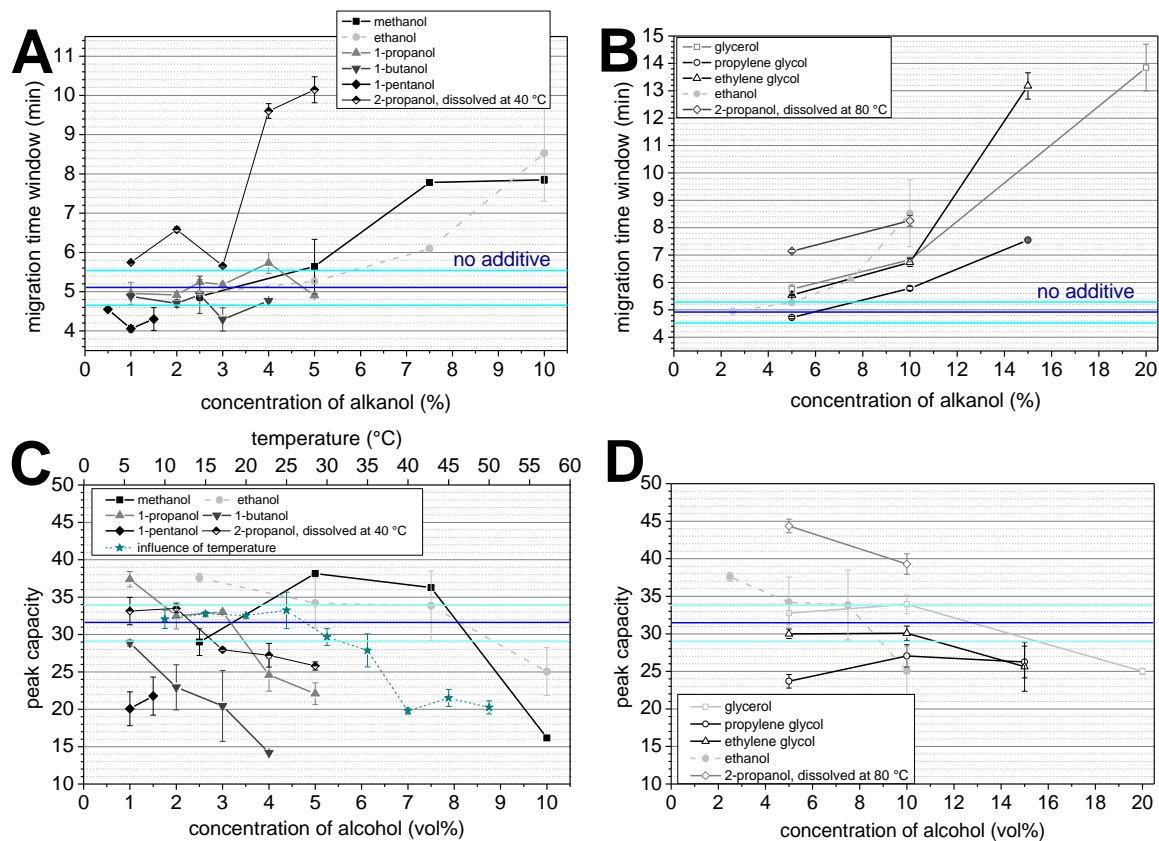


Figure 6: Migration time windows for **A:** Homologous series of n-alkanols from methanol to 1-pentanol and 2-propanol (dissolving PEO at 40 °C). Alkanols with higher carbon content cannot be successfully added at concentrations of 0.5 % or higher. **B:** Migration time windows determined for poly-alkanols with 2 and 3 carbons as well as 2-propanol (dissolving PEO at 80 °C). The influence of the additives and separation temperature on the peak capacity, calculated via Equation (2), is shown for **C:** homologous series of n-alkanols from methanol to 1-pentanol and 2-propanol (dissolving PEO at 40 °C) or **D:** mono- and poly-alkanols with 2 and 3 carbon atoms. ■: methanol, □: glycerol, ●: ethanol, ○: propylene glycol, ▲: 1-propanol, △: ethylene glycol, ▼: 1-butanol, ◆: 1-pentanol, ◇: 2-propanol (dissolving at 40 °C), ◇: 2-propanol (dissolving PEO at 80 °C), ★: temperature. Dark blue and light blue lines indicate the migration time window and peak capacity for measurements without additive and their standard deviation.

2.4.2. Influence of cassette temperature

The influence of temperature on the separation performance was investigated using the separation medium without additives. Increasing temperature led to a decrease in t_{mig} , as can be seen in Figure 2 B. This decrease was found to be parabolic, which is in good accordance with literature⁸⁴. Above 35 °C the formation of gas bubbles occurred visible as spikes in the electropherogram, see Figure 2 B. Measurements above 50 °C were not conducted successfully.

INVESTIGATION OF TEMPERATURE AND ADDITIVE INFLUENCES ON SDS-CE PART 1: A SET OF MODIFICATIONS FOR EITHER FAST OR HIGH RESOLVING SEPARATIONS USING PEO WITH A SINGLE MOLECULAR WEIGHT ONLY

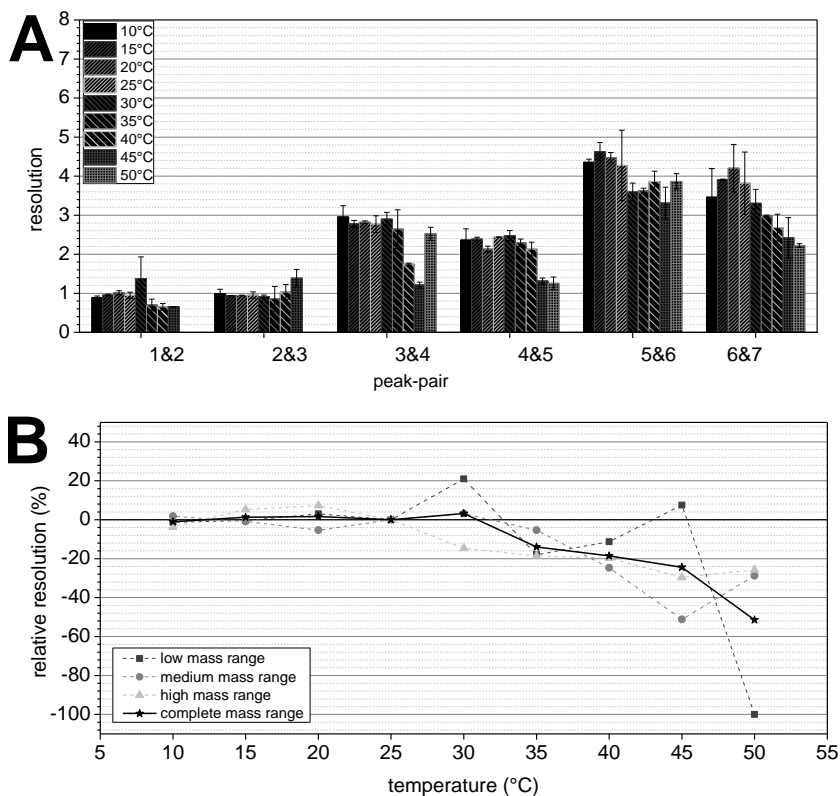


Figure 7: Influence of temperature on resolution. A: Resolution of each peak-pair in measurements conducted at temperatures between 10 and 50 °C, increment 5 °C. B: Relative resolution for the three mass ranges, calculated by comparison with the respective measurements at 25 °C, conducted within the same day.

The resolution values for all peak-pairs at each temperature are displayed in Figure 7 A. For a better understanding $r_{\%}$ is shown in Figure 7 B for all three mass ranges (gray shaded dashed lines). $r_{\%}$ was calculated using the measurement at 25 °C as reference and averaging peak-pair-values for the three mass ranges. Additionally, $r_{\%}$ of the complete mass range was calculated (black solid line). It can be seen that $r_{\%}$ was approx. 0 % for each mass range at temperatures between 10 °C and 30 °C. This indicates that low temperatures do not influence separation performance. However, temperatures of 35 °C and higher gave negative $r_{\%}$ -values for each mass range (except low mass range at 45 °C) and thus decreased separation performance. Only for the low mass range at 30 °C a positive $r_{\%}$ -value with 20 % was observed, but at this temperature a simultaneous decrease in resolution for the separation in the medium, high and complete mass range was present, too.

2.4.3. Variation of the detection aperture

Various detection aperture sizes and their influence on the resolution were investigated. Therefore, pin- and slit-holes were prepared using aluminum foil which was inserted into the manufacturers' capillary alignment interface for UV-detection.

The electropherograms of the measurements at aperture sizes of 14 %, 27 %, 96 % and 100 % ($n = 1$) are presented in Figure 8 A. Differences in t_{mig} are linked to the fact that the measurements were performed with different capillaries and sieving polymer solution. Almost identical electropherograms were obtained for each aperture size.

INVESTIGATION OF TEMPERATURE AND ADDITIVE INFLUENCES ON SDS-CE PART 1: A SET OF MODIFICATIONS FOR EITHER FAST OR HIGH RESOLVING SEPARATIONS USING PEO WITH A SINGLE MOLECULAR WEIGHT ONLY

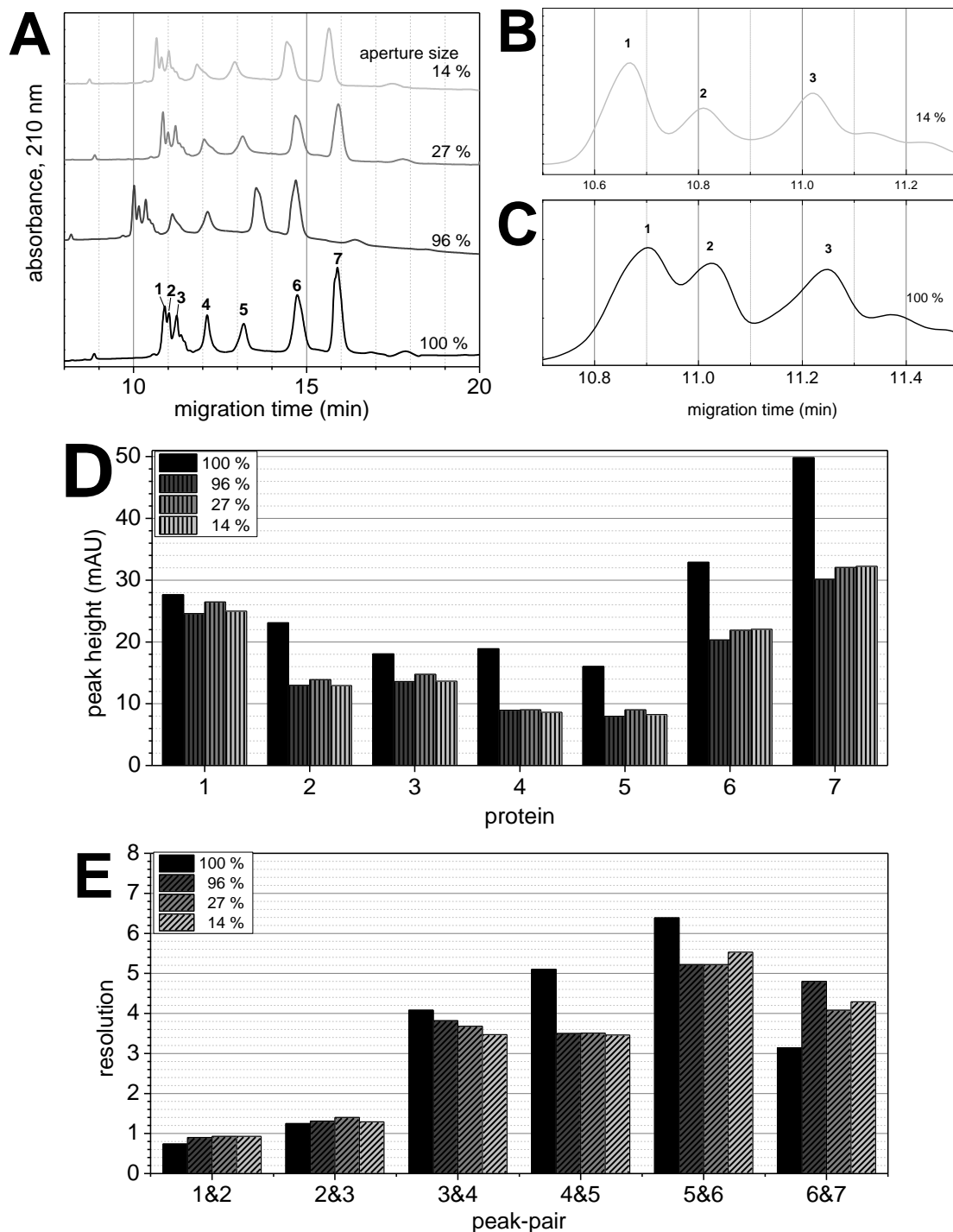


Figure 8: Electropherograms obtained for various aperture sizes. **A:** From top to bottom: electropherograms obtained for 14 %, 27 %, 96 % and 100 % (original size) of manufacturer’s aperture size. **B & C:** Close-ups of the low-mass region for 14 % and 100 % aperture size (offset = 0.2 min). **D:** Peak heights of each protein obtained at different aperture sizes. **E:** Resolution values obtained for the different aperture sizes.

For lysozyme (1), almost no change in peak height is observed with the implementation of a smaller aperture. For all other proteins, a decrease in peak height compared to 100 % aperture size is observed for each aperture modification. It is worth noting, that decreasing the peak aperture below 96 % leads to no further decrease in peak height-values.

Interestingly, for smaller aperture sizes a beneficial increase in resolution is observed only for the lowest mass range (peak-pairs 1&2, 2&3) and the high end of the high mass range (peak-pair 6&7). For all other peak-pairs, a strong decrease in resolution was found. For carbonic anhydrase **4** and BSA **6**, peak broadening seemed to occur, however, in fact, partial resolution of protein isoforms is likely with decreasing aperture size. The most significant changes were observed in the low mass range, as can be seen comparing Figure 8 B with Figure 8 C: Comparing electropherograms for the smallest vs. original aperture size, it can easily be seen, that the separation efficiency increases between the first and the second as well as between the second and the third protein peak with decreasing aperture size. This trend can also be seen by the increasing resolution for these two peak-pairs (1&2 and 2&3) with decreasing aperture size, as presented in Figure 8 E. An increase in resolution was only observed for the low mass range (Pairs 1&2 and 2&3) and the high end of the high mass range (Pair 6&7). For Pairs 3&4, 4&5 and 5&6 a decrease in resolution was observed.

With smaller aperture sizes, light transmission is diminished. The expected strong decrease of peak heights, however, was observed for all proteins except lysozyme (Protein 1) decreasing the aperture from 100 to 96 % (see Figure 8 D). No further decrease in peak height was observed when using smaller detection windows.

Overall, the utilization of a smaller aperture had only a minor effect on the separation efficiency.

2.4.4. Combined influence of temperature and additive at 14 % aperture size

The combined influences of temperature and 2-propanol (chosen as the best additive) at various concentrations on the separation were investigated. All polymer solutions were prepared by heating to 40 °C for 2 h. 2-propanol was added at a concentration range of 0-6.0 % (increment of 1.0 %), the cassette-temperatures was varied between 10-25 °C (5 °C increment). The electropherograms obtained for the measurements at 10 °C and 15 °C with alkanol in the sieving polymer solution were void of protein signals within the first 45 min, results not shown. For the measurements performed at 25 °C and especially at 20 °C and (see Figure 9 A and B), a strong increase in t_{mig} was observed from 0.0 % over 1.0 % to 2.0 % 2-propanol, but a decrease in t_{mig} for 3.0 % 2-propanol. At 25 °C a strong increase in t_{mig} was found at 4.0 % 2-propanol followed by a minor increase at 5.0 % 2-propanol, see Figure 9 A. A similar effect can be assumed for measurements at 20 °C albeit at lower concentration of the additive as no protein signals were observed with 4.0 and 5.0 % 2-propanol within the first 90 min. Peaks width correlated with migration times, peak heights diminished at higher temperature and additive concentration accordingly. In contrast, 2-propanol concentration to up to 15 % did not yield electropherograms containing protein signals within the first 45 min of measurement.

Overall, a slightly increased separation performance compared to the results without additive at 20 °C were found for 2.0 % and 3.0 % 2-propanol concentration.

INVESTIGATION OF TEMPERATURE AND ADDITIVE INFLUENCES ON SDS-CE PART 1: A SET OF MODIFICATIONS FOR EITHER FAST OR HIGH RESOLVING SEPARATIONS USING PEO WITH A SINGLE MOLECULAR WEIGHT ONLY

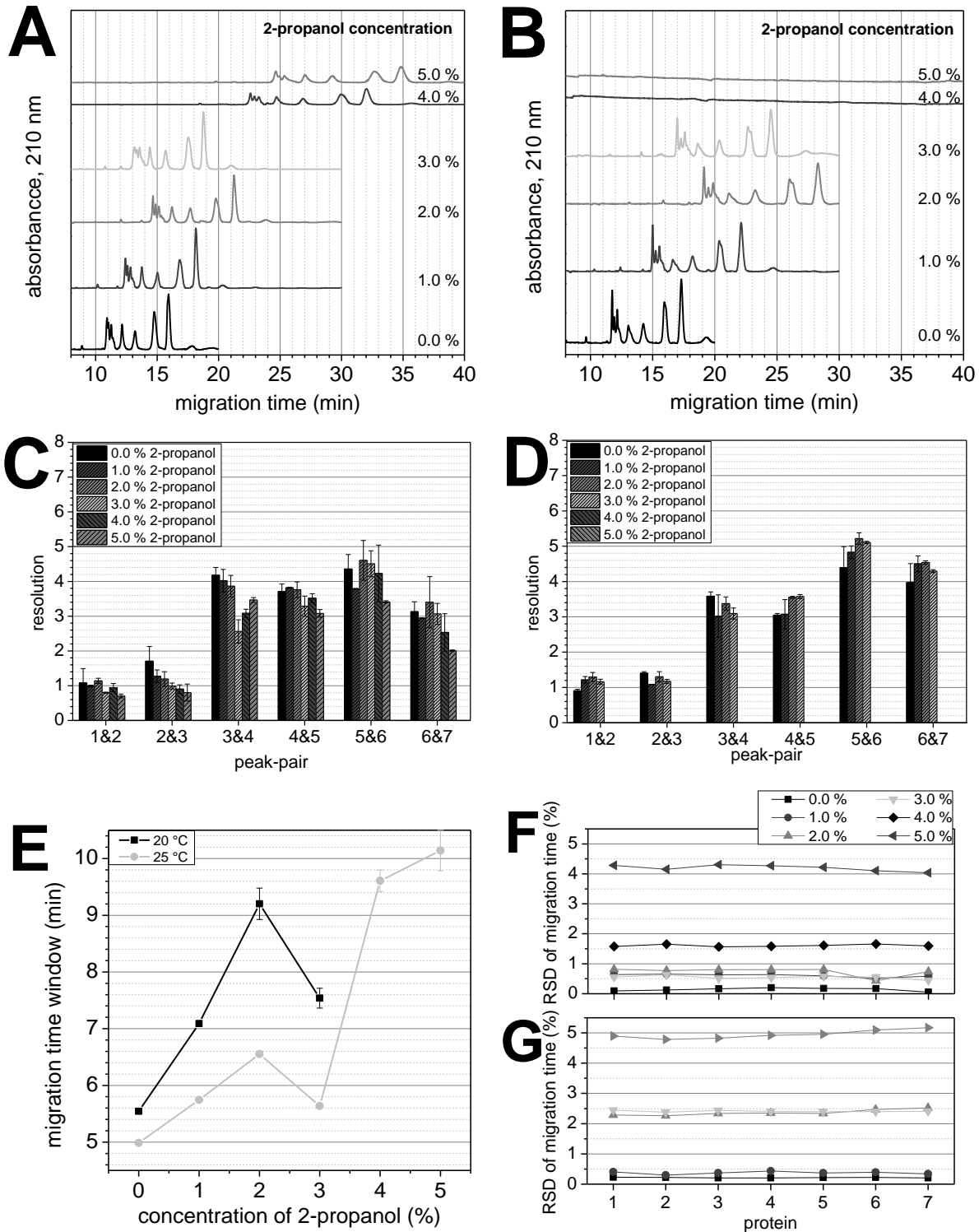


Figure 9: Electropherograms obtained for a separation system with 0.0-5.0 % 2-propanol, an aperture of 14 % and a cassette temperature of A: 25 °C and B: 20 °C. The presented electropherograms are baseline-corrected. Resolutions calculated for the electropherograms presented in A and B. Resolutions calculated for measurements ($n = 3$) at C: 25 °C and D: 20 °C. E: Migration time windows calculated for both temperatures at all 2-propanol concentrations. F, G: Repeatability at various visible by the RDS(t_{mig}) at various 2-propanol concentrations and F: 25 °C and G: 20 °C.

The migration time window (see Figure 9 E) reaches a maximum at 2.0 % 2-propanol in the separation medium for both temperatures. Overall, a high migration time precision was observed (error bars in Figure 9 E and Figure 9 F, G) with slightly better values for measuring at 25 °C.

2.4.5. Aspects of sample injection

2.4.5.1. Short-end injection

By injection of protein at the short end of the capillary, the effective capillary length decreased to a third (from 26.5 cm to 8.5 cm) so that separation times of 5 min were achieved using reversed polarity (see Figure 10 A). To obtain sufficient resolution, it was necessary to reduce the aperture size to 14 %. Injection conditions needed to be optimized (1 - 3 s at -10 kV, see Figure 10 A) to avoid overloading conditions. At higher injection times, peak heights increased but resolution decreased (see Figure 10 C), whereas migration times remained constant. Highest resolution for the medium mass range was visible at 1 s injection times, whereas at 3 s for the high mass range. Finally, an injection time of 3 s was chosen for its best signal to noise ratio, see Figure 10 B.

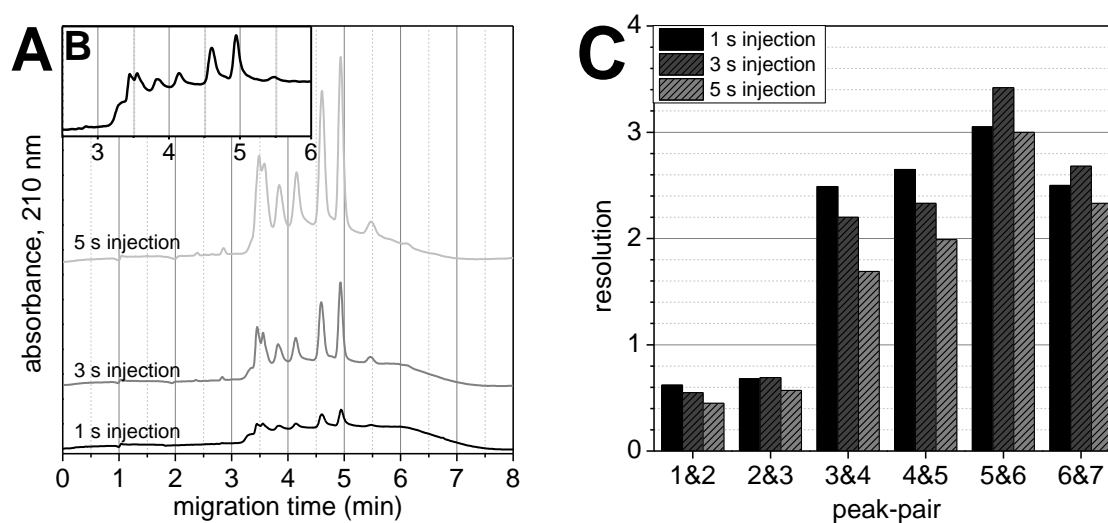


Figure 10: A: Electropherograms obtained for the optimization of injection times (1 s, 3 s and 5 s at -10 kV) using a separation system void of alkanol. B: Close-up of the measurement with injection for 1 s. Electropherograms were not baseline-subtracted. C: Resolution calculated for peak-pairs of adjacent proteins (see Table 3).

2.4.5.2. Relative quantification of protein amounts after electrokinetic injection

All results presented in this section were obtained with a separation system void of alkanols and at a temperature of 25 °C in a capillary with an inner diameter of 50 µm. These experiments were conducted at an early stage of research, when the beneficial impact of higher diameters (faster rinsing procedures and better LOD) to enhance resolution had not yet been found. Therefore, these measurements were conducted using capillaries with 50 µm instead of 100 µm in diameter. In order to determine the influence of sample constituents, I diluted the sample with the denatured proteins 1 and 4-7 ($c = 16.0\text{-}17.2 \mu\text{mol/L}$, see Section 2.3.4) with either BGE void of polymer (100 mmol/L Tris-CHES, 0.1 % SDS at pH 8.9) or with water at ratios of 1:2; 1:4; 1:8; 1:10; 1:16 and 1:20 ($n = 3$) prior to electrokinetic injection at the inlet at -10 kV and 5 s. Baseline-separation of all protein signals was reached. The LOD was estimated to be little below 1 µmol/L. The only differences in the resulting electropherograms taken in 50 v. 100 µm capillaries were a higher background and smaller peak areas. Considering Lambert-Beer's Law I propose LODs below 500 nmol/L when using capillaries with 100 µm in diameter.

An almost linear correlation of peak area vs. protein concentration was obtained in the range of 1.6 – 16.0 µmol/L (dilution ratio 1:10 – 1:1) for the dilution with BGE (Figure 11 A and B). When sample was diluted with water, a steep increase of peak area at low protein concentration was

INVESTIGATION OF TEMPERATURE AND ADDITIVE INFLUENCES ON SDS-CE PART 1: A SET OF MODIFICATIONS FOR EITHER FAST OR HIGH RESOLVING SEPARATIONS USING PEO WITH A SINGLE MOLECULAR WEIGHT ONLY

observed, which was followed by a plateau indicating diffusion-limited injection conditions. Constant peak area ratios (calculated by dividing the peak area of a protein signal by the sum of all protein peak areas) were found over the whole concentration range investigated, which proves that relative protein concentrations are well accessible.

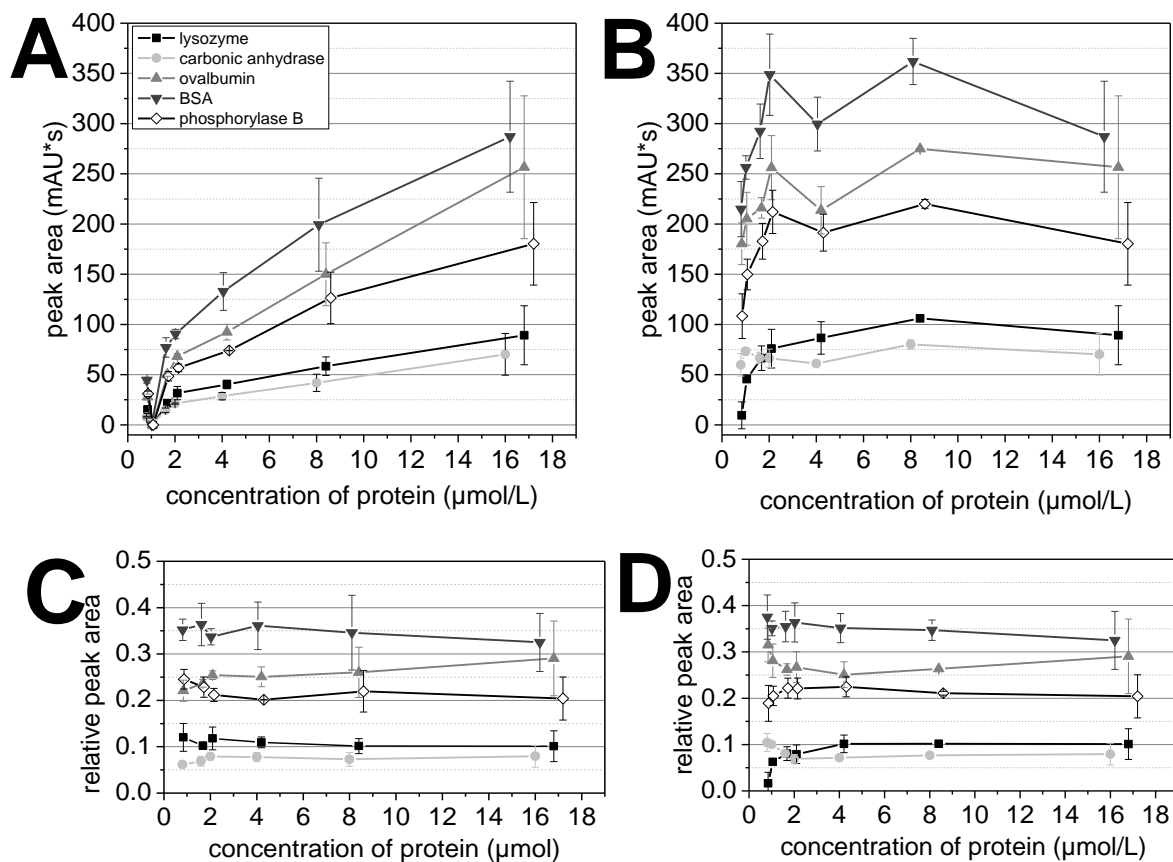


Figure 11: Peak areas (A & B) and relative peak areas (C & D) obtained from various electropherograms after electrokinetic injection for 5 s at -10 kV for samples with proteins 1 and 4-7. The protein concentrations were obtained by diluting the original sample (see Section 2.3.4) with A & C: 100 mM Tris-CHES, 0.1 % SDS at pH 8.9, no polymer or B & D: water. C & D: Relative peak areas were calculated for each protein by dividing the respective peak area with the sum of all protein peak areas in the electropherograms.

2.4.5.3. Relevance of polymer in BGE vial and enrichment-plugs on the separation performance

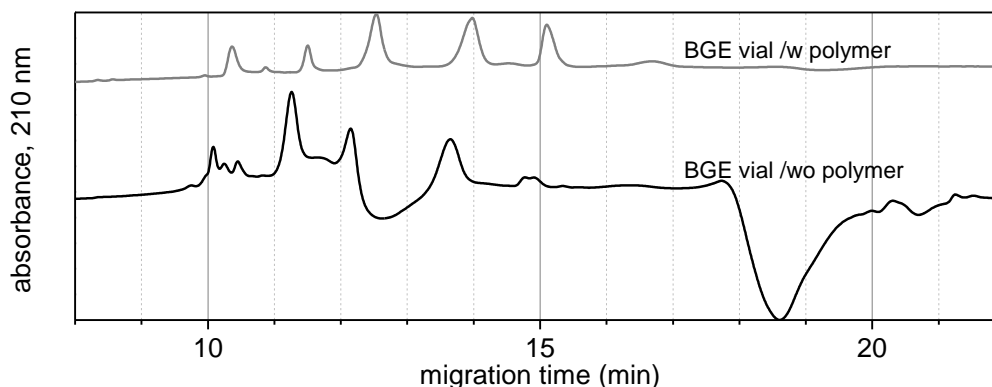


Figure 12: Electropherograms obtained for measurements of samples dissolved in BGE. BGE vials with and without 2.0 % PEO polymer were used during separation. Separation conditions are described in Section 2.3.3, electrokinetic injection of sample (bottom: the 7 proteins described in Section 2.3.4, top: protein sample void of myoglobin and β -lactoglobulin) was conducted for 5 s at -10 kV. Sample

In SDS-PAGE, stacking gels are used to enhance separation efficiency. For SDS-CE, I tested the influence of polymer present in the BGE solution during voltage application using a separation medium without alcohol additive at a temperature of 25 °C. It can be seen, that for the measurement without polymer in the BGE vial negative system peaks occur at 12-13 min and 18-19 min. Especially the first is detrimental for the identification of protein signals. The necessity of polymer in the BGE inside the capillary is obvious.

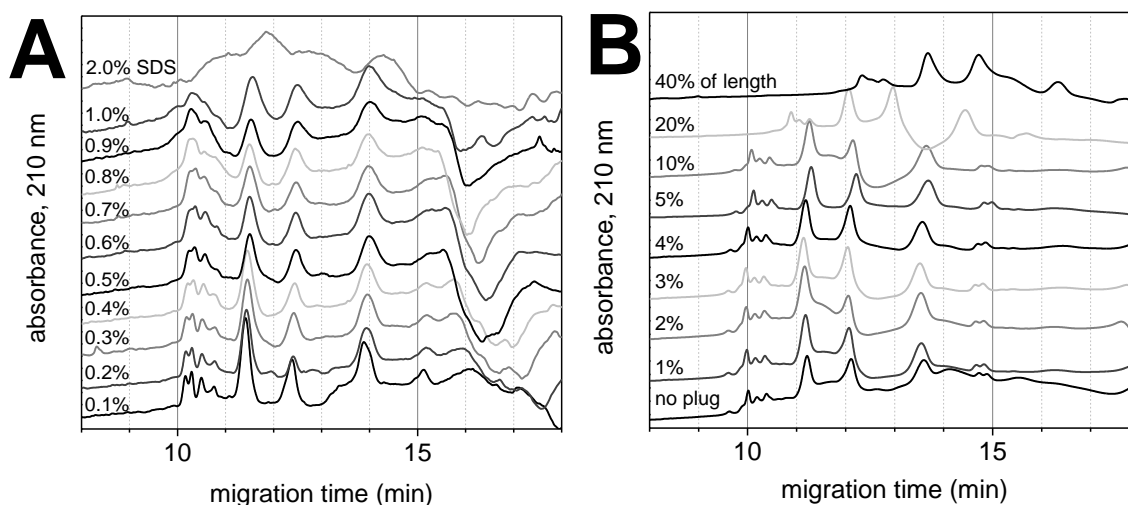


Figure 13: A: Electropherograms obtained for different concentrations of SDS in an enrichment-plug with a length of 5 % of the capillary length. B: Electropherograms obtained using various plug lengths at a fixed SDS-concentration of 0.1 %. All electropherograms were not baseline-corrected for better presentation of detrimental effects on the baseline.

For CE, enrichment plugs of low conductivity/high electric field strength are commonly injected prior to electrokinetic injection of the sample to avoid enrichment of ions directly at the capillary inlet, which hinders further injection^{85, 86}. For SDS-CE I tested if an aqueous enrichment-plug at the capillary inlet injected hydrodynamically, is advantageous regarding separation efficiency, resolution and limit of detection by evoking peak sharpening. To ensure sufficient conductivity and to avoid disaggregation of SDS-protein-agglomerates, SDS was added at low concentrations. Plug

lengths were estimated by consecutive rinsing experiments recording the time necessary to reach the detector. The SDS-concentration in the enrichment plug was varied while keeping the plug length fixed at approx. 5 % of the capillary length. Figure 13 A shows that with increasing SDS-concentration, increasing peak widths and thus decreasing separation performances are induced. For SDS-concentrations above 0.8 % no separation of proteins in the small mass range (Proteins **1 – 3**) was obtained, at a concentration of 2.0 %, electropherograms were void of protein signals within 20 min. For an SDS-concentration of 0.1 % narrowest peaks and thus best separation performance for each protein signal were observed.

For the investigation of different plug lengths, a fixed SDS-concentration of 0.1 % was chosen. As visible from Figure 13 B, plug lengths below 10 % of the capillary length do not alter t_{mig} of proteins. With a plug filling 20 % (40 %) of the capillary, t_{mig} of proteins shift to higher values by approx. 1 min (2 min), accompanied by peak broadening and deleterious effects on the baseline. Additionally, a positive (negative) system peak at 11.5 min (between 12.5 and 13.5 min) occurred, except when using a plug length of 5 %.

In summary, best separation performance and lowest baseline disturbance were observed for a separation system using polymer in the BGE and a separation plug filling 5 % of the capillary (1.75 mm) with a concentration of 0.1 % SDS. Compared to the system without plug, only minor improvements were found.

2.5. Discussion

2.5.1. The influence of alkanols and temperature on the separation

In summary, all poly-alkanols except propylene glycol provide increased separation performance (higher resolution, peak capacity and migration time window) for the low and medium mass range when added at low to intermediate concentration. For the high mass range, detrimental effects are observed for all alkanol additives except for 1- and 2-propanol (dissolving PEO at 40 °C and 80 °C), where resolution was positively affected. Polar alkanols, such as methanol and ethanol, reveal best separation performances for the low mass range at 5.0 % and 7.5 % alkanol concentration. For the medium and high mass range, a slight decrease in separation performance was often observed, in rare cases, separation efficiency and resolution increased (e.g. for 2-propanol, dissolved at 80 °C and 1-propanol at 4 % only). For non-polar alkanols with C4 to C7, no clear trends in resolution changes were observed. They can only be added at low concentration, especially when their $\log(P_{ow})$ -values are high. Overall, the addition of non-polar alkanols to the separation medium in SDS-CE is not advisable.

In contrast, of all additives tested, branched 2-propanol (dissolving PEO at 80 °C) was found to stand out due to its strong positive effects on resolution over the whole mass-range at both investigated concentrations. The small differences in $\log(P_{ow})$ between 1-propanol and 2-propanol indicate that this influence is mainly related to the branched structure of 2-propanol rather than to its polarity. Furthermore, similar $RSD(t_{mig})$ -values for all proteins in one run series (see Section 0) indicate a stable sieving medium and a homogeneous separation mechanism over the whole separation path.

Overall, stable separation conditions were achieved for each alkanol except for the non-polar butanol and pentanol with high $\log(P_{ow})$ -values, yet again proving them to be unsuitable as additives for SDS-CE. Polar poly-alkanols (ethylene glycol, propylene glycol and glycerol) had a beneficial impact on the separation stability, unlike the small alkanols methanol, ethanol, 1-propanol and 2-propanol. All of them showed a higher migration time reproducibility, indicating a more stable sieving mechanism. I thereby propose the general addition of small amounts of methanol, ethanol, 1- or 2-propanol to PEO-based SDS-CE systems to increase migration time precision.

2-propanol was outstanding with regard to the improvement of resolution, especially for protein micro-heterogeneity. The mechanistic aspects underlying these effects, will be discussed thoroughly in Chapter 3. In short, I presume that they are related to its branched structure and low polarity. Both properties seem to promote the interaction with PEO without perturbing SDS-protein-interaction. I expect 2-propanol to change the pore structure of the PEO network to induce larger pores⁸⁷. This changes SDS-protein-agglomerate-sieving without leading to partial degradation of SDS-protein-agglomerates due to their interaction with alkanols which would result in peak-broadening.

High temperatures, which lead to decreased separation performance and lowered repeatability due to formation of gas bubbles above 35 °C. Resolution increased at temperatures below the common 25 °C, however, the effect is significantly lower than the influence of organic solvent additives. In addition, lower migration time precision was observed frequently at elevated separation temperature. Especially when SDS-CE measurements are conducted during summer, temperatures of 20 °C cannot be reached by the CE instrument in a laboratory without air conditioning. Overall, from all results I prefer measurements at temperatures between 25 °C and 30 °C.

Measurements combining 2-propanol (dissolving PEO at 40 °C) additive and elevated temperature (20 °C instead of 25 °C) showed a decrease in separation performance, so obviously no synergistic effects could be reached.

2.5.2. Influence of detection and injections parameters on the separation

In order to obtain stacking conditions and enhance separation efficiency as well as loadability, I tested different injection protocols. However, the injection of enrichment plugs of low conductivity yielded separations with undesirable background and system peaks (see Section 2.4.5.3). The desired sharpening of peaks, as observed for stacking-gels in SDS-PAGE or in polymer-free CE^{85, 88, 89}, was not observed. It is worth noting that similar observations were made when the protein sample was injected hydrodynamically (data not shown). When adding sieving polymer to the injection plug *and* to the sample supported electrokinetic injection, no system peaks^{90, 91} were present anymore. Similar observations demonstrated the necessity to have sieving polymer in the BGE vials during separation (see Section 2.4.5.3). Interestingly, reproducibility of measurements was not impaired by any of these measures. However, the presence of sieving polymer in sample or BGE vials necessitated daily cleaning of electrodes and pre-punchers. The gain in separation performance was negligible, I therefore advise neither an enrichment plug nor BGE void of polymer.

The use of a smaller detection window (smaller aperture) resulted in a minor increase in resolution for the “normal-end”-injection for the 3 smallest proteins. In addition, peak heights were lower, though the influence was small given the fact that lateral peak widths are smaller than the detection window of 2 mm length (I estimate 300 µm peak widths). In contrast, the reduction of the aperture was vital for short end-injection. Here, the 3-times shorter separation path lead to high separation efficiencies, but also co-migration. Only with the reduced detection window with its increased lateral resolution, protein identification and thus quantification can be reached, which is in good accordance with the work of Mack *et al.*⁹².

For QC of monoclonal antibodies and wheat proteins, quantification relative to either a main peak or relative to an internal standard is often done^{35, 93, 94}. I prove that relative quantification in aqueous samples or samples diluted with separation medium without PEO is possible in a concentration range of at least 0.16 µmol/L – 16 µmol/L and for all proteins except carbonic anhydrase (1.6 µmol/L as lower limit).

In my work, I prefer dilution of samples with BGE to prevent dissociation of SDS-protein-agglomerates. Another, more universal problem, is the lack of convection, e.g. by stirring in the sample vial during electrokinetical injection, leading to depletion of analyte in proximity to the capillary inlet and formation of a Stern-layer⁹⁵⁻⁹⁷.

2.6. Conclusion and outlook

I here demonstrate that PEO-based sieving matrices with self-coating properties based on commercially available PEO⁵¹ are interesting for SDS-CE separations. I am aware, that better separation performances and LODs are achieved by LIF-detection^{51, 69}, the presented LOD of 160 nmol/L will thereby be easily surpassed. I showed, that 2-propanol as an additive in SDS-CE separations evokes a better separation performance, when the PEO is dissolved at 80 °C. The impact of enrichment plugs was rather disappointing and often worsened the separation and induced massive background disturbances, which I conclude to stem from heterogeneous distribution or composition of the separation medium during separation possibly due to dynamic

local changes of SDS concentration. The addition of different alcohols can improve the separation in different mass ranges, e.g. 1-propanol at 4.0 % and 2-propanol (dissolved at 80 °C) are well suited to enhance resolution of high molecular mass proteins, whereas small alkanols ethanol, 2-propanol (dissolving at both temperatures) and 1-propanol improve resolution for small proteins. The underlying mechanistical aspects that lead to this superior separation performance will be discussed in Chapter 3. Alcohol additives can thus be used for a fine-tuning of the separation, whose run times can nevertheless be kept below 20 min. This is an advantage compared to fixed commercially available kit systems. The high repeatability within measurements and the knowledge of buffer components (which is not given for commercially available kits) will hopefully have tremendous impact on the further optimization and development also of 2-dimensional-CE setups^{98, 99}.

Short-end-injection combined with a miniaturized detection window provides an interesting experimental setup to give rise to a fast screening method below 5 min run time. Overall, with the same basic separation medium, fast (short-end-injection), moderately fast (separation medium void of alcohol additive) or slow analysis (addition of 2-propanol) is applicable, strongly differing in the resolution obtained.

3. Investigation of temperature and additive on SDS-CE part 2: mechanistic investigation of the influence of alkanols and temperature on the sieving mechanism via interaction with SDS-protein-agglomerates and sieving polymer

3.1. Abstract

In the previous chapter I reported the beneficial impact of alkanols on the separation of proteins in SDS-CE, especially when using 2-propanol as additive in polyethylene oxide sieving matrix. In this study, the focus is set on the mechanistic interpretation of the results. To this end I investigate the dependence of migration times on protein molecular mass to understand which sieving mechanism is present for different separation media. Further parameters considered are separation efficiency, resolution and migration time repeatability. I show that it is possible to manipulate SDS-protein-agglomerates and SDS-PEO-interaction by the addition of different alkanols. From my results, the alkanols employed are classified into micelle-penetrating linear mono-alkanols (homologous series of methanol to heptanol as well as 1-propanol) and non-penetrating poly-alkanols (2-propanol as well as C2 and C3 poly-alkanols ethylene glycol, propylene glycol and glycerol).

I discuss two dominant mechanisms in the manipulation of size sieving. Mechanism 1: Alkanol-PEO-interaction increases the mesh-size of the sieving polymer (beneficial for Ogston-sieving) with increasing additive concentration, and Mechanism 2: alkanol-SDS-protein-agglomerate-interaction, which increases the diameter of SDS-protein-agglomerates (beneficial for Reptation-sieving) with increasing alkanol concentration. The change between the sieving mechanism upon addition of alkanols and changes of the separation temperature provides a deeper insight into the separation effects in entangled polymer sieving electrophoresis.

3.2. Introduction and motivation

The sieving mechanism behind both electrophoretic gel and entangled polymer sieving is linked to differences in the hydrodynamic radius of the SDS-protein-agglomerates and the mesh-size of the polymer network. Thus, for optimal separation results, both parameters must be controlled to alter the sieving mechanism between Ogston-sieving (larger or equally sized mesh size diameter compared to analyte diameter) and Reptation-sieving (smaller mesh size diameter than analyte diameter)¹⁰⁰⁻¹⁰⁸. The correlation between the logarithm of the electrophoretic mobility (μ) of a protein and its molecular mass (M_r) is $\log(\mu) \sim M_r^{-1}$ and $\log(\mu) \sim -\log(M_r)$ for Ogston- and for Reptation-sieving, respectively. Better resolving power in the low (high) mass range is obtained for Ogston-sieving (reptation-sieving). A distinction between both mechanisms can be found using appropriate linearization^{100, 104, 105}.

In classical SDS-PAGE the mesh-size in the gel is easily adapted to the analytical question by altering the amount of monomer and crosslinker as well as starting radical¹⁰⁹⁻¹¹² whilst keeping the SDS-protein-agglomerates at a constant size. Methods that alter the diameter of the SDS-protein-agglomerates were reported, e.g. by the addition of ethylene glycol, glycerol or n-alkanols^{113, 114}. Modification of micellar structures in capillary based methods is used for separation optimization in micellar electrokinetic chromatography¹¹⁵⁻¹¹⁷.

In SDS-CE, polymers are used as a sieving matrix and sieving occurs on highly dynamic entangled polymer networks. The polymer chain-length and/or its concentration¹¹⁸ is commonly changed to manipulate the polymer mesh size in SDS-CE. Another approach for method optimization is the addition of additives, e.g. ethylene glycol and glycerol^{75, 119}, alkanols¹²⁰ or acetonitrile¹²¹, but from the published empirical studies, no understanding of the underlying effects was gained. The group of Sumitomo *et al.*⁸⁷ studied mesh-sizes of entangled polymer solutions applied in SDS-CE separation via dynamic light scattering. They investigated PEO and other polymers of different chain lengths and concentrations. Based on their and my results as well as studies by Rösch *et al.*¹²²⁻¹²⁴, who thoroughly described the structure of PEO in crystalline form as well as in aqueous solution, I can understand why only 2-propanol gives such outstanding separation performance in SDS-CE and why this is only achieved when the sieving polymer is dissolved in the background electrolyte (BGE) at an elevated temperature of 80 °C.

My conclusion is, that PEO-alkanol-interaction (Mechanism 1) favors Ogston-sieving whereas SDS-alkanol-interaction (Mechanism 2) favors Reptation-sieving. Both can be controlled via the heating-temperature during dissolution of polymer, since Mechanism 1 is thermodynamically more favorable. I will demonstrate, that alkanol-PEO-interaction is beneficial over alkanol-SDS-interaction and that the sieving-mechanism can be effectively manipulated for optimal separation results.

3.3. Materials and methods

3.3.1. Chemicals

Lysozyme (chicken egg white, $M_r = 14.4$ kDa, **1**), myoglobin (equine heart, $M_r = 16.951$ kDa, **2**), β -lactoglobulin (bovine milk, $M_r = 18.4$ kDa, **3**), carbonic anhydrase (bovine erythrocytes, $M_r = 29$ kDa, **4**), ovalbumin (chicken egg white, $M_r = 42.8$ kDa, **5**), bovine serum albumin (BSA, bovine serum, $M_r = 66.463$ kDa, **6**), phosphorylase B (rabbit muscle, $M_r = 97.412$ kDa, **7**), sodium dodecyl sulfate (SDS, 98,5 %), methanol (HPLC grade), ethanol (reagent grade), isopropanol (LC-MS grade), n-butanol (reagent grade), n-pentanol (reagent grade), polyethylene oxide ($M_r = 600$ kDa) were purchased from Sigma-Aldrich (Steinheim, Germany). 1-propanol (reagent grade) was purchased from BASF SE (Ludwigshafen, Germany). Tris(hydroxymethyl)aminomethane (Tris), 1-hexanol (reagent grade), 1-heptanol (reagent grade), sodium hydroxide solution (NaOH, 30%, suprapur), 2-mercaptoethanol (≥ 99.9 %), were delivered by Merck (Darmstadt, Germany). 1-Butanol (reagent grade) and hydrochloric acid (HCl, 32 %, analytical grade) were purchased from VWR (Darmstadt, Germany). *N*-Cyclohexyltaurine (CHES) was obtained from Alfa Aesar (Karlsruhe, Germany). Deionized water was prepared using an ELGA-Veolia PURELAB Classic system (Celle, Germany).

3.3.2. Buffer and sieving polymer solution preparation

Background electrolyte (BGE) solutions contained 100 mmol/L Tris-CHES, 0.1 % SDS, as well as additives. BGEs were used no longer than 5 days after preparation. Sieving solutions containing polymer were prepared by the following standard procedure: 20 mg (equals 2.0 %) PEO was dissolved in 1 mL BGE in a sealed vial at 40 °C while stirring for 2 h. For polymer sieving solutions with BGEs containing poly-alkanols, heating to 80 °C was chosen, see Table 1 for further details. For 2-propanol, both temperatures were investigated. Therefore, the basic separation medium for SDS-CE utilized 2.0 % PEO, 100 mmol/L Tris-CHES and 0.1 % (3.5 mmol/L) SDS at pH 8.9. Protein stock solutions were dissolved separately in 30 mmol/L aqueous ammonium acetate, pH 6.8 at a concentration of 10 g/L (1 %) and stored at -20 °C. No degradation upon storage was visible via SDS-CE experiments.

3.3.3. Instrumentation and separation parameters

CE- and MS-parameters are described in Chapter 2.

3.3.4. Sample preparation

Sample preparation was already described in Chapter 2. In brief, a protein stock solution with a total protein concentration of 10.0 g/L (lysozyme, myoglobin, β -lactoglobulin, carbonic anhydrase, ovalbumin, BSA, phosphorylase B in a ratio of 1:1:1:2:3:4.5:7) was used. The sample injection solution for SDS-CE was prepared by mixing 78.0 μ L of this protein mixture with 109.8 μ L of a solution containing 1.0 % SDS, 5.0 % 2-mercaptoethanol and 100 mmol/L Tris-CHES at pH 8.9 to obtain an SDS:protein ratio of 1.4. The final overall protein concentration was 4.15 g/L, which equals a concentration of 11.6-15.3 nmol/L for each protein. This sample injection solution was incubated at 100 °C for 15 min. Aliquots of approx. 20 μ L were stored at -20 °C until use.

3.3.5. Data processing

Data processing was described in Chapter 2.

3.4. Results

3.4.1. Intermediate precision

Repeatability of migration times was investigated for each protein at each investigated temperature and alkanol concentration using three consecutive runs.

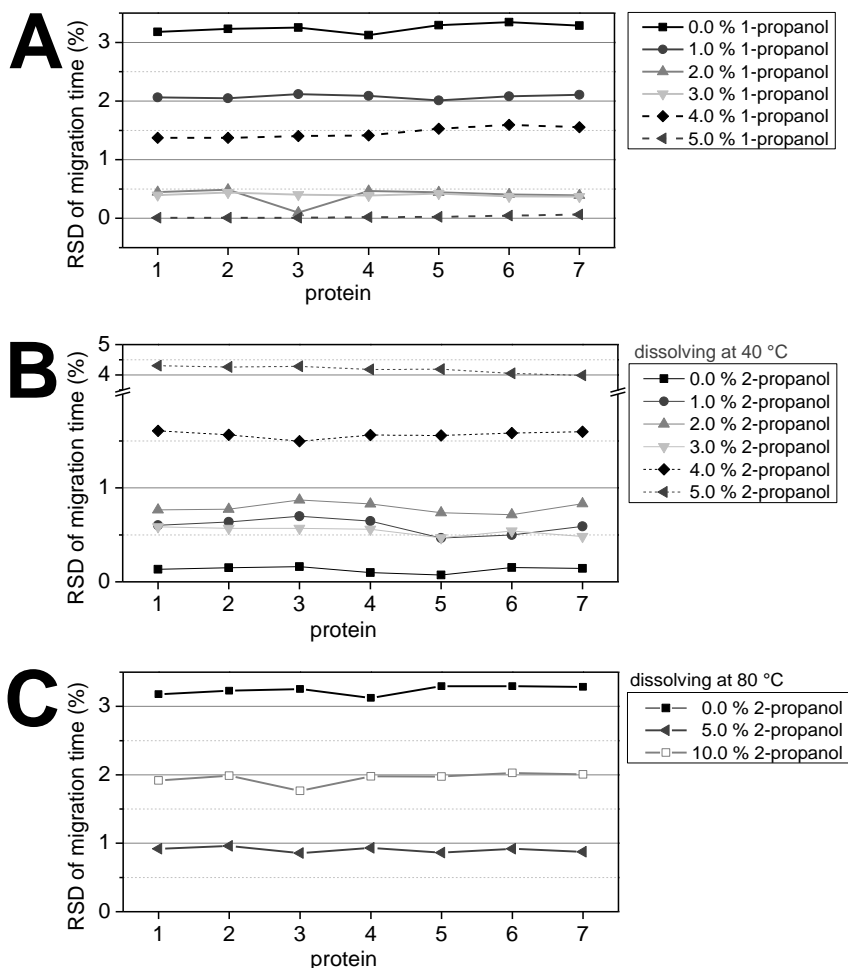


Figure 14: Standard deviations of migration time obtained by averaging 3 measurements each for A: 1-propanol, B: 2-propanol, dissolving of PEO at 40 °C and C: 2-propanol, dissolving of PEO at 80 °C. ■: 0.0 % alkanol, ●: 1.0 % alkanol, ▲: 2.0 % alkanol, ▼: 3.0 % alkanol, ◆: 4.0 % alkanol, ◄: 5.0 % alkanol, □: 10.0 % alkanol.

RSD(t_{mig})-values calculated for 1- and 2-propanol (dissolving PEO at 40 °C or 80 °C) added at different concentrations to the separation medium are exemplarily displayed in Figure 14 A - C. Clearly, the addition of alkanol decreases repeatability regardless of the concentration level. Furthermore, for almost all separation media tested, similar RSD(t_{mig})-values were observed for all proteins. This indicates a high inter-run stability of the separation mechanism, only minor run-to-run changes in μ_{EOF} may be present. It can be expected that the separation media and thus the sieving mechanism are stable. This was the case for almost each investigated separation system.

To decrease the amount of data, averaged RSD(t_{mig})-values for all proteins were calculated and are presented in Figure 15. For all organic solvents investigated see Chapter 2. Error bars derive from differences in migration time precision of different proteins. The data visualize the stability of the

separation medium and consistency of the sieving mechanism: high error bars indicate poor reproducibility of the sieving mechanism. Smaller averaged $RSD(t_{mig})$ -values in the presence of additive were always observed except for: 5 % methanol, 10.0 % ethanol, 15.0 % ethylene glycol and 20.0 % glycerol (see Figure 15). Largest error bars and thus lowest homogeneity of the sieving mechanism along the separation path were observed for nonpolar 1-butanol at 3.0 % and 4.0 %, for 1-pentanol at 0.5 % and 1.5 %, ethanol at 10 % as well as for ethylene glycol at 15.0 %. Lowest error bars were obtained for separation systems utilizing 0-7.5 % ethanol, as well as 1-propanol and 2-propanol (dissolving PEO at 40 °C or 80 °C) at every investigated concentration. It is worth mentioning, that neither the most polar nor the least polar alkanols offered best stability in sieving mechanism.

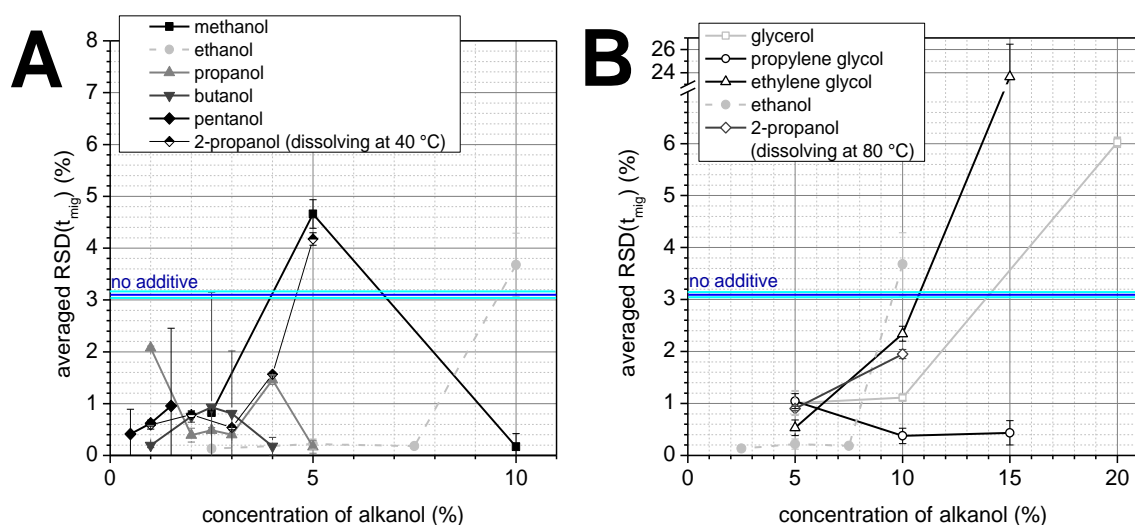


Figure 15: Averaged standard deviations in migration times versus concentration of alkanol. A: Homologous series of n-alkanols from methanol to 1-pentanol. Alkanols with higher carbon content were not successfully deployed at concentrations of 0.5 % or higher. B: Mono- and poly-alkanols with 2 and 3 carbons. Dark blue and light blue lines indicate the $SDV(t_{mig})$ for measurements without additive and their error bars, respectively. ■: methanol, □: glycerol, ●: ethanol, ○: propylene glycol, ▲: 1-propanol, △: ethylene glycol, ▼: 1-butanol, ◆: 1-pentanol, ◇: 2-propanol (dissolving PEO at 40 °C), ◇: 2-propanol (dissolving PEO at 80 °C).

3.4.2. Separation performance – Linearity of the mass scale

In SDS-CE, the migration order is determined by the molecular mass of the protein analytes with the lightest proteins migrating first. In literature, plots of the logarithmic molecular mass of proteins ($\log(M_r)$) versus t_{mig} are commonly displayed. A linear relationship is expected but never truly achieved. In Figure 16 A and Figure 16 C, these plots are shown for measurements in the sieving matrix upon addition of 1-propanol (0.0 – 5.0 %) and 2-propanol (dissolving PEO at 80 °C, 0.0 – 10.0 %).

Clearly, strong changes in the slope (m) are observed between measurements with different additive and different additive concentration. m exhibits a reciprocal correlation to the migration time window. Especially for measurements with long migration times, strong deviations from linearity are evident in low correlation coefficients and high residuals of the linear regression as displayed in Figure 16 B for a measurement without alkanol. The residuals for the lightest and heaviest proteins, lysozyme ($M_r = 14.4$ kDa) and phosphorylase B ($M_r = 97.4$ kDa), are both negative. For the medium mass range, which includes carbonic anhydrase ($M_r = 29.0$ kDa) and

ovalbumin ($M_r = 42.8$ kDa), strongly positive residuals were obtained. In contrast, myoglobin ($M_r = 17.7$ kDa), β -lactoglobulin ($M_r = 18.4$ kDa) and BSA ($M_r = 66.5$ kDa) have small residuals. Comparable results were obtained for every investigated alkanol and temperature. Contemplating the scattering of data points in the residual plot in Figure 16 B as well as in the linearization plots in Figure 16 A and Figure 16 C, a higher order regression seems conceivable for better mass determination. In Figure 16 D, a linear mass determination using solely the heaviest four proteins is shown. Here, a strongly linear behavior ($R^2 = 1.000$) is observed. It becomes obvious, that medium and high mass range proteins are separated by a different mechanism than proteins of low mass.

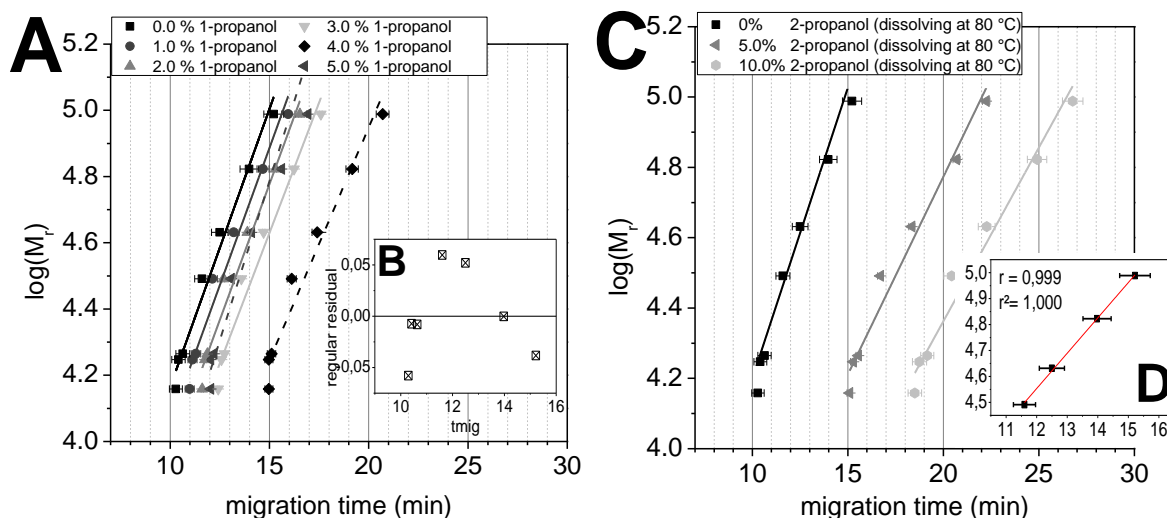


Figure 16: Linearization of the dependence of molecular mass of the protein analyte from the migration time via plotting the logarithm of molecular mass of proteins versus migration time. Measurements conducted in the separation medium (see Section 3.3.2) with addition of alkanol at various concentration. A: 1-propanol and C: 2-propanol (dissolved at 80 °C), based on the measurements shown in Figure 3 in Chapter 2. Standard deviations derive from t_{mig} errors and are indicated by the error-bars. B: The insert shows the residues of the linearization determined for a measurement without additive (0.0 % 1-propanol) presented in A. D: Linearization for a measurement without additive (0.0 % 2-propanol) by taking only the heaviest 4 proteins into account ($R^2 = 1.000$).

3.4.3. Ogston- and Reptation-sieving

Linearization according to Ogston- and Reptation-sieving is presented in Figure 17. For Ogston-sieving, well-suited for the description of the separation mechanism for small proteins, linearization was calculated via the electrophoretic mobilities of the lightest proteins **1-3**, see Figure 17 A. For Reptation-sieving, the two heaviest proteins **6** and **7** were considered, see Figure 17 B and C. It can easily be seen, that for Ogston-sieving the proteins of the high mass range deviate strongly from the linear behavior, for Reptation-sieving highest deviation is found for the low mass range. Strong changes in residuals were found when alkanols were added to the sieving medium, but only minor changes when changing the temperature, results not shown.

For a quantitative description the change in residuals from linearization was calculated for both Ogston- (O) and Reptation- (R) sieving for all proteins at each measurement condition. Exemplarily, Equation (1) shows the calculation for Ogston sieving. $RLO_{x,i}$ presents the residual in linearization of Ogston-sieving for protein i obtained for measurement condition x , e.g. $RLO_{0\% 25^\circ C, 6}$ represents the residual for Protein 6 in a measurement conducted without additive at 25 °C.

$$dRLO_{\%} = \frac{RLO_{x,i} - RLO_{0\% 25^{\circ}C, i}}{RLO_{0\%,i}} \cdot 100 \% \quad (3)$$

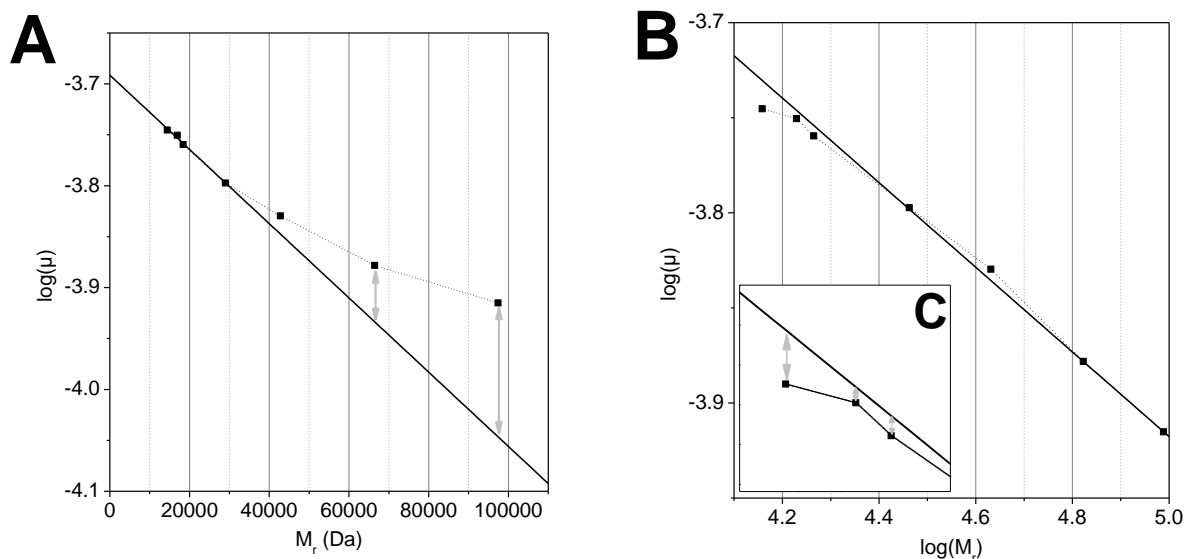


Figure 17: Linearization of a measurement void of alkanols, plotted according to the mechanism of **A:** Ogston- and **B:** Reptation-sieving. **C:** Close-up of the small mass range presented in B. The gray arrows indicate the residuals calculated as the deviation from linear regression and were taken into account for the calculation of the relative change in residuals presented in Figure 18 A & B for alkanol addition and in Figure 19 A & B for various temperatures.

Results are presented in Figure 18 for changes in alkanol content and in Figure 19 for varying temperatures. For Ogston-sieving, the values for Proteins 6 and 7 were averaged, for Reptation-sieving, for Proteins 1-3. Thus, positive values indicate an increase in residuals and thus a larger deviation from linearity. This means that the sieving mechanism underlying the linearization is less suited to describe the separation process.

As can be seen in Figure 18 A, negative values were obtained for $dRLO_{\%}$ for the large Proteins 6 and 7 when alkanols are added to the separation medium. Thus, at higher alkanol concentration, Ogston-sieving should preferably be used to describe the separation mechanism. Lowest values were not found for 2-propanol (dissolving at 80 °C), which comes as a surprise, considering that it proved superior regarding separation performance, see Chapter 2.

For Reptation-sieving, values comprise a broader range from -3000 % to 1000 % indicating strong effects on the separation mechanism upon alkanol addition. Polar ethylene and propylene glycol gave positive values and thus a shift away from Reptation-sieving and towards Ogston-sieving for Proteins 1-3. For glycerol, no change was observed. The addition of non-polar 1-pentanol and 1-butanol revealed very small negative values indicating that the separation mechanism is well described via Reptation sieving. Considering poor separation performance and extremely low $dRLR_{\%}$ -values for both alkanols, I assume, that shifting of the sieving-mechanism towards Reptation-without-stretching occurs using these alkanols. The other alkanols gave no such remarkable trends and are not discussed further.

Overall, the addition of 2-propanol lead to increased Ogston-sieving, which tremendously improved mass-resolution in the small molecular weight range. This is especially desired for the application

INVESTIGATION OF TEMPERATURE AND ADDITIVE ON SDS-CE PART 2: MECHANISTIC INVESTIGATION OF THE INFLUENCE OF ALKANOLS AND TEMPERATURE ON THE SIEVING MECHANISM VIA INTERACTION WITH SDS-PROTEIN-AGGLOMERATES AND SIEVING POLYMER

in antibody-characterization. I was not yet able to find conditions where a similarly high separation performance was achieved in the high mass range.

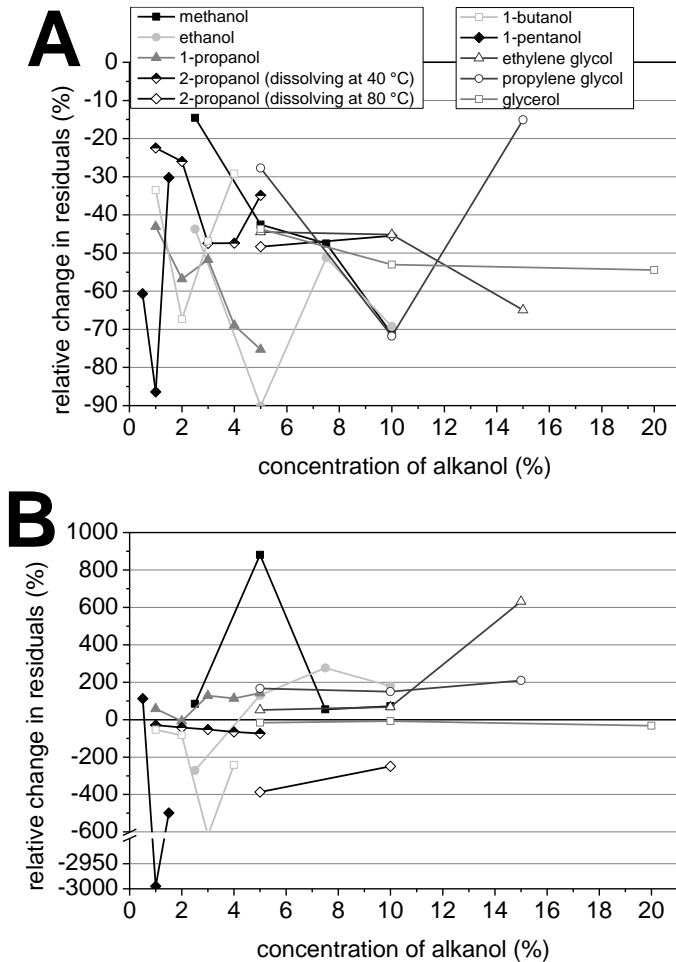


Figure 18: Relative change in residuals calculated according to Equation (1) for all alkanols investigated, with A: dRLO% values for the investigation of Ogston-sieving, averaged over the single values of Proteins 6 and 7 (see arrows in Figure 17). B: dRLR% values for the investigation of Reptation-sieving, averaged over the single values of Proteins 1-3 (see arrows in Figure 17).

3.4.4. Influence of cassette temperature

The dependence of the relative residual values from temperature are shown in Figure 19 for Ogston-sieving and Reptation-sieving. The negative dRLO% values at temperatures below 25 °C indicate a minor promotion of this mechanism. Lowest dRLO% values were obtained for a cassette temperature of 30 °C. Thus, Ogston-sieving is the prominent separation mechanism here. Increasing cassette temperature lead to increasing positive dRLO% values and thus decreased Ogston-sieving.

dRLR% values of Reptation-sieving are shown in Figure 19 B. Here, slightly positive dRLR% values are obtained for temperatures below 25 °C, indicating decreasing accordance to the Reptation-sieving mechanism. Concerning the results found for Ogston-sieving at this temperature, a shift of sieving-mechanism from Ogston- towards Reptation-sieving is assumed. For 35 °C and higher, negative dRLR% values and thereby a more pronounced Reptation-sieving is observed. At 50 °C both dRLR%

INVESTIGATION OF TEMPERATURE AND ADDITIVE ON SDS-CE PART 2: MECHANISTIC INVESTIGATION OF THE INFLUENCE OF ALKANOLS AND TEMPERATURE ON THE SIEVING MECHANISM VIA INTERACTION WITH SDS-PROTEIN-AGGLOMERATES AND SIEVING POLYMER

and dRLO%-values increase. I thereby propose that the influence of temperature does not impair the sieving mechanism.

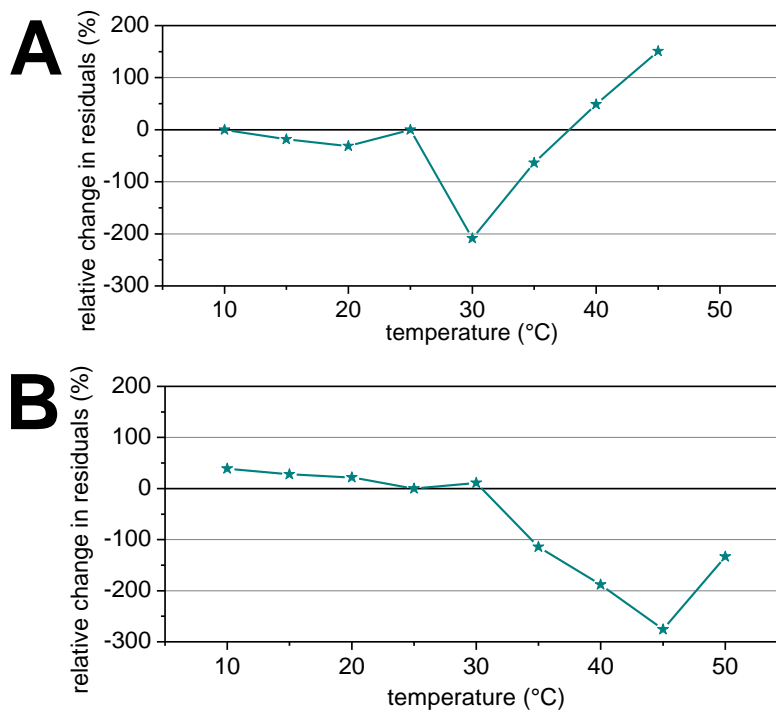


Figure 19: A: dRLO%-values averaged for Proteins 6 and 7 and B: dRLR%-values averaged for Proteins 1-3, obtained at various temperatures relative to measurements at 25 °C.

3.5. Discussion

Numerous effects were observed in this chapter and in Chapter 2: migration time drifts towards higher and lower times, in- and decreasing resolution, peak capacity and intermediate precision as well as changes between Ogston-sieving and Reptation-sieving. In the following I will use literature to identify temperature and solvent dependent effects.

3.5.1. The non-linearity of mass determination as an intrinsic property of sieving mechanisms

For the discussion of the sieving mechanism, the correlation of migration time or electrophoretic mobility and protein mass is important. As discussed above, different sieving mechanisms have a different dependence. In literature on SDS-CE the logarithm of the molecular mass of each protein ($\log(M_r)$) is plotted versus t_{mig} or vice versa. In my study, I use the addition of alkanols to the separation medium and changes in the temperature to better understand the importance of the sieving mechanism underlying the separation process on the resolution obtained in protein separation. For this, I compare literature data with my results and discuss the influence of additives and temperature on the mesh-size of the polymer and protein-SDS agglomerates.

3.5.1.1. Non-linearity in literature: is it really an influence of sieving-polymer and BGE or is it an intrinsic property of SDS-CE?

Linearization of the logarithmic protein molecular mass versus t_{mig} according to literature was presented in Section 3.4.2. This simple method of linearization via linear regression always leads to residuals with highest values for both the high and low mass range, which indicates the necessity of a higher order fitting. Precise molecular mass determination of unknown proteins is limited. The group of Csapo *et al.* tackled this problem and proposed data regression using a second degree polynomial function for better mass determination¹²⁵. The molecular mass of a protein analyte can then be determined by interpolation, with an error of only 0.25 kDa for a protein with $M_r = 30$ kDa.

In the following I will compare the results of Csapo *et al.*¹²⁵ to ours to start a discussion about possible influences for the non-linear dependence. Csapo *et al.* used linear polyacrylamide (LPA, $M_r = 700$ -1000 kDa) in a BGE containing 50 mmol/L Tris, 50 mmol/L *N*-tris-(hydroxymethyl)methyl-4-aminobutanesulfonic acid (TAPS) and 0.05 % SDS at pH 8.4. Therefore, they used a "GOOD buffer"-system with linear polymer and low concentration of SDS at alkaline pH. SDS and buffering species had half the concentration compared to the separation medium in this work. I regard the miniaturized separation system of Csapo *et al.* comparable to the capillary setup presented here.

Hydrophilic LPA as sieving matrix is known to give best results in size-sieving electrophoresis of DNA. A downside is the lack of self-coating ability^{70,126}, which makes a covalent surface modification necessary. Csapo *et al.*¹²⁵ used larger proteins, the low mass range was not considered. Similar proteins in the medium and partly high mass range as in this study were used, such as carbonic anhydrase (29 kDa), ovalbumin (42.8 kDa), BSA (66.5 kDa) and phosphorylase B (97.4 kDa).

In contrast to the results for the medium to high mass range (see Figure 16 A and B) Csapo *et al.*¹²⁵ observed a deviation from linearity when plotting $\log(M_r)$ vs. migration time and linked it to the use of non-covalent markers for LIF-detection. According to the authors, these may alter the electrophoretic mobility of the investigated proteins. However, other aspects may be taken into account: Changes in protein form/size due to reduced protein-SDS agglomeration below saturation

at an SDS:protein ratio of 1:4, possibly evoked by the relatively low ionic strength and SDS concentration in the BGE. There may be differences in the effective electrophoretic mobility of the protein analytes from incomplete SDS agglomeration. Differences in protein-SDS agglomerate size/form may also change the sieving mechanism, e.g. for some proteins Ogston-sieving may already be present. As a different sieving polymer of different chain length is used, the direct comparison of the sieving mechanism is not possible.

With the sieving matrix dextran ($M_r = 2000$ kDa) and a BGE identical to ours (100 mmol/L Tris-CHES and 0.1 % SDS at pH 8.6), Reif *et al.* showed comparable results to this study. Again, only the medium to high mass range was investigated using carbonic anhydrase (29 kDa), ovalbumin (42.8 kDa), BSA (66.5 kDa) and phosphorylase B (97.4 kDa). Identical correlation coefficients of ($R > 0.998$) were observed (see Figure 16 D and ⁶⁵). The similarities between my study and the one of Reif *et al.* point out that the chemical structure of sieving polymer has no influence on the linearity of mass determination and presumably the sieving mechanism, at least for the medium and high mass range. This is in good accordance with the theory of size-sieving mechanism, where the chemical structure of polymer is rendered irrelevant¹²⁷.

I pointed out, that especially low molecular weight proteins are hardly included in literature studies on the investigation of linearization. In this study, lysozyme (14.4 kDa), myoglobin (17.0 kDa) and β -lactoglobulin (18.4 kDa) were investigated, representing the low mass range. For all three, see Section 3.4.2, lower t_{mig} s than expected were observed from linearization via the common (M_r) vs. t_{mig} plot. These observations can be either linked to (i) a low SDS-binding capacity at the SDS-protein-agglomerates and thus differences in effective electrophoretic mobilities even without sieving matrix present or (ii) different sieving mechanisms between low and high weight proteins.

For protein-SDS-agglomerates, a uniform charge-to-mass ratio is commonly postulated in literature dealing with SDS-CE and -PAGE. This antiquated model, which is based on viscometry-studies¹²⁸, derives from the assumption, that reduction of proteins in the presence of SDS yields unscrambled protein-SDS-agglomerates which are shaped like a prolate ellipsoid, with a semi-minor axis diameter of approximately 0.18 nm. Assuming identical binding sites for SDS at each amino acid in the protein, the length and charge of this SDS-protein-agglomerate would be proportional to the protein chain length and thereby its molecular weight. However, there is plenty of research about SDS-protein binding ratios which gives good insight into the actual binding characteristics. An identical charge-to-mass ratio would result in identical effective electrophoretic mobility (μ_{el}) in the absence of polymer sieving matrix. However, the possibility of identical μ_{el} was already refuted in literature by Takagi *et al.*¹²⁹ who demonstrated differences in μ_{el} higher than 100 % found for SDS-protein-agglomerates of proteins with a molecular mass below 10 kDa. Limitations in size determination by SDS-CE and SDS-PAGE were discussed for proteins with different binding sites as discussed e.g. for strongly non-polar and strongly folded membrane proteins and especially for strongly acidic and basic proteins due to their intrinsic charge. Several NMR-studies^{130, 131} as well as small-angle neutron scattering experiments¹³² further supported these assumptions looking at SDS-protein binding. To overcome this limitation, the Ferguson analysis presents a useful tool for better mass determination by additional measurements at various polymer concentrations and extrapolation to the relative electrophoretic mobility¹³³. However, these methods are very time-consuming and require polymers of well-defined chain length and size distribution.

In conclusion I can say that the influence of the polymers' chemical structure on the separation can be neglected. The influence of the BGE will be predominantly via ionic strength effects. Further research is required for a detailed understanding.

I was not able to find literature investigating the influence of BGE with respect to linearity and thus relative μ_{el} . The influence of BGE cannot be investigated without further research, since comparable research often neglects the investigation of mass determination. The fact, that proteins with exceptionally high P_{ow} -values and extreme pI -values deviate from the general linear dependence is known in literature. I assume that the influence of alkanols and temperature presented in this work is independent from such influence, since I used the same protein samples during this research, as will be discussed in the following.

3.5.2. Preliminary remarks about the addition of alkanols to the sieving medium and the influence of temperature

There are numerous aspects on how alkanols can influence the separation. One dominant effect I observed was the change in t_{mig} for increasing alkanol concentration with an additional large step-wise increase at a specific alkanol concentration coming along with a strong decrease in separation efficiency (see Chapter 2).

3.5.2.1. General influences of organic solvent additives in CE

Viscosity and dielectric constant change upon addition of organic solvents to BGEs in capillary electrophoresis. Both parameters influence the electrophoretic and electroosmotic mobilities:

(i) Changes in viscosity are related to temperature, addition of organic solvents and changes in polymer entanglement which itself depends on the separation medium. Higher t_{mig} are expected for increased viscosity of the separation medium. As expected, I obtained highest t_{mig} in the presence of the most viscous alkanol glycerol. But even for the addition of methanol with its lower viscosity than water, increasing t_{mig} were observed. Changes in the viscosity of an aqueous solution are neither linear nor steady for increasing alkanol concentration¹³⁴. However, as increasing t_{mig} were observed for each alkanol, I assume that the impact of increased viscosity on t_{mig} is not the most dominant influence. Further influences will be discussed in the following section.

(ii) Decreasing EOF upon alkanol addition may be the reason for decreasing t_{mig} , I observed at low concentration of additive, since the low EOF is directed towards the capillary inlet (measurements were conducted at inverted polarity). However, Sarmini *et al.*¹³⁵ discussed that, for SDS-CE, decreases in EOF due to organic quota in aqueous sieving media are negligible. It is more likely that the presence of organic solvents increases the solubility of PEO and thus its self-coating ability, which leads to increased EOF and lowered t_{mig} -values.

Both phenomena occur above a certain threshold concentration of alkanol, with (i) measurable as an increase in t_{mig} and (ii) measurable as a disproportionately high decrease in t_{mig} . Regarding data presented for 1-propanol in Chapter 2, Figure 3 it can be seen, that t_{mig} first increases (0.0 % - 4.0 %, additionally the sieving mechanism was manipulated) which was then followed by a strong decrease (1-propanol at 5.0 %, inherent with decreased separation efficiency). The latter is associated with decreased PEO-adsorption on the capillary and increased EOF (see (ii)) which is

associated with peak-broadening and ultimately followed by electropherograms void of protein signals (1-propanol above 6.0 %, EOF increases strongly and μ_{EOF} exceeds μ_{el} of proteins).

3.5.2.2. Influences of alkanols and temperature on SDS-CE

Beside these general aspects, parameters specific for SDS-CE have to be considered, which include changes in the sieving mechanism due to effects of alkanols on both the polymer mesh and the SDS-protein-agglomerates. One additional effect is the inadvertent interaction between sieving polymer and SDS. SDS-PEO-interaction is prevented by CHES¹³⁶, however, various changes in the interaction between PEO, CHES and SDS in the presence of alkanol or at different temperatures are possible.

(iii) The influence of temperature on the sieving mechanism is complex. For temperatures below 25 °C I observed negative dRLR% but positive dRLO% values. The opposite was observed above 40 °C with positive dRLR%- and negative dRLO%-values. These results are in good accordance with the hypothesis, that the dominant separation mechanism at low temperature is Ogston-sieving, whereas elevated temperature favors Reptation-sieving. Above 50 °C both Ogston- and Reptation-sieving become less pronounced indicating that another mechanism, e.g. Reptation-without-stretching, occurs. I hypothesize that at elevated temperature, thermal movement of polymer chains overcomes inter-chain interaction so that a very dynamic mesh with varying mesh sizes is present. This allows analytes (SDS-protein-agglomerates) to push the polymer-chains aside while migrating through the capillary and the sieving mechanism is altered. The effect of temperature and sieving can be seen in the respective electropherograms in Chapter 2, Figure 7: Electropherograms at elevated (lowered) temperature showed narrower (broader) peaks at lower (higher) migration times but also smaller (larger) migration time windows. The resolution decreased for temperatures above and below 25 °C.

The pronounced Ogston-sieving mechanism at low temperatures can be explained when discussing both (i) the rigidity of sieving-polymer meshwork and its pore-size¹⁰³ as well as (ii) the size of SDS-micelles¹³⁷ or SDS-protein-agglomerates. First, decreasing temperature leads to more rigid and thus less flexible polymer meshes with relatively fixed mesh size. In parallel, larger SDS-protein-agglomerates evolve due to intercalation of alkanols in the SDS-protein-agglomerates. Considering both Reptation-sieving may be expected at low temperature. The opposite is observed in my experiments. I assume that the temperature dependence of the kinetics of Reptation-sieving as described by Cottet *et al.*¹⁰³ is the reason for the observed effects. Cottet *et al.* also found, that in SDS-CE experiments Reptation-sieving is favored at elevated temperature. I assume the following: Reptation sieving needs flexible SDS-protein-agglomerates. This kinetic phenomenon dominates over the discussed steric aspects. Cottet *et al.* furthermore described that the kinetics of Reptation-sieving are proportional to the temperature, so higher temperatures allow Reptation-sieving to take place. These kinetic aspects are negligible for the addition of alkanols.

(iv) The interaction between the buffer components SDS, CHES and alkanol is prone to result in decreased CHES-PEO interaction and thus increased SDS-PEO interaction due to an alkanol-mediated SDS-PEO interaction. Increased PEO-SDS-interaction leads to increased charge at the PEO-chains, forcing them to migrate towards the anode at the capillary outlet in the electric field, which would result in decreased t_{mig} (as observed for e.g. the addition of 5.0 % 1-propanol). In

addition, PEO-SDS interaction diminishes PEO's self-coating abilities, making silanol groups accessible to proteins. According to the observations of Sumitomo *et al.*¹³⁶, this is commonly accompanied by either co-migration of proteins or electropherograms void of protein signals. The latter observation is due to adsorption of SDS-protein-agglomerates on the capillary surface, which is now free of PEO, leading to peak broadening. Decreasing t_{mig} were only observed for 5.0 % 1-propanol, 12.5 % ethanol and for 3.0 % 2-propanol (dissolving PEO at 40 °C), compared to the next lower concentrations, see Figure 3 in Chapter 2. The first two examples are utilized to separation media using the highest alkanol concentrations possible, with higher concentrations leading to electropherograms void of protein signals, which does not comply with acceleration of SDS-PEO-agglomerates towards the capillary outlet.

Based on these observations I propose that increased SDS-PEO interaction takes place due to alkanol-induced depletion of CHES from PEO, which leads to SDS-PEO-agglomerates and thus movement of the sieving medium to the anode in the electric field. Simultaneously the self-coating abilities of PEO are diminished, resulting in an increase of the EOF towards the cathode. The resulting EOF at the given pH can be expected to be higher than the mobility of bulky SDS-PEO-agglomerates, so an overall protein transport towards the cathode results.

(v) The interaction between the sieving polymer (PEO) and alkanol leads to a change in polymer mesh-size (ζ) and thereby changes in the sieving-mechanism¹⁰⁰⁻¹⁰⁸. Adaptation of the mesh size to access different mass-regions for separation is a common technique established in gel electrophoresis, since the accessible mass-range is linked to the difference between the pore size of the sieving matrix and size of SDS-protein-agglomerates. This topic is thoroughly discussed for polyacrylamide gels¹⁰⁹⁻¹¹², where different mesh sizes are obtained by variation of polymerization conditions, e.g. concentration of cross-linker and starter radical. For entangled polymer solutions used in capillary-based systems, Sumitomo *et al.*⁸⁷ described the relation between protein's t_{mig} and μ_{el} , to be strongly dependent on ζ . In contrast, effects of additives on SDS-CE separations are rarely discussed.

Numerous studies on PEO properties when dissolved in various solvents or solvent mixtures have been published from which information relevant to understand the here presented results in SDS-CE can be deduced. When dissolved in water, originally solid PEO changes its conformation to a staggered meander-like structure where each oxygen atom in the polymer chain is chelated by two water molecules in the first hydration sphere as described by Rösch *et al.*¹²²⁻¹²⁴. Despite this change in conformation inherent to the dominant formation of intermolecular water-PEO hydrogen bonds over intramolecular PEO-PEO dipole interactions, the PEO chains keep a rigid gauche configuration^{138, 139}. For a synthetic polymer, PEO offers surprisingly good solubility in water due to its chemical structure; the spacing between ether oxygens is almost identical to the next nearest spacing of oxygen atoms in "ordinary" ice 1h, the hexagonal structure of ice, which is common at ambient pressure¹⁴⁰. The entropic distortion of the water structure caused by the dissolution of PEO is thereby minimal at low temperatures. It is therefore not surprising, that PEO precipitates at higher temperatures from aqueous solutions by an increase of the entropic effects¹³⁸. Whether this is caused due to the loss of only the first or also higher hydration spheres is unknown. Furthermore, increased flexibility prior to precipitation is noted in literature¹⁴⁰.

There are studies concerning the influence of temperature on PEO solvation in the given BGE, but neither with the investigated molecular weight ($M_r = 600$ kDa) of PEO nor over the investigated temperature range (10 – 50 °C)¹⁴¹. My investigations on the influence of temperature on the size-sieving in SDS-CE help to better understand the influence of alkanols on the flexibility of the polymer mesh: It was pointed out in Section 3.4.4 that increased temperature leads to a preference of Ogston-sieving. Reptation-sieving was preferred at low temperature. This indicates that alkanols promoting Ogston-sieving (e.g. 1- and 2-propanol, ethanol and methanol at certain concentrations) increase flexibility and dynamics the polymer meshwork, resulting in higher ζ , whereas alkanols promoting Reptation-sieving reduce the flexibility of the polymer meshwork (e.g. methanol, ethanol and 2-propanol), resulting in lower ζ . These examples were chosen to show, that this influence is not as simple as it seems: methanol and ethanol give both increasing Ogston- and Reptation-sieving, see Figure 18.

To describe the interaction of PEO with solvents other than water, solubility experiments give good insight. PEO is soluble in pure methanol, ethanol and 2-propanol, but hardly in 1-propanol. For methanol and 2-propanol, higher solubility is achieved by the addition of water¹³⁹. This indicates that water is better suited for the chelation of ether groups in the first hydration sphere than methanol and 2-propanol. As a consequence, the distortion of the solvent structure is reduced. Similar effects can be expected for ethanol. PEO can neither be dissolved in less polar n-alkanols nor very polar alkanols such as ethylene glycol and glycerol¹³⁹. This clearly indicates, that steric aspects must be considered as well. Overall, both the chelation of PEOs ether oxygen upon dissolution, transferring PEO from its staggered conformation (solid) to its meander structure (dissolved), as well as the coordination of solvent around the ethylene group of PEO play important roles.

It is known, that in a solution void of alkanol, aggregation of PEO-polymer-chains requires a certain concentration, called entanglement threshold^{142, 143}. PEO-PEO interaction is weakened or even inhibited by the addition of methanol,¹⁴⁴ with intermolecular interactions between methanol and PEO's ether and ethylene groups. For SDS-CE this means that a more flexible meshwork with higher ζ is present. Alkanols in which PEO is easily dissolved, e.g. methanol, ethanol and 2-propanol, are prone to yield a high flexibility of PEO mesh. This was indicated by the high impact of solvent additives on the separation performance in the low mass range, see Chapter 2, which can be identified as an influence on the sieving mechanism. Both changes in $dRLO_{\%}$ - and $dRLR_{\%}$ -values were negative, indicating, that both mechanisms play an important role. Yet, Ogston-sieving comprises a larger mass range when the solvents are added and was thus favored over Reptation-sieving, as can be seen in Figure 18. Depending on the mass of the protein, changes in sieving mechanism occur because of alkanol induced softening of mesh-work.

Both PEO interaction sites (ethylene group and ether oxygen) need to be solvated to a certain extent, as indicated by the solubility of PEO in both very polar (ethylene glycol and glycerol) and nonpolar (1-propanol, 1-pentanol, etc.) solvents. I showed, that only small alkanols had a beneficial impact on sieving mechanism and separation performance. I postulate that any compound with a nonpolar residue is able to interact with the ethylene group of PEO. Long (more than four carbons) n-alkyl chains seem to be detrimental for the PEO-PEO interaction. Amphiphilic alkanols act as

solubilizer towards water and thereby inhibit PEO-PEO-interaction. This effect then leads to softening of the sieving polymer meshwork.

The interaction between PEO and sterically demanding and amphiphilic SDS is prone to be even more complex: it is evident that the dodecyl substituent of SDS and the ethylene groups of PEO interact with each other, as both are non-polar. The large and ionic sulfate group of SDS is not competitive to water in its interaction with PEOs ether oxygen due to steric hindrance and the low polarization of ether oxygen.

When I utilize alkanols in polymer sieving solutions in SDS-CE, the best separation performance was obtained for 2-propanol (dissolving PEO at 80 °C) and the second best for 1-propanol and 2-propanol (dissolving at 40 °C). This difference can primarily be linked to the branched structure of 2-propanol, which allows for the preferred interaction with PEO rather than intercalation into SDS-protein-agglomerates, as will be discussed in (vi). The enhanced performance of 2-propanol (dissolving PEO at 80 °C) is either linked to overcoming the kinetic barrier for 2-propanol intercalation or to vaporization of 2-propanol during heating. The latter would result in lower 2-propanol concentration and thus lowered intercalation into the SDS micelles. However, vaporization of 2-propanol is unlikely as sealed vessels were used. I here postulate that the addition of polar and sterically non-demanding alkanols (e.g. ethanol, 1- and 2-propanol) on PEO entanglement and thus the dynamics of the mesh and its pore size is advantageous for SDS-CE separation while the influence of non-polar and sterically demanding alkanols (e.g. 1-pentanol) on the SDS-protein-agglomerates is detrimental for the separation performance.

The absolute differences in separation performance and changes in t_{mig} between 1- and 2-propanol (dissolving PEO at 40 °C), are very small. However, it is worth noting that for 2-propanol both effects are observed at lower alkanol concentration than for 1-propanol.

(vi) The interaction between SDS-protein-agglomerates and alkanol leads to numerous effects: First of all, alkanol intercalation into the micellar region of the SDS-protein-agglomerates reduces intermolecular SDS repulsion of sulfate groups, which also influences SDS-protein interaction. Both effects promote swelling of proteins' micellar SDS-regions¹⁴⁵. This evokes an increased diameter of SDS-protein-agglomerates (d_{SPA}). Depending on the magnitude of this effect, a shift from Ogston- to Reptation-sieving is possible for proteins of intermediate mass and thereby changes in sieving-mechanism. Penetrating alkanols (non-polar n-alkanols with high $\log(P_{ow})$) can be expected to have a stronger effect than non-penetrating alkanols (polar (poly)-alkanols with low $\log(P_{ow})$). Thus, a distinction between alkanols inflicting the sieving polymer (polar and sterically non-demanding) and SDS-protein-agglomerates (non-polar with no steric preference) can be found. Secondly, a decrease in charge density of SDS-protein-agglomerates due to substitution of SDS by alkanols is likely. Decreased μ_{el} and therefore increased t_{mig} are then expected with increasing alkanol concentration, as observed in this study¹⁴⁶. The resolution changes for protein micro-heterogeneities leads to an apparent peak-broadening in UV detection due to partial separation. A third aspect is that the addition of alkanol also leads to a decrease in the BGE polarity, which either results in an increase in the critical micellar concentration of SDS and/or the formation of mixed alkanol-SDS-micelles¹⁴⁷. Dissolution of monomeric SDS is enhanced by non-polar alkanols due to diminished entropic effects of the non-polar SDS residue. Mixed SDS-alkanol micelles are favored

over pure SDS-micelles due to reduced inter-molecular repulsion of sulfate residues. Alkanols offer thermodynamically more stable aggregation regions for SDS than proteins and may thus promote dissociation of SDS-protein-aggregates, which may become visible in the loss of protein signals in the electropherograms.

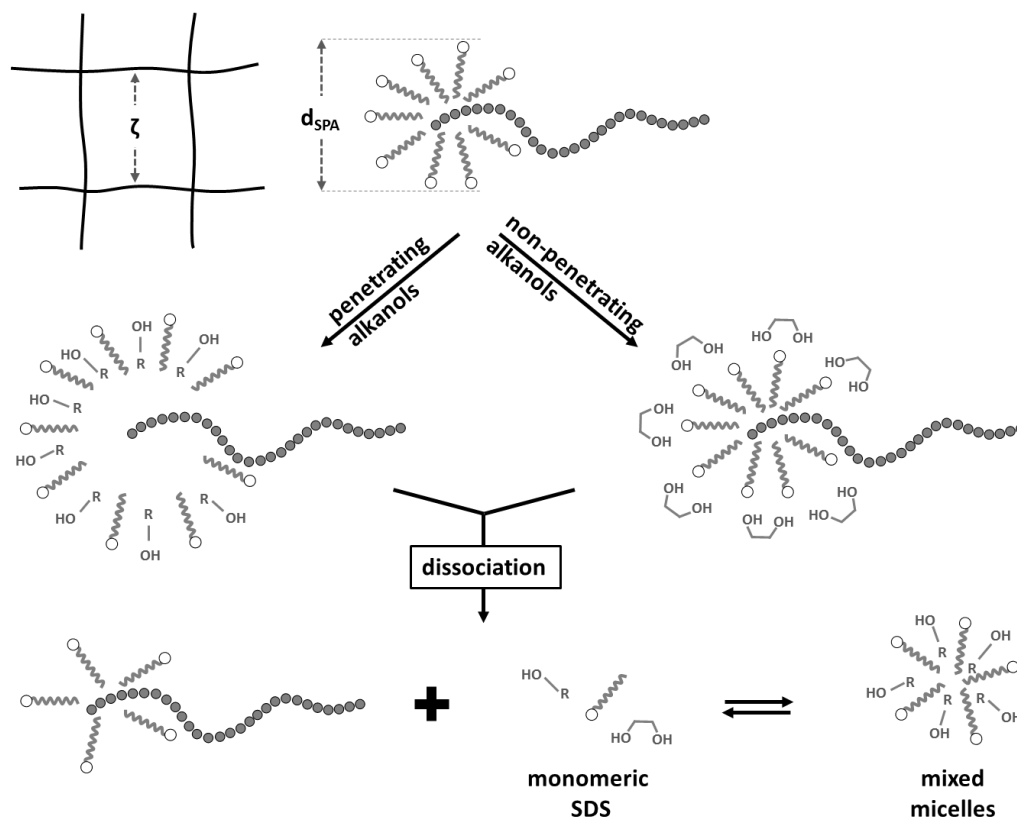


Figure 20: Schematic display of the changes of the diameter of SDS-protein-agglomerates (d_{SPA}) with increasing alkanol concentration. Strongest swelling of proteins' micellar regions is achieved by penetrating alkanols, non-penetrating alkanols add to the corona region of the micelles and result in little to no swelling¹⁴⁷. With increasing concentration of alkanols, dissociation of SDS-protein-agglomerates favoring the formation of free SDS and mixed SDS-alkanol-micelles is observed. Changes in the sieving mechanism are expected also when the mesh-size ζ of the meshwork does not change simultaneously.

The processes of (vi) are schematically summarized in Figure 20. When taking the sieving mechanism into consideration both the diameter of SDS-protein-agglomerates (d_{SPA}) as well as the mesh-size of the entangled polymer network ζ need to be discussed. The importance of these two effects can be discussed on the basis of the observed sieving mechanism, as clearly presented by Guttman *et al.*¹⁴⁸.

vii) Entropic effects due to the addition of alkanols can be understood when taking into account effects well described when heating of PEO-solutions: precipitation of polymer is observed with increasing temperature¹³⁸. The formation of a hydration sphere around PEO or alkanols requires water molecules to orient themselves according to partial induced charges, which is entropically unfavorable. This effect strongly determines PEO and alkanol solubility. Likewise, I can expect that the presence of both PEO and alkanol, changes their solubility compared to pure aqueous media.

For the most polar additives, ethylene glycol and glycerol, the distortion of the water structure is expected to be small due to hydrogen bonds similar to water, resulting in good PEO solubility even

when these additives are present. This is supported by the high concentrations of those additives that could be utilized in this work, see Chapter 2.

In simple aqueous-organic mixtures without surfactants and PEO, increasing amounts of n-alkanol evoke a decrease in n-alkanol-water interaction, inherent with increased water-water- and n-alkanol-n-alkanol interaction, commonly leading to phase separation. When surfactant is present, intercalation into micelles occurs, as discussed in (vi). Both phenomena force entropically unfavorable coordination of water structure and will impair PEO solubility.

In summary, I showed, that both alkanol and temperature influence the sieving mechanism. This happens due to the increased flexibility of the polymer mesh, which is beneficial for Ogston-sieving and for the performance in the low weight range. A decrease of PEO-PEO interaction is assumed for increasing $\log(P_{ow})$ -value of the additive. Yet, intercalation of alkanols in SDS-protein-agglomerates occurs, leading to microheterogeneities in SDS-protein-agglomerates becoming partially separated. Nonpolar n-alkanols preferably interact with SDS and SDS-protein-agglomerates. This effect also becomes more pronounced with increasing $\log(P_{ow})$ -value. Considering PEO-alkanol-interaction discussed in (v) I furthermore postulate, that methanol, ethanol, 1- and 2-propanol, and presumably 1-butanol have the largest impact on PEO and thus the mesh without additional alkanol-SDS-protein-agglomerate interaction. Branching of alkanols is another important factor as indicated by the differences between 1- and 2-propanol: 2-propanol is both (i) more efficient in the interaction with PEO, which is the desired effect for the alteration of the sieving mechanism and (ii) less efficient in its interaction with SDS. The branched structure allows better interaction with PEO but hinders the intercalation into micellar structures such as SDS-micelles and SDS-protein-agglomerates.

3.6. Conclusion and outlook

I investigated the influence of temperature (between 10 °C and 50 °C) and addition of alkanols (up to 20 %) on the PEO ($M_r = 600$ kDa) as separation medium. I investigated the underlying influence on the protein mass dependent change from Ogston- to Reptation-sieving using both literature and my results. Temperatures below and above 25 °C showed to enhance Ogston-sieving for the small mass range whilst Reptation-sieving was beneficial only at temperatures below 25 °C for large proteins. For temperatures above 25 °C, kinetically dominated stretching of sieving polymer and a third sieving mechanism, presumably Reptation-without-stretching, were assumed.

I conclude, that the addition of alkanols to the sieving medium has two dominant effects: it inflicts the stability of or SDS-binding in SDS-protein agglomerates as well as polymer mesh size ζ . Effects on viscosity, EOF, interaction with buffer components and entropic reasons are either minor or come into play only at high alkanol concentrations, when measurements become instable.

The here presented results provide an understanding of the SDS-CE sieving mechanisms and give rise to further research to tailor sieving media apt for each mass range of interest. 2-propanol was shown to be best for the mass range below 30 kDa.

To distinguish influences on EOF and viscosity from those on sieving mechanism directly from electropherograms, I propose to consider the changes in the migration time window upon solvent addition. In addition, on-line determination of μ_{EOF} and measurement of viscosities as well as DLS-experiments for the determination of ζ -values will help to gain further understanding of the influence of alkanols and temperature on SDS-CE sieving mechanism.

4. Novel approach for the synthesis of a covalently bound, highly polar and pH-persistent N-acryloylamido ethoxyethanol capillary coating for capillary electrophoresis-mass spectrometry part 1: strategy, performance and stability

4.1. Abstract

Capillary coatings are of crucial importance in capillary electrophoresis, especially in the separation of peptides and proteins. Often, dynamic coatings in combination with phosphate, borate or “GOOD buffers” are used for highest separation efficiencies and migration time precision. However, the non-volatile buffer components impair MS-detection desirable for proteomic research. To achieve MS-hyphenation whilst suppressing protein and peptide adsorption, statically adsorbed and covalently bound capillary coatings are of crucial importance. Published coating strategies and commercially available coated capillaries have a limited pH-stability so that the analysis at strongly acidic pH is limited, or harsh rinsing procedures for biological sample analysis cannot be applied.

I here present a covalently bound capillary coating based on N-acryloylamido ethoxyethanol (AAEE) with a new synthetic strategy including LiAlH₄ surface reaction and a parallelized setup for the capillary coating procedure. I show my investigations on the optimization of AAEE-coating preparation with emphasis on stability and reproducibility applying harsh rinsing procedures (strong acid, strong base and organic solvents), using the electroosmotic mobility and separation efficiency of tryptic peptides as measures.

My improved synthesis procedure of covalently bound AAEE-capillary surfaces via Si-H-surface coupling includes chlorination and hydration and provides full advantage of T³-group and Si-C-linkage stability. Complete synthesis is performed in less than 2 days for up to 8 capillaries of more than 16 m total length. The importance of the dryness of solvent during hydration was investigated. Intra- and inter-batch reproducibility using 5 and 7 capillaries were determined regarding electroosmotic mobility (μ_{EOF}) and separation efficiency and migration time precision in CE-MS separation of tryptically digested bovine serum albumin. Coating stability (one capillary of each batch) towards rinsing with strong acid (1 mol/L HCl), organic solvent (acetonitrile) and strong base (1 mol/L NaOH) was investigated. Outstanding performance was found for single capillaries. However, inter-capillary reproducibility is discussed critically.

The new coating was successfully applied for reproducible CE-MS separation of large proteins, medium-sized peptides and small and highly charged polyamines using a very acidic background electrolyte containing 0.75 mol/L acetic acid and 0.25 mol/L formic acid (pH 2.2). Complex samples such as serum and fish egg extracts were successfully measured without further sample processing.

4.2. Introduction and motivation

Capillary based separation of proteins is often performed using background electrolytes (BGE) containing non-volatile phosphate, borate or zwitterionic buffers, sometimes with polymer additives or detergents¹⁴⁹⁻¹⁵³. The latter act as dynamic coatings and thus prevent the adsorption of analytes on the silica surface. For hyphenation with MS, volatile BGEs such as ammonium and low-weight carboxylic acids, predominantly formic and acetic acid, are crucial¹⁵⁴. These compounds lack self-coating abilities so that appropriate capillary coating strategies to realize separation of peptides and proteins are required. Prominent capillary coatings are e.g. polyvinyl alcohol (PVA)¹⁵⁵, poly(diallyldimethylammoniumchloride)(DADMAC)¹⁵⁶⁻¹⁵⁸, polybrene^{156, 159-161} or successive multiple ionic layer-coatings (SMIL)^{154, 162, 163, 164}. Capillaries with PVA-coating are commercially available but their applicability is restricted regarding pH of the BGEs. A pH-range from 2.5 to 9.5 is recommended by the manufacturer¹⁶⁵. The use of rinsing procedures for capillary regeneration with concentrated acid or base solutions¹⁶⁶ strongly reduces capillary lifetimes.

In recent years, fewer studies addressing novel or improved syntheses for capillary coatings apt for peptide and protein separation were published. Most research considering the performance and stability of various capillary coatings was published between 1990 and 2005^{150, 156, 158, 167, 168}. However, there is still a lack of robust neutral capillary coatings which can stand harsh cleaning conditions including very high or low pH and organic solvents. Screening the literature, my attention was caught by a study using covalently bound *N*-acryloylamido ethoxyethanol (AAEE) as a monomer for a neutral, covalently bound capillary coating, which was shown to offer high separation efficiency for intact proteins in CE-UV¹⁵⁰ and high pH-stability towards hydrolysis whilst being strongly hydrophilic preventing protein adsorption^{150, 169}. Hydrolytic inertness of polymeric AAEE itself is remarkably high; only slow degradation occurs in 1 mol/L sodium hydroxide solution at 70 °C¹⁷⁰.

To access the full potential of this polymer, successful covalent binding to the surface is crucial. Starting from a silicium hydride (Si-H)-species, Chu *et al.* presented Speier-catalytic linkage of allyl methacrylate to the surface, followed by grafting through of AAEE¹⁷¹. Generally, the formation of a silica surface with Si-H functionality is possible via 4 prominent approaches as presented in Figure 21 A. a) Silanol linkage of silanol precursors to an existing silica surface, also referred to as "silanization process": here, the new surface groups involve bridged Si-O-Si-H; b) transfer of surface silanol groups into Si-Cl groups followed by reduction with an inorganic hydride (direct formation of Si-H from Si-OH); c) preparation of a new poly hydro siloxane (PHS) network from hydrolyzable precursors, which has the chemical composition $(\text{HSiO}_{3/2})_n$ ¹⁷²; d) chemisorption of hydrogen onto a pyrolytically activated (methyl) silica surface¹⁷³⁻¹⁷⁵. Methods c) and d) were not investigated in this work due to technical limitations: for c) it would have been necessary to build a capillary from silica precursors, for d) the capillary would have had to be heated to 600-800°C, which would destroy the outer polyimide coating. The focus of this work was on Method b) due to the intrinsically higher hydrodynamic stability of the silica-species in the resulting coating, as I elaborate in the following.

Sandoval *et al.*¹⁷⁶ described the differences in Si-H surfaces formed with respect to the molecular surface of the capillary and came to the following considerations: (i) A bare fused silica surface consists of a dense and packed surface layer with a large number of Q³-groups (Si surrounded by four O and three further Si, see Figure 21 B. (ii) Turning Q³-groups into T³-groups (Si surrounded by

three O and three further Si, see Figure 21 B, e.g. to Si-Cl or Si-H can easily be performed and it is assumed that this reaction proceeds to completeness, see Figure 21 A, Scheme b). Subsequent modifications of these surfaces via hydrosilylation^{176, 177}, via Grignard reagents^{178, 179} or via organolithium intermediates¹⁸⁰ are supposed to yield surfaces void of residual silanol groups. In the following, this approach is referred to as “direct linkage”. (iii) Surface modification via silanol chemistry, see Strategy a) in Figure 21 A, is assumed to leave a number of residual silanol groups proportional to the steric hindrance of the attached substituent - the larger the substituent, the higher the number of residual silanol groups¹⁷⁶. On first sight, a difference between approach a) and b) is not easy to understand. The main reason for the lower residual silanol group population found for coatings prepared via direct linkage is, that T³-groups are barely formed via silanol chemistry due to steric aspects. For silanol chemistry, preferentially T² and T¹ (see Figure 21 B) groups are formed. These are less stable towards hydrolysis, so not only a higher number of residual silanol groups is present but also inferior stability at high or low pH^{176, 181, 182}. Higher μ_{EOF} -values can thus be expected for coatings synthesized via silanol chemistry. Furthermore, an increase in EOF velocity and a decrease in performance when using aqueous BGEs is expected, when extreme pH-values are chosen.

PART 1: STRATEGY, PERFORMANCE AND STABILITY

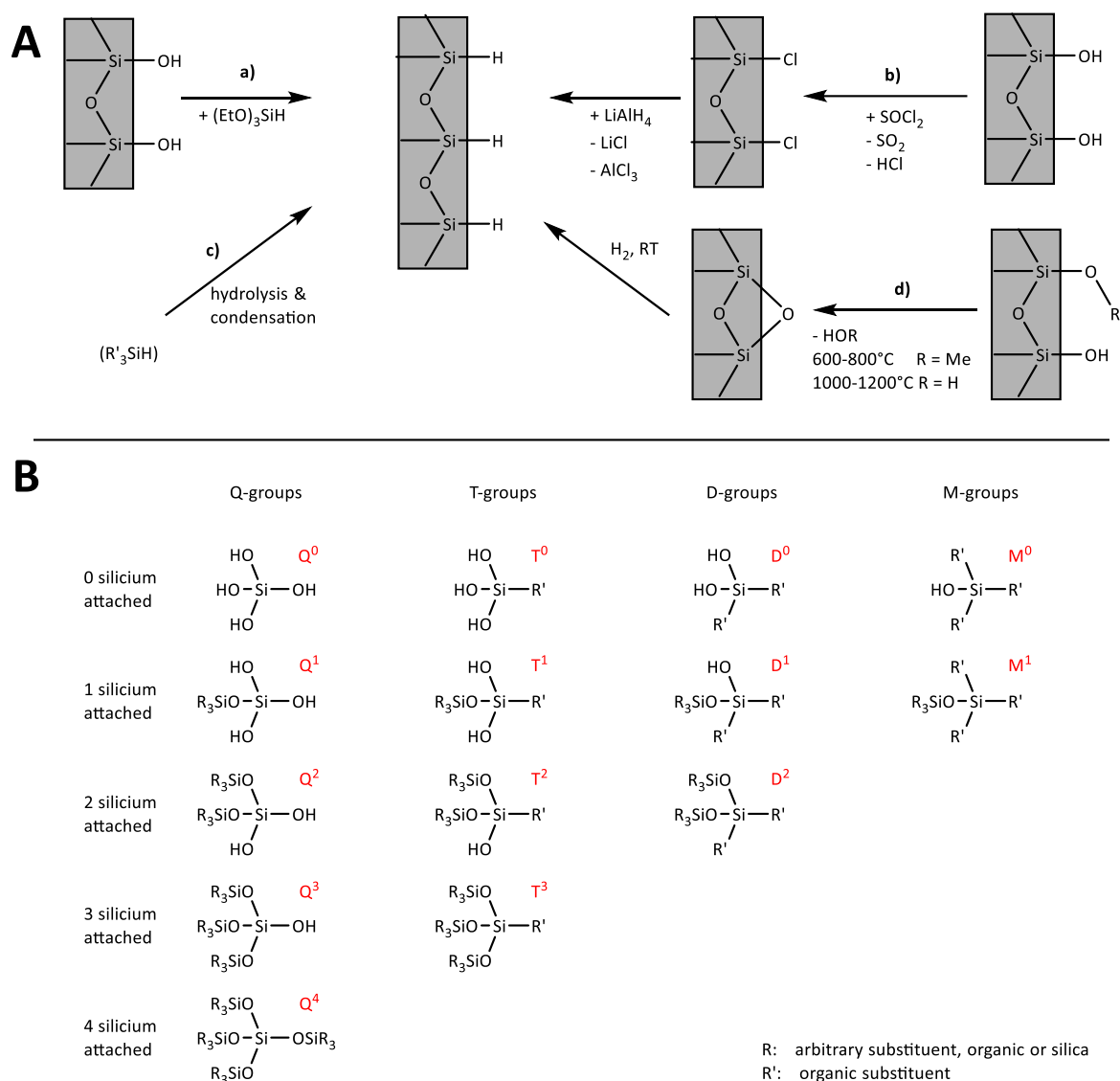


Figure 21: A: Established methods for the formation of a Si-H surface: a) modification of an existing silica-surface using silanol chemistry¹⁵⁰, b) transformation of Si-OH into Si-Cl using thionyl chloride followed by reduction to Si-H using LiAlH₄, c) preparation of a new bulk material using sol-gel chemistry starting from silanol species exhibiting desired Si-H-group, d) chemisorption of hydrogen onto a pyrolytically activated (methyl) silica surface¹⁷³⁻¹⁷⁵. **B:** Nomenclature of relevant silica species¹⁸³. Highest hydrolytic stabilities are assumed for high numbers of attached silicium atoms and various organic substituents. For T species the proposed trend of hydrolytic stability is T³>T²>T¹>T⁰.^{176, 181} R: arbitrary substituent (organic or silica), R': organic substituent

Chu *et al.*¹⁷¹ used silanol chemistry with expectable inferior stability, although the same group presented the formation of Si-H via Approach b) as a superior alternative to silanol chemistry before¹⁸⁴. For both silica particles and polyacrylamide-coated capillary surfaces, this Approach b) was presented to yield surfaces with splendid properties regarding degradation, even at extreme pH-values^{67, 168, 171, 185-187}. When optimizing the presented synthetic approach, starting with this procedure, I experienced challenges with reproducibility of the coating process. I here describe the optimization of the coating process and the stability of the capillaries coated with AAEE towards rinsing with strong base and acid (1 mol/L NaOH or HCl), demonstrating excellent performance. A technical innovation allows us to coat up to 8 capillaries of 2.1 m in length each simultaneously.

4.3. Materials and methods

4.3.1. Instrumentation and methods

4.3.1.1. Capillary electrophoresis

Fused silica capillaries with an inner diameter of 50 μm and an outer diameter of 365 μm were purchased from Polymicro (Kehl, Germany). If not stated otherwise, capillaries had a length of approx. 65 and 75 cm and an inner diameter of 50 μm . For CE analysis, an Agilent 7100 CE system (Agilent, Waldbronn, Germany) with UV-detection was used. For the determination of the electroosmotic mobility (μ_{EOF}), the chosen wavelengths were 210 nm and 280 nm with a spectral width of 10 nm and a reference wavelength of 360 nm. To decrease measurement times for EOF determination, caffeine-double injection was performed as follows: rinsing of capillary with BGE (here: 30 mmol/L aqueous NH_4OAc , pH 6.8) for 3 min with 1 bar followed by injection of a 1 g/L caffeine-solution containing 10 % BGE for 5 s at 100 mbar. A voltage of +30 kV was applied for 2-5 min prior to another injection of caffeine-solution for 5 s at 100 mbar. Hydrodynamic mobilization at 100 mbar for 10 min yielded 2 signals in the electropherogram allowing calculation of μ_{EOF} ^{188, 189}.

MS parameters for CE-MS measurements are described in Section 4.3.1.2. For CE-MS, measurements were performed as follows: rinsing the capillary with aqueous BGE (here: 0.75 mol/L acetic acid and 0.25 mol/L formic acid at pH 2.2, see also Pattky *et al.*¹⁴⁶) for 3 min with 1 bar followed by sample injection for 5 s at 100 mbar (tryptically digested BSA, see Section 4.3.3) and separation for 15-20 min at +30 kV with an additional pressure of 10 mbar. Injection of samples was performed hydrodynamically at various conditions.

After coating capillaries were conditioned prior to their first run by flushing with BGE for 10 min followed by application of +30 kV voltage for 5 min. After use, capillaries were consecutively rinsed 3 min with phosphate buffered saline (PBS), 2 min with water and 2 min with air, each at 1 bar.

4.3.1.2. Mass spectrometry

A quadrupole time-of-flight mass spectrometer 6550 (QTOF 6550) from Agilent (Santa Clara, CA, United States) with a sheath liquid interface from Agilent (Agilent Technologies, Waldbronn, Germany) was utilized by implementing an Agilent isocratic pump 1260 (Agilent Technologies, Waldbronn, Germany) at a flow rate of 5 $\mu\text{L}/\text{min}$. A jetstream electrospray ionization (ESI) source was operated with a nebulizer pressure of 275 and 345 mbar, for coated and non-coated capillaries, respectively. The drying gas temperature was 150°C. A flow rate of 11 L/min and a fragmentor voltage of 175 V were applied. Skimmer voltage was set to 65 V and octopole voltage to 750 V. The mass range was 100-3000 m/z with a data acquisition rate of 2 spectra/s. A 1:1 (v/v) mixture of 2-propanol/water was used as sheath liquid, containing 0.1 % formic acid as well as a few nanogram of 3 selected calibrants for internal calibration (Agilent Technologies, Waldbronn, Germany, m/z = 121.0508, 322.0481 and 922.0097).

During stability tests of capillary coatings, corrosion of sprayer would occur while rinsing with 1 mol/L HCl and 1 mol/L NaOH, if the sprayer would be mounted inside the source. Therefore, the sprayer tip with the mounted capillary was placed in a solution of 50 mmol/L NH_4OAc during rinsing with acid and base.

4.3.2. Chemicals

Lysozyme (chicken egg white), β -lactoglobulin (bovine milk), carbonic anhydrase (bovine erythrocytes), bovine serum albumin (BSA, bovine serum), sodium chloride (NaCl, $\geq 99\%$), *N,N,N',N'*-tetramethylene diamine (TEMED, $\geq 99\%$), ammonium peroxodisulfate (APS, $\geq 98\%$), 2-propanol (iPrOH, LC-MS grade), lithium aluminum hydride (LiAlH_4 , 1 mol/L solution in THF), tetrahydrofuran (THF, LC-MS grade), chloroplatinic acid hexahydrate ($\text{H}_2\text{PtCl}_6 \cdot 6\text{H}_2\text{O}$, ACS reagent, $\geq 37.50\%$ Pt basis), allyl methacrylate (AMA, $\geq 98\%$ with 50-185 ppm *p*-methoxyphenol as inhibitor), acetonitrile (ACN, LC-MS grade), spermine ($\geq 97\%$), spermidine ($\geq 99\%$), putrescine (analytical standard) and formic acid (LC-MS grade) were purchased from Sigma-Aldrich (Steinheim, Germany). Trypsin (sequencing grade modified) was purchased from Promega (Mannheim, Germany). Ammonium hydrogen carbonate (NH_4HCO_3 , $\geq 99.5\%$) was delivered from Fluka (München, Germany). Sodium hydroxide solution (NaOH, 10 mol/L, suprapur), ammonium acetate (NH_4OAc , ACS reagent grade $\geq 97\%$), thionyl chloride ($\geq 99.0\%$, reagent grade) and glacial acetic acid ($\geq 99.9\%$) were delivered by Merck (Darmstadt, Germany). Hydrochloric acid (32 % in water, analytical grade) and 1,4-dithiothreitol (DTT, $\geq 99\%$ electran for microbiology) were purchased from VWR (Darmstadt, Germany). Sodium dihydrogen phosphate dehydrate (NaH_2PO_4) was purchased from Caelo (Hilden, Germany). RapiGest was bought from Waters (Eschborn, Germany). Methanol (MeOH, HPLC-grade) was obtained from Honeywell (Seelze, Germany). Toluene (HPLC grade) was purchased from Fisher Scientific (Schwerte, Germany). *N*-acryloylamido ethoxyethanol (AAEE, $\sim 50\%$ solution in water, $\geq 98\%$, with $\sim 0.01\%$ hydroquinone as stabilizer) was purchased from Santa Cruz Biotechnology (Heidelberg, Germany). Caffeine (water free, pharmaceutical purity) was delivered from Fagron (Barsbüttel, Germany). Deionized water was prepared using an ELGA-Veolia PURELAB Classic system (Celle, Germany).

Dry toluene and THF (reagent grade, Sigma Aldrich, Steinheim, Germany) were obtained using a M. Braun Solvent Purification System (SPS, Garching, Germany).

4.3.3. Preparation of tryptically digested BSA and PBS

Tryptic digestion of BSA was performed using a modified protocol as reported previously¹⁴⁶. In brief, 2 μL BSA solution ($c = 10\text{ g/L}$ in water) were mixed with 15 μL of a 0.1 % RapiGest-solution and with 1.3 μL 50 mmol/L aqueous DTT-solution, both containing 50 mmol/L NH_4HCO_3 . The mixture was incubated for 1 h at 60 °C. 4 μL of a 50 mmol/L iodoacetamide solution in water has been added followed by mixing and incubation in the dark for 30 min at ambient temperature. 20 μL of a 10 mg/L trypsin-solution containing 500 $\mu\text{mol/L}$ acetic acid, 86 % acetonitrile and 14 % water were added prior to incubation at 37 °C overnight.

The phosphate-buffered saline (PBS) was made of 150 mmol/L NaCl and 10 mmol/L NaH_2PO_4 . The pH was adjusted to 7.4 by conductometric titration with 10 mol/L NaOH utilizing a WTW inoLab pH7110 pH meter (WTW, Dienslaken, Germany).

A freshly prepared protein solution containing the four proteins BSA, lysozyme, β -lactoglobulin and carbonic anhydrase in mass-ratios 64:16:4:1 and an overall protein concentration of 10 g/L in PBS was used.

4.3.4. Preparation of fish egg samples

Fish egg samples from genetically modified zebrafish (*Danio rerio*) were obtained using a single fish egg. Preparation was as follows: 1 fish egg was incubated in 50 μ L methanol in an ultra-sonification bath. Sample preparation included precipitation of interfering substances with 5 μ L of a 5 mol/L HCl and protein precipitation upon addition of 140 μ L acetonitrile followed by centrifugation for 15 min at 3000 x g. 20 μ L of the resulting solution were used for injection.

4.3.5. Preparation of serum samples and extraction of protein signals

Blood was obtained from a healthy male subject using citrate vacutainer blood extraction tubes (SARSTEDT S Monovette 3 mL, 66 x 11 mm, Citrat 3.13 %, sterile, Sarstedt AG & Co., Sarstedt, Germany). Freshly obtained blood was directly centrifuged for 10 min at 2500 x g using a 5417R centrifuge (Eppendorf Vertrieb Deutschland GmbH, Wesseling-Berzdorf, Germany). Supernatant serum was then directly aliquoted in fractions of 1 mL and stored at -80 °C until use.

Protein signals in human serum samples: Identification of proteins in the sample was conducted using Agilent MassHunter Qualitative Analysis B.06.00 software for molecular feature extraction for large molecules (proteins and oligos). Only a small selection of identified proteins is presented here, the EICs are as follows: S1: $m/z_{\text{experimental}} = 1281.511$, deconvoluted molecular mass = 17926.65 Da, S2: $m/z_{\text{experimental}} = 1327.542$, deconvoluted molecular mass = 17926.65 Da, S3: $m/z_{\text{experimental}} = 1145.500$, deconvoluted molecular mass = 54939.14 Da, S4: $m/z_{\text{experimental}} = 1614.502$, deconvoluted molecular mass = 69372.83 Da, S5: $m/z_{\text{experimental}} = 1814.687$, deconvoluted molecular mass = 29020.77 Da, S6: $m/z_{\text{experimental}} = 840.934$, deconvoluted molecular mass = 32755.59 Da, S7: $m/z_{\text{experimental}} = 868.031$, deconvoluted molecular mass = 28612.14 Da.

4.3.6. Capillary coating

4.3.6.1. Autoclave for parallelized rinsing of multiple capillaries with corrosive solvents

To avoid corrosion of expensive CE-devices, coated capillaries were prepared using a stainless-steel autoclave, see Figure 22. This device was designed and manufactured in-house and offers the possibility to coat up to 8 capillaries in parallel. Capillaries with lengths of up to 2.1 m were successfully utilized using a raw pressure of 8 bar. Longer capillaries were not investigated but are expected to be applicable. Common 100 mL beakers with the different coating solutions were placed inside, offering the possibility of excessive rinsing over long periods. In Figure 22, only 4 of 8 capillaries were mounted using polyether ether ketone (PEEK) F-300x micro-ferrules with F-113 micro ferrule and F-385 sleeves from IDEX (Oak Harbor, WA, USA) whilst blocking and sealing the remaining 4 holes using screws and Teflon tape.



Figure 22: Stainless steel autoclave used for parallelized capillary coating with corrosive solvents. Up to 8 capillaries with lengths up to 2.1 m were flushed at once, longer capillaries were not investigated but are expected to be utilizable.

4.3.6.2. Preparation of hydrated capillary surface (Si-H-capillaries)

Capillary coatings were prepared as follows: preconditioning of capillaries by consecutive rinsing with methanol, 1 mol/L HCl, 1 mol/L NaOH and water, each for 10 min at 8 bar. The capillaries were then rinsed with thionyl chloride for 1.5 h at 8 bar, followed by 45 min with toluene and 20-22 h with 30 mmol/L LiAlH₄ solution, prepared by diluting a 1 mol/L LiAlH₄ solution in THF with a 1:1 mixture of toluene and THF. Two synthetic approaches differing in the dryness of the solvents used in this synthesis step were evaluated to determine the relevance of solvent dryness. One was performed using solvents dried using an SPS (dry solvents, Batch 1) and one was performed using non-processed solvents (regular solvents, Batch 2). Capillaries were then rinsed with THF for 15 min, followed by air for 5 min. Then, the EOF was determined before proceeding with the polymerization step.

4.3.6.3. Preparation of covalently bound *N*-acryloylamido ethoxyethanol (AAEE-capillaries)

Capillaries with a Si-H-surface were consecutively rinsed with MeOH and air for 5 min at 8 bar followed by incubation at 100 °C for 30 min. The capillaries were then filled hydrodynamically with a freshly prepared solution consisting of 26 mmol/L H₂PtCl₆ · 6H₂O in 74 % AMA and 26 % iPrOH at 1 bar for approx. 40-50 sec followed by incubation at 100 °C for 30 min. Afterwards, capillaries were rinsed with air at 8 bar for 1-3 min until air-bubbles were observed in the outlet vial. This step was directly followed by filling the capillaries with an aqueous solution containing 0.04 % APS, 0.04 % TEMED and 1.5 % AAEE using a pressure of 1 bar, followed by incubation at ambient temperature for 1 h. Capillaries were then emptied from reaction solution by subsequent rinsing at 8 bar for

NOVEL APPROACH FOR THE SYNTHESIS OF A COVALENTLY BOUND, HIGHLY POLAR AND PH-PERSISTENT N-
ACRYLOYLAMIDO ETHOXYETHANOL CAPILLARY COATING FOR CAPILLARY ELECTROPHORESIS-MASS SPECTROMETRY

PART 1: STRATEGY, PERFORMANCE AND STABILITY

5 min with air, 10 min with water and 10 min with ACN. For storage, the capillary was then rinsed with air for 5 min at 8 bar.

Capillaries can be stored under air and at ambient temperature for at least 2.5 years prior to first use as well as between different uses. Longer storage times were not investigated. Rinsing with aqueous BGE for 15 min proved to be sufficient for capillary preconditioning.

4.4. Results

To investigate the quality of capillary coatings, EOF-measurements and separation performance in CE-MS with tryptically digested BSA as model sample (both $n = 5$) were considered, see Section 4.3.1.1. The experimental design is depicted in Figure 23: After coating synthesis, each capillary was cut into three pieces of 65 to 75 cm in length, which were used either for EOF determination or for the determination of CE-MS performance parameters, thus avoiding possible hysteresis effects or different numbers of measurements conducted with each capillary. The third piece was kept as backup. The differences in final lengths of the capillaries investigated here (approx. 75 cm for Batch 1 and approx. 65 cm for Batch 2) were mainly due to clogging, which occurred more frequently in Batch 2 during hydration-step. Capillaries had to be shortened by up to 20 cm to ensure permeability, resulting in total capillary lengths of approx. 1.9 m instead of 2.1 m before cutting the capillary into three separation columns.

To judge separation performance in CE-MS and investigate inter-batch precision and coating stability towards harsh rinsing conditions (HCl, ACN, NaOH, see Figure 23) plate height (H), peak area (A) and effective electrophoretic mobility (μ_{eff}) of 6 tryptic peptides were taken into consideration. Overall, longer storage times between series of measurements were avoided for better comparison.

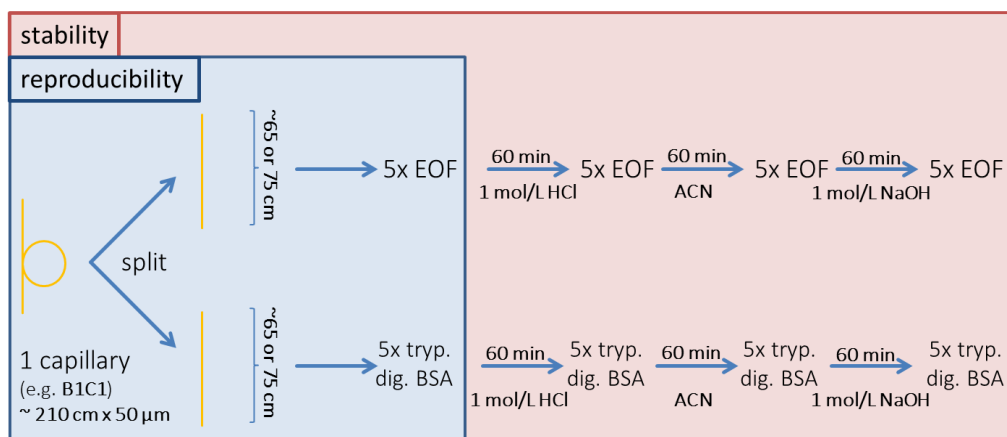


Figure 23: Scheme illustrating the approach for the investigation of reproducibility (blue) and stability (red). **Blue square:** Each capillary from the two both batches (differing in the dryness of the solvents THF and toluene) was cut into 3 pieces of which 2 pieces were approx. 65 cm (Batch 2) and 75 cm (Batch 1) in length. One piece of each capillary was investigated regarding EOF mobility. The separation efficiency and precision for a model tryptic digest of BSA were determined for 4 capillaries from Batch 1, and 2 capillaries for Batch 2. **Red square:** Measurements regarding stability were conducted for one capillary piece from each batch (e.g. B1C1 for Batch 1) subsequent to measurements regarding reproducibility to assure like storage conditions for all capillaries.

4.4.1. Reproducibility of capillary coatings

4.4.1.1. Extent of surface-coverage depicted via μ_{EOF}

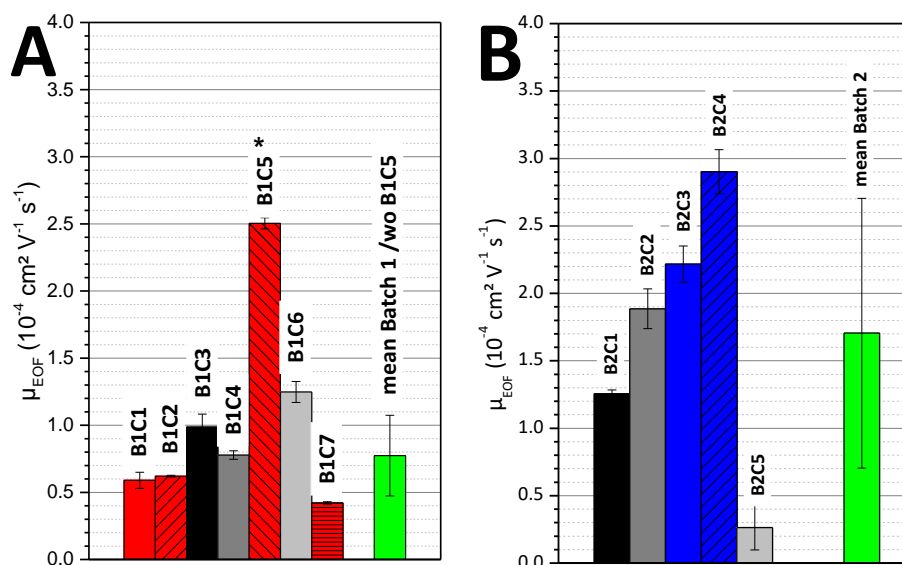


Figure 24: μ_{EOF} -values determined for each capillary of A: Batch 1 (B1): Batch with dry solvents and B: Batch 2 (B2): Batch with regular solvents, $n = 5$. C1-7: Capillary numbers within the batch. Black, gray and red columns represent data for a single capillary, labels above represent batch-number B and capillary number C in a 4-letter pattern, e.g. B1C5 for Capillary 5 of Batch 1. The bar marked with * was an outlier (Grubbs). The green bars represent the intra-batch average after exclusion of outliers (*). The pattern-scheme of red bars is uniform to that in Figure 26, allowing correlation between μ_{EOF} and its separation performance towards tryptically digested BSA.

μ_{EOF} -values were determined for each capillary from the two batches via caffeine-double-injection ($n=5$), see Section 4.3.1.1. Capillaries prepared in the same batch exhibited different absolute μ_{EOF} -values, as can be seen in Figure 24 A for Batch 1 (dry solvents during the hydration step) and in Figure 24 B for Batch 2 (regular solvents). In case of Batch 1, 1 of 8 capillaries but for Batch 2, 3 of 8 capillaries clogged during the hydration step, which already demonstrates the importance of using dry solvents. 5 of the 7 permeable capillaries of Batch 1 (71 %) exhibited $\mu_{\text{EOF}} \leq 1 \cdot 10^{-4} \text{ cm}^2 \text{ V}^{-1} \text{ s}^{-1}$, one of them even smaller than $0.5 \cdot 10^{-4} \text{ cm}^2 \text{ V}^{-1} \text{ s}^{-1}$. Only one capillary was found to have a high $\mu_{\text{EOF}} \approx 2.5 \cdot 10^{-4} \text{ cm}^2 \text{ V}^{-1} \text{ s}^{-1}$, identified as an outlier (Grubbs-outlier-test, marked with an asterisk in Figure 24 A). For Batch 2, one capillary revealed $\mu_{\text{EOF}} = 0.3 \cdot 10^{-4} \text{ cm}^2 \text{ V}^{-1} \text{ s}^{-1}$ and was found not to be an outlier, although the other 4 capillaries had $\mu_{\text{EOF}} > 1.2 \cdot 10^{-4} \text{ cm}^2 \text{ V}^{-1} \text{ s}^{-1}$, see Figure 24 B. Grubbs-outlier-test parameters were performed as follows: Batch 1 (g -value = 2.09 > $g_{\text{crit}, \alpha=0.05, n=7} = 2.02$, outlier confirmed) and Batch 2 (g -value = 1.44 < $g_{\text{crit}, \alpha=0.05, n=5} = 1.72$, outlier neglected).

The mean electroosmotic mobility μ_{EOF} of a batch was calculated via the means ($n=5$) of each capillary ($n = 7$ (5) for Batch 1 (2)). Similar results were obtained combining the results for all single measurements ($n = 35$ (25) for Batch 1 (2)). When comparing the mean of both batches using a t -test (2 tailed, assuming different variances and averages), the results were found not to be significantly different ($p = 0.11$). Therefore, electroosmotic mobilities were found to be independent from the kind of solvent used. However, higher error-bars in μ_{EOF} -values were observed for every capillary in Batch 2 compared to Batch 1. This indicates inferior run-to-run reproducibility for capillaries prepared using regular solvents.

4.4.1.2. Separation performance towards triptically digested BSA

Preliminary remarks: Separation performance but also stability measurements (see Section 4.4.2) were performed within 48 h using CE-MS with the same measuring conditions, sample and BGE solution. BGE in the separation vial was exchanged after 5 consecutive measurements. Six peptides detected in tryptically digested BSA were chosen for the determination of capillary performance. They show a wide range of m/z -values, a broad range of migration times and resolution including only partial resolution for some peptides. The respective m/z -values were determined and peptides numbered with increasing migration time t_{mig} as follows: **1:** 417.197, **2:** 473.883, **3:** 379.700, **4:** 526.240, **5:** 395.224 and **6:** 740.370, see also Figure 25.

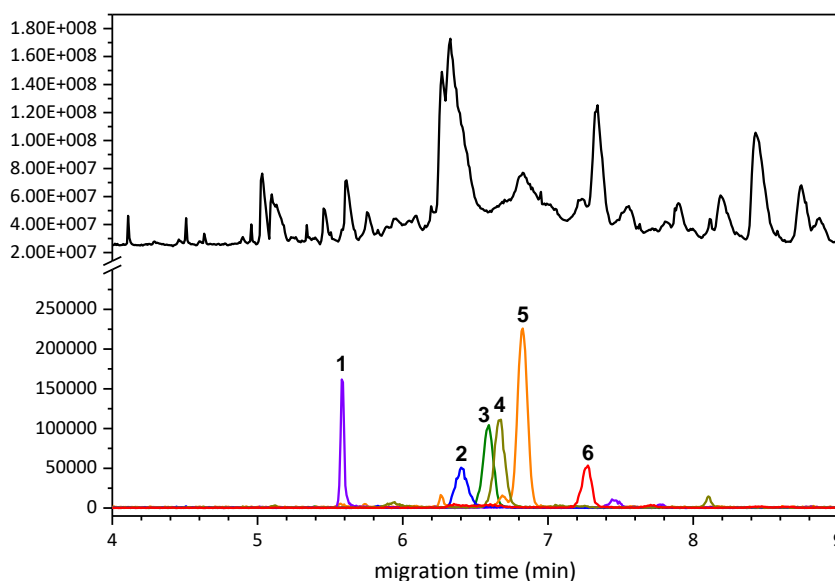


Figure 25: Exemplary CE-MS-electropherogram from B1C1 ($L = 75.5$ cm), showing the total ion current (TIC, black) as well as the EICs of peptides 1-6 from a tryptic digest of BSA. m/z -values extracted are: **1:** 417.197, **2:** 473.883, **3:** 379.700, **4:** 526.240, **5:** 395.224 and **6:** 740.370. Samples with tryptically digested BSA, prepared according to Section 4.3.3, were injected hydrodynamically at 100 mbar for 5 s. Separation was carried out in 0.75 mol/L acetic acid and 0.25 mol/L formic acid at 30 kV and an additional pressure of 10 mbar for 15 – 20 min.

Since capillaries with different lengths were used effective electrophoretic mobilities (μ_{eff}) were calculated assuming zero EOF at this low pH to determine the repeatability for each peptide in repeated measurements in a single capillary, see Figure 26 A for results. Instead of resolution and plate number, plate height (**H**) was determined to describe separation efficiency to eliminate the influence of different capillary lengths, see Figure 26 B. Quantitative precision was evaluated via peak areas (**A**) of each peptide signal for measurements in different capillaries, see Figure 26 C.

Calculation of RSDs was performed as follows:

- I define intra-capillary differences as the precision of μ_{eff} , H and A obtained for repeated analysis of tryptically digested BSA ($n = 5$) using a single capillary (repeatability). RSDs for single capillaries were calculated for each of the six peptides ($n = 5$) separately (see Figure 26). Since the RSDs of different peptides were always comparable, the RSDs presented in Table 4 for single capillaries were obtained by averaging the RSDs of all six peptides.
- I discuss inter-capillary differences via intra- vs. inter-batch differences. RSDs were first calculated for each peptide using the median values of μ_{eff} , H and A per capillary of Batch 1 and

2. Intra-batch differences were calculated for 4 capillaries (Batch 1) or 2 capillaries (Batch 2), whereas inter-batch differences used results for all 6 capillaries. The RSD (range) of μ_{eff} , H and A was considered. The obtained values were comparable for all 6 peptides and are thus displayed as a mean in Table 4.

Intra-capillary differences: Averaged RSDs for all peptides were calculated and are presented in Table 4 for the capillaries with best (**B1C2** and **B2C3**) and poorest (**B1C2** and **B2C4**) separation performance in both batches. Additionally, medians over capillaries were calculated. Therein, RSD(μ_{eff}) ranged from 0.9 % to 2.4 %, RSD(H) from 3.4 % to 13.8 % and RSD(A) from 4.5 % to 16.5 %, which indicates a slightly better reproducibility of μ_{eff} but about two times better reproducibility of A and H for Batch 1. The results show that (i) similar trends in RSDs for μ_{eff} , A and H were observed increasing in the order **B1C2**, **B2C3**, **B2C4** and **B1C1** (see Table 4). This shows that the coating quality is vital for all parameters of a separation including quantitative precision. (ii) Overall, lower RSDs and thus higher precision were obtained for capillaries of Batch 1, pointing out the importance of solvent dryness during the hydration step as already indicated by the number of clogged capillaries and higher EOF repeatability (Section 4.4.1.1). However, the strong differences in precision comparing the results from different capillaries also shows that the synthesis is not yet fully reproducible.

For Batch 1 and 2, I calculated the intra-batch capillary relative standard deviation for μ_{eff} , A and H for each peptide in all capillaries of one batch. For Batch 1 (Batch 2) RSDs were: RSD(μ_{eff}) = 12.6 % (11.6 %), RSD(H) = 33.8 % (34.0 %) and RSD(A) = 19.0 % (26.2 %). Except for peak area RSDs were comparable for Batch 1 and Batch 2. High intra-batch variances were observed for migration time, peak area as a quantitative parameter and plate height as a measure for separation efficiency, but these were observed to be independent from the dryness of the solvent used in the hydration step.

Table 4: Standard-deviations of effective electrophoretic mobility μ_{eff} , plate height H and peak area A for intra-capillary- (run-to-run-precision), intra-batch- and inter-batch-characterization regarding repeatability and reproducibility. All values are in %.

	Batch 1			Batch 2		
	RSD(μ_{eff}) (%)	RSD(H) (%)	RSD(A) (%)	RSD(μ_{eff}) (%)	RSD(H) (%)	RSD(A) (%)
intra-capillary	0.9 ^a 2.4 ^b 1.9 ^e	3.4 ^a 13.8 ^b 3.9 ^e	4.5 ^a 16.2 ^b 6.8 ^e	1.0 ^c 2.0 ^d 1.5 ^f	6.7 ^c 11.0 ^d 8.9 ^f	8.8 ^c 14.1 ^d 11.5 ^f
intra-batch	12.6 ^g	33.8 ^g	22.1 ^g	11.6	34.0	26.2
	RSD(μ_{eff}) (%)		RSD(H) (%)		RSD(A) (%)	
inter-batch	18.3		55.7		22.5	

Data obtained using ^aB1C2 (best capillary of Batch 1), ^bB1C1 (poorest capillary of Batch 1), ^cB2C3 (best capillary of Batch 2) and ^dB2C4 (poorest capillary of Batch 2). ^eMedian of intra-capillary RDS for both capillaries of Batch 1. ^fMedian of intra-capillary RDS for all capillaries of Batch 2. ^gIntra-batch-standard deviations of Batch 1 when omitting B1C5 as outlier calculated as described in the text.

NOVEL APPROACH FOR THE SYNTHESIS OF A COVALENTLY BOUND, HIGHLY POLAR AND PH-PERSISTENT N-ACRYLOYLAMIDO ETHOXYETHANOL CAPILLARY COATING FOR CAPILLARY ELECTROPHORESIS-MASS SPECTROMETRY
PART 1: STRATEGY, PERFORMANCE AND STABILITY

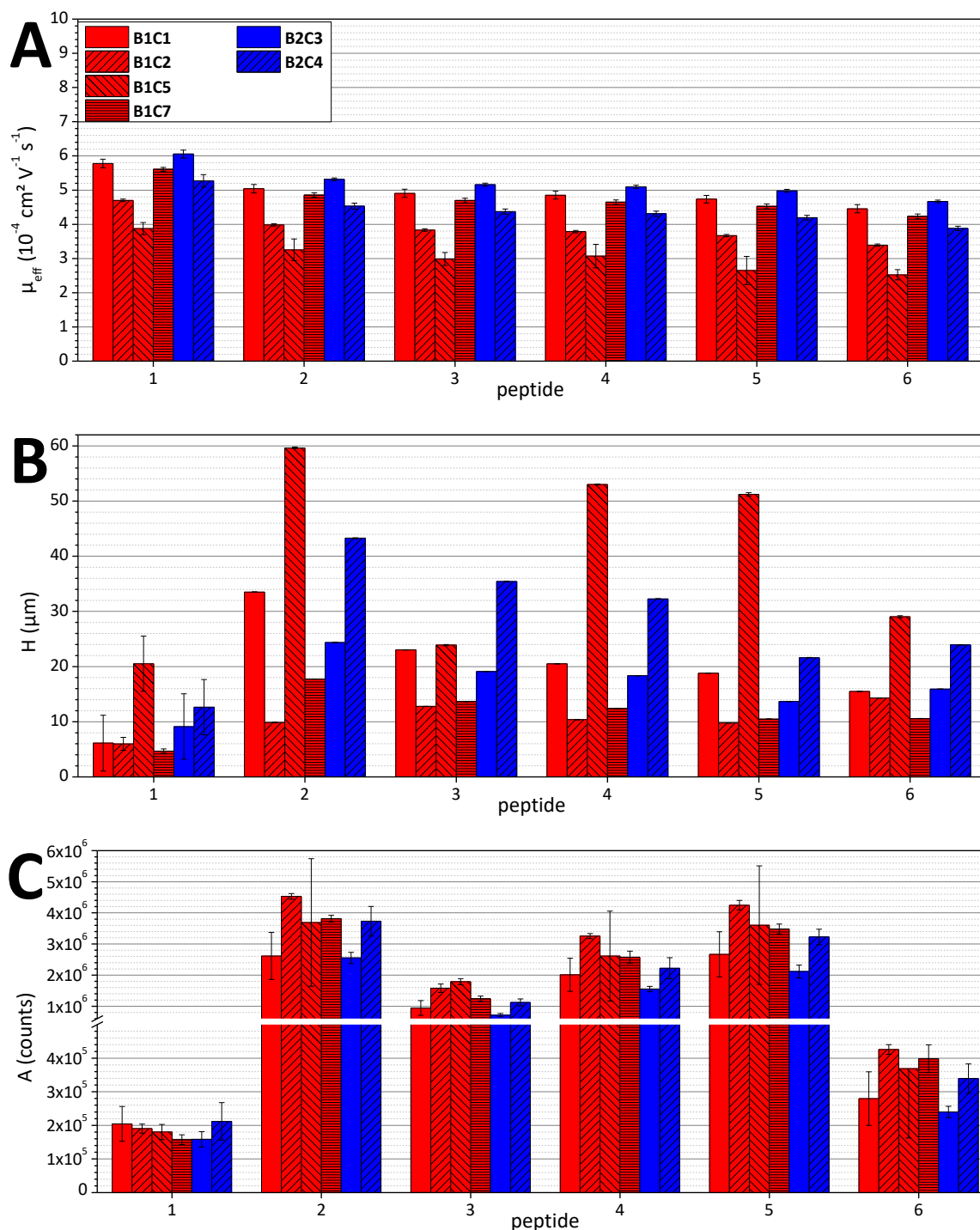


Figure 26: A: Effective electrophoretic mobility μ_{eff} , B: plate height H and C: peak area A determined for each of the 6 peptides detected in tryptically digested BSA for different capillaries (see legend) ($n = 5$). A representative electropherogram is presented in Figure 25. Red bars belong to Batch 1 (dry solvents) and blue bars to Batch 2 (regular solvents). Representative capillaries of both batches were chosen. The same color code as in Figure 24 was used, allowing correlation between a capillaries μ_{EOF} and its separation performance for tryptically digested BSA.

Inter-batch comparability is visible comparing differences in μ_{eff} , A and H for capillaries of one batch in Figure 26 A. For μ_{eff} , trends are consistent for all peptides: No significant differences were found between both batches regarding μ_{eff} (p-values between 0.33 and 0.36), H (p-values between 0.46 and 0.92) as well as A (p-values between 0.20 and 0.95). The overall precision from all 30

measurements (4+2 capillaries) with 5 consecutive runs each, named inter-batch capillary precision can be determined to: $RSD(\mu_{\text{eff}}) = 18.3 \%$, $RSD(H) = 55.7 \%$ and $RSD(A) = 22.5 \%$. All results are summarized in Table 4.

4.4.2. Stability towards harsh rinsing conditions

The stability of AAEE-surfaces against harsh rinsing solutions (1 mol/L HCl, acetonitrile and 1 mol/L NaOH), commonly utilized for cleaning bare-fused silica capillaries in CE-UV-setups, was investigated. On total, 20 measurements were made. After the first 5 measurements the capillary was rinsed with 1 mol/L HCl for 1 h at 1 bar. Directly afterwards, 5 new measurements were made, followed by rinsing with acetonitrile at the same conditions and, finally, after 5 further measurements by rinsing with 1 mol/L aqueous NaOH solution. The experiment was finalized with a further series of measurements ($n = 5$) as depicted in Figure 27. Capillaries with poorest separation efficiency for tryptically digested BSA of both batches (**B1C1** with $\mu_{\text{EOF}} = 0.7 \pm 0.0 \cdot 10^{-4} \text{ cm}^2 \text{ V}^{-1} \text{ s}^{-1}$ and **B2C4** with $\mu_{\text{EOF}} = 2.3 \pm 0.1 \cdot 10^{-4} \text{ cm}^2 \text{ V}^{-1} \text{ s}^{-1}$) were chosen in order to prove that even poorest coating surfaces offer good properties regarding stability of the Si-C bond and do not show accelerated degradation even under extreme pH conditions.

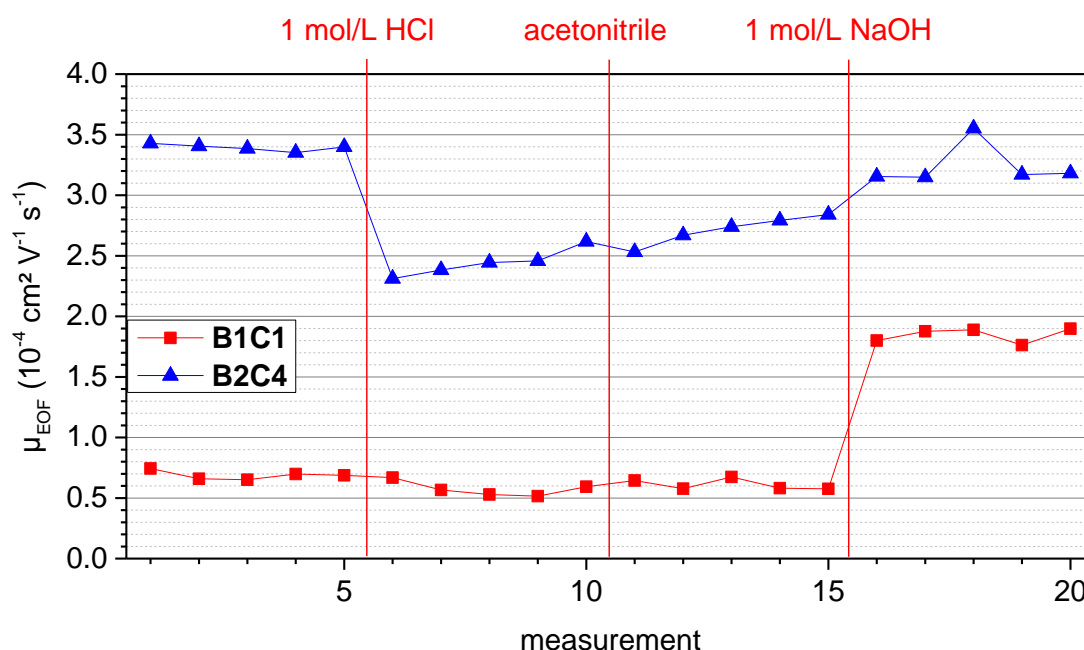


Figure 27: μ_{EOF} -values obtained during stability testing. The stability of the covalently bound coating was investigated using one capillary from each batch (B1C1, indicated by the red squares and B2C4, indicated by the blue triangles). The capillary was rinsed with (i) 1 mol/L HCl, acetonitrile and 1 mol/L NaOH for 1 h at 1 bar each. The electroosmotic mobility was determined before and after rinsing steps ($n = 5$) as described in Section 4.3.1.1. Vertical lines indicate the measurements in-between which rinsing was conducted.

μ_{EOF} -values were determined for every measurement according to Section 4.3.1.1. For capillary **B1C1** from Batch 1 no significant change in μ_{EOF} -values was observed prior to rinsing with 1 mol/L NaOH (t-test, 2 tailed, assuming different variances and averages, p -value = 0.00). After this rinsing step μ_{EOF} -values almost doubled, indicating a degradation of the surface-bound polymer. For the capillary from Batch 2 (**B2C4**) overall higher μ_{EOF} -values than for Batch 1 were observed. After rinsing with 1 mol/L HCl, μ_{EOF} -values decreased from 3.4 to $2.3 \cdot 10^{-4} \text{ cm}^2 \text{ s}^{-1} \text{ V}^{-1}$, followed by a steady

increase in μ_{EOF} -values afterwards. This indicates remaining silanol-groups at the surface which leads to prolonged equilibration of surface charges, due to hysteresis¹⁹⁰. After rinsing with 1 mol/L NaOH μ_{EOF} -values were insignificantly lower than those found for the original surfaces. Overall, this indicates a minor degradation of the surface coating despite the harsh rinsing conditions.

For separation performance for a tryptic digest of BSA the capillary **B1C1** showed decreased μ_{eff} for each peptide after rinsing with 1 mol/L HCl, see Figure 28 A. In contrast, resistance to further changes regarding rinsing with acetonitrile and 1 mol/L NaOH was observed. Comparable observations were made for **B2C4** except for Peptides 5 and 6, which exhibited higher μ_{eff} -values after rinsing with 1 mol/L HCl resulting in faster migration than Peptide 2.

Rinsing with 1 mol/L HCl furthermore revealed increased separation efficiency for each peptide for both capillaries as can be seen by the decrease of H in Figure 28 B. For **B1C1** no change in separation efficiency was observed for Peptides 2-6 after rinsing with acetonitrile and 1 mol/L NaOH. After rinsing with 1 mol/L NaOH, the separation efficiency of Peptide 1 signal declined to a level inferior to that obtained from the original coating. For **B2C4** no change in separation efficiency with additional rinsing was observed for Peptides 2, 4 and 5. For Peptides 1, 3 and 6 separation performance declined again upon rinsing with acetonitrile or 1 mol/L NaOH and reached the original values.

Peak areas A slightly decreased for Peptides 2-6 after rinsing with 1 mol/L HCl in **B1C1**. No significant changes were observed for **B2C4**. However, for both capillaries peak areas of Peptide 1 seemed to be lowered by a factor of 2 after rinsing with 1 mol/L HCl. However, the peak width was too small to allow for a reliable quantification at the data rate of 2 spectra/s.

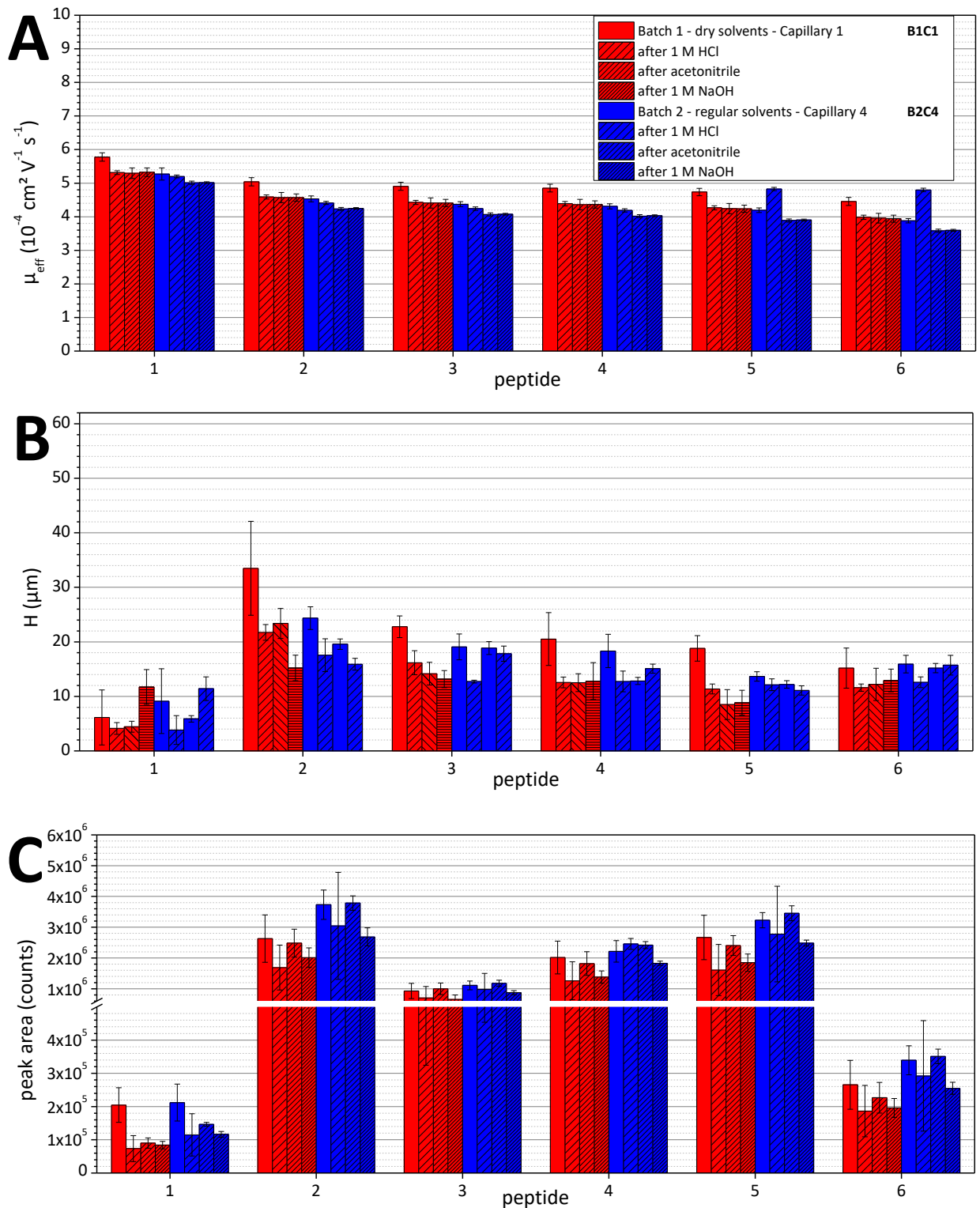


Figure 28: A: Effective electrophoretic mobility μ_{eff} , for 6 different peptides (see Figure 25), B: plate height H, and C: peak area A determined prior to and after each rinsing step (1 h, 1 bar). Red bars belong to B1C1, blue bars to B2C4. For detailed assignment see legend in A. Data were calculated as the mean of 5 consecutive measurements with error bars.

4.4.3. Application of AAEE-coated capillaries to complex samples

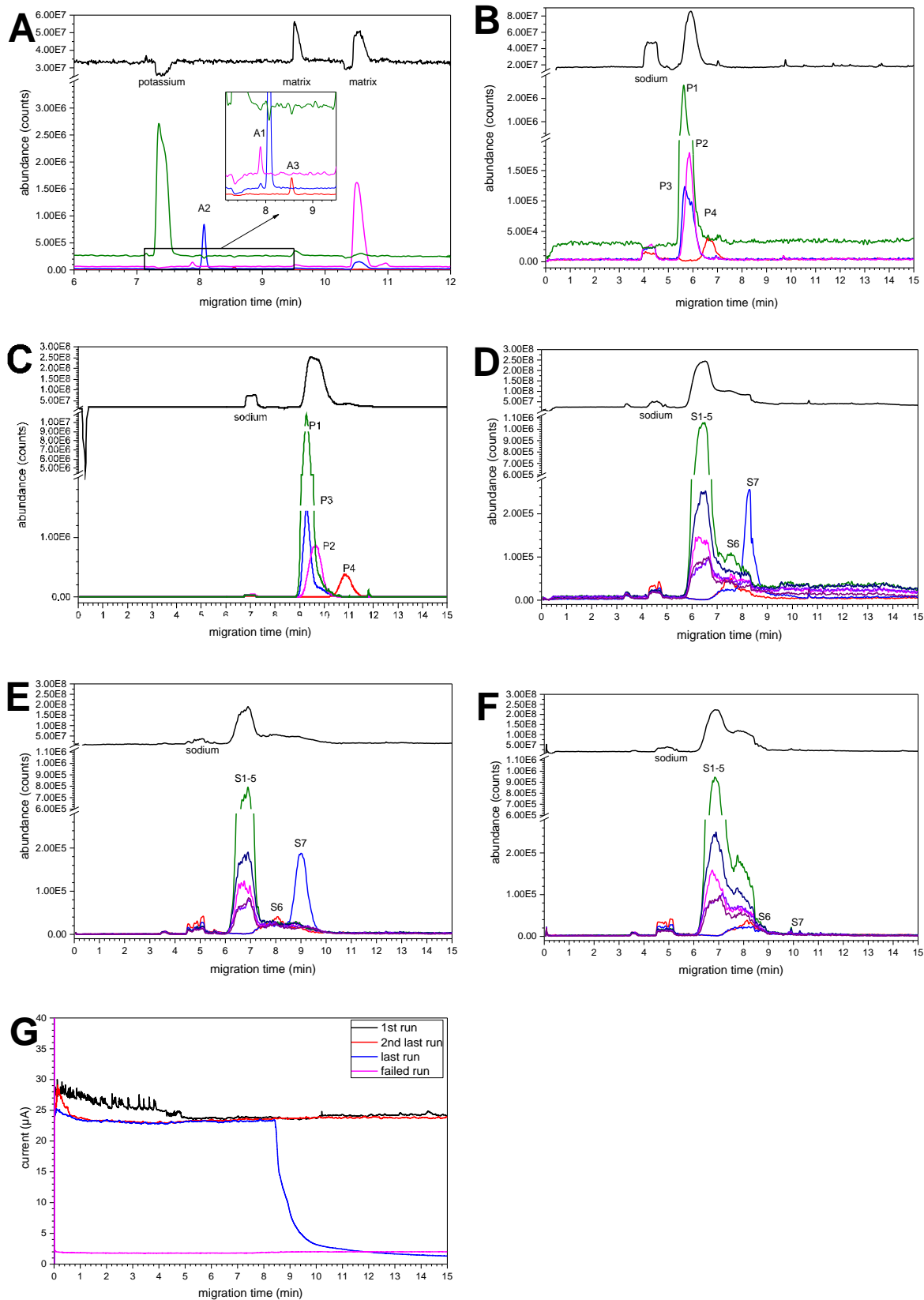


Figure 29: Representative electropherograms obtained using CE-MS utilizing the presented capillaries. BGE: 0.75 mol/L HOAc and 0.25 mol/L FA. Separation conditions: +30 kV and 20 mbar (A) or 100 mbar (B-G), MS parameters see Section 4.3.1.2. Electropherograms in B and D – F as well as currents presented in G were obtained using capillary B1C1 (73 cm in length). The electropherograms presented in A and C were recorded using a capillary (100 cm in length) from another batch with three years storage at ambient conditions in between. A: The electropherogram of a separation of a fish egg-sample, prepared from a single fish egg, is shown. Sample preparation was as described in Section 4.3.4. In-between runs the capillary was rinsed with BGE for 300 s. Injection was conducted for 7 s at 100 mbar. EICs of compounds of interest¹⁹¹ are as follows: A1: $m/z_{\text{theoretical}} = 203.224$ (spermine), A2: $m/z_{\text{theoretical}} = 146.166$ (spermidine), A3: $m/z_{\text{theoretical}} = 89.108$ (putrescine). Separation of analytes from the macrocomponent potassium in the sample is shown in green, which indicates the potassium adduct of an internal tune-mass ($m/z_{\text{experimental}} = 959.966$). B and C: Standard protein mixture in PBS with $c_{\text{protein}} = 4.2$ g/L, mass-ratio of BSA : lysozyme : β -lactoglobulin : carbonic anhydrase = 64:16:4:1. EICs of protein isoforms (not further identified) are plotted: P1 lysozyme ($m/z_{\text{experimental}} = 1431.542$, deconvoluted molecular mass = 14305.34 Da), P2 BSA ($m/z_{\text{experimental}} = 1359.170$, deconvoluted molecular mass = 66550.40 Da), P3 β -lactoglobulin ($m/z_{\text{experimental}} = 1219.520$, deconvoluted molecular mass = 18277.52 Da) P4 carbonic anhydrase ($m/z_{\text{experimental}} = 830.325$, deconvoluted molecular mass = 29026.04 Da). D-F: Protein signals in human serum samples, diluted 1:1 with PBS. For protein signal generation via MS software, see Supporting information. The first (D) and last (E) successful separation are shown together with the results for the first measurement after clogging (F). G: Current recording for the measurements shown in D-F. Injection of sample in B - F was conducted for 4 s at 100 mbar followed by BGE for 10 s at 100 mbar. In between runs for protein and serum analysis, the capillary was rinsed with 50 mmol/L HCl for 2 min at 1 bar prior to preconditioning described in Section 3.1.1.

Capillaries covalently coated with AAEE via an Si-C linkage were applied for the separation of large intact proteins as well as small and highly charged polyamines using the acidic BGE of acetic and formic acid during the reproducibility and robustness testing.

4.4.3.1. Analysis of highly charged polyamines in fish eggs

An AAEE capillary was successfully applied for the separation of the polyamines spermine, spermidine and putrescine in an egg from a genetically modified zebrafish (*Danio rerio*) to investigate biosynthesis¹⁹¹. Three samples were investigated, each an acidified aqueous extract of a single fish egg. A high separation efficiency of $N = 2.4 \cdot 10^5$, $H = 4.1$ μm and peak base widths of 6-12 s (see Figure 29 A) also manifests in the uniformly high resolution R ($R \approx 7.1$ between putrescine and spermidine and $R \approx 2.9$ between spermidine and spermine). The high repeatability of migration times ($\text{RSD}(t_{\text{mig}}) = 0.4$ % for aqueous standard samples and $\text{RSD}(t_{\text{mig}}) < 3$ % for fish eggs) and peak area ($\text{RSD}(A) = 6.4 - 17.3$ %) are remarkable given that these amines are normally used as dynamic coating agents in CE-UV experiments¹⁶⁴. Lower reproducibility regarding both peak area and t_{mig} , was observed for the fish egg samples due to the influence of matrix. No signs of degradation or contamination of the capillary surface were observed during the series of 27 experiments. No rinsing step except rinsing for 300 s (500 s) with BGE was necessary.

4.4.3.2. Separation of intact protein standards and intact human serum proteins

Electropherograms for intact proteins revealed symmetrical peaks, both for pure proteins dissolved in PBS (Figure 29 B and C) and proteins in serum mixed with PBS 1:1 (see Figure 29 D-F).

This indicates low adsorption on the capillary surface. For capillaries with a length of 73 cm (see Figure 29 B, D-F), peak-widths at the base in the range of 1 min and broader were obtained for the proteins. Good separation from sodium ions is visible. At this low pH, the overall analysis time was below 10 min. Insufficient separation of proteins was due to sample-induced transient isotachopheresis (tITP). Successful separation was achieved by using a longer capillary (100 cm in length), as shown in Figure 29 C. $\text{RSD}(t_{\text{mig}})$ -values obtained were different for each protein. These were reduced from 2.3 – 7.3 % for the 73 cm long capillary to 1.9 – 2.0 % for the 100 cm long

capillary. Further attempts to increase the separation performance (e.g preliminary reduction of sodium concentration or varying BGE composition regarding e.g. pH or composition), were not made. For intact protein standards, 40 consecutive runs were made without changes in the performance. Rinsing with 50 mmol/L HCl for 2 min followed by rinsing with BGE for 3 min, both at 1 bar, was sufficient.

Afterwards, human serum, only 1:1 diluted with PBS was injected. A representative electropherogram is shown in Figure 29 D (1st measurement of serum on this capillary, conducted directly after measurements of standard proteins) with some mass traces of intact proteins not further identified. Peak base widths of 1 min and higher were obtained. Broader signals were obtained, presumably due to the higher complexity of both protein isoforms and sample matrix. In Figure 29 E and F the electropherograms of the last two measurements (no. 28 and 29) with serum are shown. Afterwards, all conducted measurements exhibited very low current (approx. 2 μ A), high background, and no protein signals were detected. When taking the rapidly decreasing current for the last successful measurement at approx. 9 min in Figure 29 G into account it is obvious, that clogging of capillary occurred, most likely due to protein agglomeration. Compared to the first measurement with serum no peak broadening can be observed for the last successful measurement.

Overall, more than 140 electropherograms (approx. 100 h measurement time) were recorded with intact proteins and serum samples. I expect a better applicability when using appropriate rinsing protocols or some sample preparation.

4.5. Discussion

4.5.1. Novelty in preparation procedure

Despite the problems during the hydration step regarding moisture, which are discussed in literature¹⁷¹, I was able to design a synthetic strategy to covalently couple AAEE to the silica surface via stable Si-C bonds. Si-H surfaces were prepared using pure thionyl chloride and 30 mmol/L LiAlH₄. An inert atmosphere was not required for this reaction step. Using dried solvents in this reaction step did not impact electroosmotic flow velocities or separation efficiency. However, the reaction procedure had to be optimized to reduce clogging events by: (i) using pure thionyl chloride, (ii) using a low concentrations of LiAlH₄ in a 1:1 mixture of THF and toluene and (iii) collecting the rinsing solvent in hydride-quenched THF:toluene. With a simple pressurized vessel, I was able to coat up to 8 capillaries in parallel, each 2.1 m long giving rise to up to 24 capillaries suitable for CE-MS analysis. Longer capillaries were not tested. The batch-wise processing reduces the coating procedure per capillary to 2.5 h per capillary. I want to stress that the capillary surfaces were stable enough to allow long-term storage at ambient conditions even after use.

Compared to the coating of particles for chromatography, rinsing allowed us to work with at least 10.000 – 100.000-fold excess of thionyl chloride and LiAlH₄¹⁸⁴. I assume this circumstance to strongly favor both Si-Cl and Si-H surface group formation. The capillary format revealed further advantages: drying capillaries after Si-H formation took only 1 h instead of 6 h in particle coating reactions, and Speier-catalytic linkage was strongly accelerated from 24 h to 30 min due to a 100-fold higher amount of the catalyst compared to literature^{171, 184}. Overall preparation times were thereby reduced to 2 days.

4.5.2. Reproducibility and stability of prepared capillaries

For intra-capillary repeatability, very good results were found for each capillary with RSD(μ_{eff}) varying between 0.9 % to 2.4 %, see Table 4. For capillary-to-capillary reproducibility RSD(μ_{eff}) was found to be 11.6 % and 12.6 % for intra-batch and 18.3 % for inter-batch. Regarding the fact, that this topic is sparsely investigated in literature for CE-capillaries, in the following I compare separation performances regarding RSD(μ_{eff}) with RSD values of retention factors RSD(k). The group of Guiochon *et al.* presented RSD(k)-values in the range of 0.5 – 0.6 % obtained with commercially available Kromasil C₁₈-columns¹⁹². There, differences in performance were mainly discussed by variations in particle size and packing of columns but not surface degradation or adsorption.

I assume that the major factor still contributing to high inter- and intra-batch differences is the highly amorphous and heterogeneous bare fused silica surface, which is not fully homogenized by the current preconditioning procedure^{193,194}. Chromatographic particles prepared using sol-gel-synthesis are expected to be more homogeneous and can be produced with a higher reproducibility, leading to the excellent column-to-column reproducibility often observed¹⁹². For non-charged and statically adsorbed PVA, Xu *et al.*¹⁹⁵ observed column-to-column RSD(t_{mig}) < 1 % in CE-UV using phosphate buffer (n = 10 capillaries, 3 runs each). Belder *et al.*¹⁹⁶ reported RSD(t_{mig}) = 1.2 % (single capillary, n > 900 runs), also utilizing CE-UV and phosphate BGE.

I emphasize that, to the best of my knowledge, no literature is known dealing with capillary-to-capillary reproducibility of covalently bound and non-charged coatings with CE-MS hyphenation. Only highly charged capillaries prepared via successive multiple ionic polymer layers (SMIL) exhibit

the desired capillary-to-capillary reproducibility in CE-MS. The typically high thickness (up to 1 μm) of polymer-layers results in complete shielding of inhomogeneous silica which then results in the desired reproducibility. For instance, the group of Asakawa *et al.*¹⁴⁹ presented $\text{RSD}(\mu_{\text{EOF}}) < 1\%$.

4.5.3. Stability of capillary surfaces due to preparation via Si-H-route

In my study I especially focused on a protocol for a neutral covalently coupled coating which can withstand very harsh rinsing conditions and separation at very low pH often applied for CE-MS analysis of peptides and proteins. The ruggedness of surface coating both for capillary surfaces and for particles decreases in the order $\text{Si-O-C} > \text{Si-O-Si-C} > \text{Si-C}$ ^{179, 197, 198}. The latter coupling approach was chosen accordingly. In addition, the polymer AAEE was used known to have an excellent stability at high pH conditions¹⁷⁰. I demonstrate that especially capillaries from Batch 1 were well suited as they withstood both acid- and base-induced degradation rinsing with 1 mol/L HCl and NaOH, see Figure 24, without obvious surface degradation. Overall, surface coverage was high, visible by the lack of hysteresis effects in contrast to Batch 2 capillaries. However, with the very harsh rinsing conditions chosen here, some minor degradation processes may be assumed: First, base-induced dissolution of Q^3 -silica (Si-OH) from non-coated regions of the capillary may occur. This degrades previously stable T^3 - to hydrolytically unstable T^2 -entities (Si-C), as discussed by the group of Yoreo *et al.* for Q^3 and Q^2 -silica¹⁹⁹. Bleeding of surface-bound polymer would result, which was, however, not observed in CE-MS. A further coating optimization would thus have to consider a complete transfer of Si-OH into Si-H groups and a complete reaction of Si-H Si-C functions. Then, this type of degradation will not be observed, and degradation stability of surface-bound polymer matches or (due to steric reasons) exceeds stability of free polymer. Secondly, degradation of surface bound polymer species could occur. However, I presume this influence to be negligible as the here used rinsing times at ambient temperature are small especially considering the long-term stability of free polymeric AAEE in both 0.1 mol/L HCl and NaOH at 70 °C as published by Chiari *et al.*¹⁷⁰.

These observations show that especially surface coverage needs to be further optimized. I thereby propose more drastic protocols for silanol surface activation prior to surface modification or implement grafting conditions. Another option would be to increase the thickness of the polymer e.g. via cross-linking so that penetration by base is hindered.

4.5.4. Application of coated capillaries for complicated separations

Polyamines: High stability and excellent separation performance were achieved for the separation of polyamines, which are otherwise often used as dynamic coating agents in the BGE themselves^{156, 164, 200}. Slightly lower intermediate precision was observed for fish egg samples due to matrix effects. Direct analysis of acidic extracts from only one fish egg was possible without the need for derivatization of the polyamines²⁰¹. No carryover effects, no decrease in performance or drifts in migration times were observed during my experiments as observed in CE-UV analysis using phosphate and citrate BGEs on a non-coated capillary²⁰², where the authors observed shifts in migration times of up to 1 min despite rinsing with 0.1 mol/L NaOH between runs, presumably due to unwanted coating of the capillary surface with polyamines left underivatized during sample preparation. The analysis of non-derivatized polyamines was successfully conducted using CE-MS with slightly better $\text{RSD(A)} \approx 4.6\% - 5.9\%$ for standard samples compared to my study. The

quantitative precision for the samples under investigation (white and red wines) was similar to this study with RSDs > 10 %²⁰³.

Intact proteins: The separation of intact, acidic proteins using CE-UV and AAEE-coated capillaries was presented by Chiari *et al.*¹⁵⁰ who first used an AAEE-coating with excellent separation efficiencies and precision with $RSD(t_{mig}) = 0.5 - 2 \%$ but lower precision for the more hydrophobic polyacrylamide coating ($RSD(t_{mig}) = 1 - 5 \%$). In this study with covalently coupled AAEE I also achieved $RSD(t_{mig}) \leq 2 \%$ when using long capillaries necessary to dissolve the sample-induced tITP-state. However, in the approach by Chiari *et al.*¹⁵⁰ a high coating stability for long measurement series (300 runs of 20 min, 100 h) at pH 8.5 was only achieved when combined with a statically adsorbed coating at the inlet and outlet of the capillary using methylcellulose every 15 h. In my approach, 140 runs over 100 h measuring time were conducted using **B1C1**, see Section 4.4.3.2. No further treatment was necessary except for rinsing with 50 mmol HCl and BGE between runs, even when serum samples diluted 1:1 with PBS were analyzed. However, clogging due to protein coagulation and matrix effects occurred after about 30 consecutive runs with serum samples. Clogging of microfluidic devices is a known problem as e.g. observed for nanoLC-MS²⁰⁴.

Despite the good repeatability presented here, I was not able to achieve as high separation efficiencies (plate numbers $N < 2000$) as Chiari *et al.*¹⁵⁰ ($N = 1.3 - 5.9 \cdot 10^5$), which can at least in part be explained by the different BGE used which had to be MS compatible for this study and thus precluded the use of methylcellulose and “GOOD-buffers”, which have been shown to be advantageous for protein separation already at low concentrations by de Jong *et al.*²⁰⁵. As described in Section 4.3.2, an acidic BGE at pH 2.2¹⁴⁶ was used here, which is in good accordance to typical practice in CE-MS¹⁶². Very fast separations of small proteins were presented by Banks *et al.*²⁰⁶ using a statically adsorbed amine coating with a very high EOF at the low pH BGE (FWHM around 2 s with separation times below 3 min), however, no data on precision or stability were presented.

4.6. Conclusion and outlook

In this study I demonstrate that covalent coupling of the hydrophilic polymer AAEE to the capillary surface is possible with a direct linkage via Si-C. bonds. Superiority of the presented approach over regular covalent coating approaches using silanol chemistry is due to the formation of Si-C in T³-groups, as presented in Section 4.2. The coating procedure was parallelized to allow simultaneous coating of 16 m of capillary with similar performance over the whole length. Parallelized coating is possible and desirable due to the possibility of long-time storage (at least 3 years), even after use. Overall, capillary coating times of 2.5 h per capillary were achieved. The optimized synthesis was straight-forward without the need for an inert atmosphere. The high excess of thionyl chloride and LiAlH₄ during rinsing steps allowed us to speed up the reactions compared to particle coatings for LC. My results demonstrate that the coating gives reproducible results for both small molecules known to easily adsorb to capillary surfaces, as well as peptides and proteins. Matrix effects were low, only for 1:1 diluted serum clogging occurred, but no signs of coating degradation were observed. The coated capillaries proved stable also upon long-term storage at ambient conditions even after use. Further improvement will focus on bringing preconditioning methods for more homogeneous capillary surfaces into play to further increase both stability and capillary-to-capillary reproducibility.

NOVEL APPROACH FOR THE SYNTHESIS OF A COVALENTLY BOUND, HIGHLY POLAR AND PH-PERSISTENT N-
ACRYLOYLAMIDO ETHOXYETHANOL CAPILLARY COATING FOR CAPILLARY ELECTROPHORESIS-MASS SPECTROMETRY

PART 1: STRATEGY, PERFORMANCE AND STABILITY

The presented capillary coating offers excellent separation performances towards polyamines and peptide as well as high reproducibility and long time stability towards the separation of intact proteins even in serum matrix. To conclude, further improvements of the capillary coatings may be obtained when using harsher preconditioning methods such as rinsing with strong base at elevated temperature.

5. Novel approach for the synthesis of a covalently bound, highly polar and pH-persistent *N*-acryloylamido ethoxyethanol capillary coating for capillary electrophoresis-mass spectrometry part 2: Etching with supercritical water as capillary pretreatment

5.1. Abstract

Synthetic strategies for covalently coupled coatings may suffer from low robustness due to surface inhomogeneities of the silica surface of the capillary. Commonly, harsh rinsing steps with strongly alkaline and acidic solutions are applied, partly with heating. I here investigate a novel pre-conditioning protocol using etching with supercritical water for the formation of Si-C bonds between the capillary surface and the neutral polymer *N*-acryloylamido ethoxyethanol (AAEE). The advantage of Si-C coupled AAEE is the high stability over a wide pH range, the very low electroosmotic flow and high prevention of peptide and protein sorption. However, I observed limitations regarding the repeatability of the coating process. The etching process with supercritical water was optimized to obtain surfaces with a defined surface roughness between 75 nm and 1000 nm. Periodic surface structures were observed. The etched capillaries showed extremely high reactivity due to a high extent of silica dissolution and re-aggregation upon rinsing with 1.0 mol/L HCl and NaOH was observed.

In addition, using scanning electron microscopy, I present novel insight into the reaction mechanism of Si-H-group formation using thionyl chloride and LiAlH_4 solution on the capillary surface. This first step was followed by Speier coupling of allyl methacrylate to form Si-C-groups, and in a third step, AAEE is grafted on the surface via radical chemistry. The results show that mechanisms described in literature are not sufficient to explain the surface reactions as my results indicate, that the formation of polymeric $\text{Al}(\text{O})_x\text{H}_y$ ($x+y = 3$) plays an important role in the formation of the active capillary surface layer for the polymerization step. This active layer presumably provides metal-hydride species for Speier-catalytic linkage of allyl methacrylate in the second step of the coating protocol. Especially surfaces with a roughness of 1000 nm provide an increased number of adsorption sites and thus thick layers of this species. Varying some parameters in the synthesis, I show that the formation of this aluminate-layer on the surface is a mechanism coexisting with Si-H-formation.

5.2. Introduction and motivation

I previously presented research considering the separation performance, stability and reproducibility of covalently bound *N*-acryloylamido ethoxyethanol (AAEE) capillary coating, see Chapter 4. Excellent stability and separation performance were observed, but capillary-to-capillary reproducibility was not satisfactory. I pointed out, that inhomogeneity of fused silica species is an intrinsic property of bare-fused silica capillaries. Appropriate preconditioning procedures for surface homogenization are thus required. This is a common problem in microfluidics in general and capillary electrophoresis in particular. Common preconditioning procedures consist of incubation under highly concentrated (12 mol/L) HCl at 80 °C overnight^{207, 208}, sometimes followed by incubation in ammonium hydrogen difluoride, rinsing with nitrogen and heating²⁰⁸. Fluoride and ammonium remain in the silica surface giving it novel and sometimes desired properties²⁰⁹ but more often the surface acquires unpredictable properties.

To avoid these contaminations, I used supercritical water at 400 °C and 400 bar for surface preconditioning using a self-made device, see earlier publications of Karásek *et al.*^{210, 211}. Contamination of surface with inorganic residue is avoided and at the given conditions I was able to etch and activate the surface without un-wanted etching of the capillary in a cylindrical shape.

As will be shown in this research the etched capillaries exhibit higher surface activity and reactivity towards the further surface modifications. More efficient and denser “packing” of the coating is a result. Longer and denser polymer chains result not only in thicker polymer layers on the surface, but formation of an entangled polymer meshwork in the capillary might also occur which is prone to offer higher lifetimes than gels²¹², but regenerating via rinsing with BGE is still possible.

5.3. Materials and methods

5.3.1. Instrumentation

5.3.1.1. Capillary etching

Capillary etching was conducted as previously described by Karásek *et al.*²¹⁰. In brief: a self-made assembly was used with a commercially available pressure system, a heating filament under nitrogen atmosphere and liquid nitrogen cooling for exhausted water.

5.3.1.2. Capillary electrophoresis

Fused silica capillaries with an inner diameter of 50 μm and an outer diameter of 365 μm were purchased from Polymicro (Kehl, Germany). If not stated differently, capillaries with approx. 65 or 75 cm in length and an inner diameter of 50 μm were used. For CE analysis, an Agilent 7100 CE system (Agilent, Waldbronn, Germany) with UV-detection was used. For determination of μ_{EOF} , the chosen wavelengths were 210 nm and 280 nm with a spectral width of 10 nm and a reference wavelength of 360 nm. To decrease measurement times for EOF determination, caffeine-double injection was performed as follows: rinsing of capillary with BGE (here: 30 mmol/L NH_4OAc , pH 6.8) for 3 min with 1 bar followed by injection of a 1 g/L caffeine-solution containing 10 % BGE for 5 s at 100 mbar. Voltage was applied for 2-5 min prior to another injection of caffeine-solution for 5 s at 100 mbar. For normal and reversed EOF determination a voltage of +30 kV and -30 kV was applied for 2 min. Hydrodynamic mobilization at 1 bar for 5 min yielded 2 signals in the electropherograms allowing calculation of μ_{EOF} , see Chapter 4 for further information. Lower pressures lead to electropherograms void of peaks within the first 15 min. Normal EOFs were observed for AAEE-coated capillaries, reversed EOFs were observed for capillaries after hydration using LiAlH_4 .

For MS conditions during CE-MS measurements see Section 4.3.1.2. CE-MS measurements were performed as follows: rinsing of the capillary in-between runs with BGE (here: 0.75 mol/L acetic acid and 0.25 mol/L formic acid at pH 2.2, see also Pattky *et al.*¹⁴⁶) for 3 min with 1 bar followed by injection of sample for 5 s at 100 mbar (tryptically digested BSA, see Section 4.3.3) and separation for 9 min at 100 mbar and +30 kV. Lower pressures led to interruption of electric current within the first 60 s of each run.

Measurement conditions for CEC-MS measurements without voltage application (investigation of wall coated open-tubular column mass spectrometry (WCOTC-MS)) were as follows: injection of tryptically digested BSA at 100 mbar for 5 s followed by hydrodynamic mobilization with 100 mbar for 9 min. In-between runs, capillaries were rinsed with BGE for 3 min at 1 bar.

Freshly prepared capillaries were conditioned prior to their first use by flushing with BGE for 10 min followed by application of +30 kV voltage for 5 min. After use and for storage, capillaries were consecutively rinsed 3 min with PBS, 2 min with water and 2 min with air, each at 1 bar.

5.3.1.3. Mass spectrometry

A quadrupole time-of-flight mass spectrometer 6550 (QTOF 6550) from Agilent (Santa Clara, CA, United States) with a sheath liquid interface from Agilent (Waldbronn, Germany) was used by implementing an Agilent isocratic pump 1260 (Agilent Technologies, Waldbronn, Germany) producing a flow rate for the sheath liquid of 5 $\mu\text{L}/\text{min}$. A jetstream electrospray ionization (ESI) source was operated with a nebulizer pressure of 275 and 345 mbar, for coated and non-coated

capillaries, respectively. The drying gas temperature was 150°C, a flow rate of 11 L/min and a fragmentor voltage of 175 V were applied. Skimmer voltage was set to 65 V and octopole voltage to 750 V. The mass range was 100-3000 m/z with a data acquisition rate of 2 spectra/s. A 1:1 (v/v) mixture of 2-propanol/water was used as sheath liquid, containing 0.1% formic acid as well as a few nanogram of 3 selected calibrants for internal calibration (Agilent Technologies, Waldbronn, Germany, m/z = 121.0508, 322.0481 and 922.0097).

For CE-MS, six arbitrarily chosen peptides found in tryptically digested BSA were taken for the evaluation of the capillary performance. The m/z-values of these peptides were determined experimentally and are numbered with increasing t_{mig} as follows: **1**: 417.1968, **2**: 473.8831, **3**: 379.6995, **4**: 526.2403, **5**: 395.2235 and **6**: 740.3700.

5.3.1.4. Scanning electron microscopy (SEM)

SEM-measurements were conducted using a MIRA3 (Tescan, a.s, Brno, Czech Republic) in InBeam mode at 5 kx, 10 kx, 25 kx, 50 kx and 100 kx magnification at 10 kV acceleration voltage and a sample-to-lens distance of approx. 5.2-5.3 mm. Samples for SEM were prepared in duplicates using a capillary piece of 2 cm in length which was cut in 2 pieces of 1 cm in length.

5.3.1.5. Energy dispersive x-ray (EDX)

EDX-measurements were conducted using a Hitachi 8030 SU (Hitachi Ltd., Tokyo, Japan) with an acceleration voltage of 5.0 kV at 35 kx magnification, a sample-to-lens distance of approx. 17.2-17.3 mm whilst utilizing the lower detector.

5.3.2. Chemicals

Bovine serum albumin (BSA, bovine serum), sodium chloride (NaCl, ≥99 %), *N,N,N',N'*-tetramethylenediamine (TEMED, ≥99 %), ammonium peroxodisulfate (APS, ≥98 %), 2-propanol (iPrOH, LC-MS grade), lithium aluminum hydride (LiAlH₄, 1 mol/L solution in THF), tetrahydrofuran (THF, LC-MS grade), chloroplatinic acid hexahydrate (H₂PtCl₆ · 6H₂O, ACS reagent, ≥37.50% Pt basis), allyl methacrylate (AMA, ≥98% with 50-185 ppm *p*-methoxyphenol as inhibitor), acetonitrile (ACN, LC-MS grade) and formic acid (LC-MS grade) were purchased from Sigma-Aldrich (Steinheim, Germany). Trypsin (sequencing grade modified) was purchased from Promega (Mannheim, Germany). Ammonium hydrogen carbonate (NH₄HCO₃, ≥99.5 %) was delivered from Fluka (München, Germany). Sodium hydroxide solution (NaOH, 10 mol/L, suprapur), thionyl chloride (≥99,0%, reagent grade) and glacial acetic acid (≥99.9 %) were delivered by Merck (Darmstadt, Germany). Hydrochloric acid (HCl, 32 %, analytical grade) and 1,4-dithiothreitol (DTT, ≥99 % electron for microbiology) were purchased from VWR (Darmstadt, Germany). Sodium dihydrogen phosphate dehydrate (NaH₂PO₄) was purchased from Caelo (Hilden, Germany). Rapidigest was purchased from Waters (Eschborn, Germany). Methanol (MeOH, HPLC-grade) was obtained from Honeywell (Seelze, Germany). Toluene (HPLC grade) was purchased from Fisher Scientific (Schwerte, Germany). *N*-acryloylamido-ethoxyethanol (AAEE, ~50% solution in water, ≥98%, with ~0.01% hydroquinone as stabilizer) was purchased from Santa Cruz Biotechnology (Heidelberg, Germany). Deionized water was prepared using an ELGA-Veolia PURELAB Classic system (Celle, Germany). Dry Toluene and THF were obtained using an M. Braun Solvent Purification System (SPS, Garching, Germany).

5.3.3. Preparation of tryptically digested BSA

Tryptic digestion of BSA was performed using a modified protocol as reported previously¹⁴⁶. In brief, 2 μL of a BSA solution with a concentration of 10 g/L in water were mixed with 15 μL of a 0.1 % Rapidigest-solution and with 1.3 μL 50 mmol/L DTT-solution, both containing 50 mmol/L NH_4HCO_3 . The mixture was incubated for 1 h at 60 °C. 4 μL of a 50 mmol/L iodoacetamide solution in water is added followed by mixing and incubation in the dark for 30 min at ambient temperature. 20 μL of a 10 mg/L trypsin-solution containing 500 $\mu\text{mol/L}$ acetic acid, 86 % acetonitrile and 14 % water were added prior to incubation at 37 °C overnight.

5.3.4. Capillary coating

The coating synthesis was conducted in an autoclave with up to 8 capillaries in parallel in order to protect the CE instrument from aggressive solvents. Details can be found in Chapter 4.

5.3.4.1. Preparation of hydrated capillary surface (Si-H-capillaries)

Capillary coatings were prepared as follows: preconditioning of capillaries by consecutive rinsing with methanol, (0.1 mol/L) 1 mol/L HCl, (0.1 mol/L) 1 mol/L NaOH and water, each for 10 min at 8 bar. The capillaries were then rinsed (or not rinsed) with thionyl chloride for 1.5 h at 8 bar, followed by 45 min with toluene and 20-22 h with 30 mmol/L LiAlH_4 , prepared by mixing 1 mol/L LiAlH_4 with equal amounts of toluene and THF. Only solvents dried using an SPS were used during this step. Capillaries were then rinsed with THF for 15 min, followed by air for 5 min. Sample abbreviations and the respective synthesis procedures are listed in Table 5.

Table 5: Abbreviations of capillaries including the different synthetic procedures.

Abbreviation	Concentration of preconditioning solution ^b	Thionyl chloride ^c
etched ^a	1	✓
0.1/woTC	0.1	✗
1/woTC	1	✗
0.1/wTC	0.1	✓
1/wTC	1	✓

^aEtched capillaries with various surface roughnesses, the precise surface roughness is given as e.g. "etched 1000 nm" for the capillary with 1000 nm surface roughness. ^bConcentration of HCl and NaOH-solution during preconditioning in mol/L. ^cIndication, whether rinsing with thionylchloride was conducted (/wTC) or not (/woTC).

5.3.4.2. Preparation of covalently bound N-acryloylamido ethoxyethanol

For the preparation of AAEE-capillaries, Si-H-capillary surfaces are required. Capillaries prepared according to Section 4.3.6.2 were used for this reaction step. Si-H-capillaries were consecutively rinsed with MeOH and air for 5 min at 8 bar followed by incubation at 100 °C for 30 min. The capillaries were then filled hydrodynamically at 1 bar for approx. 40-50 s with a freshly prepared solution consisting of 26 mmol/L $\text{H}_2\text{PtCl}_6 \cdot 6\text{H}_2\text{O}$ in 74 % AMA and 26 % iPrOH followed by incubation at 100 °C for 30 min. Afterwards, capillaries were rinsed with air at 8 bar for 1-3 min until the formation of air bubbles was observed. This step was directly followed by filling the capillaries at 1 bar with an aqueous solution containing 0.04 % APS, 0.04 % TEMED and 1.5 % AAEE and incubation at ambient temperature for 1 h. Capillaries were then emptied from the reaction solution by subsequent rinsing at 8 bar for 5 min with air, 10 min with water and 10 min with ACN. For storage, the capillaries were then rinsed with air for 5 min at 8 bar.

5.4. Results

5.4.1. SEM-investigation

5.4.1.1. Impact of etching procedure on silica surfaces

Capillaries etched with supercritical water were prepared via rinsing with water at 400 °C and 400 bar, as previously described by Karásek *et al.*²¹⁰. The obtained surface roughness was controlled regarding rinsing time, pressure and incubation prior to rinsing. Capillaries with a roughness between 75 nm and 1000 nm were manufactured. Representative SEM-pictures are presented in Table 6 and Table 7. Due to the cumbersome etching process, only a single capillary was used for each investigated surface roughness. The capillary coating procedure optimized for non-etched capillaries was transferred for these capillaries.

5.4.1.2. Stability of etched silica surfaces towards NaOH and HCl

I investigated the stability of etched capillaries towards pH. When rinsing with 0.1 mol/L HCl (pH 1) and NaOH (pH 13) no change of the surface compared to original capillaries was observed in SEM. In contrast, rinsing with 1 mol/L HCl (pH 0) and NaOH (pH 14) led to a degradation of the silica surface, which was observed in SEM, see Table 6 and Table 7. With increasing surface roughness, stronger surface degradation was evident by the formation of “needles” on the surface, see Table 7. This observation was not made for non-etched capillaries: two non-etched capillaries were investigated over a length of approx. 50 cm, cutting the capillary in 1 cm pieces and analyzing each piece via SEM. All SEM images were similar, results not shown.

5.4.1.3. Thickness of aluminate and polymer layers

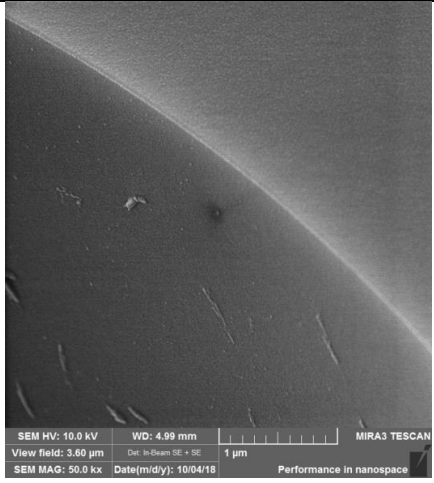
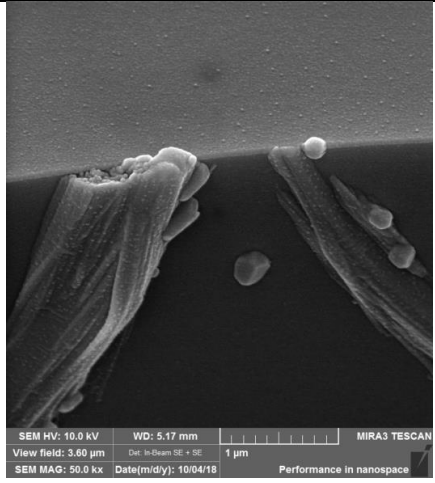
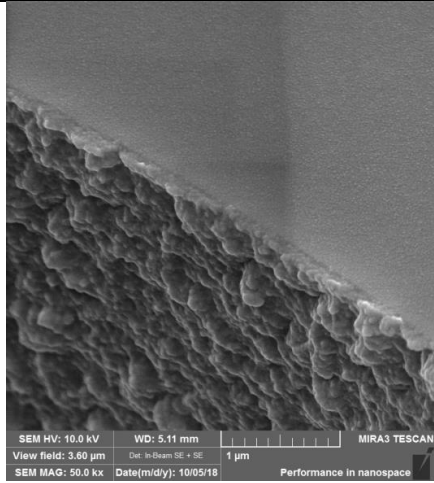
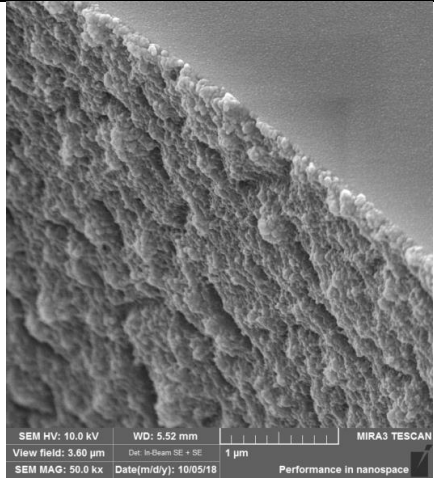
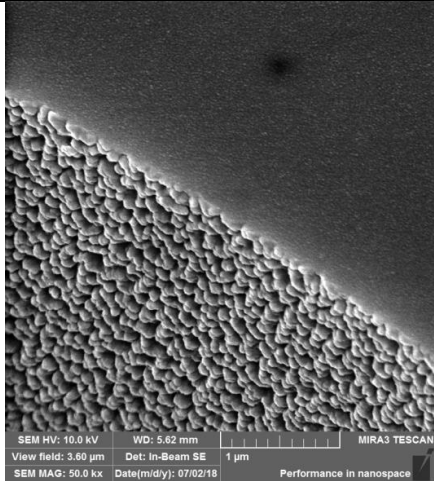
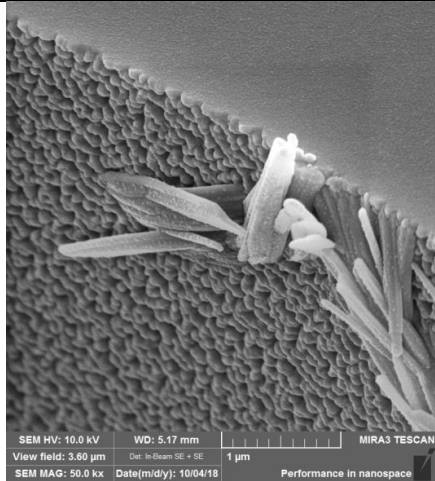
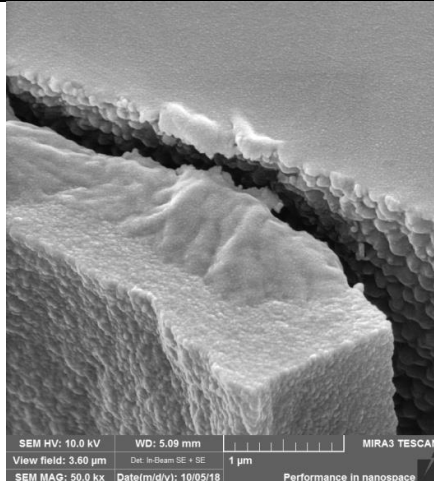
Subsequent rinsing with thionyl chloride and hydration with a solution of LiAlH_4 resulted in the formation of deposits on the capillary surface. On non-etched capillaries, the small deposits formed layers with a thickness well below 100 nm and a relatively homogeneous surface coverage all over the capillary. For 75 nm and 150 nm surface roughness, these small deposits agglomerated in thick layers of approx. 1 μm thickness, covering the capillary only to a low extent, possibly due to shrinking after drying. For capillaries with a surface roughness of 250 nm, 400 nm and 750 nm, agglomeration of small deposits in dense layers on and in-between the rough capillary surface was observed. For the capillary with 1000 nm roughness, both debris in form of agglomerates and dense layers was observed.

Coating with AAEE never increased the layer thickness as could be observed with SEM. This indicates, that the polymer layer thickness is in the nm-range. This is in accordance to the strong decrease in μ_{EOF} -values after coating with polymer, see Section 5.4.2.

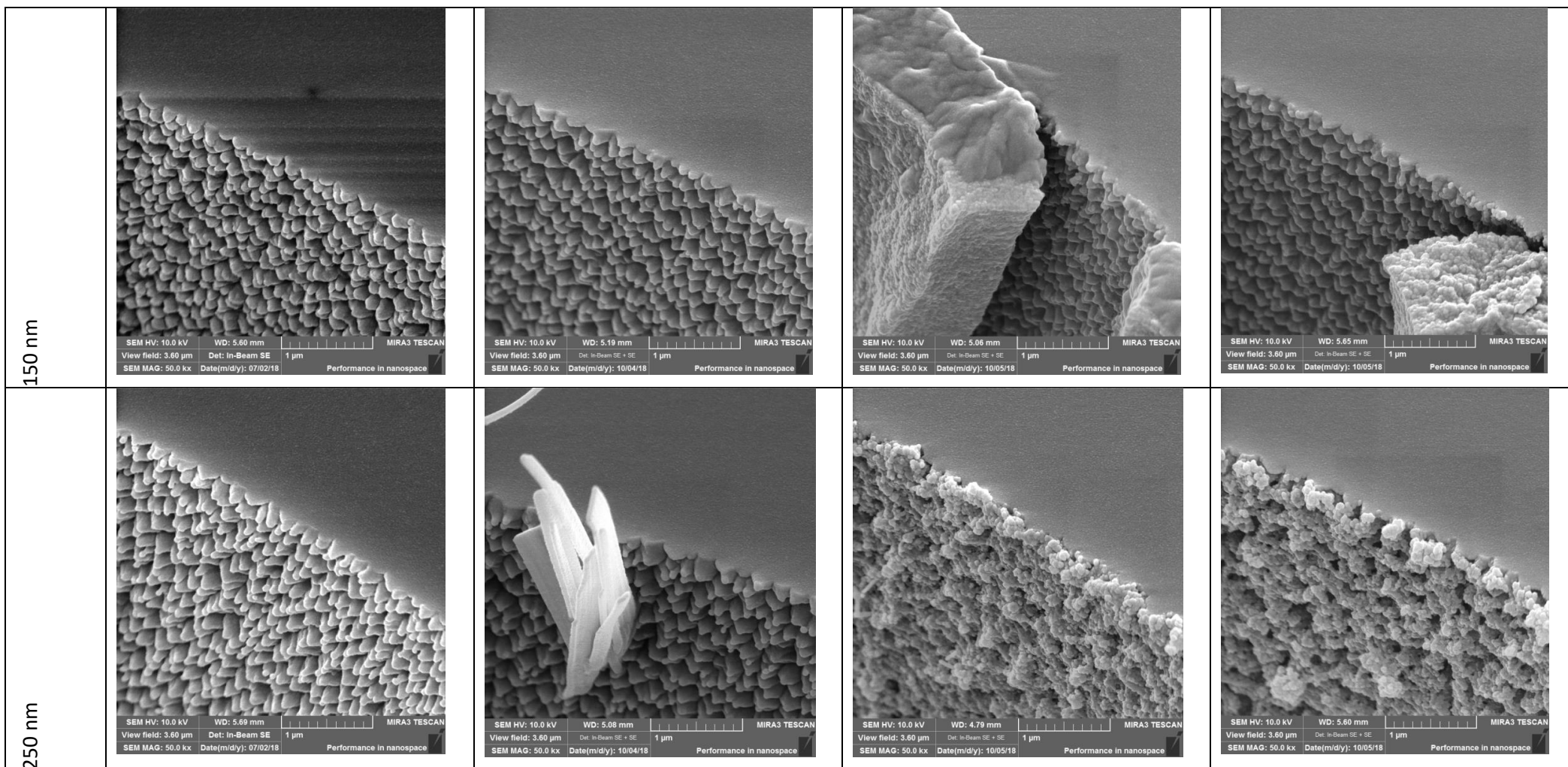
I assume that the debris consists of $\text{Al}_2(\text{O})_{x/2}\text{H}_y$ ($x+y = 6$). For identification, EDX-measurements of the surfaces after the hydration step were made. The results indicate the formation of a layer with very low conductivity, so no meaningful EDX data could be obtained. In contrast, bare-fused silica and AAEE-coated surfaces allowed EDX analysis. Thus, EDX analysis can support the hypothesis of the formation of an insulating layer of $\text{Al}_2(\text{O})_{x/2}\text{H}_y$ deposit.

NOVEL APPROACH FOR THE SYNTHESIS OF A COVALENTLY BOUND, HIGHLY POLAR AND PH-PERSISTENT N-ACRYLOYLAMIDO ETHOXYETHANOL CAPILLARY COATING FOR CAPILLARY ELECTROPHORESIS-MASS SPECTROMETRY PART 2: ETCHING WITH SUPERCRITICAL WATER AS CAPILLARY PRETREATMENT

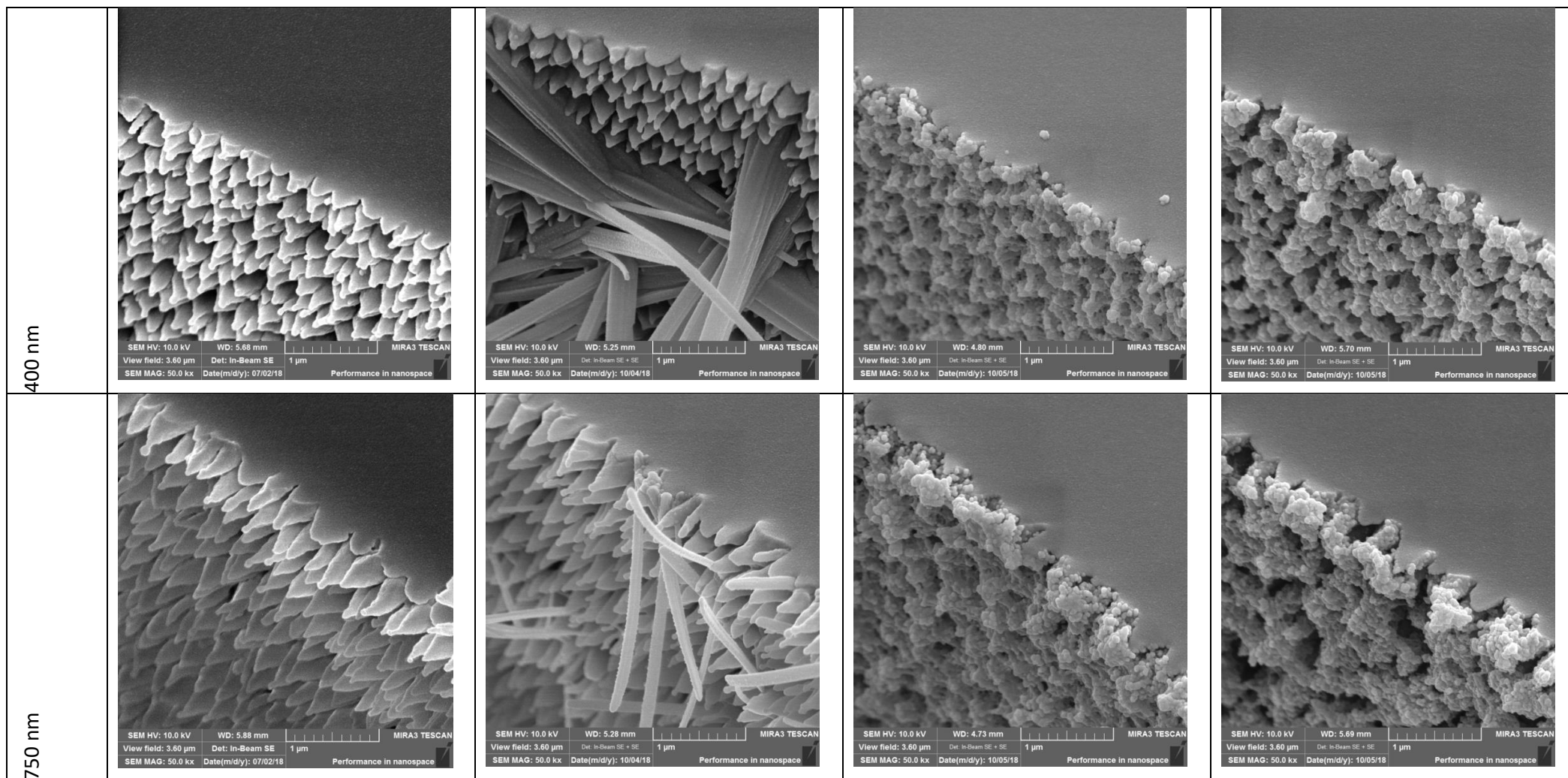
Table 6: SEM-pictures taken on capillaries with various surface roughness after different steps of the coating procedure. From each capillary 2 cm pieces were cut, SEM pictures were taken at two positions of each capillary piece. One representative picture with 50000-fold magnification is shown each. For measurement settings see Section 5.3.1.4.

Surface roughness	After preconditioning with 0.1 mol/L HCl and NaOH	After preconditioning with 1 mol/L HCl and NaOH	After LiAlH ₄	After AAEE
Non-etched				
75 nm				No picture, capillary clogged during coating procedure

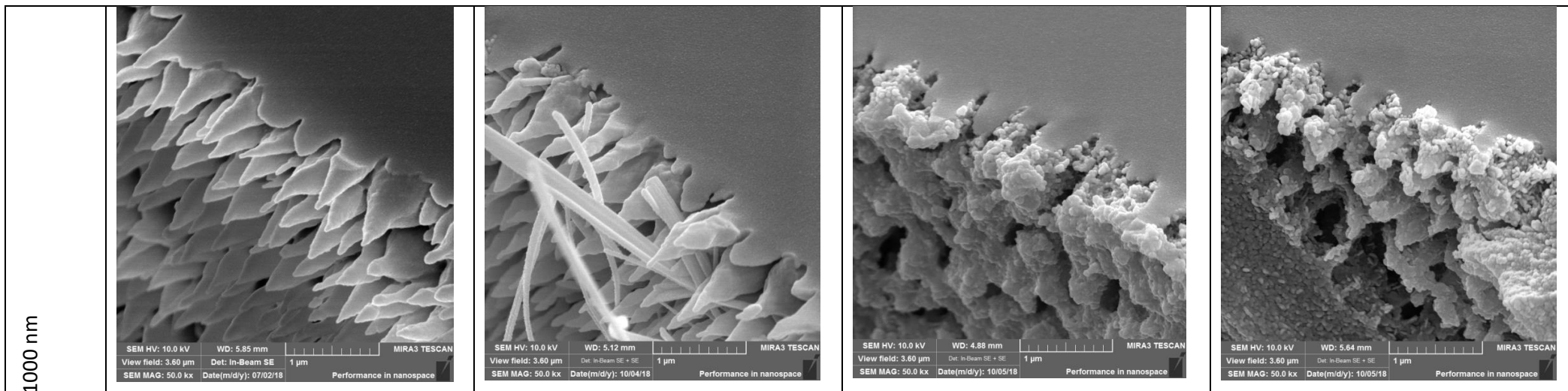
NOVEL APPROACH FOR THE SYNTHESIS OF A COVALENTLY BOUND, HIGHLY POLAR AND PH-PERSISTENT N-ACRYLOYLAMIDO ETHOXYETHANOL CAPILLARY COATING FOR CAPILLARY ELECTROPHORESIS-MASS SPECTROMETRY PART 2: ETCHING WITH SUPERCRITICAL WATER AS CAPILLARY PRETREATMENT



NOVEL APPROACH FOR THE SYNTHESIS OF A COVALENTLY BOUND, HIGHLY POLAR AND PH-PERSISTENT N-ACRYLOYLAMIDO ETHOXYETHANOL CAPILLARY COATING FOR CAPILLARY ELECTROPHORESIS-MASS SPECTROMETRY PART 2: ETCHING WITH SUPERCRITICAL WATER AS CAPILLARY PRETREATMENT

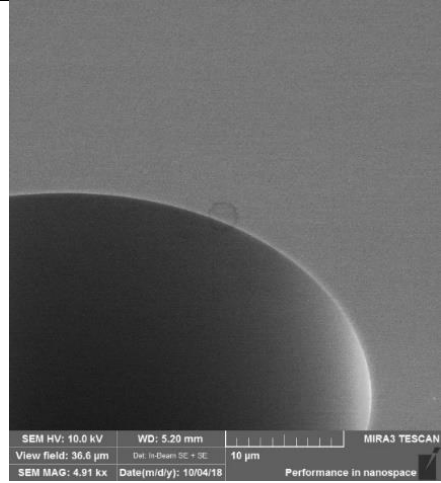
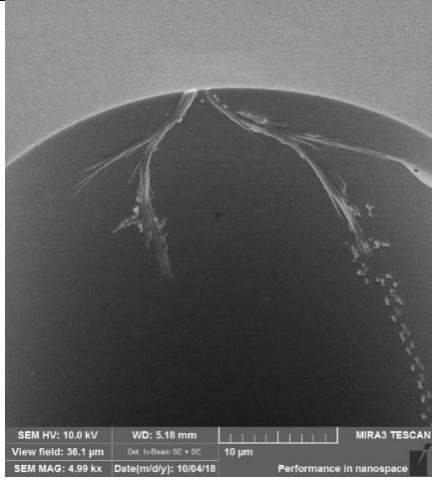
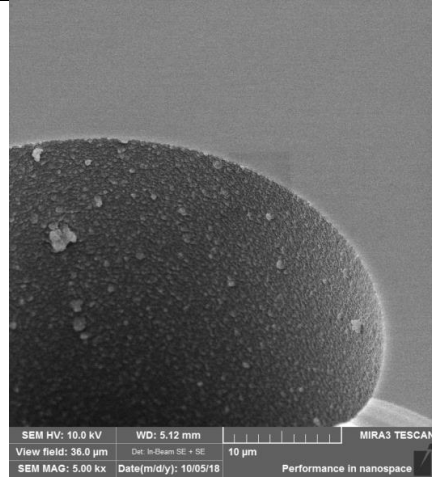
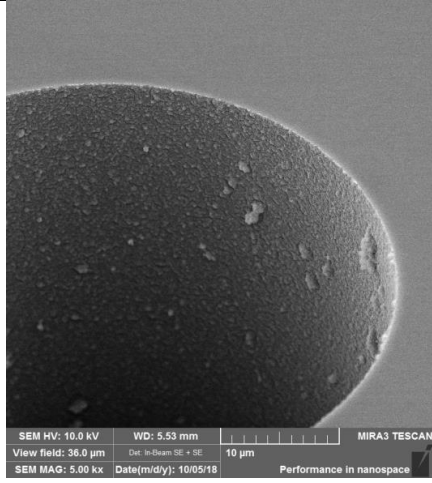
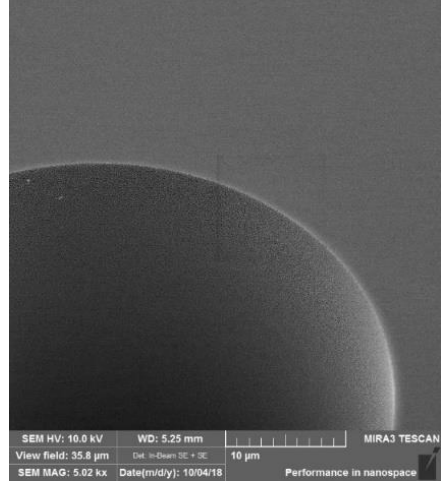
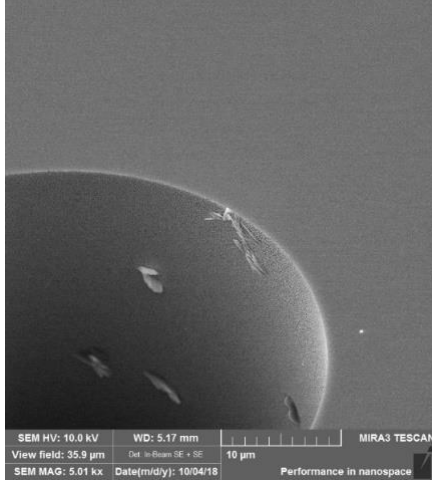
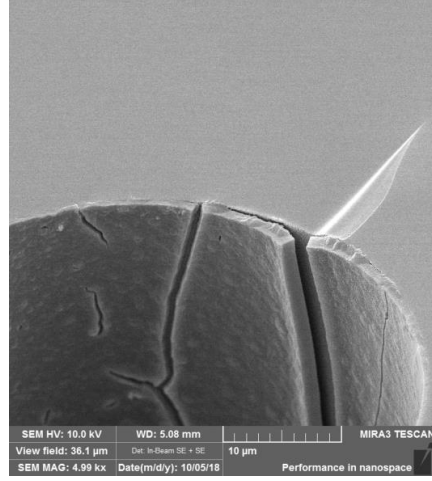


NOVEL APPROACH FOR THE SYNTHESIS OF A COVALENTLY BOUND, HIGHLY POLAR AND PH-PERSISTENT N-ACRYLOYLAMIDO ETHOXYETHANOL CAPILLARY COATING FOR CAPILLARY ELECTROPHORESIS-MASS SPECTROMETRY PART 2: ETCHING WITH SUPERCRITICAL WATER AS CAPILLARY PRETREATMENT

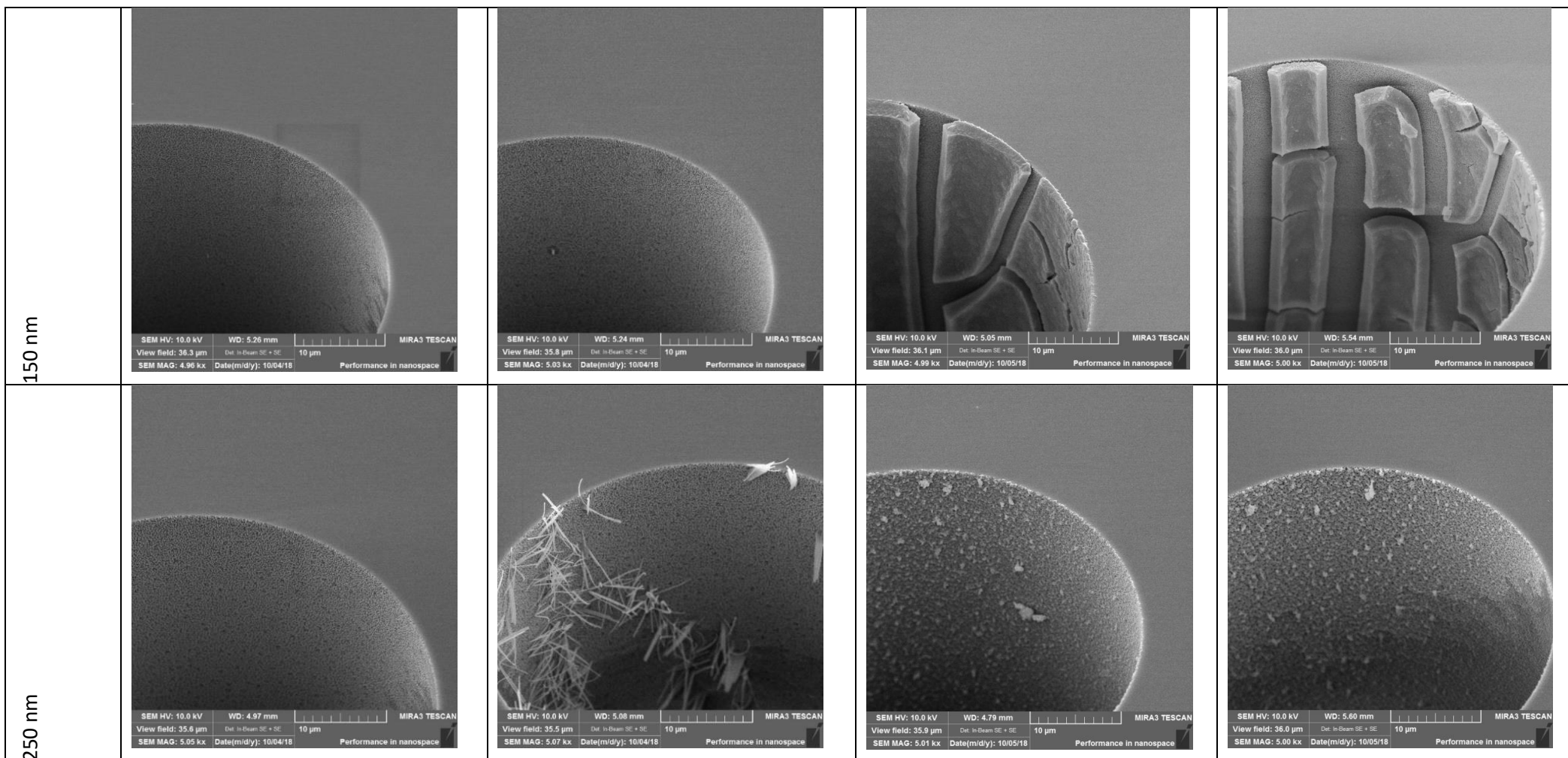


NOVEL APPROACH FOR THE SYNTHESIS OF A COVALENTLY BOUND, HIGHLY POLAR AND PH-PERSISTENT N-ACRYLOYLAMIDO ETHOXYETHANOL CAPILLARY COATING FOR CAPILLARY ELECTROPHORESIS-MASS SPECTROMETRY PART 2: ETCHING WITH SUPERCRITICAL WATER AS CAPILLARY PRETREATMENT

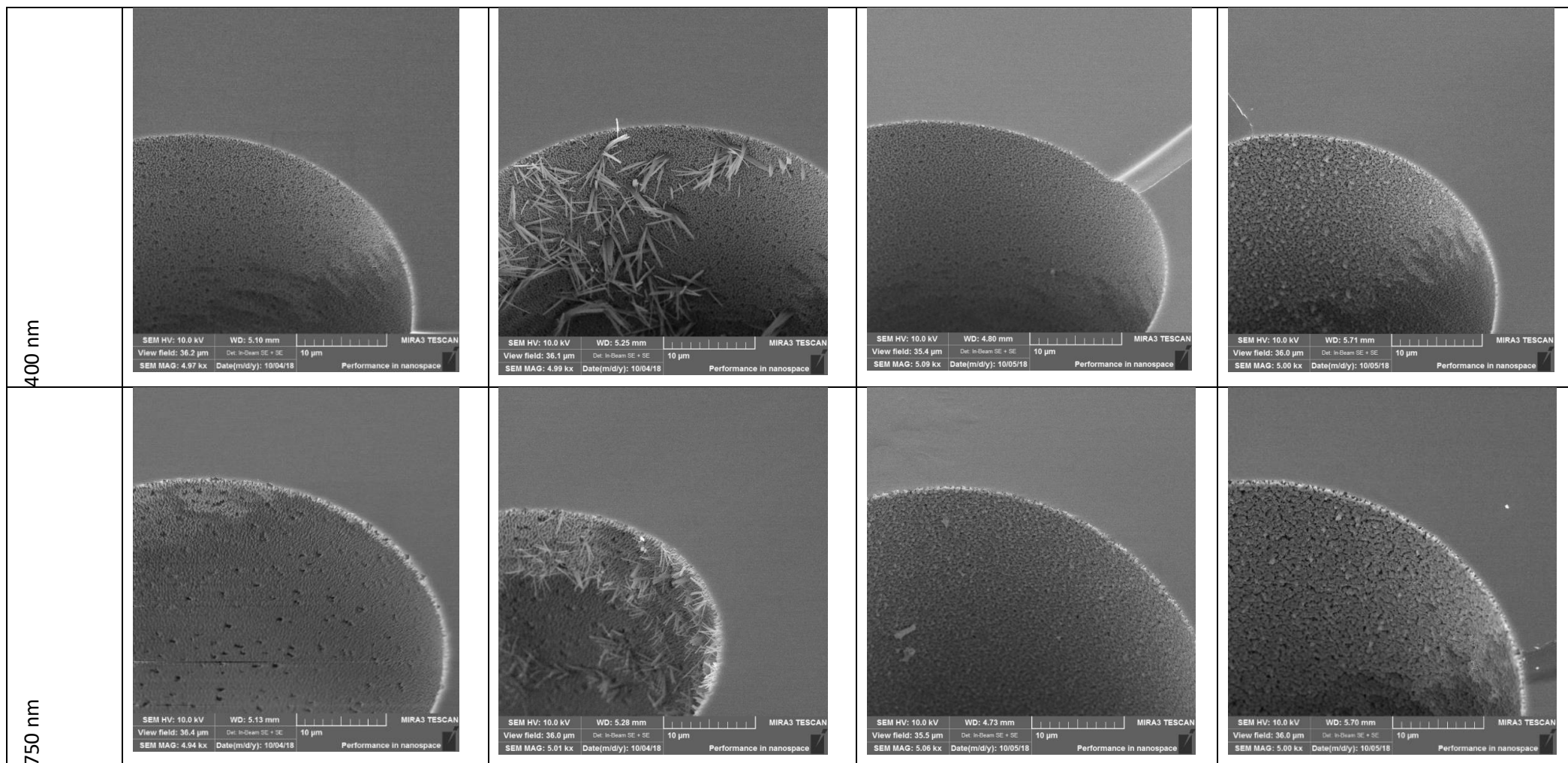
Table 7: SEM-pictures taken on capillaries with various surface roughnesses at different steps of the coating procedure. The same capillary was used for each surface roughness by cutting 2 cm pieces, SEM was measured at two positions of each capillary piece. No significant differences were found within one capillary. One representative picture with 5000-fold magnification is shown each. For measurement settings see Section 5.3.1.4.

Surface roughness	After preconditioning with 0.1 mol/L HCl and NaOH	After preconditioning with 1 mol/L HCl and NaOH	After LiAlH ₄	After AAEE
Non-etched				
75 nm				No picture, capillary clogged during coating procedure

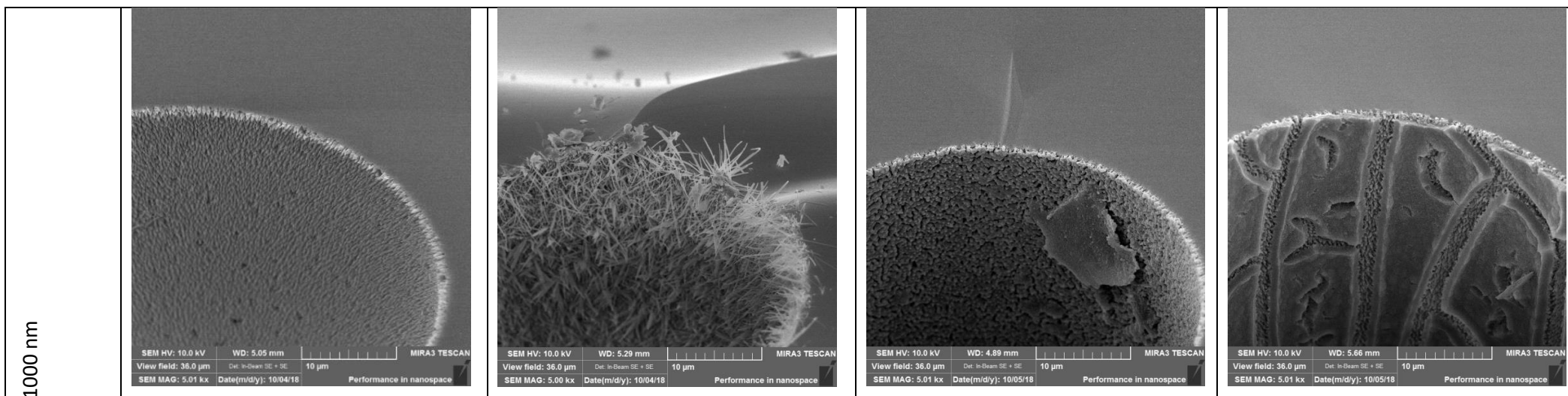
NOVEL APPROACH FOR THE SYNTHESIS OF A COVALENTLY BOUND, HIGHLY POLAR AND PH-PERSISTENT N-ACRYLOYLAMIDO ETHOXYETHANOL CAPILLARY COATING FOR CAPILLARY ELECTROPHORESIS-MASS SPECTROMETRY PART 2: ETCHING WITH SUPERCRITICAL WATER AS CAPILLARY PRETREATMENT



NOVEL APPROACH FOR THE SYNTHESIS OF A COVALENTLY BOUND, HIGHLY POLAR AND PH-PERSISTENT N-ACRYLOYLAMIDO ETHOXYETHANOL CAPILLARY COATING FOR CAPILLARY ELECTROPHORESIS-MASS SPECTROMETRY PART 2: ETCHING WITH SUPERCRITICAL WATER AS CAPILLARY PRETREATMENT

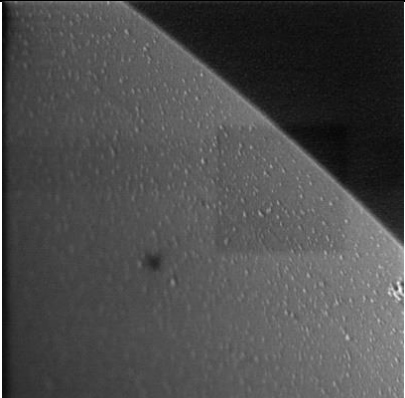
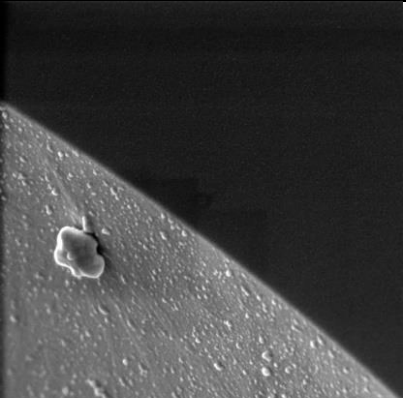
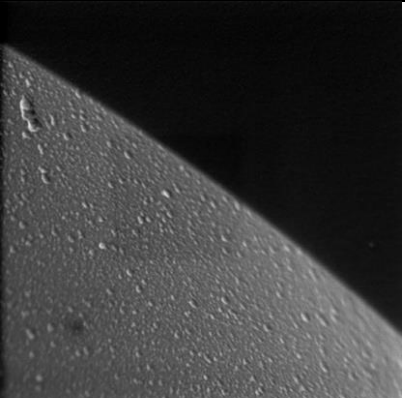
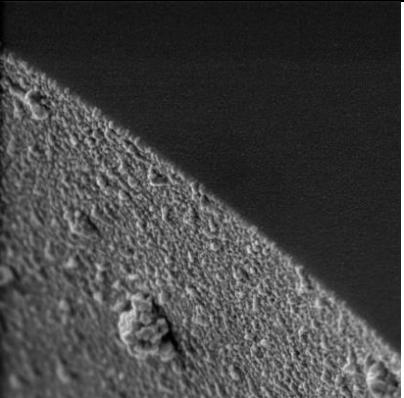


NOVEL APPROACH FOR THE SYNTHESIS OF A COVALENTLY BOUND, HIGHLY POLAR AND PH-PERSISTENT N-ACRYLOYLAMIDO ETHOXYETHANOL CAPILLARY COATING FOR CAPILLARY ELECTROPHORESIS-MASS SPECTROMETRY PART 2: ETCHING WITH SUPERCRITICAL WATER AS CAPILLARY PRETREATMENT

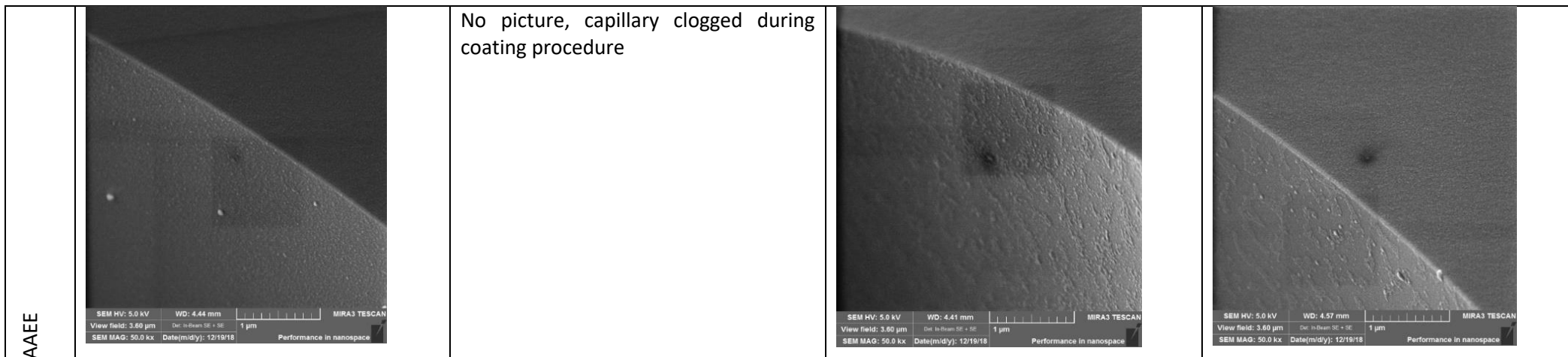


NOVEL APPROACH FOR THE SYNTHESIS OF A COVALENTLY BOUND, HIGHLY POLAR AND PH-PERSISTENT N-ACRYLOYLAMIDO ETHOXYETHANOL CAPILLARY COATING FOR CAPILLARY ELECTROPHORESIS-MASS SPECTROMETRY PART 2: ETCHING WITH SUPERCRITICAL WATER AS CAPILLARY PRETREATMENT

Table 8: SEM-pictures taken on capillaries prepared using different synthesis procedures, either by altering preconditioning procedures (0.1 mol/L vs 1 mol/L HCl and NaOH) as well as reaction procedure (using vs. relinquishing rinsing with thionyl chloride). SEM-measurements were conducted after both hydration step using LiAlH_4 and after coating with AAEE and both pictures were taken from a single capillary by cutting a piece with a length of 2 cm. Therein, SEM was measured on two positions of each capillary piece and each synthesis condition was investigated using two capillaries. No significant differences between all four measurements (2 measurements per capillary, 2 capillaries for each synthesis procedure) were found. One representative picture with 5000-fold magnification is shown each. Measurement settings see Section 5.3.1.4

After...	0.1 mol/L HCl and NaOH without thionyl chloride	1 mol/L HCl and NaOH without thionyl chloride	0.1 mol/L HCl and NaOH with thionyl chloride	1 mol/L HCl and NaOH with thionyl chloride
LiAlH_4	 <p>SEM HV: 5.0 kV WD: 3.34 mm MIRA3 TESCAN View field: 3.60 µm Det: In-Beam SE 1 µm SEM MAG: 50.0 kx Date(m/d/y): 12/11/18 Performance in nanospace</p>	 <p>SEM HV: 5.0 kV WD: 4.47 mm MIRA3 TESCAN View field: 3.60 µm Det: In-Beam SE 1 µm SEM MAG: 50.0 kx Date(m/d/y): 12/17/18 Performance in nanospace</p>	 <p>SEM HV: 5.0 kV WD: 3.26 mm MIRA3 TESCAN View field: 3.60 µm Det: In-Beam SE 1 µm SEM MAG: 50.0 kx Date(m/d/y): 12/11/18 Performance in nanospace</p>	 <p>SEM HV: 5.0 kV WD: 3.46 mm MIRA3 TESCAN View field: 3.60 µm Det: In-Beam SE 1 µm SEM MAG: 50.0 kx Date(m/d/y): 12/11/18 Performance in nanospace</p>

NOVEL APPROACH FOR THE SYNTHESIS OF A COVALENTLY BOUND, HIGHLY POLAR AND PH-PERSISTENT N-ACRYLOYLAMIDO ETHOXYETHANOL CAPILLARY COATING FOR CAPILLARY ELECTROPHORESIS-MASS SPECTROMETRY PART 2: ETCHING WITH SUPERCRITICAL WATER AS CAPILLARY PRETREATMENT



5.4.1.4. Variation in synthesis protocol

Various modifications of the coating synthesis were investigated for non-etched capillaries (see Table 5). More deposit aggregates were observed for both higher concentration of acid and base during preconditioning as well as for rinsing with thionyl chloride, as can be seen in Table 8. Thickest layers were obtained when both high concentrations of NaOH and HCl during preconditioning and thionyl chloride in the hydration step were applied.

5.4.2. Electroosmotic mobilities

EOF determinations were made to judge the influence of rinsing protocols with HCl and NaOH on the reaction and the importance of thionyl chloride in the formation of the additional layers as described in Section 5.4.1. Investigations according to Table 5 were conducted using 2 capillaries for each condition. Capillary **1/woTC II** clogged during the coating procedure. For all capillaries coated with AAEE, EOF values below $0.5 \cdot 10^{-4} \text{ cm}^2 \text{ V}^{-1} \text{ s}^{-1}$ were determined (see Figure 30 A). This is approx. 10 % of the μ_{EOF} -value found for non-coated capillaries at the same pH. No dependence on the etching duration or surface roughness was present. In addition, low relative standard deviations of EOF mobilities indicate sufficient stability of the coating surface. Higher μ_{EOF} -values are commonly observed when rinsing with thionyl chloride is neglected. Preconditioning with 0.1 and 1 mol/L HCl and NaOH gave comparable results.

Both higher reproducibility of μ_{EOF} -values as well as lower μ_{EOF} -values were obtained for etched capillaries, see Figure 30 A.

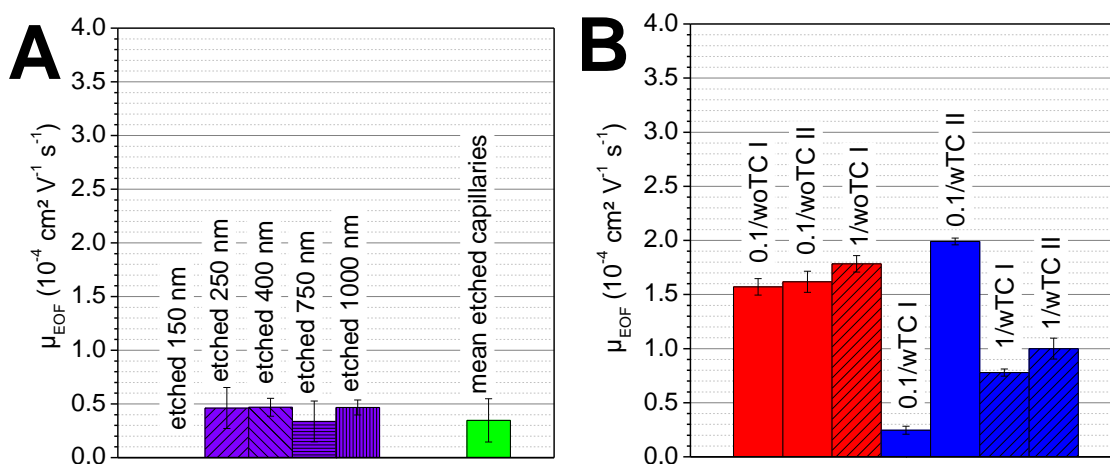


Figure 30: μ_{EOF} -values determined in AAEE-coated capillaries, synthesis and measurement procedures see Table 5. **A:** μ_{EOF} -values obtained for capillaries with etched surfaces ($n = 5$). The whole coating protocol according to Section 5.3.4 was applied here. **B:** μ_{EOF} -values obtained for AAEE-coated capillaries where a rinsing step with thionyl chloride was implemented during synthesis (wTC) are shown in blue, those, where the rinsing step was omitted (woTC) are shown in red. I and II refer to replicates, since each coating procedure was conducted in duplicates. Capillaries were preconditioned with 0.1 mol/L (0.1/) or 1 mol/L (1/) HCl and NaOH.

The relevance of the reaction step with thionyl chloride was investigated for non-etched capillaries, see Figure 30 B. Overall, electroosmotic mobilities were mostly higher than for etched capillaries (Figure 30 A). The use of thionyl chloride in the coating synthesis revealed lower μ_{EOF} -values (0.1/wTC I, 1/wTC I and 1/wTC II, blue bars). When thionyl chloride was omitted in the synthesis (0.1/woTC I, 0.1/woTC II and 1/woTC I, red bars) somewhat higher EOF was present on average.

The high μ_{EOF} -value of **0.1/wTC II** is in good accordance with the observations made previously, see Chapter 4. There, μ_{EOF} -values between $0.5 \cdot 10^{-4} \text{ cm}^2\text{V}^{-1}\text{s}^{-1}$ and $2.5 \cdot 10^{-4} \text{ cm}^2\text{V}^{-1}\text{s}^{-1}$ were observed. A t-test for μ_{EOF} -values presented in Figure 30 B with previously synthesized capillaries of Batch 1 in Chapter 4 revealed significant differences for capillaries obtained using synthesis procedures without thionyl chloride ($p = 0.00042$) and good correlation for those obtained using thionyl chloride ($p = 0.42$), showing the importance of this reagent in the coating protocol. μ_{EOF} -values were identical for both concentrations in the preconditioning solution (0.1 or 1 ml/L NaOH and HCl, see Figure 30 B).

5.4.3. CE-MS

Capillary performance analyzing a peptide sample (tryptically digested BSA, see Section 4.3.3) was characterized as described previously in Chapter 4.

During CE-MS measurements, high hydrodynamic resistance towards rinsing was observed for all etched capillaries; approx. 3 times higher rinsing times at a pressure of 1 bar were necessary to transport a sample plug through capillaries which were etched in contrast to non-etched capillaries, results not shown. Preconditioning with BGE was kept at 3 min at 1 bar, which is identical to the preconditioning for non-etched capillaries, see Chapter 4. In contrast, for measurements at 30 kV, the internal pressure needed to be increased from 10 mbar (non-etched capillaries, see Chapter 4) to 100 mbar (etched capillaries) to obtain similar effective electrophoretic mobilities (μ_{eff}) of Peptide 1 between $4.0 - 6.6 \cdot 10^{-4} \text{ cm}^2\text{V}^{-1}\text{s}^{-1}$ as in non-etched capillaries. This is worth noting, since the vastly higher internal pressure would normally result in much lower apparent μ_{eff} -values, especially as shorter capillaries (lengths of 54.1 – 60.3 cm) were used here.

Despite this increased hydrodynamic resistance, peak areas (**A**) were only approx. 2-times smaller for etched capillaries compared to non-etched capillaries, see Figure 32 C and Figure 26 C in Chapter 4. An exception was observed for the surface roughness of 1000 nm; peak area of Peptides 1-4 and 6 was 10 % of the peak area observed for non-etched capillaries whereas the peak area of Peptide 5 was approx. 50 % higher. A significantly lower separation performance for etched capillaries was observed: Plate heights (**H**) were between 120 – 1200 μm and thus at least 20 times higher than those observed for non-etched capillaries.

I observed that the separation selectivity was altered when etched capillaries were used, visible in altered migration order compared to non-etched capillaries. For capillaries etched with a final surface roughness larger than 150 μm , Peptide 6 co-migrated with Peptide 3 and thus migrated faster than Peptides 4 and 5, see Figure 31. An altered separation mechanism with chromatographic interaction at the capillary surface and thus wall coated open tubular capillary electrochromatography (WCOTC) or a size sieving with polymer inside the separation path may be the reason. WCOTC could be excluded as a major separation mechanism, when pumping the sample plug through the etched capillaries after AAEE coating as described in Section 5.3.1.2 ($n = 5$). Identical retention times were observed for each peptide precluding significant chromatographic interaction with the capillary surface. Further investigations would be necessary to understand the selectivity changes.

NOVEL APPROACH FOR THE SYNTHESIS OF A COVALENTLY BOUND, HIGHLY POLAR AND pH-PERSISTENT N-ACRYLOYLAMIDO ETHOXYETHANOL CAPILLARY COATING FOR CAPILLARY ELECTROPHORESIS-MASS SPECTROMETRY
PART 2: ETCHING WITH SUPERCRITICAL WATER AS CAPILLARY PRETREATMENT

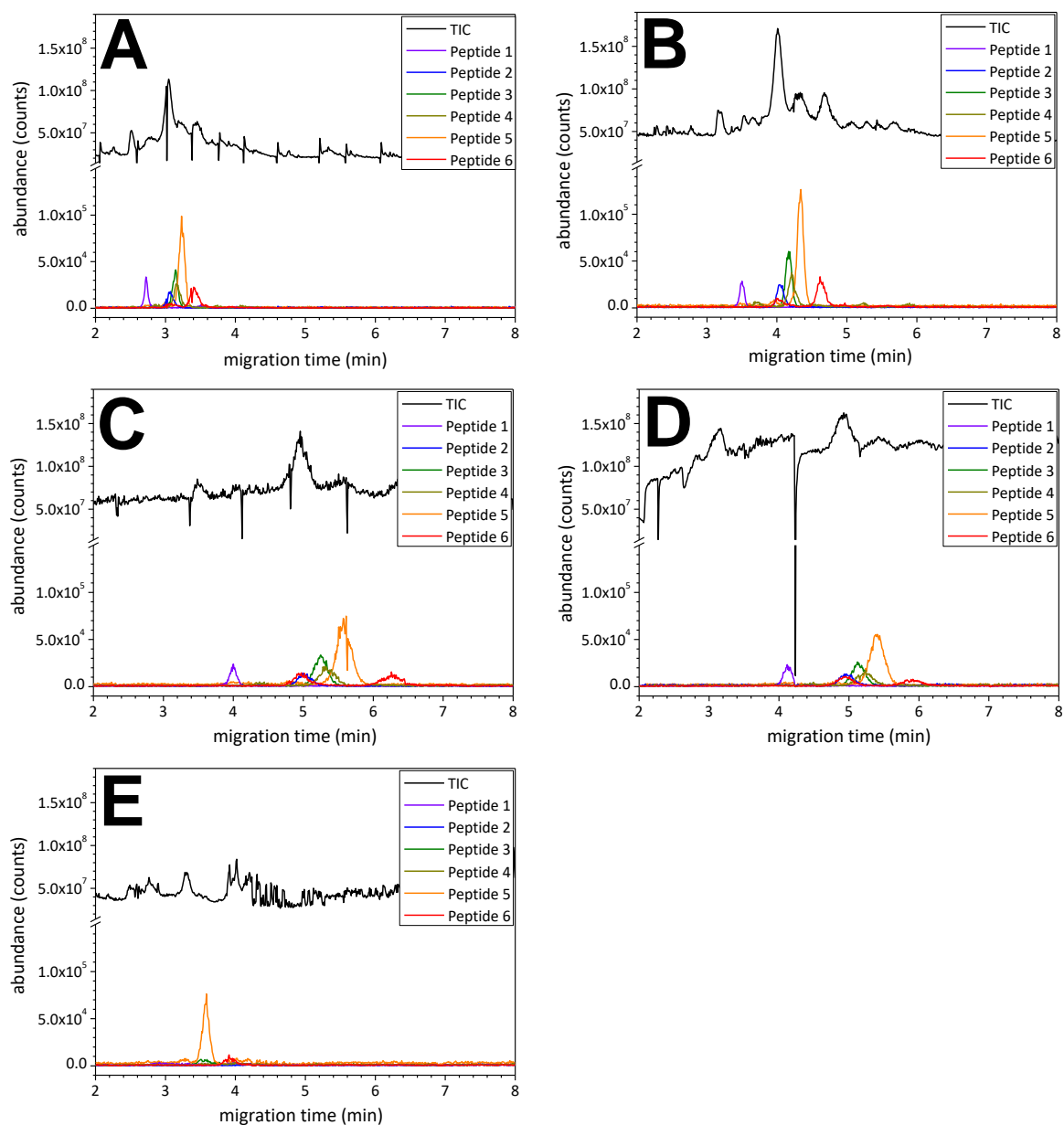


Figure 31: Exemplary CE-MS-electropherograms (total ion current (TIC) and extracted ion current (EIC)) obtained using AAEE-coated capillaries with a surface roughness (and length) of A: 150 nm (L = 57.8 cm), B: 250 nm (L = 58.8 cm), C: 400 nm (L = 54.1 cm), D: 750 nm (L = 60.3 cm), E: 1000 nm (L = 51.9 cm), showing the total ion current (TIC, black) as well as the 6 EICs of peptides 1-6 (colors) for estimation of separation performance. *m/z*-values of peptides are as follows: 1: 417.1968, 2: 473.8831, 3: 379.6995, 4: 526.2403, 5: 395.2235 and 6: 740.3700. Capillaries were rinsed with BGE for 3 min at 1 bar in-between runs and prior to the first analysis. Measurement parameters can be found in Section 5.3.1.2.

NOVEL APPROACH FOR THE SYNTHESIS OF A COVALENTLY BOUND, HIGHLY POLAR AND PH-PERSISTENT N-ACRYLOYLAMIDO ETHOXYETHANOL CAPILLARY COATING FOR CAPILLARY ELECTROPHORESIS-MASS SPECTROMETRY
PART 2: ETCHING WITH SUPERCRITICAL WATER AS CAPILLARY PRETREATMENT

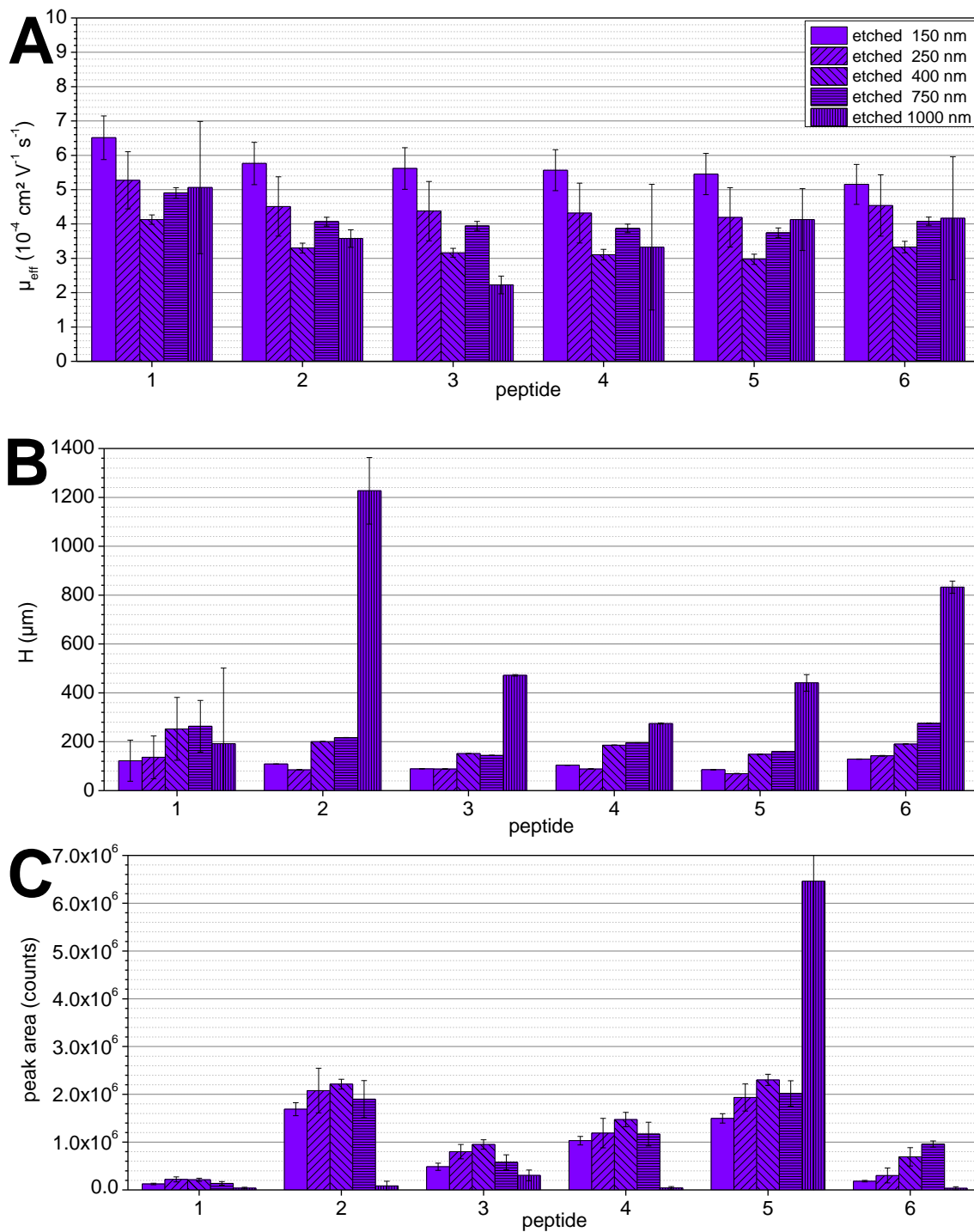


Figure 32: A: Effective electrophoretic mobility μ_{eff} , for 6 different peptides, see Chapter 4, Figure 25 for further information, B: plate height H, and C: peak area A determined for each of the 6 peptides detected in tryptically digested BSA for measurements in AAEE coated capillaries with different surface roughness (see legend) (n = 5). The same patterns as in Figure 30 A were used. Representative electropherograms for each capillary are presented in Figure 31..

5.5. Discussion

5.5.1. Etched surfaces during coating procedure

I tried to take representative capillaries pieces for the SEM measurements, overall representing 4 cm in length. Nevertheless, large differences in the respective SEM-images of capillaries after hydration (see Table 6 and Table 7) were found, especially when comparing the SEM-pictures of the capillary with 1000 nm surface roughness with the non-etched surface. The debris was irregularly spread over the capillary inner surface. High dispersity of surface coverage with these deposits is thereby assumed for etched capillaries. In contrast, very homogeneous layers were observed for non-etched capillaries, as noted in Section 5.4.1.3. To demonstrate that my results are not an artefact at one end of a capillary, SEM-measurements have to be taken over the whole capillary, analogous to those described for non-etched capillaries in Section 5.4.1.2. However, with the clear dependence on the surface roughness, an artefact is unlikely.

The formation of needles observed in SEM of preconditioned capillaries after rinsing at extreme pH-values (pH 0 and 14 for 1 mol/L HCl and NaOH, respectively), see Section 5.4.1.2, is presumably due to pH-induced silanol chemistry. I suggest that dissolution and re-crystallization of silanol takes place. The fact, that this phenomenon correlates well with the surface roughness is presumably linked to a weakened (highly amorphous) silica structure also at deeper layers. This observation is in good accordance with the fact, that the solubility of silica increases dramatically in supercritical solvents, especially water^{213, 214}. Weakened surface structure after treatment with supercritical water is indicated by my results. Faster dissolution rates are achieved. I did not find studies, explicitly investigating the origin of increased activity of silica surfaces after supercritical water treatment.

Since I did not work under inert conditions I assume, that moisture induced the oxidation of LiAlH_4 -species to a material of unknown composition, which formed small crystalline structures in solution, finally present on the capillary surface as debris. For non-etched capillaries, only a thin layer of this debris formed (see Section 5.4.1.3). In contrast, for etched capillaries, the needles formed during preconditioning may have acted as crystallization nuclei for the formation of thick layers and larger structures (see Table 6 and Table 7).

With regard to the identification of these layers formed, I have hints from the insulating properties of this layer observed during EDX. I presume that aluminate-species²¹⁵ are formed. From the reactants in the reaction solutions, the only other option would be formation of solid NaOH, which is, however, unlikely.

Ionic bonds between aluminates and silica species are very favorable and stable²¹⁵⁻²¹⁷, which is due to their similar metal-oxide distances in oxides (181 pm for Al_2O_3 and 161 pm for SiO_2)²¹⁸. The observed aggregation of aluminate-species on the surface of activated silica is thus not surprising.

5.5.2. Advantages of preconditioning with supercritical water

High capillary-to-capillary reproducibility of etched capillaries and the low overall μ_{EOF} -values after formation of AAEE surfaces indicate not only successful but also superior preconditioning of the inner surface. Clearly, etching with the harsh conditions of supercritical water provides more homogeneous surfaces than using concentrated acid and base alone (see also Chapter 4). regarding

the depletion of Si-OH. The similar μ_{EOF} -values for all capillaries preconditioned with supercritical water indicate, that surface homogenization plays a more important role than surface etching to obtain different surface roughness.

For capillaries with a surface roughness higher than 150 nm, two effects were observed: changes in separation selectivity, a decrease in separation efficiency and increased hydrodynamic resistance when trying to rinse the capillaries, see Section 5.4.3.

The investigation of CEC, as described in Section 5.4.3, proved that a chromatographic separation mechanism is unlikely. I assume, that some sort of capillary sieving electrophoresis (CSE) occurs. The high hydrodynamic resistance indicates that either a strong decrease in capillary diameter (not supported by SEM to this extent) occurred or AAEE polymer chains extend into the capillary inner volume, inducing hydrodynamic resistance and CSE. I do not expect the polymer chains to be long enough to produce a homogeneous network over the whole capillary inner diameter, but only over a few μm . SEM pictures clearly show that the surfaces coating is not homogeneous, see Table 6 and Table 7. From this, it is easy to understand that peak-broadening, as visible in Figure 31 for peptide separation, occurs. It becomes pronounced for capillaries with high degrees of etching during the preconditioning with supercritical water.

Precluding chromatographic interaction in a CEC mechanism, it is likely, that the reactions at the surface were very fast and efficient due to the good surface activation. I assume that a polymer network evolved at the capillary surface and extends into the capillary inner volume. If this is the case, the reaction times could be shortened significantly, especially the reaction with LiAlH_4 to achieve the same surface coating quality as for non-etched capillaries. In addition, this will occur on a homogeneous surface to provide higher repeatability of the coating process.

5.5.3. Co-existence of aluminate layer and Si-H-groups

Observations made for non-etched capillaries and various rinsing conditions, shown in Section 5.4.1.4, indicate that thionyl chloride plays an important role in the suppression of the EOF. In Chapter 4 I described, that a highly suppressed EOF indicates a high and homogeneous coverage of the capillary surface. This is possible by reducing the access to Si-OH groups at the capillary surface either via the formation of Si-C-groups or via the shielding of Si-OH groups. Capillaries rinsed with thionyl chloride had thickest layers of aluminate, see SEM-pictures in Table 8. However, only thionyl chloride allows transformation of Si-OH over Si-H to Si-C-groups. I clearly showed that at least for non-etched capillaries, the addition of thionyl chloride as reactant is important to obtain a low EOF (see Section 5.4.1.4). From my experimental results, it is not yet clear, if both the formation of the aluminate layer and Si-H formation at the capillary surface determine the quality of the coating process. Possibly, for etched capillaries, silanol groups are efficiently shielded already by the aluminate layer so that thionyl chloride can be omitted. Thus, further experiments are necessary to verify that the surface layers observed are aluminate (e.g. using TOF-SIMS) and to determine the dependence of the separation performance and EOF on the presence of the thionyl chloride in combination with the thickness of the aluminate layer. The latter can surely be adjusted for each surface roughness by reaction times.

5.6. Conclusion and outlook

My results show, that etching with supercritical water is a new possibility for surface activation, homogenization and preconditioning prior to the synthesis of covalent capillary coatings. Higher capillary-to-capillary reproducibility of the coating formation can be obtained. I assume, that the surface roughness itself plays a minor role, therefore quick capillary etching pulses for an efficient surface activation is worth to be investigated in future in order to shorten the overall synthetic protocol. The protocols will also have to be adapted to the higher reactivity of the etched surfaces. I think, that even omitting rinsing steps with acid and base is possible, since surfaces are already cleaned and activated using supercritical water.

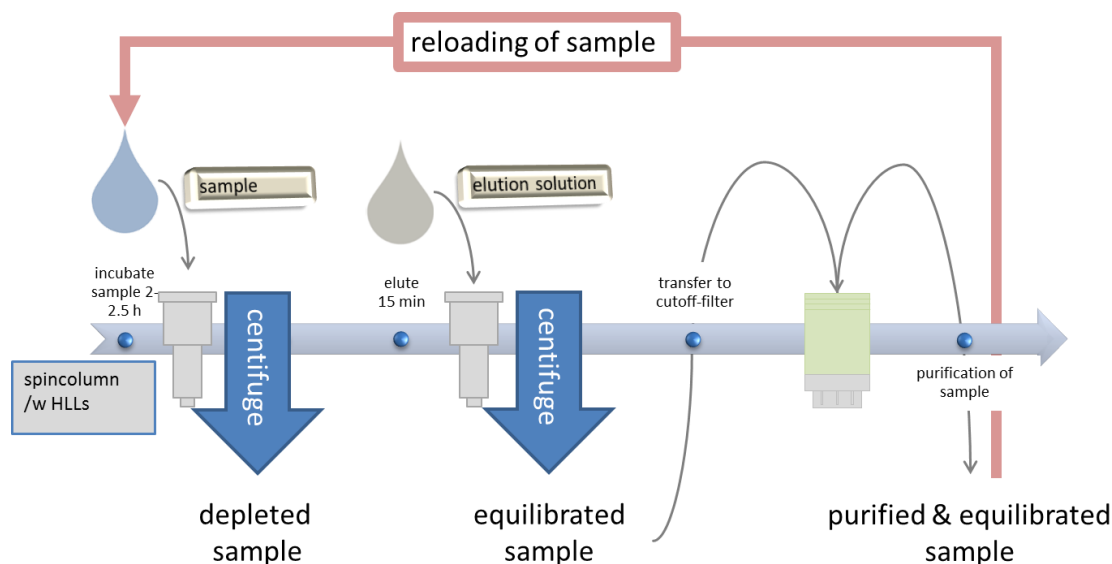
With the identification of the layer composition, for which I propose aluminate species, new and extremely stable covalently coupled coating (pH, organic solvents) can be envisaged, when the last reaction step of polymerization is understood. Currently, I do not know, if accessible Si-H groups are still present despite the aluminate layer or if the polymerization occurs only on the aluminate surface in case of strongly etched capillaries with thick aluminate layers. In general, aluminate is very stable and obviously, the layers formed allow for an efficient shielding of surface silanol groups as the major source for adsorption of biomolecules.

6. Step-wise equilibration of protein samples using hexapeptide ligand libraries. Optimization of the elution and purification protocols to enable reloading

6.1. Abstract

Hexapeptide ligand libraries (HLL) are a useful, non-depleting tool for proteomic investigations as well as for pharmaceutical product development and control. A deep insight into the proteome is difficult due to the high sample amounts that would be necessary to account for low abundance proteins in the presence of high abundance ones. I therefore present an enhanced equilibration method which needs significantly smaller sample volumes by developing a protocol for step-wise equilibration via HLLs. Using a smaller amount of beads in the consecutive reloading steps, an overall better equilibration can be reached.

Step-wise protein equilibration was investigated using a protein solution consisting of 4 standard proteins with concentration differences of up to 1:64, as well as serum samples. Three elution solutions for HLL-experiments with urea and five elution solutions based on sodium dodecyl sulfate (SDS) were investigated with respect to the possibility of purifying the proteins to regain loading conditions using cut-off-filters. Various washing and centrifugation as well as recovery and pre-equilibration protocols were investigated with the aim of step-wise reloading the purified sample on a novel fraction of HLLs. Highest recoveries from HLLs and purification of proteins were observed for a sample containing 8 mol/L urea, 5 % acetic acid and 2 % CHAPS. After purification, up to two further equilibration steps were performed. Characterization of the equilibration efficiency was based on relative concentrations of different proteins and their isoforms after quantification of the intact proteins by capillary electrophoresis-mass spectrometry.



Graphical Abstract: Flow chart for the consecutive equilibration of protein samples. After sample incubation on HLLs using spin-columns, various elution protocols were investigated. The best elution protocol (8 mol/L urea, 2 % CHAPS and 5 % acetic acid) was utilized in consecutive equilibration, using cut-off-filters for depletion of HLL elution solution. Purified samples can be reloaded and equilibrated multiple times. Thereby, depleted samples as well as purified and equilibrated samples are obtained.

6.2. Introduction and motivation

The search for easily accessible proteins as biomarkers in e.g. urine, blood and saliva is still ongoing¹⁻¹². Protein biomarkers are especially hard to obtain for blood, where the concentration range of proteins reaches over 12 orders of magnitude with albumin and the globulins present in a mass concentration above 90 %. These most abundant proteins hinder detection of low abundant proteins¹⁵⁻¹⁷. No analytical technique is capable to deal with this vast concentration range since abundance of few proteins impairs both selectivity and sensitivity for low concentrated proteins. Therefore, sample pre-treatment techniques to lower this concentration range became prominent in proteomics research. Commonly, antibody-based depletion-techniques for the most abundant 6-20 proteins are used to make low-abundant proteins detectable¹⁸. This solid-phase-extraction of proteins of interest using target-specific antibodies^{19, 219, 220} followed by elution in low volumes is very successful albeit expensive. Depletion efficiencies are generally very high, however, no relative enrichment of low abundance proteins takes place so that their concentration is still below the limit of detection. Furthermore co-depletion of low concentrated proteins is problematic^{221, 222}. The depletion of the high-abundance proteins leads to lower interferences in MS-based analytical techniques.

When sub-proteomes with a specific post-translational modification (PTM) are targeted, special enrichment techniques offer the possibility to enrich low concentrated proteins with this modification and simultaneously obtain a versatile sub-proteome such as the phosphoproteome²²³⁻²²⁸, ubiquitinome^{229, 230}, glycoproteome^{231, 232} and acetylome²³³, to name only a few. Serial enrichment to obtain several of these sub-proteomes from a single sample are known, too²³⁴. These techniques often reveal high protein concentrations due to the possibility to use small elution volumes.

Hexapeptide ligand libraries (HLL) offer an alternative approach to reduce the concentration range of proteomes^{10, 235}: Instead of enriching a specific type of post-translationally modified protein, proteins are bound nonspecifically via their amino acid backbone. Ideally, the beads have the same binding capacity for all proteins. Even the presence of PTMs such as glycosylation gives no bias on the equilibration, as published by Huhn *et al.*^{26, 236}. HLL are designed to provide various non-specific binding sites, offering numerous binding sites so ideally, each protein finds a suitable ligand. With the same binding capacity for each protein, protein equilibration is obtained under overloading conditions, where excess of high abundance proteins remains in the liquid phase and is washed away¹³.

The synthesis procedure is illustrated in Figure 33. HLLs are polymeric (polyhydroxyethyl methacrylate²³⁷) particles with a defined and modified surface. Starting with an amine function covalently bound to the surface, N-terminally protected amino acids are grafted by a so-called “split-couple-recombine” synthesis. This synthesis is presented exemplarily in Figure 33 for the synthesis of a tripeptide surface consisting of 3 different amino acids. Here, particles with an amine function are “split” into 3 reaction vessels followed by “coupling” of one specific amino acid (here: alanine A, glycine G and valine V) onto each surface. Particles are then purified, “recombined”, protection groups are removed, and the particles are “split” into 3 reaction vessels again. Thereby, $3^2 = 9$ different surfaces are obtained. The HLLs applied in this work are commercially available (BioRad, München, Germany) and consist of a hexapeptide surface using 20 amino acids, resulting in $20^6 = 6.4 \cdot 10^7$ different surfaces¹³.

STEP-WISE EQUILIBRATION OF PROTEIN SAMPLES USING HEXAPEPTIDE LIGAND LIBRARIES. OPTIMIZATION OF THE ELUTION AND PURIFICATION PROTOCOLS TO ENABLE RELOADING

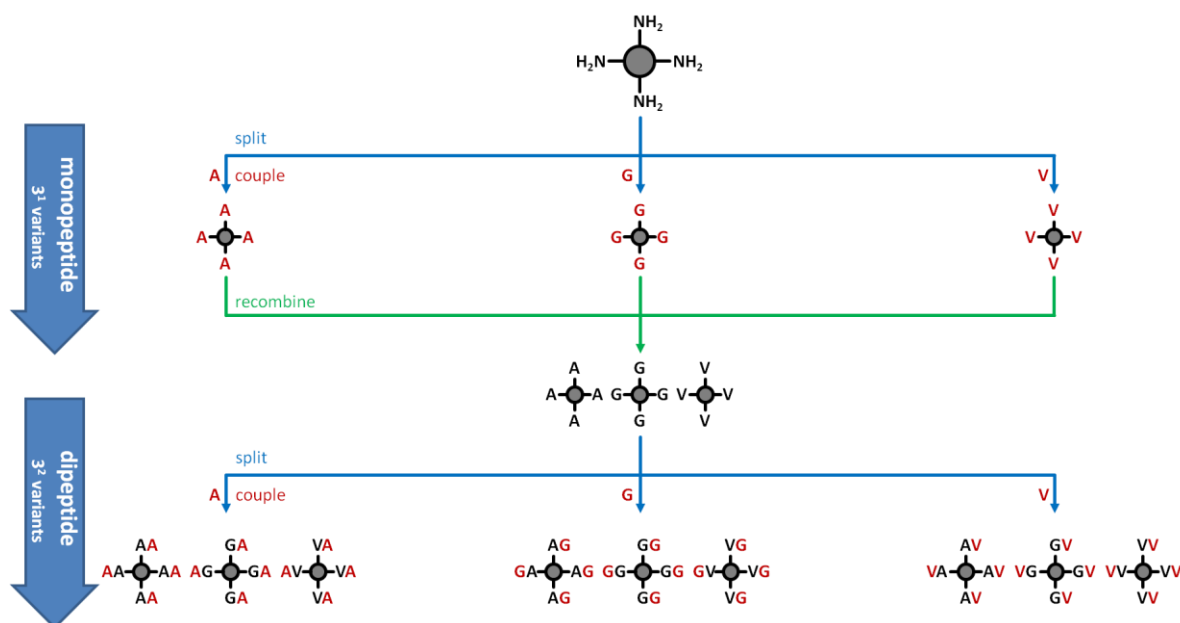


Figure 33: Synthesis of tripeptide ligand libraries based on 3 different amino acids (alanine A, Glycine G and valine V) starting from a particle exhibiting amine functions on its surface. Splitting before synthesis guarantees uniform amino acid sequence on each particle, recombination guarantees increased versatility of surfaces. Figure based on Boschetti *et al.*⁷ and Furka *et al.*²³⁸. Permission was kindly granted by Elsevier.

Elution of equilibrated proteins from HLLs using a small volume of appropriate elution solvent results in samples of high overall protein concentration and high complexity. Using manufacturer protocols, a protein-equilibration to a factor 40 to 50 can be reached. In literature, protocols using high amounts of sample at comparatively low amount of ligand libraries (up to 150 mL serum, which equals approx. 7.5 g overall protein and 500 μ L settled bead volume / 52.5 mg dry beads) are known, resulting in an enormous equilibration and thus a deeper look inside the proteome (estimated factor 7500)²³⁹. However, co-depletion and other effects on the binding capacity are likely. Equilibration using high sample amounts is difficult, e.g. in clinical diagnosis or early-stage pharmaceutical research, where only small sample amounts are available. Therefore, a method for the consecutive equilibration of proteins using HLLs is developed during this work. In my proof of concept study, an equilibration factor of 250 from serum was aimed at using step-wise equilibration (factor 50 followed by factor 5) from only 1.0 mL (50 mg) of protein sample instead of single-step equilibration using 5 mL on the same amount of beads.

Re-application of the protein sample after elution needs purification, which is achieved by using 10 kDa molecular weight cut-off-filters (cut-off-filter). To fully restore binding conditions, various washing and centrifugation procedures were investigated. The main general challenges of their applicability towards the processing of protein samples are protein adsorption on membranes as well as the formation of a protein-concentration-gradient during centrifugation that often results in loss of sample due to protein precipitation. Especially, excessive centrifugation followed by appropriate recovery steps for the sample has proven to be troublesome. Few work-flows and protocols tackling these issues are discussed on corresponding websites rather than in scientific literature²⁴⁰⁻²⁴². Incubation of filter-units with surfactant²⁴³ or “sticky” proteins such as BSA has been claimed as an adequate measure to avoid adsorption. For this work, I decided against such measures in order to minimize the presence of protein and nonprotein interfering compounds. In addition, these measures are not appropriate to avoid precipitation.

In literature, time-consuming screening techniques, such as 2D-PAGE^{1, 7, 244, 245}, sometimes followed by digestion and MALDI-MS⁶³ or other 2D-separation techniques are often used after digestion of proteins, among others. For an overview, I like to refer to several excellent reviews²⁴⁶⁻²⁴⁸. Here, I used a fast CE-MS-technique with high resolution MS (qTOF) to quantify intact native proteins, offering all necessary information on equilibration efficiency, high automation and measurement times of only approx. 20 min per sample. I successfully conducted CE-MS in triplicate using only a fraction of equilibrated samples (approx. 10 μ L, this equals 1/10 of original sample and 5 μ g or 0.35 nmol as detection limit for the lowest concentrated protein). Overall, high precision was observed for the analytical replicates. High MS-resolution as well as highly protein repulsive capillary coatings allow characterization of intact proteins without the necessity of digestion which increases complexity of samples and enforces consecutive characterization using data-base supported algorithms. The model protein sample chosen consists of 4 proteins with a broad range of molecular weight and physicochemical properties, such as pI and log(P_{ow}) with an overall concentration range of 1:64.

Since each protein is present with numerous isoforms, not only equilibration between proteins (via the “inter-protein equilibration”), but also the equilibration of isoforms for each protein (called “intra-protein equilibration”) is investigated. All isoforms considered from CE-MS analysis are listed in **Table S 1**. Evaluation of elution protocols, pre-equilibration and protein-recovery from cut-off-filters was done two-fold: first, via relative equilibration and enrichment using inter- and intra-protein equilibration and secondly via the evaluation of recovery using the overall yield of proteins. The latter is the summed weight of each protein and its respective isoforms.

6.3. Materials and methods

6.3.1. Instrumentation

6.3.1.1. Capillary electrophoresis

For CE analysis, an Agilent 7100 CE system (Agilent, Waldbronn, Germany) with UV-detection was used. For SDS-CE, the chosen wavelengths were 210 nm and 280 nm with a spectral width of 10 nm and a reference wavelength of 360 nm. For CE-MS measurements and hyphenation see Section 4.3.1.2. Fused silica capillaries with an inner diameter of 50 μm or 100 μm and an outer diameter of 365 μm were purchased from Polymicro (Kehl, Germany). Measurements in Section 4.4.1 and 6.4.3.1 were conducted using capillaries with a self-made covalent capillary coating with a hydrophilic *N*-acryloylamido ethoxyethanol (AAEE) surface, see Chapter 4. If not stated otherwise, capillaries with 100 cm in length and an inner diameter of 50 μm were used for CE-MS-measurements. During separation at +30 kV, an additional pressure of 100 mbar was applied. The running buffer (BGE) contained 0.75 mol/L acetic acid and 0.25 mol/L formic acid in water at pH 2.2¹⁴⁶. In between measurements, capillaries were rinsed with 50 mmol/L for 2 min at 1 bar followed by BGE for 3 min at 1 bar. Capillaries were stored dry until use.

6.3.1.2. Mass spectrometry

A quadrupole time-of-flight mass spectrometer 6550 (QTOF 6550) from Agilent (Santa Clara, United States) with a sheath liquid interface from Agilent (Waldbronn, Germany) was used by implementing an Agilent isocratic pump 1260 (Agilent Technologies, Waldbronn, Germany) at a flow rate of 5 $\mu\text{L}/\text{min}$. A jetstream electrospray ionization (ESI) source was operated with a nebulizer pressure of 275 and 345 mbar, for coated and non-coated capillaries, respectively. The drying gas temperature was 150°C. A flow rate of 11 L/min and a fragmentor voltage of 175 V were applied. Skimmer voltage was set to 65 V and octopole voltage to 750 V. The mass range was 100-3000 m/z with a data acquisition rate of 2 spectra/s. A 1:1 (v/v) mixture of 2-propanol/water was used as sheath liquid, containing 0.1 % formic acid as well as a few nanogram of 3 selected calibrants for internal calibration (Agilent Technologies, Waldbronn, Germany, m/z = 121.0508, 322.0481 and 922.0097). If not stated otherwise, injection of sample was performed hydrodynamically at 100 mbar for 5 s.

Compounds were identified using Agilent MassHunter Qualitative Analysis B.06.00 software using an algorithm for molecular feature extraction for large molecules (proteins and oligos). It takes the following parameters into account: extraction of peaks with heights ≥ 50 counts, including hydrogen-, sodium-, potassium-, ammonium- and chloride-adducts as well as loss of hydride. A quality score ≥ 80 % was set.

For quantification via CE-MS, external calibrations were performed within the same sequence-run, see Section 6.4.1 for further details. Data evaluation was done using Agilent MassHunter Quantitative Analysis B.06.00 software considering a single m/z -value for each analyte. Respective values are summarized in Table S 1 for proteins and protein microheterogeneities investigated in this work.

6.3.2. Chemicals

Lysozyme (chicken egg white, M_r = 14.4 kDa), β -lactoglobulin (bovine milk, M_r = 18.4 kDa), carbonic anhydrase (bovine erythrocytes, M_r = 29 kDa), ovalbumin (chicken egg white, M_r = 42.8 kDa),

bovine serum albumin (BSA, bovine serum, $M_r = 66.463$ kDa), sodium dodecyl sulfate (SDS, 98,5 %), ethanol (reagent grade), sodium chloride (NaCl, ≥ 99 %), acrylamide (AA, ≥ 99 %), *N,N'*-methylenebis-acrylamide (bAA, 99 %), trichloroethylene (TCE, ≥ 99.5 %), *N,N,N',N'*-tetramethylethylenediamine (TEMED, ≥ 99 %), ammonium peroxodisulfate (APS, ≥ 98 %), 2-propanol (LC-MS grade), polyethylene oxide ($M_r = 600$ kDa), 3-[(3-Cholamidopropyl)dimethylammonio]-1-propanesulfonate hydrate (CHAPS, 98 %) and formic acid (FA ≥ 99 %) were purchased from Sigma-Aldrich (Steinheim, Germany). Tris(hydroxymethyl)aminomethane (Tris), aqueous sodium hydroxide solution (NaOH, 10 mol/L, suprapur), 2-mercaptoethanol (≥ 99.9 %) and glacial acetic acid (≥ 99.9 %) were delivered by Merck (Darmstadt, Germany). Hydrochloric acid (HCl, 32 %, analytical grade), methanol (≥ 99.8 %), Coomassie brilliant blue G-250 (Coomassie) and 1,4-dithiothreitol (DTT, ≥ 99 % electran for microbiology) were purchased from VWR (Darmstadt, Germany). *N*-Cyclohexyltaurine (CHES) was obtained from Alfa Aesar (Karlsruhe, Germany). Sodium dihydrogen phosphate dehydrate (NaH_2PO_4) was purchased from Caelo (Hilden, Germany). Deionized water was prepared using an ELGA-Veolia PURELAB Classic system (Celle, Germany).

6.3.3. Preparation of sample, HLL elution solutions and PBS

The phosphate-buffered saline (PBS) was made of 150 mmol/L NaCl and 10 mmol/L NaH_2PO_4 . The pH was adjusted to 7.4 by conductometric titration with 10 mol/L NaOH using a WTW inoLab pH7110 pH meter (WTW, Dienslaken, Germany). Aqueous solutions of urea-PBS consisted of 8 mmol/L urea. They were freshly prepared daily and stored on ice prior to use.

Two different samples were used in this project: **Sample A:** The sample used for the optimization of purification protocols with cut-off-filter was a protein solution containing 8 g/L BSA and 2 g/L lysozyme in PBS or water, giving an overall protein concentration of 10 g/L. **Sample B:** For HLL-experiments, a protein solution containing the four proteins BSA, lysozyme, β -lactoglobulin and carbonic anhydrase in mass-ratios 64:16:4:1 and an overall protein concentration of 40.5 g/L in PBS was used.

Table 9: Composition of the investigated HLL elution solutions and elution conditions. The component categories are: buffer, surfactant additive and reducing agent.

#	buffer	surfactant	reducing agent	elution condition
i	100 mmol/L Tris-CHES	1 % SDS	3 % 2-mercaptoethanol	15 min at 95 °C
ii	100 mmol/L Tris-CHES	1 % SDS	none	15 min at 95 °C
iii	water	1 % SDS	none	15 min at 95 °C
iv	water	10 % SDS	none	15 min at 95 °C
v	water	10 % SDS	3 % DTT	15 min at 95 °C
vi	8 mol/L urea, 5 % HOAc	2 % CHAPS	none	15 min at AT ^a
vii	8 mol/L urea	2 % CHAPS	none	15 min at AT
viii	8 mol/L urea	none	none	15 min at AT

^aambient temperature (AT)

STEP-WISE EQUILIBRATION OF PROTEIN SAMPLES USING HEXAPEPTIDE LIGAND LIBRARIES. OPTIMIZATION OF THE
ELUTION AND PURIFICATION PROTOCOLS TO ENABLE RELOADING

All eluents to elute proteins from the HLL (referred to as HLL elution solutions) are listed in Table 9 and were prepared on the day of use. Solutions **i-v** were prepared using stock solutions of 10 wt% SDS and 200 mmol/L Tris-CHES at pH 8.9 which were stored at room temperature and used within 3 months. Solutions **vi-viii** were freshly prepared and stored on ice prior to use.

6.3.4. Preparation and application of HLLs and protein cleanup with 10 kDa cut-off-filters

Hexapeptide ligand libraries and spin columns designed for HLL-experiments were purchased from BioRad (München, Germany) under the brand name Proteominer Beads. Preparation of HLLs was performed according to manufacturer recommendations. In brief, lyophilized HLLs were rehydrated in 20 % aqueous ethanol at 4 °C for 18 h while shaking to reach the final concentration of 0.86 wt% (5.25 mg, 20 µL settled bead volume (SBV) equaling the manufacturer's low capacity enrichment-kit) or 4.30 wt% (26.25 mg, 100 µL settled bead volume (SBV), normal capacity enrichment-kit). Commonly, aliquots of 500 µL were taken and filled into spin columns. Supernatant was removed via centrifugation at 1000 x g for 60 s. This step was followed by washing each HLL fraction 3 times after incubation in 600 µL PBS for 5 min while shaking followed by centrifugation at 1000 x g for 60 s.

Protein samples according to Section 4.3.3 were added to HLL and incubated at ambient temperature for 2 h while shaking. With normal capacity enrichment-kits, 1.25 mL (50.6 mg) protein solution of Sample B were equilibrated at an equilibration ratio of 1:50, the theoretical overall amount of equilibrated protein then equals 1.00 mg⁸. For low capacity enrichment-kits (used for 2-fold equilibration with a binding capacity of 1:5) and for investigation of pre-equilibration of HLLs, the respective protein solution was diluted to approx. 10.1 g/L with PBS.

To purify protein eluates from SDS and urea from the elution step to obtain rebinding conditions to a new HLL, MRCPR010 Microcon-10 kDa centrifugal filter units with Ultracel-10 membrane, here referred to as cut-off-filters, were purchased from Merck Millipore Ltd. (Cork, Ireland) and used according to manufacturer's instructions. For centrifugation a Labofuge 400R (Heraeus, Hanau, Germany) was used. In brief, cut-off-filters were conditioned prior to sample loading via a washing step using 100 µL PBS or water. Samples were loaded and centrifugation times were adjusted according to sample volume. Four consecutive sample washing steps were performed with 100 µL PBS or water, each followed by centrifugation at 14.000 x g for 13 min. For samples containing SDS, 4 preliminary washing steps with an aqueous solution of 8 mol/L urea were conducted to deplete SDS²⁴⁹. Sample elution was conducted in two different ways: For "normal elution" (n), samples were recovered either by 4 consecutive recovery steps adding 25 µL water or PBS, yielding an overall sample volume of 100 µL. For another elution protocol, referred to as "reverse centrifugation" (r), cut-off-filters were placed upside-down in the centrifugation tubes. Here, I loaded 100 µL of water or PBS on the outlet of the cut-off-filter and centrifuged upside-down for 20-25 min at 7.000 x g. This step was repeated three times for each sample and elution fractions were characterized independently. A lower centrifugation speed was used to avoid dislocation of the filter membrane observed at 14.000 x g.

6.3.5. Sodium dodecyl sulfate polyacrylamide gel electrophoresis (SDS-PAGE)

Protein samples for SDS-PAGE analysis were prepared by heating them in an aqueous solution containing 1 % SDS, 100 mmol/L Tris-CHES and 5 % 2-mercaptoethanol. Separation of protein samples in the slab gel was conducted using a discontinuous gradient gel with a stacking gel. The discontinuous separation gradient gel was prepared via a "GM-100 mixer for 2x gradient gels" using equal amounts of a 15.0 wt% and 7.5 wt% AA solution with 3.3 wt% bAA each in separation buffer. Both contained 0.0007 % APS, 0.13 % TEMED, 0.73 % TCE. The solution with the higher AA

concentration also contained 1.0 % glycerol. The overall buffer composition in the separation gel was 375 mmol/L Tris and 0.5 wt% SDS at pH 8.8. Buffer composition in the collector gel was 125 mmol/L Tris and 0.5 % SDS at pH 6.8. Polymerization took place over night at 4 °C.

Size sieving separation of samples via SDS-PAGE was conducted in a PEQLAB-cell from VWR (Darmstadt, Germany) at 180 V and approx. 128 mA and ambient temperature for 2 h. Identification of protein was done by incubation of the slab-gel sheet for 30 min in a solution containing 0.1 % Coomassie, 45 % methanol, 45 % water and 10 % acetic acid followed by consecutive washing with water and incubating four times for 10-15 min in a solution containing 50 % methanol, 44 % water and 6 % glacial acetic acid. A final incubation step in the mentioned solution overnight yielded the final slab gel sheets presented in this work.

6.3.6. Sodium dodecyl sulfate capillary electrophoresis

Sample composition and measurement conditions are described in Chapter 2. Briefly, samples were denaturated in a solution containing 1 % SDS, 5 % 2-mercaptoethanol and 100 mmol/L Tris-CHES at pH 8.9 to obtain an SDS:protein ratio of 1.4:1.

Measurements were performed using a CE instrument as follows: rinsing the capillary (with an overall length of 35 cm, an effective length of 26.5 cm and an inner diameter of 100 µm) with 0.1 mol/L NaOH, 0.1 mol/L HCl and water for 1 min at 1 bar, followed by rinsing with the polymer solution (2 % PEO ($M_r = 600$ kDa) in 100 mmol/L Tris-CHES, 0.1 % SDS at pH 8.9, see Chapter 2) for 3 min at 1 bar. Excessive polymer sticking to the capillary outer surface and electrodes was removed by dipping both capillary ends into water. The sample was injected electrokinetically for 5 s at -10 kV followed by the separation at -8.20 kV (-234 V/cm) for 20 min.

6.4. Results

6.4.1. Quantification of proteins by CE-MS

Standard proteins were separated by CE-MS using a separation capillary which was covalently coated with AAEE, see Chapter 4 providing a hydrophilic surface to reduce adsorption and the possibility to conduct harsh rinsing procedures with e.g. concentrated aqueous NaOH, HCl or acetonitrile. In order to quantify proteins in HLL eluates, compatibility with components in the eluate, here mainly salts from PBS buffer, was investigated. Representative electropherograms are presented in Figure 34 A showing a partial separation of lysozyme and BSA with a good separation efficiency given the basicity of especially lysozyme²⁵⁰. All m/z -values and molecular masses were determined in preliminary experiments.

6.4.2. Compatibility with eluate composition

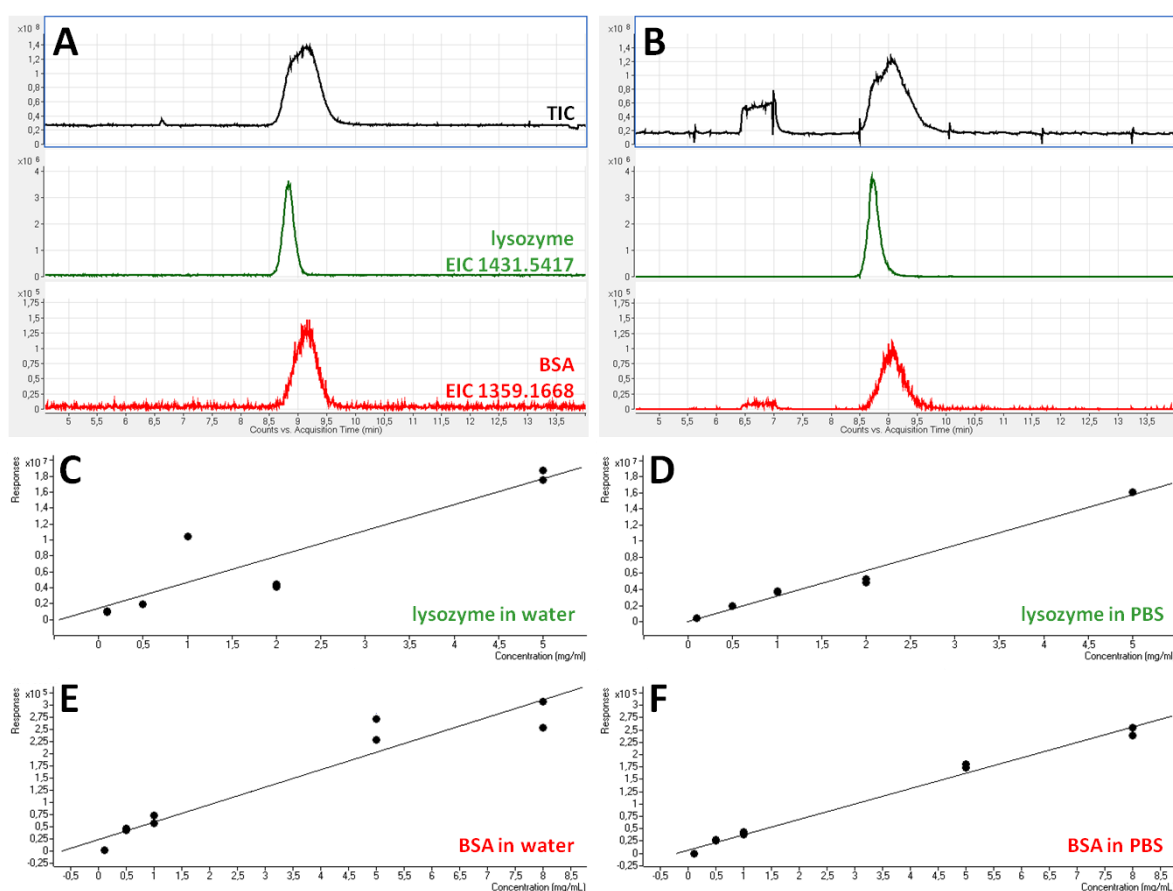


Figure 34: A and B: From top to bottom the total ion currents (TIC) of a representative separation with the extracted ion currents (EIC) of lysozyme (Lys1, $m/z_{\text{theoretical}} = 1431.5417$, deconvoluted molecular mass = 14305.34 Da) and the EIC of BSA (BSA3, $m/z_{\text{theoretical}} = 1359.1668$, deconvoluted molecular mass = 66550.40 Da) are presented for samples dissolved in A: deionized water and B: PBS. The electropherograms show the separation of lysozyme ($c = 2 \text{ mg/L}$) and BSA ($c = 8 \text{ mg/mL}$), see Section 4.3.3. For calibration, proteins were injected separately. Separations were conducted after injection for 4 s at 100 mbar on a 50 μm wide and 100 cm long AAEE capillary using following parameters: internal pressure of 100 mbar and separation current of 30 kV for 15 min. Calibration curves ($n = 2$) obtained for C & D: lysozyme and E & F: BSA in water (C & E) and PBS (D & F).

In order to evaluate the compatibility of CE-MS with the composition of eluates, proteins were dissolved in water or PBS (see Figure 34 and Section 4.3.3). The electropherograms obtained for the samples in water and in PBS, see Figure 34 A and B, yielded almost identical electropherograms with respect to migration time (t_{mig}) and intensity. The TIC in B shows a strong, square-shaped signal

from sodium (PBS) in the time segment from 6.5-7.0 min. EICs of samples in PBS showed this square-shaped signal at 6.5-7.0 min, too, which was assigned to different clusters of sodium acetate and formate. Furthermore, it can be seen, that separation performance was not influenced by the sample composition. Only minor differences were found for the peak-shapes of both lysozyme and BSA; minor fronting of the lysozyme peak with the protein dissolved in PBS was observed, see Figure 34 B.

For external calibration, lysozyme and BSA were injected separately using the following concentration steps: 5.0; 1.0, 0.5; 0.1 g/L. Results for the proteins dissolved in water are shown in Figure 34 C and E. For both lysozyme and BSA, linear correlation was unsatisfactory with respect to the R^2 -values (0.77939 for lysozyme and 0.92518 for BSA). For calibrations in PBS, better linear correlations were obtained ($R^2 = 0.98750$ for lysozyme and 0.98925 for BSA). In addition, precision was improved (see Figure 34). At 0.1 g/L BSA the LOD was reached for both sample types. For lysozyme the signal-to-noise (S/N) ratio was 17.0 in PBS and 142.8 in water at this concentration, therefore detection limits are lower than 0.1 g/L. Overall, 10-times higher sensitivity was thus determined for lysozyme compared to BSA regardless of the sample solvent. Inferior R^2 -values were observed for aqueous samples but higher sensitivity than in samples with PBS (lysozyme 13.3 % higher and BSA 3.2 % higher).

6.4.2.1. Quantitative analysis in the presence of excess comigrating protein

In HLL model experiments, Sample B with 4 proteins was used to investigate equilibration performance. In order to assess the influence of co-migration of proteins present in excess, Sample B was injected for CE-MS analysis at dilution quota of 1, 0.5, 0.2, 0.1, 0.05, 0.02 and 0.01 keeping the concentration ratios of proteins constant. The respective total protein concentrations were 40.5, 20.3, 8.10, 4.05, 2.03, 0.81 and 0.41 g/L in the different dilutions in PBS. Exemplarily, concentrations of lysozyme (the second highest concentrated protein in the mixture) were 7.62, 3.81, 1.52, 0.76, 0.38, 0.15 and 0.08 g/L, comparable to Section 6.4.2. In Figure 35 C, an electropherogram of undiluted Sample B is presented with the EICs of all 4 proteins. Peak-heights are normalized to equal heights. It is worth noting, that isoforms of each protein comigrated, therefore one EIC of each protein (Lys1, BSA3, bLa2 and CAn1) is presented exemplarily. It can be seen, that lysozyme and β -lactoglobulin fully co-migrate. BSA is only partially separated from both. Only carbonic anhydrase migrates at higher t_{mig} .

Exemplarily, two calibration curves for lysozyme are depicted in Figure 35 A and B being representative also for the other investigated proteins (lysozyme: 7.62 g/L and 3.81 g/L at overall protein concentrations of 40.5 and 20.3 g/L). Further details can be found in Table S 1). As can be seen for lysozyme in Figure 35 A, linearity was not granted over the whole concentration range, unlike to the observations made in Figure 34 F for the pure standard. This deviation from a linear fit was observed for all proteins except carbonic anhydrase, where a linear response over the whole concentration range was found. For co-migrating proteins, diminished charge deconvolution during the ESI-process leads to the curvature of the calibration curve²⁵¹. Yet, a very good second order logarithmic fit ($y = a + m \cdot \ln(x) + n \cdot \ln(x)^2$, with a: intercept, m, n: slopes) was calculated over the whole concentration range. Excellent linearity was observed in the low concentration range, see Figure 35 B, since charge convolution is not influenced by other proteins. Quantification of co-migrating proteins is possible at every concentration with higher precision for overall protein concentrations below 10 g/L.

STEP-WISE EQUILIBRATION OF PROTEIN SAMPLES USING HEXAPEPTIDE LIGAND LIBRARIES. OPTIMIZATION OF THE ELUTION AND PURIFICATION PROTOCOLS TO ENABLE RELOADING

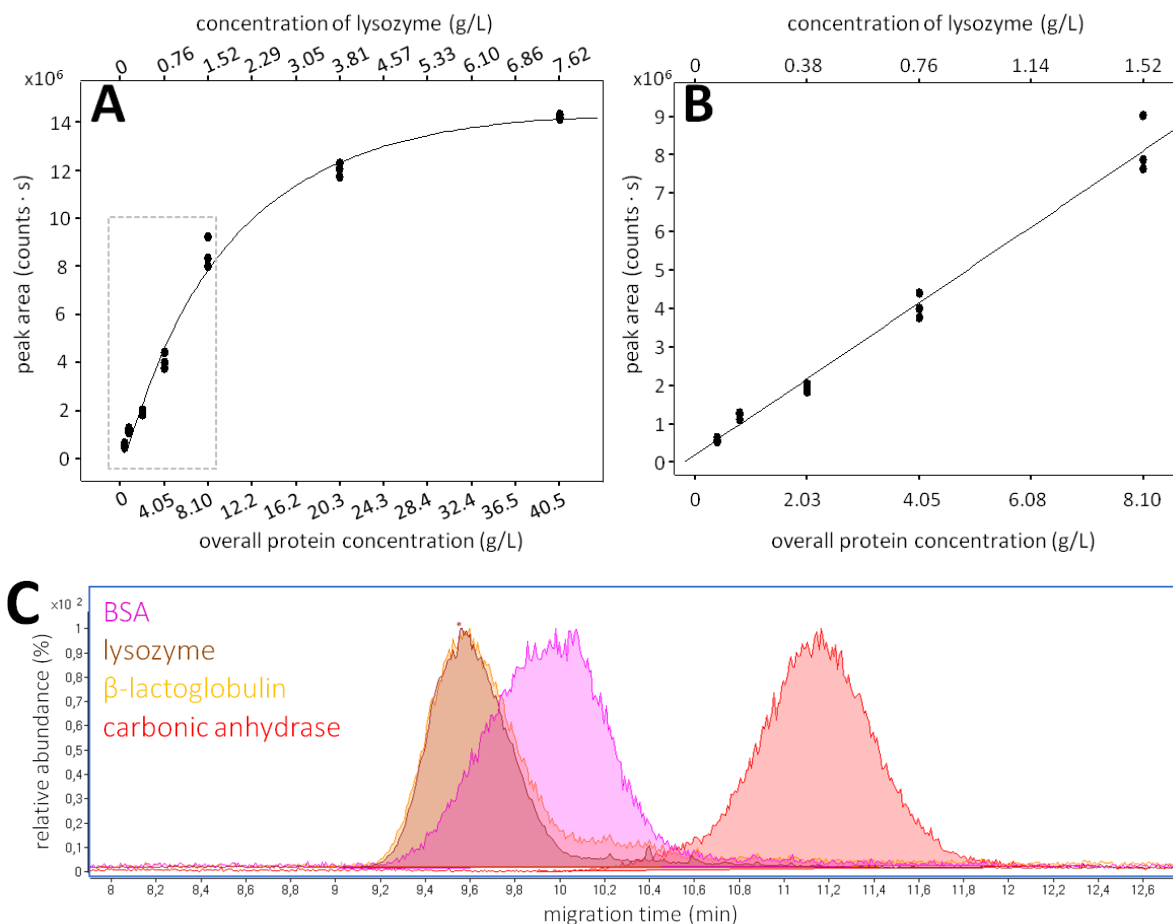


Figure 35: A & B: Calibration curves ($n = 3$) obtained for lysozyme (Lys1, $m/z_{\text{experimental}} = 1431.5417$, deconvoluted molecular mass = 14305.34 Da, see Table S1) in PBS. A protein solution designed for HLL-experiments containing 4 proteins (Sample B, see Section 4.3.3) at a fixed concentration ratio and different dilutions in PBS (up to 1:100). The overall concentration of protein is indicated by the bottom x-axis. A: A second order logarithmic (ln) fit. Overall peak area is plotted versus protein concentration and concentration of lysozyme. A good correlation between data and curve with $R^2 = 0.99090$ is obtained. The gray box indicates the data taken into consideration for B. B: A linear fit is conducted, considering dilutions of the concentration range of 0.01-0.2 only (equals a lysozyme concentration of 0.08-1.52 g/L and an overall concentration of 0.41-8.10 g/L). C: Electropherogram of undiluted Sample B. EICs presented are those of lysozyme (brown, Lys1), BSA (magenta, BSA3, $m/z_{\text{experimental}} = 1359.1668$, deconvoluted molecular mass = 66550.3979 Da), β -lactoglobulin (yellow, bLa2, $m/z_{\text{experimental}} = 1219.5164$, deconvoluted molecular mass = 18277.52 Da) and carbonic anhydrase (red, CAn1, $m/z_{\text{experimental}} = 830.3254$, deconvoluted molecular mass = 29026.0413 Da), for details see Table S1. Peak-heights are normalized to equal heights. Complete co-migration of lysozyme and β -lactoglobulin as well as partial co-migration of BSA with both is observed. The peak of carbonic anhydrase is almost base-line-separated from the other 3 protein signals. Separations were conducted after injection for 4 s at 100 mbar on a 50 μm wide and 100 cm long AAEE capillary followed by a separation at 100 mbar and 30 kV for 15 min.

For BSA (lysozyme), a 77.0 (12.6) times higher slope and thus sensitivity was found compared to Section 6.4.2, whereas at the lowest investigated BSA (lysozyme) concentration of 0.31 g/L (0.08 g/L) better S/N-ratios of $S/N = 5.0$ (14.1) compared to Section 6.4.2 were obtained. For BSA the S/N was 1.4 at 0.5 g/L. I assume that differences in sensitivity observed for lysozyme and BSA are primarily linked to (i) inter-day-variances such as temperature changes in the laboratory and (ii) a different sample preparation, see Section 4.3.3. (i) emphasizes the necessity of an air-conditioned laboratory and frequent calibration of the measurement system. (ii) would provide results other than expected, since Sample B offers higher amounts of proteins and thereby quenching, yet higher slopes and S/N-ratios were observed.

6.4.3. Protein purification and recovery from cut-off-filters

In order to be able to rebind the protein eluate to a lower amount of HLL for further concentration equilibration, binding conditions need to be re-established in the eluate after the first enrichment step. For this, I tested low molecular weight cut-off-filters. Recovery and removal of interfering eluate components were investigated. For a graphical illustration of the protocols see Figure 36.

6.4.3.1. Investigation of protein recovery from cut-off-filters

Due to the defined cut-off of the filters (exact product-name see Section 6.3.4), recovery rates for proteins of up to 95 % are claimed by the manufacturer. For the investigation of protein recovery 125 μ L aliquots of protein solution (Sample A, Section 4.3.3) and 125 μ L PBS were loaded (on total, 1.00 mg BSA and 0.25 mg lysozyme in 250 μ L). The sample was centrifuged at 14.000 x g for 30 min to remove sample solvent. The influence of washing steps on sample recovery was investigated by three different protocols; (I) single washing step using PBS and centrifugation, (II) 4 consecutive washing steps with PBS only or (III) 4 consecutive washing steps with 8 mol/L urea followed by 4 more washing steps with either PBS or water. Each washing step was performed using 100 μ L of the respective washing solution followed by centrifugation at 14.000 x g for 13 min. As a rule of thumb, approximately 1 min centrifugation per 8 μ L solution was necessary.

Two protocols to recover the proteins from the filters were investigated called normal and reverse recovery, see Section 6.4.3.2. For sample recovery via reverse centrifugation, the filter was placed upside-down in the centrifuge tube and the recovery solution was loaded at the bottom of the filter. 3 consecutive centrifugation steps using 100 μ L recovery solution (PBS or water) each were investigated. Here, centrifugation was performed at 7000 x g for 26 min to avoid loosening of the filter membrane. Only the first aliquot contained detectable amounts of protein as determined by CE-MS. This observation was independent from both the protein investigated, and the solution used for recovery (data not shown). For normal recovery, 4 x 25 μ L of water or PBS solution were added to the filter and the solutions were taken up by a pipette via mixing until formation of foam and pooled. Depending on the amount of solvent remaining in the filter after centrifugation, sample volumes up to 200 μ L were obtained. Sample volume was determined gravimetrically assuming a density of 1 g/mL.

Protein concentrations in eluates, washing and recovery solutions were quantified by CE-MS with external calibration. The results of the calculated recovery rates are presented in Figure 37.

STEP-WISE EQUILIBRATION OF PROTEIN SAMPLES USING HEXAPEPTIDE LIGAND LIBRARIES. OPTIMIZATION OF THE ELUTION AND PURIFICATION PROTOCOLS TO ENABLE RELOADING

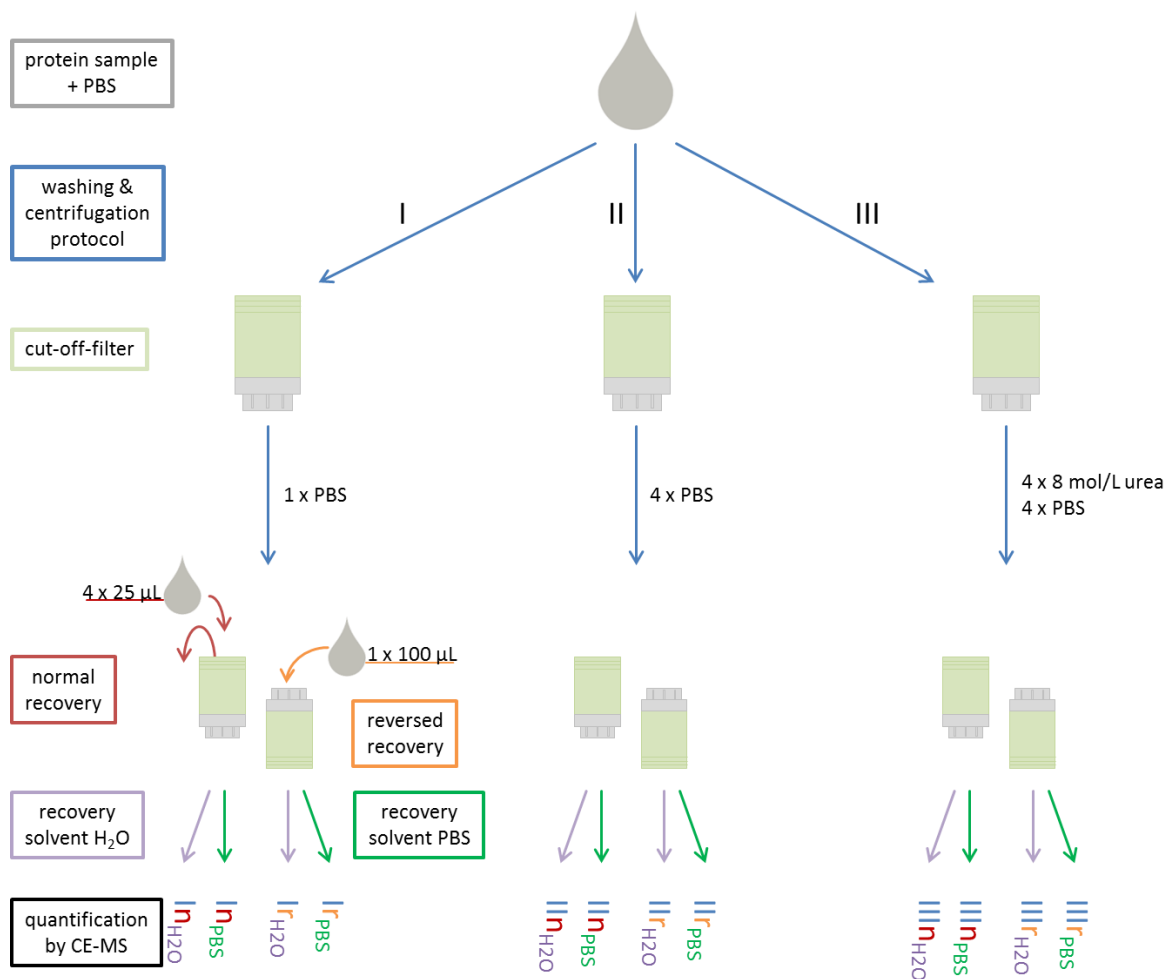


Figure 36: Scheme illustrating the approach of protein purification and recovery using cut-off-filters. Sample A dissolved in PBS was used. Three different washing and centrifugation protocols were used; I: washing once with 100 μ L PBS, II: four consecutive washing steps with 100 μ L PBS each, III: four consecutive washing steps with 100 μ L 8 mol/L urea each, followed by four consecutive washing steps with 100 μ L PBS each. Centrifugation of 125 μ L protein sample and 125 μ L PBS was conducted at 14.000 x g for 30 min prior to washing & centrifugation protocols. Each washing step was followed by centrifugation at 14.000 x g for 13 min. Centrifugation to complete dryness was avoided. Two different modes of sample recovery were tested: normal recovery washing 4 times with 25 μ L PBS or water, reversed recovery inverting the filter units and centrifuging in 100 μ L of PBS or water at half the rotary speed. Exact sample volumes and thus amount of protein were determined gravimetrically assuming a density of the aqueous solution of 1 g/mL and quantification by CE-MS. Abbreviations of the samples obtained thereby indicate the procedures and are given in the figure. They are built as follows: Xy_z with X: washing and centrifugation protocol (I, II or III), y: recovery protocol (n or r) and z: recovery solvent (H_2O or PBS).

Comparing **normal and reverse recovery mode**, normal recovery yielded higher recoveries in almost every case, as can be seen when comparing Figure 34 A vs. B, C vs. D and E vs. F as well as G vs. H. The only difference was observed for lysozyme in the samples III_nH_2O and III_rH_2O (Protocol III with water) where reversed recovery gave higher recoveries, see Figure 37 E and F, as well as for III_nPBS and III_rPBS where no significant difference was found for the treatments, see Figure 37 G and H. Overall, the normal recovery mode gave better results than the reversed one and was used for further experiments.

For the influence of the **number of washing and centrifugation steps** on the recovery, Protocols I, II and III were compared. Normal recovery with PBS gave higher recovery rates in case of fewer washing and centrifugation steps ($I_nPBS > II_nPBS > III_nPBS$), as can be seen in Figure 37 C and G for both

STEP-WISE EQUILIBRATION OF PROTEIN SAMPLES USING HEXAPEPTIDE LIGAND LIBRARIES. OPTIMIZATION OF THE ELUTION AND PURIFICATION PROTOCOLS TO ENABLE RELOADING

lysozyme and BSA. Overall, highest recovery rates were obtained for $I_{n_{PBS}}$ (normal recovery with PBS via Protocol I). For the reverse recovery utilizing PBS, see Figure 37 D and H, no significant difference in recovery rates were observed between Protocols I and II for both lysozyme and BSA (p -values of 0.167 and 0.193 in paired t-test, respectively). For $III_{r_{PBS}}$ increased recovery-rates for both proteins were determined for both proteins compared to $I_{r_{PBS}}$ and $II_{r_{PBS}}$, indicating higher recovery with higher number of washing steps ($I_{r_{PBS}} \approx II_{r_{PBS}} < III_{r_{PBS}}$).

For normal recovery using water, an increase in recovery rates with additional washing and centrifugation steps was observed for lysozyme (recovery rate $I_{n_{H_2O}} < II_{n_{H_2O}} < III_{n_{H_2O}}$), see Figure 37 E. For BSA, no continuous trend for the recovery of proteins and the number of washing and centrifugation steps was observed, see Figure 37 A. Analogous observations were made for the reverse recovery using water, see Figure 37 E and F.

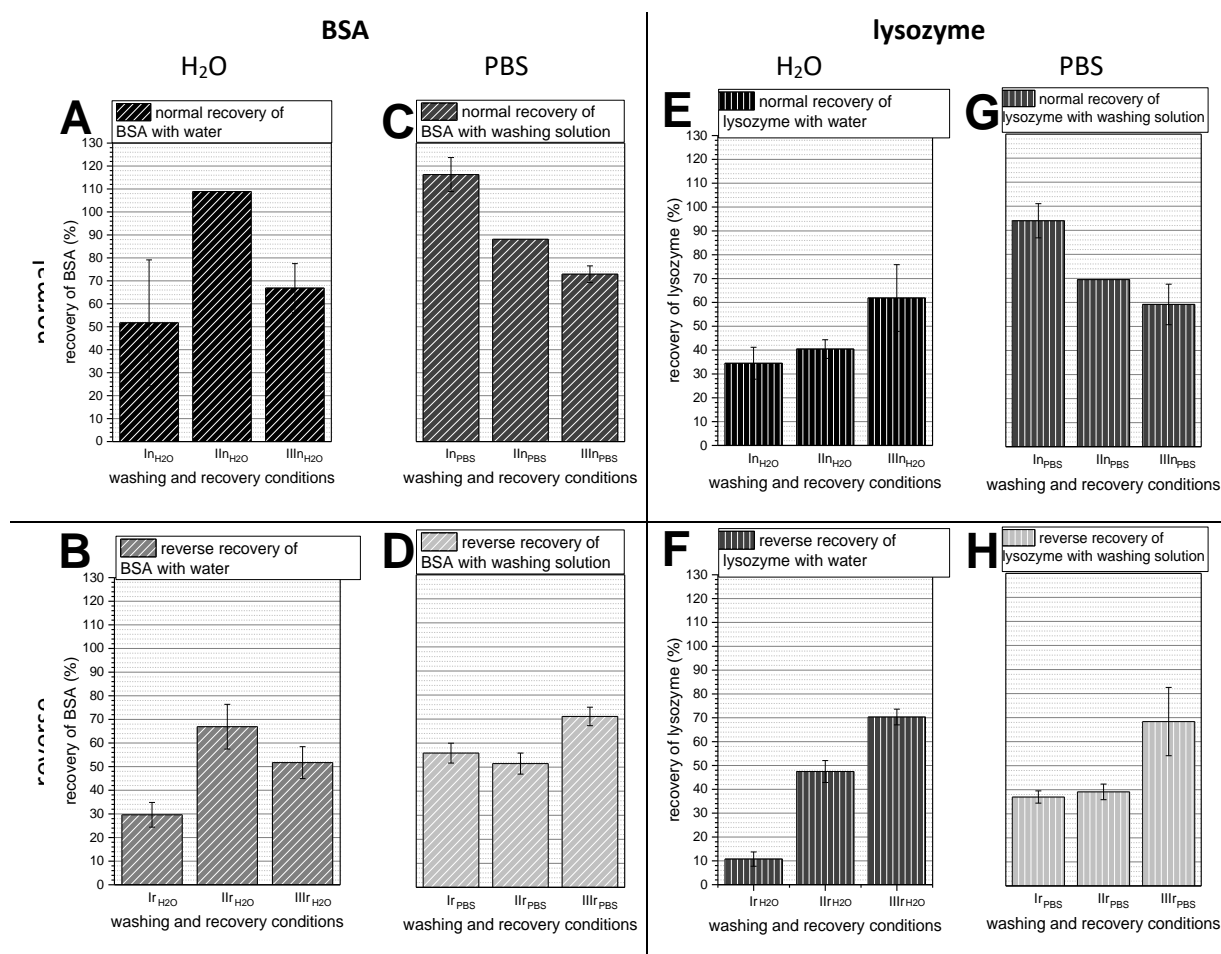


Figure 37: Recovery of proteins by washing (I) once with 100 µL PBS, (II) 4 consecutive times with 100 µL PBS each and (III) 4 consecutive times with 100 µL 8 mol/L urea each, followed by washing 4 times with 100 µL PBS each, according to Figure 36. All washing steps were performed by centrifugation at 14.000 x g for 13 min using 10 kDa cut-off-filters. Sample A in PBS was used. The recovery rates obtained for A-D: BSA and E-H: lysozyme are shown. On top (A, C, E, G), recovery rates for the normal recovery procedure are given, on the bottom (B, D, F, H) those obtained for the reverse centrifugation. Protein-amounts were determined via CE-MS. Separations were conducted after injection for 4 s at 100 mbar (further CE-MS parameters as in Figure 35).

These observations show, that the choice of the recovery solution (**water or PBS**) is most significant for optimal recovery with PBS giving best results. In addition, repeatability of CE-MS quantification was better, visible from the smaller error-bars for the recovery with PBS (compare Figure 37 C vs. A, D vs. B, G vs. E and H vs. F). Although higher absolute recovery rates were found for the normal

recovery of BSA with water via Protocol II, the lower precision as well as the large difference in recovery rates between lysozyme and BSA limits the usability of water for recovery.

Future experiments were thus conducted with PBS solution via Protocol I, which is of advantage also regarding the following equilibration step on HLL. It is worth noting that the recovery rates for BSA were always higher than those of lysozyme. These **differences in recovery rates between BSA and lysozyme** were observed regardless of the protocol used. Lysozyme recovery was always lower for normal recovery (compare Figure 37 C vs. G and D vs. H), presumably due to sorption of this basic protein. BSA recovery rates of 110-120 % for Protocol I (see Figure 37 C) are assumed to be within measurement uncertainty.

For best recoveries of both BSA and lysozyme, a final purification and recovery protocol using one single washing and centrifugation step (Protocol I) and recovery with 4 x 25 μ L PBS was chosen (In_{PBS}).

6.4.3.2. Applicability of cut-off-filters to remove SDS and urea from HLL-eluates

The feasibility of cut-off-filters to remove SDS and urea from HLL protein eluates was investigated for the HLL elution solutions **i-viii**, see Table 9, by mixing 125 μ L of each HLL elution solution with 125 μ L of protein Sample A in water directly in preconditioned cut-off-filters (see Section 6.3.4), giving an overall sample volume of 250 μ L and an overall protein amount of 1.25 mg. Sample purification was investigated by consecutive washing steps using the optimized recovery-protocol $n_{\text{H}_2\text{O}}$ as described in Section 6.4.3.1 with normal recovery and single washing steps using washing Protocol II (see Figure 38) for samples **vi-viii** which are void of SDS and washing Protocol III for SDS-containing samples **i-v**. Investigation of Protocol I was not further considered since removal of HLL elution solutions were of primary interest here. Slight modifications were made for washing and centrifugation of SDS-containing samples **i-v**: Native sample was centrifuged for 60 min at 14.000 x g (instead of 30 min) and washing and centrifugation was conducted at 14.000 x g for 20-45 min (instead of 13 min). I assume that SDS-micelles clog the pores of the cut-off-filters and thereby reduce flow-rates. Sample recovery was performed with water using the normal recovery method only. The influence of PBS in the sample solution was not investigated here.

Protein sample (supernatant (S_0)), washing solutions containing urea ($W_{1,x}$ with $x = 1-4$), washing solutions containing PBS ($W_{2,x}$ with $x = 1-4$) and solutions containing recovered protein (P_3) were collected and stored at -20°C until further analysis via CE-MS. The index-numbers indicate the succession in which the fractions were collected. The full process is illustrated in Figure 38. In order to determine recoveries and possible sample loss in the different protocols, BSA and lysozyme were quantified in S_0 , $W_{1,x}$, $W_{2,x}$ and P_3 . In addition, SDS was analyzed in $W_{1,x}$ to characterize urea-assisted SDS-removal, see Figure 39. Quantification was achieved using CE-MS.

In Figure 39 A, the concentrations of lysozyme and BSA in P_3 are shown to assess recoveries. Overall amounts of protein found in all solutions together never exceeded 30 % of the loaded sample solution, see Figure 39 C. When comparing the overall amount of BSA recovered in the different solutions (see Figure 39 C) to the recovered amount of protein P_3 presented in Figure 39 A, it can be seen, that almost equal amounts of lysozyme and BSA were obtained.

For SDS-containing HLL elution solutions (**i-v**), insufficient recovery rates between 2-6 % for BSA and between 0-4 % for lysozyme were determined. For HLL elution solutions **vi-viii**, 2-4 times higher recovery rates for BSA and 10-20 times higher recovery rates for lysozyme compared to **i-v** were

observed. In general, recovery rates were higher for BSA than for lysozyme by a factor of about 2 for HLL elution solutions void of SDS (**vi-viii**). For HLL elution solutions **i-v**, almost twice as high recovery rates were found for BSA. The observations made for **vi-viii** are in good accordance with those described in Section 6.4.3.1 for the investigation of filter recovery rates for aqueous or PBS containing samples and for observations made by CE-MS-quantification, see Section 6.4.1. In all supernatants **S₀** a lysozyme fraction of about 0.2 % was found, whereas 1.5-3.6 % of BSA were detected in **S₀** from HLL elution solutions **i-v**, and between 0.3 and 0.6 % in case of HLL eluates **vi-viii**. Similar concentrations of BSA were determined in the washing solutions **W** when SDS was present in the sample (**i-v**), see Figure 39 C. The large error-bars are most certainly linked to measurement uncertainty (quantification with label-free CE-MS and external calibration, see Section 6.4.1) and to the use of water as recovery solvent, see Section 6.4.3.1. For samples containing urea (**vi-viii**), two observations are worth noting: (i) except for **W_{2,1}** using HLL elution solution **vi** (with urea and CHAPS), about 1 % of the applied BSA was detected in each of the collected fractions and (ii) increasing amounts of BSA were observed in consecutive washing and centrifugation steps. Amounts of lysozyme were always below 0.2 % for each washing solution, results not shown.

SDS was quantified in separate runs using CE-MS at reverse polarity and lower internal pressure (-30 kV and +30 mbar). The respective base-peak used was $m/z_{\text{experimental}} = 289.1445$ m/z, which equals $[M+H]^+$. Analyzing the SDS content in different washing steps with urea, it is clear that most SDS was depleted already in the first washing step, see Figure 39 E and F. For HLL elution solutions **i-iii** with 1 % SDS, SDS was only detected in washing solutions containing urea. For HLL elution solutions **iv** and **v** (10 % SDS), SDS-depletion was observed to continue also in washing steps with PBS, as can be seen in Figure 39 D and E. When comparing the relative amounts of SDS in Figure 39 E to the absolute amounts in Figure 39 F, it is apparent, that SDS can efficiently be removed even when high quantities of SDS are present (approx. 1 mg per washing step for **W_{1,1}** and HLL elution solutions **iv** and **v** which contain 10 % SDS). However, only a further fraction of approx. 10-20 % of SDS remaining is removed within each consecutive washing step. Thereby, SDS removal is inefficient especially when low concentrations of SDS are present in late urea or PBS washing steps. Therefore, only elution solutions **vi**, **vii** and **viii** were used for further experiments.

STEP-WISE EQUILIBRATION OF PROTEIN SAMPLES USING HEXAPEPTIDE LIGAND LIBRARIES. OPTIMIZATION OF THE ELUTION AND PURIFICATION PROTOCOLS TO ENABLE RELOADING

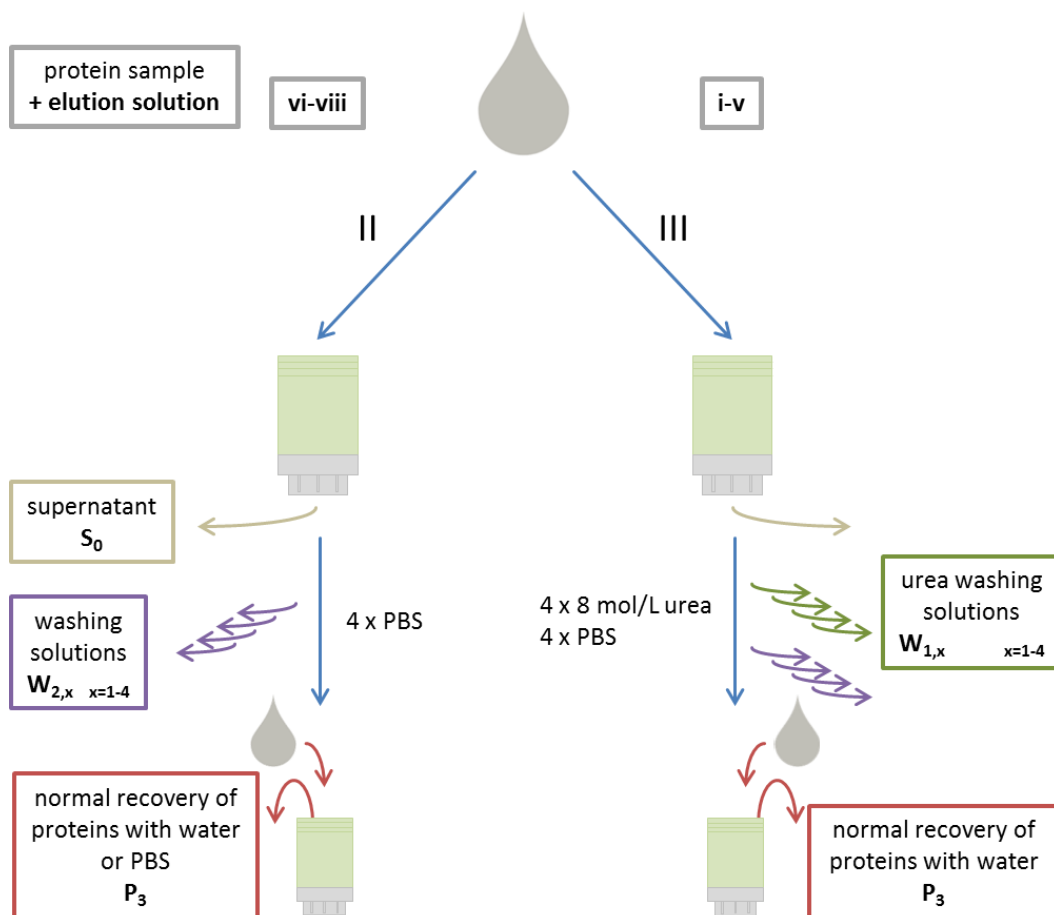


Figure 38: Flow chart for the optimization of SDS and urea removal from HLL eluates using cut-off-filters. The starting point is a mixture containing 125 μL Sample A in water and 125 μL of an HLL elution solution containing SDS or urea (see Table 9), giving an overall sample volume of 250 μL . The sample is loaded into the cut-off-filter followed by centrifugation at 14.000 $\times g$ for 30 min. For HLL elution solutions i-v (containing SDS), centrifugation for 60 min was necessary to quantitatively remove the solution whilst avoiding complete dryness as recommended by the manufacturer. Washing and centrifugation were conducted via Protocol II and III, see Section 6.4.3.1. For HLL elution solutions i-v, which contain SDS, washing with solutions containing urea-washing was necessary to break SDS-protein-interaction. The centrifugation times were 20-45 min, depending on the amount of solution in the filter after centrifugation. Fractions from washing and centrifugation were collected: Sample filtrate (S_0), filtrate from urea-washing steps ($W_{1,x}$) and filtrates from PBS-washing steps ($W_{2,x}$). The index X indicates the number of the washing step. W_1 fractions were only taken for HLL elution solutions i-v. Purified samples P_3 were obtained from the residue by filling the cut-off-filter 4 times with 25 μL water each and collecting the solution by pipetting.

STEP-WISE EQUILIBRATION OF PROTEIN SAMPLES USING HEXAPEPTIDE LIGAND LIBRARIES. OPTIMIZATION OF THE ELUTION AND PURIFICATION PROTOCOLS TO ENABLE RELOADING

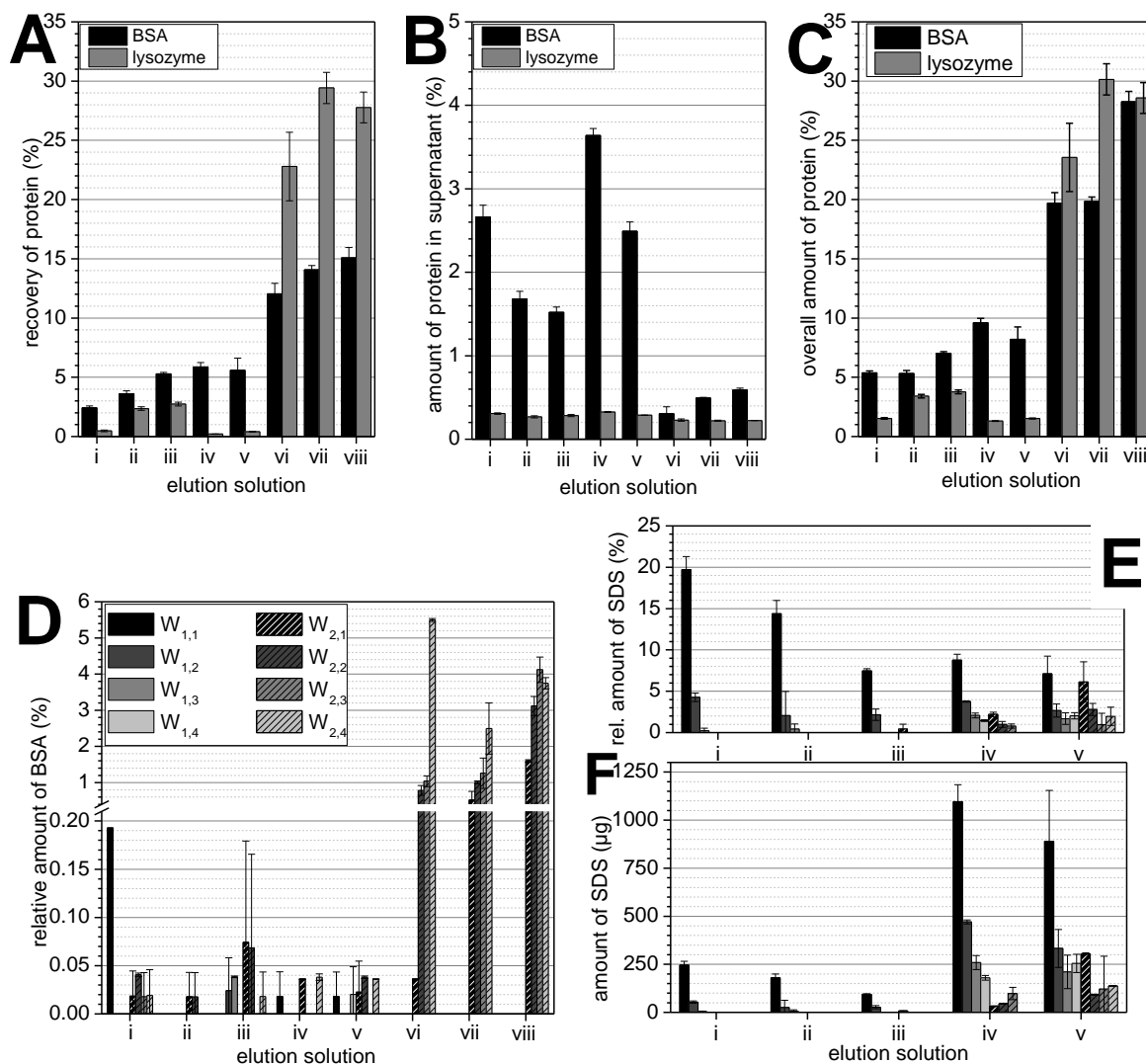


Figure 39: Quantification of lysozyme and BSA content in S₀, W_{1,x}, W_{2,x} and P₃ was achieved via CE-MS, see Section 6.4.1 for more details. Relative amounts were calculated relative to the concentration in the original sample (100 % or 1 g/L of BSA and 0.25 g/L lysozyme). A: Recovery of lysozyme and BSA retained in the cut-off filter (Sample P₃) was calculated relative to the original sample. B: Amount of protein detected in supernatant S₀. C: Sum of BSA and lysozyme content in all samples (S₀, W_{1,x}, W_{2,x} and P₃) relative to original sample. D: Amount of BSA detected in washing solutions W_{1,x} and W_{2,x} relative to original sample. E: relative amounts of SDS detected in washing solutions relative to HLL elution solutions i-v. F: Calculated absolute amount of SDS detected in each washing solution. For A & B n = 3, for C-D n = 2 replicates were analyzed. Separations were conducted by CE-MS after direct injection without further treatment for 4 s at 100 mbar on a 50 µm wide and 100 cm long AAEE capillary at 100 mbar and 30 kV, further parameters see Section 4.3.1.2. For quantification of SDS in W_{1,x} and W_{2,x} via CE-MS ($[M+H]^+$: $m/z_{\text{experimental}} = m/z_{\text{theoretical}} = 289.1445$ Da), additional measurements were performed at 30 mbar and -30 kV in the same separation buffer.

6.4.4. Investigation of elution protocols for one-fold HLL equilibration

CE-MS analysis of the proteins (p) BSA, lysozyme, β-lactoglobulin and carbonic anhydrase (see Sections 4.3.1.2 and 4.3.3) as single protein samples revealed the presence and relative abundance of isoforms for all investigated proteins. The protein isoforms (pi) are presumably linked to micro-heterogeneities from deamidation products, oxidation and other modifications. First of all, deconvoluted molecular mass, base peaks and relative abundances of the isoforms (a_{pi}) were determined experimentally injecting the protein standards in PBS at a concentration of 10 g/L.

Indices are put together as follows: a_{pi} indicates the abundance (a) of a proteins' (p , p = BSA or Lys or bLa or CAn) isoform (i , i = integer number), e.g. a_{BSA3} is the abundance of BSAs' isoform BSA3. Values corresponding to the whole protein lack the "i" and are understood as sum over all isoforms investigated e.g. $m_{abs,BSA} = \sum_{i=1}^8 m_{abs,BSAi}$.

For quantification of proteins and their isoforms, some simplifying assumptions were made: (i) equal ionization efficiencies for all isoforms and (ii) no or identical quenching effects for each protein isoform upon co-elution. Data analysis was achieved using Qualitative Analysis Software, results are presented in Table S 1 in the SI.

The equilibration procedure can be expected to also equilibrate the relative abundance of the isoforms if fully unspecific binding on the HLL is reached. The isoforms were used to evaluate HLL equilibration within a protein species, called **intra-protein equilibration**. Equilibration using HLLs was conducted using Sample B and a normal elution kit as described in Section 6.3.4. A binding ratio of 1:50 was assumed. HLL elution solutions listed in Table 9 were used and will be referred to as Protocol **vi**, **vii** and **viii**. The relative concentration of an isoform ($c_{rel,pi}$), was determined relative to the overall concentration of all protein isoforms in the sample ($c_{s,p}$) from signal areas in CE-MS-experiments using external calibration, see Section 6.4.1.

Absolute concentrations of isoforms ($c_{abs,pi}$) were calculated using Equation (4). For the calculation of the absolute amount of recovered protein isoform ($m_{abs,pi}$), the volume of sample (V_s) was determined gravimetrically as described in Section 6.4.3.1. Calculations were conducted via Equation (5).

$$c_{abs,pi} = c_{rel,pi} \cdot c_{s,p} \cdot a_{pi} \quad (4)$$

$$m_{abs,pi} = c_{abs,pi} \cdot V_s \quad (5)$$

To judge **inter-protein-equilibration**, the **absolute amount of each protein** ($m_{abs,p}$) was calculated as the sum of all isoforms of the respective protein. The data presented for the native sample were normalized to an overall protein amount of 1 mg, which equals the maximal overall amount of protein which can be recovered from HLL, for better comparison of protein yields with equilibrated sample. Here it is worth noting that $m_{abs,p}$, as presented in Figure 40 A, is little below 1 mg since only the isoforms stated in **Table S 1** were taken into consideration but further small signals had to be neglected.

Eluting the proteins from the HLL using Protocol **vi**, **vii** and **viii** gave protein amounts well below 1 mg, see Figure 40 A. This indicates that binding to or elution of proteins from HLLs using Protocols **vi**, **vii** and **viii** was incomplete.

Yet, inter-protein equilibration was clearly successful, as the relative amounts (r_i) of lysozyme (2nd highest concentrated protein) and β -lactoglobulin (3rd highest concentrated protein) obtained for **vi** and presented in Figure 40 B were higher than in the native sample. r_p was calculated using Equation (7) as the quotient between $m_{abs,p}$ and y based on the protein yields determined for the different elution protocols.

The overall protein yields for each elution protocol (y) were calculated using Equation (6) and are presented in Figure 40 B. Together with r_p equilibration can be judged regardless of the overall yield in protein. The relative change in protein amounts Δr_p allows for quick comparison with the relative protein concentration in the native sample $r_{p,0}$, see Equation (8). Another approach for the

evaluation of equilibration is the binding capacity **b**, see Equation (9). By dividing $\sum_p^n \mathbf{m}_{abs,p}$ by the settled bead volume of HLLs (V_{SBV}) used, protocols using different amounts of HLL can be compared. According to manufacturer, **b** = 10 µg/µL equals **y** = 100 %.

$$y = \frac{\sum_p^n m_{abs,p}}{\sum_p^n m_{abs,p,0}} \cdot 100\% \quad (6)$$

$$r_p = \frac{m_{abs,p}}{y} \cdot 100\% \quad (7)$$

$$\Delta r_p = \frac{r_p - r_{p,0}}{r_{p,0}} \cdot 100\% \quad (8)$$

$$b = \frac{\sum_p^n m_{abs,p}}{V_{SBV}} \quad (9)$$

Error-bars were calculated using Gaussian error-propagation. Results are shown in Figure 40 C.

By taking both Figure 40 B and C into consideration, depletion of BSA is obvious for all three HLL elution solutions investigated. Highest depletion of BSA by almost 40 % was found for Protocol **vi**. For lysozyme, a strong increase in relative amounts was observed for all three HLL elution solutions, with an increase of almost 120 % for Protocols **vi** and **vii**. Only half the increase was present using Protocol **viii**. For β -lactoglobulin, a very strong enrichment was observed for Protocols **vi** and **viii**, but a strong decrease using Protocol **vii**. For carbonic anhydrase, only decreasing protein amounts were found for each investigated HLL elution solution, no enrichment was obtained.

For the investigation of **intra-protein-equilibration**, a selection of isoforms of each protein, summarized in Table S 1, was taken into account. All data on $\mathbf{m}_{abs,pi}$ and \mathbf{r}_{pi} are present in Figure S 1 in the SI. First of all, for almost every protein isoform lower absolute amounts were found after equilibration, see Figure S 1 A-D except for Protocol **vi** for the isoforms BSA6, Lys2, bLa1, bLa3 and bLa5. This observation is strongly linked to low **y**, see Figure 40. Protocol **vi** was the elution protocol with the highest $\mathbf{m}_{abs,pi}$ for each isoform of each protein. This is in good accordance with the observations made for **y** for inter-protein equilibration. Results for inter-protein equilibration, \mathbf{r}_{pi} are presented in Figure S 1 E-H.

For carbonic anhydrase very similar ratios of isoforms, clearly differing from the native samples, were observed for Protocols **vii** and **viii**, see Figure S 1 H. It appears that a lower degree of equilibration was reached using Protocol **vi**. However, this is most likely due to limited elution of CAn-isoforms in Protocols **vii** and **viii**. Especially \mathbf{r}_{pi} values of the most abundant isoforms CAn1-3 were significantly higher for Protocol **vi**. For all protocols highest abundant CAn1 was depleted, showing that inter-protein equilibration of carbonic anhydrase occurred. Furthermore, different elution rates for the isoforms for different HLL elution solution are indicated by these results.

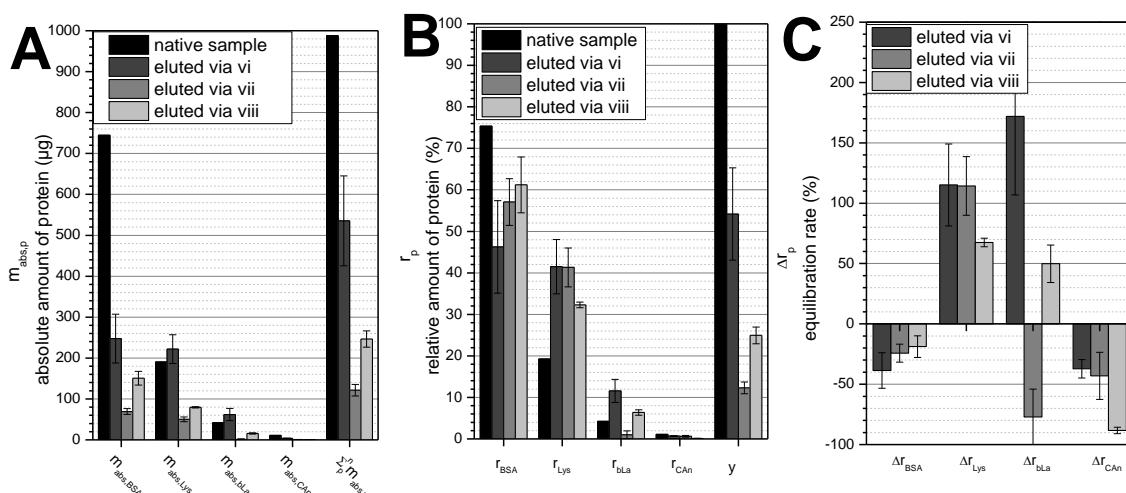


Figure 40: A: Absolute amount of each investigated protein in P_3 , calculated as the sum of the amounts found for each variant. 100 % yield would mean that approx. 1.00 mg protein is present in the eluate, independent from the type of protein. B: Relative amounts of proteins in P_3 and overall yield in protein. C: Relative change in protein amount found for each of the 4 proteins investigated.

For β -lactoglobulin, r_{pi} determined for all three HLL elution solutions are alike. High differences in $m_{abs,pi}$, corresponding to differences in y , are found. This indicated comparable elution rates for each isoform towards all HLL elution solutions applied. Surprisingly, enrichment of bLa1 and depletion of bLa2 were observed while r_{pi} of bLa3-5 did not change significantly. Inferior binding-capacity for bLa2 compared to the other 4 isoforms and/or non-competitive binding between bLa1 and bLa3-5 can be assumed.

For lysozyme (see Figure S 1 F), highest $m_{abs,pi}$ were achieved for Protocol **vi**, even for Lys1. Regarding r_{pi} , most Lys1 was present in eluates of Protocols **vii** and **viii**. Protocol **vi** is thus more efficient in eluting Lys1 than Protocols **vii** and **viii**. Regarding $m_{abs,pi}$ and r_{pi} of each other isoform it is apparent, that these can only be satisfactorily eluted using Protocol **vi**. Intra-protein equilibration between Lys1 and Lys2 is possible via Protocol **vi**. Lys3 and Lys4 are either poorly equilibrated due to lack of HLL-binding sites (or low competitiveness towards existing ones) or they hardly eluted using the given procedures due to strong interaction with binding-sites occupied.

BSA (see Figure S 1 E), BSA2, BSA5 and BSA8 showed minor changes for each elution protocol as can be seen for r_{pi} . Enrichment of BSA 6 was observed for each elution protocol, accompanied even by increasing $m_{abs,pi}$. Satisfactory depletion of BSA1 whilst enriching BSA4 was only found for Protocol **vi**. Accelerated or favorable elution of BSA1 compared to other isoforms in HLL elution solutions other than **vi** is expected to be the reason for this observation. Intra-protein equilibration is best achieved using Protocol **vi**. Regarding the absence of equilibration of BSA2 and BSA5, comparable binding situations can be discussed. Regarding decreasing r_{pi} of low abundant BSA7 and BSA8 either low binding or poor elution of both can be presumed.

6.4.5. Consecutive equilibration

To investigate the re-applicability of protein eluates from HLLs, Sample B was treated according to the scheme illustrated in Figure 42. The optimized procedures discussed previously were used (Sections 6.4.3 and 6.4.4) with elution from HLL using Protocol **vi**. Protocol **I** for washing and centrifugation was slightly modified to reduce protein precipitation and adsorption: eluate samples

were mixed until formation of foam using a pipette every 10 min during centrifugation. During washing and centrifugation, mixing until formation of foam was performed prior to centrifugation. Supernatants of one- and two-fold HLL-equilibration were kept for analysis (S_0 1x and S_0 2x). Washed proteins were recovered from cut-off filters using normal recovery. For two-fold equilibration, 80 % of the protein sample from purified eluates (P_3 1x) was loaded on fresh HLL with a settled bead volume 80 % lower than used during one-fold equilibration. 20 % of sample was kept for CE-MS analysis. Ideally, complete sorption of proteins on HLLs during the second equilibrations step and comparable protein profiles for P_3 1x and P_3 2x would be obtained.

6.4.6. Reproducibility and ruggedness of 1-fold equilibration

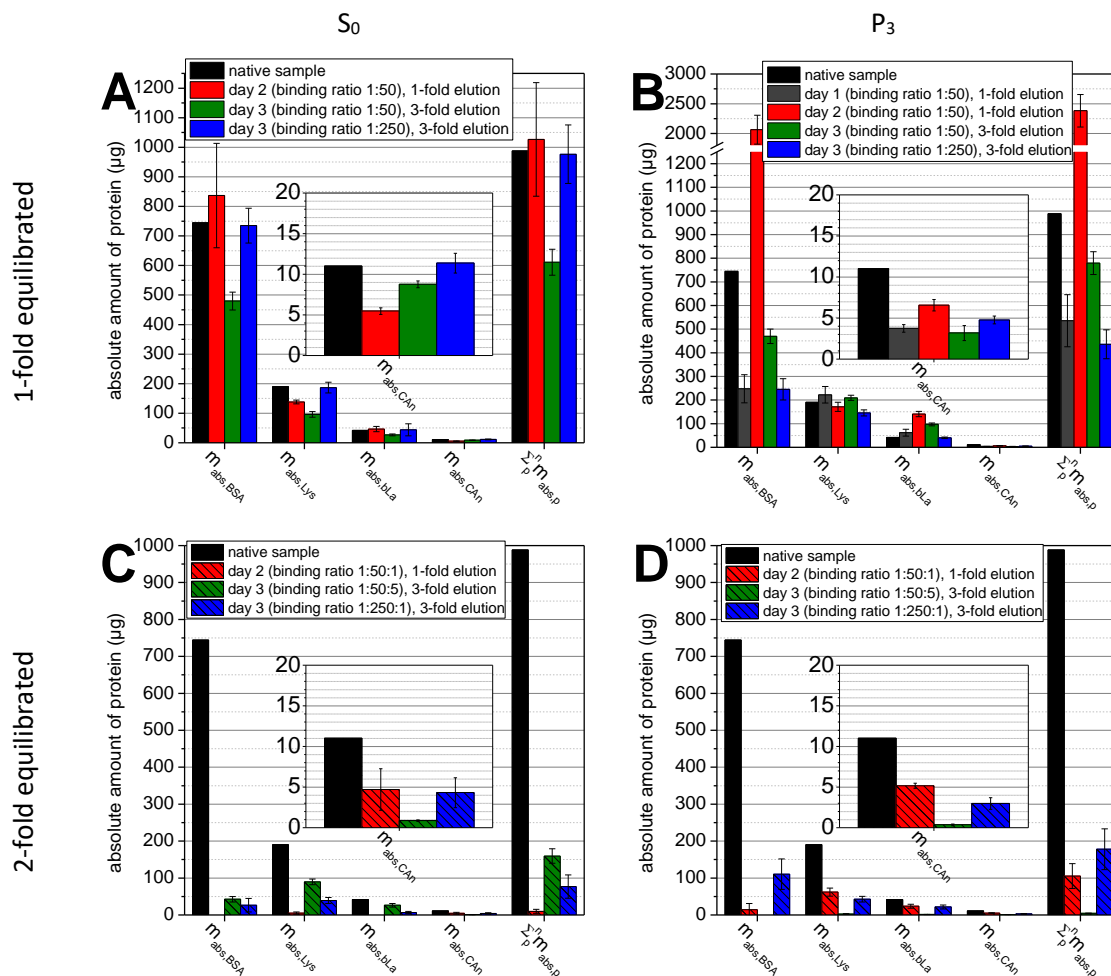


Figure 41: Absolute amount of each investigated protein, calculated as the sum of the amounts of each isoform, calculated for 1-fold (2-fold) equilibrations on 3 (2) different days. Binding ratios of 1:50 and 1:250 followed by elution using Protocol vi, either 1- or 3-fold, were investigated. Assignment via color-code, 1-fold equilibration is presented without fill-pattern, 2-fold equilibration has a striped fill-pattern. For exact assignment see figure legend. A & C: supernatants after 1-fold & 2-fold equilibration (S_0 1x & S_0 2x) and B & D: recovered protein after 1-fold & 2-fold equilibration (P_3 1x & P_3 2x). The results indicated by the gray bar are identical to those presented in Section 6.4.4 for Protocol vi.

Single equilibration was conducted on 3 different days and at 2 different binding ratios (1:50 and 1:250). Furthermore, elution Protocol vi was modified towards 3 consecutive elution steps¹⁰ with 3 x 100 µL of an aqueous solution consisting of 8 mol/L urea, 2 % CHAPS and 5 % acetic acid.

Inter-protein-equilibration:

Except for one experiment (green bar), supernatants (**S₀ 1x**) contained BSA- and bLa-amounts similar to the native sample, see Figure 41 A, as can be expected. The amounts of Lys and CAn were either lower or equal to those in the native sample. Both is in good accordance with the fact, that only 2 % (1/50th) of protein is depleted from the solution, which is well within the measurement uncertainty, depictable by the error bars. Relative protein amounts, shown in **Figure S 3 A**, verify that no significant change in inter-protein-profiles was obtained. The supernatant of one experiment (gray bar) was not investigated due to spilling of sample.

3-fold elution of HLL (**P₃ 1x**) yielded approx. 80 % of expected protein amounts for a binding ratio of 1:50 (green bar) and approx. 60 % for a binding ratio of 1:250 (blue bar), see **Figure S 3 B**. The latter showed no significant difference ($p > 0.05$) to the yield determined for 1-fold elution performed on another day (gray bar). Thus, I cannot confirm increased yields for consecutive elution as published by Guerrier *et al.*¹⁰. The differences between the two identically conducted experiments with a binding ratio of 1:50 and 1-fold elution (gray and red bar), namely the vastly higher amount of BSA observed during the experiments represented by the red bar (238 % \pm 27 %), indicate low reproducibility of the HLL-procedure. A positive aspect is demonstrated by the experiments represented by the red bar: despite the strong change of BSA concentration, the absolute amount of lower concentrated Lys, bLa and CAn is comparable to those found in the other experiments, see Figure 41 A. Yet, no relative enrichment of low abundant proteins occurred but a depletion of Lys and CAn (r_{Lys} and r_{CAn} decreased by approx. 50 %, see **Figure S 3 B**). For all other experiments, r_{Lys} were either increased by approx. 50 % (green and blue bar) or approx. doubled (gray bar). r_{bLa} was doubled in every case and r_{CAn} did not change significantly.

Overall, acceptable reproducibility regarding the inter-protein-profiles was obtained, however, with very low reproducibility of yields. Furthermore, I observed that higher amounts of BSA in P₃ correlate with higher amounts of bLa, see binding capacities in **Figure S 4 A** and Figure 41 A. I thus assume that CAn and Lys primarily bind on HLL-binding sites whilst interaction of BSA and bLa is likely leading to co-depletion or co-enrichment.

6.4.6.1. Two-fold equilibration: proof of principle

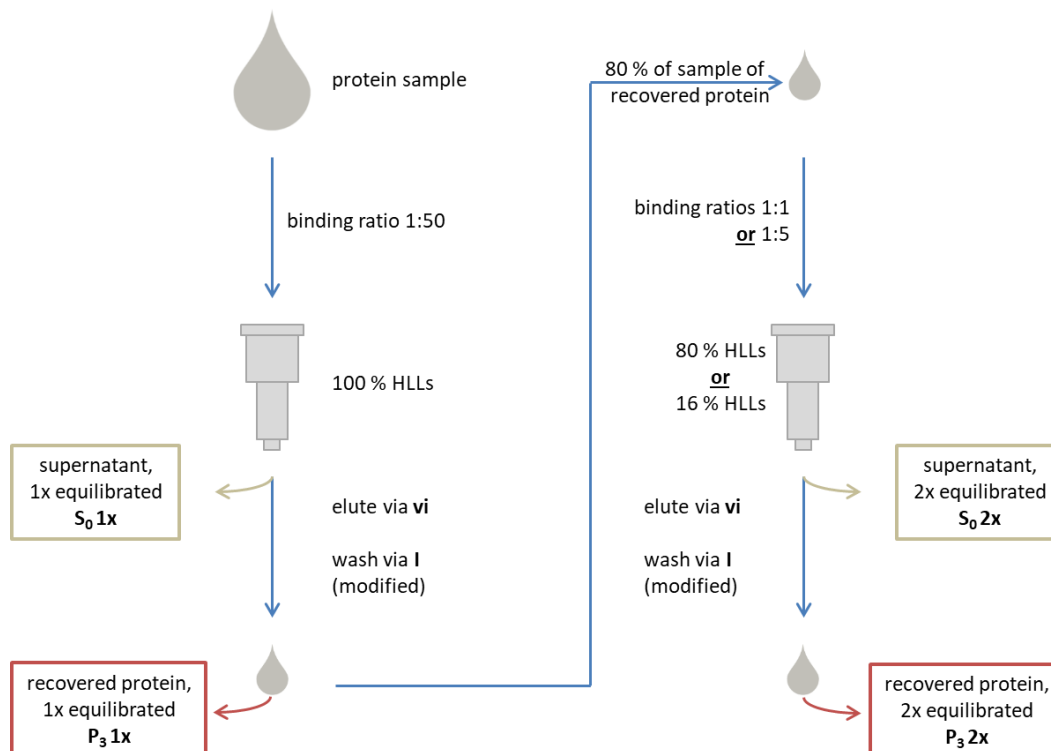


Figure 42: Scheme for the two-fold equilibration of a protein sample (Sample B). Elution was performed using Protocol vi. For washing and centrifugation using cut-off filters Protocol I was slightly modified as follows: during centrifugation samples were mixed every 10 minutes using a pipette until formation of foam. For two-fold equilibration 80 % of the amount of recovered protein obtained after 1x equilibration (P₃ 1x) was reapplied on 80 % of the HLL amount used previously.

Inter-protein-equilibration:

Expectation: Due to the HLL and sample amount chosen for reloading leading to binding ratios of 1:1, consecutive loading of equilibrated P₃ 1x is expected to give rise to supernatants (S₀ 2x) void of protein (red and blue striped bars in Figure 41 C) and approx. 80 % of the absolute amount of protein found in P₃ 1x when a binding ratio of 1:5 is established (green bar). P₃ 2x is expected to be identical to P₃ 1x for binding ratios of 1:1 (red and blue striped and non-patterned bars in Figure 41 B and D). P₃ 1x using a binding ratio of 1:250 (blue bar, no pattern in Figure 41 B) is expected to be identical with P₃ 2x using consecutive equilibration with binding ratios of 1:50 followed by 1:5 (1:50:5, green striped bar in Figure 41 D).

From the results presented in Figure 41, it can easily be seen that S₀ 2x of experiments with binding ratios of 1:1 are almost void of protein as expected (10 % ± 5 % of the expected protein amount), so almost complete rebinding is achieved. S₀ 2x of the experiment with a binding ratio of 1:5 in the second step gave significantly lower protein amounts than expected (approx. 16 % ± 2 % instead of 80 %), see Figure S 3 C. In addition, P₃ 2x of this equilibration step was almost void of proteins (γ ≈ 2 %, green striped bar in Figure 41 D). I link this observation to the lower amount of HLLs that were used to establish a binding ratio of 1:5 (only 16 % of the amount used in the first step in contrast to using 80 % for 1:1 reloading). Equilibration experiments indicated by the red bar gave γ ≈ 105 % ± 36 %. I assume that this is mainly linked to the extremely high amounts of BSA present P₃ 1x. The experiment indicated by the blue bar gave only γ ≈ 23 ± 7 %.

The results of the experiment (1:250:1) indicate a lacking of equilibration, since r_{BSA} , r_{Lys} and r_{CAn} were almost identical to the native sample, only r_{bLa} increased by approx. 100 %. Regardless of the composition of P3 1x, the other two experiments revealed both strong decreases in r_{BSA} (for the experiment (1:50:5) the amount of BSA was lower than LOD), tripled r_{Lys} and increases in r_{bLa} by 300 to 400 %. The amount of the lowest concentrated protein CAn increased by approx. 400 % (experiment 1:50:1) and 700 % (experiment 1:50:5), see Figure 41. This proves, that, in principle, 2-fold equilibration works well under conditions of overload, however, yields are not yet acceptable.

This is also well reflected comparing 1-fold equilibration with a binding ratio of 1:250 to the 2-fold equilibration with a binding ratio of 1:50:5, which—despite the same overall enrichment ratio—revealed strongly different results regarding both yields and equilibration capacity. I presume that irreversible binding sites at the HLLs are responsible for the low yields when binding ratios of 1:1 are used, well below conditions of overloading.

6.4.7. Pre-equilibration of HLLs

To avoid developing cumbersome and harsh elution procedures to be able to elute all proteins, I decided to test if it is possible to saturate these irreversible binding sites via pre-equilibration using protein solutions, either Sample B or BSA alone. The process is summarized in the scheme in Figure 43.

Good yields obtained for the 2-fold equilibration experiment when using 1:50:5 binding ratios (see Section 6.4.6.1), where BSA is present in a large excess, give rise to the assumption, that BSA is able to block irreversible binding sites on HLLs. Therefore, I investigated the pre-equilibration of HLLs using BSA (50 g/L in PBS) and Sample B, both at a binding ratio of 1:50, and PBS as a blind ($n = 3$). Equilibration was allowed to take place for 2 h and HLLs were then treated using Protocol **vi** with 3-fold elution, see Section 6.4.6.1. S_0 and P_3 -fractions of this step were discarded.

To reestablish binding conditions on these HLLs, 3-fold elution using Protocol **vi** and 3-fold washing using PBS and single washing with water were performed. Sample B diluted to an overall protein concentration of 10 g/L was then loaded onto the pre-equilibrated HLLs at a binding ratio of 1:1. S_0 - and P_3 -fractions obtained were analyzed by CE-MS ($n = 3$). All supernatants except the ones from bead eluates equilibrated in PBS only from a 1:1 binding ratio (called **S_0 none 1:1 I-III**, see Figure 43) (9 – 14 % of protein amount of initial sample) were void of protein, indicating quantitative binding of proteins to HLL.

In Figure 44 B the overall yield in protein found for all P_3 -fractions is shown. For pre-equilibration in PBS, samples **P_3 none 1:1 I-III**, showed relatively low yields between 10 – 16 % of the loading sample were found. These yields are significantly lower than those for a previous comparable experiment presented Section 6.4.6.1 (indicated by the blue bar in Figure 41), without pretreatment. I assume that the difference is due to elution of pre-equilibrated proteins with Protocol **vi** which presumably leads to surface degradation of HLLs. In contrast, pretreatment with BSA led to significantly better yields, ranging between 22 – 37 % for **P_3 BSA 1:1 I-III**. Pre-equilibration using Sample B lead to P_3 -fractions void of protein, see Figure 44, samples **P_3 F4 1:1 I-III**.

STEP-WISE EQUILIBRATION OF PROTEIN SAMPLES USING HEXAPEPTIDE LIGAND LIBRARIES. OPTIMIZATION OF THE ELUTION AND PURIFICATION PROTOCOLS TO ENABLE RELOADING

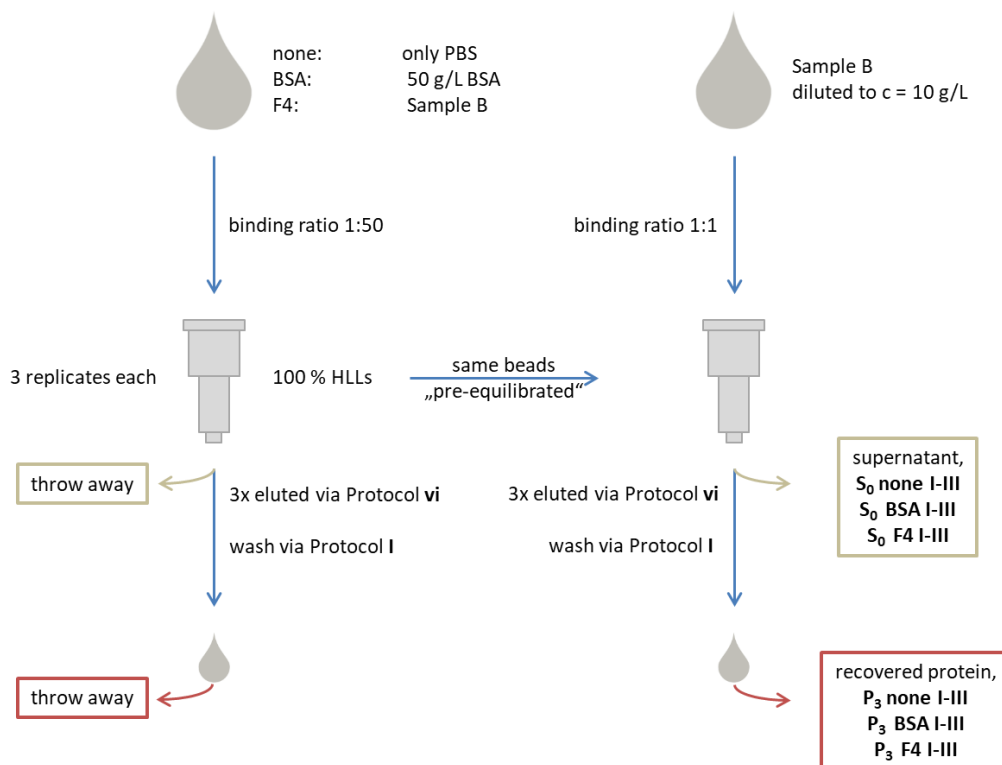


Figure 43: Scheme for the pre-equilibration of HLLs using either 50 g/L BSA in PBS or Sample B. Incubation with PBS was taken as control. After elution and washing, Sample B diluted 1:4 with PBS (overall protein concentration 10 g/L) was loaded on pre-equilibrated HLLs at a binding ratio of 1:1. After pre-equilibration, 3-fold elution was performed using Protocol vi. For washing and centrifugation using cut-off filters, modified Protocol I was used, see Section 6.4.6.1. All samples were analyzed using CE-MS ($n = 3$).

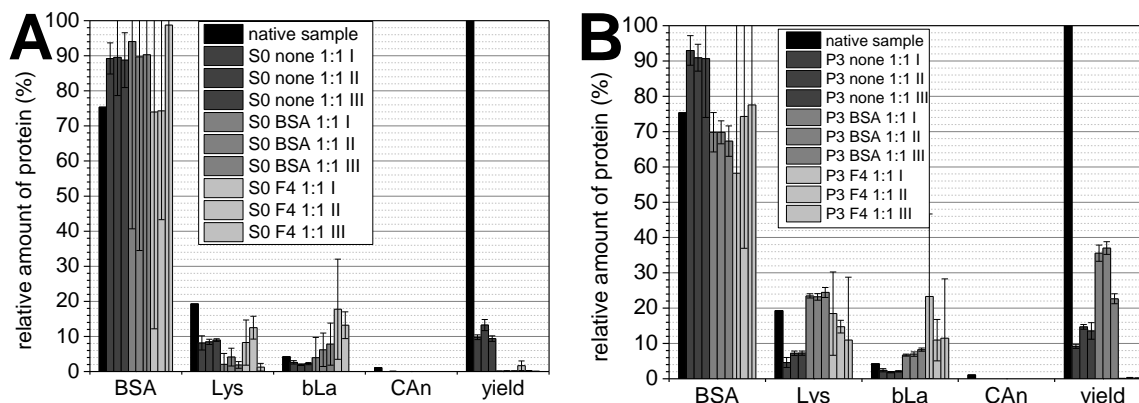


Figure 44: Relative protein amounts and yields obtained in A: supernatants S_0 and B: eluted proteins P_3 . HLL beads pre-equilibrated in PBS (“none”) in BSA solution (“BSA”), in Sample B (F4). For details see Figure 43.

No inter-protein equilibration was observed in P_3 none 1:1 I-III, but depletion of the low abundant proteins Lys and bLa, see Figure 44 B. Pre-equilibration with BSA on the other hand led to a good enrichment of Lys (increase by 20 – 30 %) and bLa (increase by 60 – 100 %) in P_3 BSA 1:1 I-III. CAn was not detected during these measurements due to poor performance of MS at this day.

6.4.8. Intra-protein equilibration

For intra-protein equilibration, the concentration change of the isoforms of each protein was investigated using Equation (8). To reduce data and make results comprehensible, color-coded tables for 1-fold and 2-fold equilibration are presented in Table S 2 and Table S 3. Red color indicates

a decrease in the concentration of this isoform with $\Delta r_p < -20\%$ and green color indicates an increase of this isoform with $\Delta r_p > 20\%$. Gray color indicates either low or no change in isoform abundance with $-20\% \leq \Delta r_p \leq 20\%$.

6.4.8.1. 1-fold equilibration

For BSA, either depletion of most-abundant BSA1 or only minor changes in relative isoform abundance were observed. For BSA2 unambiguous results were found: either depletion, enrichment or no significant change in abundance was observed. BSA3 was only depleted using higher binding ratios (**day 3 (binding ratio 1:250), 3-fold elution**) or when the insufficient elution Protocol **vii** was used. Pre-equilibration using BSA even led to increasing concentrations of this isoform. BSA7 was also only enriched using pre-equilibration with BSA and Sample B but depleted using other protocols. BSA5 and BSA8 were always depleted, whilst BSA4 and BSA6 were always enriched.

For Lysozyme, Lys2 was always enriched, except for **day 1 (binding ratio 1:50), 1-fold elution and P₃ BSA 1:1 III**. Most abundant Lys1 was either depleted or did not change in concentration, whilst Lys3 and Lys4 gave unambiguous results except when pre-equilibration with BSA was conducted. Here, enrichment of both Lys3 and Lys4 was observed.

For β -lactoglobulin, especially bLa1, bLa3 and bLa5 were enriched during the equilibration procedures, whereas bLa2 and bLa4 were either depleted or their amounts did not change. An exception to this observation were pre-equilibration experiments using BSA. Despite the fact, that inter-protein investigation showed that the relative amount of bLa almost doubled (see Section 6.4.7), **P₃ BSA 1:1 I (P₃ BSA 1:1 II)** gave increasing relative amounts of bLa5 (bLa1) only. It seems, that not intra-protein equilibration but enrichment of certain isoforms occurs regardless of their relative abundance in the original sample.

For carbonic anhydrase, depletion of CAn1 and enrichment of CAn2 was always observed. Except for **day 2 (binding ratio 1:50), 1-fold elution**, CAn3 - 5 were either enriched or did not change in concentration.

1-fold equilibration using a binding ratio of 1:1 revealed almost the same sample composition as **P₃ none 1:1 I-III** but comparably strong changes were observed in **P₃ BSA 1:1 I-III**. Regarding the overall yields discussed in Section 6.4.7, pre-equilibration is found to be a useful tool against protein loss due to irreversible binding. In both cases, CAn-isoforms were not detected due to poor sensitivity of MS at this day.

6.4.8.2. 2-fold equilibration

2-fold equilibration (details in Section 6.4.6.1) led to higher relative amounts of BSA4 and BSA6, Lys2, bLa1 and bLa5, as well as CAn2 - 5. All these isoforms were already equilibrated towards higher ratios using 1-fold equilibration. It is important to note that all other isoforms were depleted. This is presumably linked to the overall low yields, see Section 6.4.5. This frequently led to isoform concentration below LOD.

6.4.9. Application to serum samples and method comparison to SDS-PAGE

6.4.9.1. Detection of low abundant proteins in serum samples

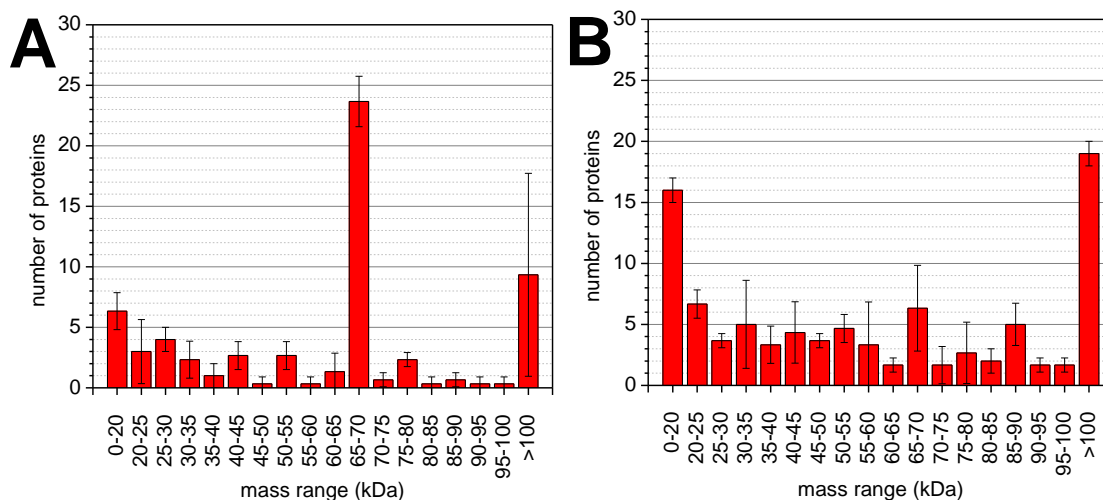


Figure 45: Number of proteins in serum A: before (number of proteins: 62 ± 6) and B: after 1-fold equilibration (number of proteins: 92 ± 12) using a binding ratio of 1:50, elution via Protocol vi (1-fold). Values were obtained from CE-MS data, further details see Chapter 4, followed by data treatment according to Section 4.3.1.2. CE-MS measurements were conducted using an AAEE-coated capillary with 100 cm in length using a separation voltage of 30 kV and an internal pressure of 100 mbar.

The capillary coating presented in Chapter 4 was also used to investigate samples equilibrated using HLLs.

The number of proteins identified via Agilent MassHunter in both native serum and a 1-fold equilibrated sample (1:50 binding ratio, elution via Protocol vi), are grouped via different molecular mass ranges and presented in Figure 45. For serum, at least 25 different proteins were detected in the mass range of 65 – 70 kDa. This is the mass range which includes albumin and its isoforms. For all other mass ranges, 6 or less proteins were found, except for the mass range >100 kDa. Here, coagulation products may be present.

After equilibration, two effects were observed: (i) the number of detectable albumin isoforms strongly decreases to approx. 6 and (ii) the number of proteins in each mass range increases, mostly in the mass range below 20 kDa and above 100 kDa.

Measurements using SDS-CE and SDS-PAGE were conducted using native serum (Trace 1) and serum after 1-fold (Traces 4&5) and 2-fold (Trace 2&3) equilibration after processing according to Protocol vii and Section 6.3.6. 1-fold and 2-fold equilibrated serum were analyzed by SDS-PAGE in duplicates, thus two traces each. The major differences between equilibrated and native serum samples visible in SDS-PAGE, see Figure 46 B, are due to the low yields, as already discussed in Section 6.4.4. The same holds for the low peak areas and heights in SDS-CE electropherograms, see Figure 46 A. During these early experiments, no attempts were made to increase yields e.g. via successive elution of HLLs or via optimized filter protocols, as described in Sections 6.4.3 and 6.4.5.

After 1-fold equilibration, a strong decrease in the number of proteins in the mass-range of 50 - 80 kDa is linked to the depletion of albumin and its isoforms and is in good accordance with the results from CE-MS experiments. Additional signals especially in the mass range below 50 kDa were observed after HLL equilibration in SDS-PAGE, which is well corroborated by the results

obtained from CE-MS experiments. I also conducted 2-fold equilibration with serum. Interestingly, an increase in overall protein amounts (and thereby a high yield) was obtained, indicated by both higher contrast in SDS-PAGE and larger peak areas in SDS-CE. I link these high yields to the large amount of albumin in the 1-fold equilibrated sample, see Traces 4&5 in Figure 46, leading to overloading conditions and thus saturation of (irreversible) HLL binding sites. These results are in good accordance with those presented for standard proteins, especially the results found for the experiment indicated by the red bar in Figure S 3 D, where high protein yields were obtained under overloading conditions at high albumin concentration.

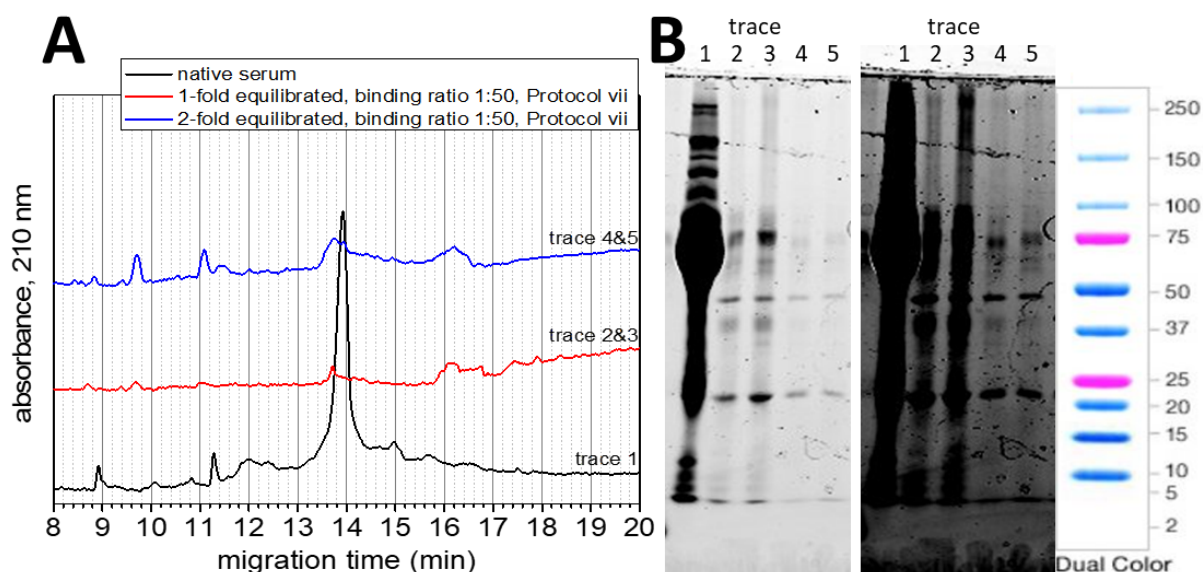


Figure 46: A: Electropherograms obtained using SDS-CE, see Chapter 2, of serum (Trace 1) as well as 2-fold (Trace 2&3) and 1-fold (Trace 4&5) equilibrated. Elution Protocol vii was used. Equilibration ratios were 1:50 and 1:50:5, with 100 μ L and 16 μ L settled bead volume, respectively, see Figure 42. Eluted and purified samples were processed according to Section 6.3.6 prior to analysis. B: SDS-PAGE of the identical samples presented in 2 different shades of gray. Trace numbering here is identical to those in A and B.

The information depth that can be reached by SDS-PAGE is clearly lower than for CE-SDS or CE-MS. More detailed information can be obtained using 2D-CE, see Boschetti *et al.*⁷. However, experimental time will increase likewise. Here, the CE-MS method with AAEE coated capillaries I developed proved advantageous with regard to information depth, speed and automation.

6.4.9.2. Detection of impurities for quality control

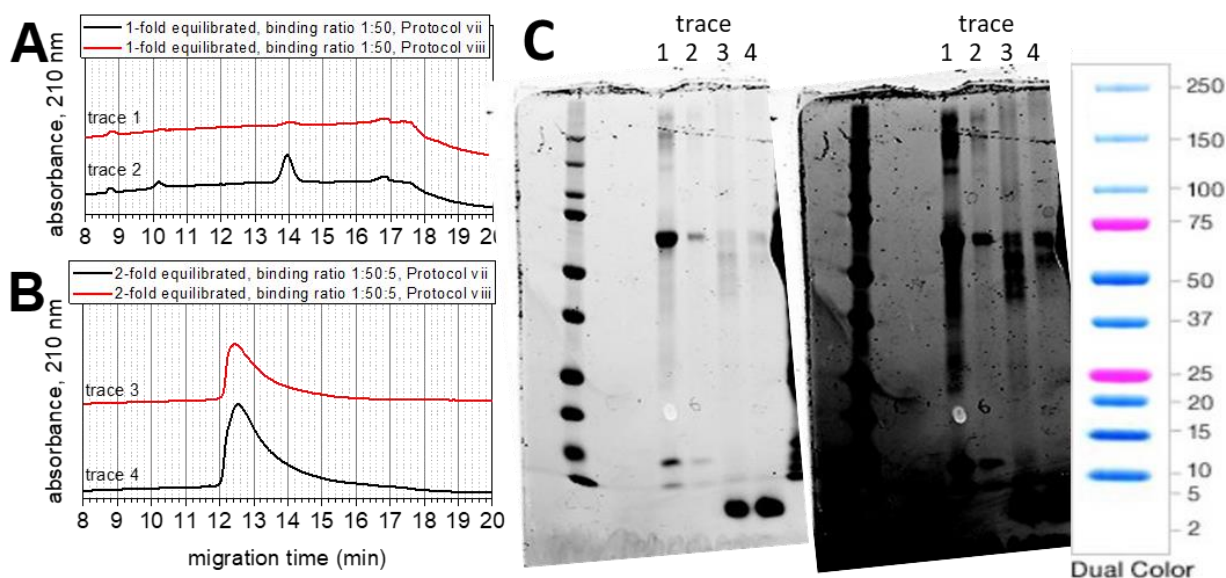


Figure 47: Electropherograms obtained using SDS-CE, see Chapter 2, of Sample A that was **A:** 1-fold equilibrated by 1:50 and **B:** 2-fold equilibrated. Elution Protocols **vii** (red traces, Traces 1 and 3) and Protocol **viii** (black traces, Traces 2 and 4). Equilibration ratios were 1:50:5, with 100 μ L and 16 μ L settled bead volume, respectively, see Figure 42. Eluted and purified samples were processed according to Section 6.3.6 prior to analysis. **C:** SDS-PAGE (see Section 6.3.5) of the identical samples presented in 2 different shades of gray. Trace numbering here is identical to those in A and B.

The use of HLLs in quality management of proteins was presented in literature by Guerrier *et al.*⁹. I applied 2-fold equilibration on Sample A using a binding ratio (settled bead volume) of 1:50 (100 μ L) and 1:5 (16 μ L) in the first and second equilibration step, respectively. The strategy is identical to the one presented in Figure 42. Elution Protocol **vii** and **viii** were used, with cut-off filter treatment protocol **IInH₂O** (see Figure 42). SDS-CE and SDS-PAGE were compared.

1-fold equilibration using a binding ratio of 1:50 revealed no equilibration compared to native Sample A (results not shown). The major difference between elution Protocol **vii** and **viii** was the overall concentration in protein, indicated by peak areas in SDS-CE and gray shading in SDS-PAGE, see Traces 1 and 2 in Figure 47 A and C. 2-fold equilibration on the other hand revealed a high number of novel protein signals above LOD in SDS-PAGE, predominantly in the mass ranges 40 – 75 kDa and 130 – 200 kDa. The enrichment of these proteins presumably originates from impurities in BSA, which had a purity of $\geq 98\%$ and was prepared via agarose gel electrophoresis by the manufacturer. Lysozyme was depleted.

Similar experiments were conducted by the group of Guerrier *et al.*⁹, where they investigated 3 different proteins including 2 different albumins. The purities of their samples ranged from 95% - 99%, and protein amounts (sample volumes) of 0.5 – 3 g (10 – 100 mL with 10 – 50 g/L, equal to 10 to 60 times higher amounts of proteins compared to us) were equilibrated using HPLC columns packed with 0.5 – 1 mL settled bead volume (5 to 10 times more than I used), leading to equilibration ratios of 1:100 and 1:300. Using these tremendously higher sample amounts, SDS-PAGE results comparable to us, namely the drastic relative increase in protein impurities concentrations, were observed.

STEP-WISE EQUILIBRATION OF PROTEIN SAMPLES USING HEXAPEPTIDE LIGAND LIBRARIES. OPTIMIZATION OF THE
ELUTION AND PURIFICATION PROTOCOLS TO ENABLE RELOADING

Overall, I present a method for cumbersome, yet promising analysis of small sample amounts using 2-fold equilibration. Besides the successful equilibration of BSA-impurities, the high comparability between SDS-PAGE and SDS-CE is demonstrated by these results.

6.5. Discussion

6.5.1. Quantification via CE-MS and compatibility with sample composition and excess co-migrating protein

CE-MS quantification depended on the sample solvent as differences for aqueous samples vs. samples in PBS were observed, see Section 6.4.1. I assume that either precipitation of proteins or adsorption to the sample vial due to the low ionic strength of the aqueous sample solution occurred, which impairs quantitative precision. Migration times and migration time precision were comparable for both sample types (see Figure 34 A and B), however, the smaller peak-widths observed for samples dissolved in PBS indicate the presence of sample-induced transient isotachopheresis (tITP) with sodium as transient leader. Therefore, beneficial assets with respect to separation efficiency are obtained when utilizing PBS as sample solution. For intact protein analysis, further BGE optimization is required as comigration of proteins occurred, which will impair quantification due to signal suppression. Eventually, also changes in the charge envelope at higher protein concentrations (Figure 35 A) may occur. Some imprecision due to changes in intra-protein profiles can thus be expected upon equilibration. Nevertheless, quantification was possible for all model proteins at concentration between 0.5 g/L and 10 g/L.

6.5.2. Applicability of cut-off-filters for protein purification to re-establish binding conditions

6.5.2.1. Recovery of proteins from cut-off-filters

Cut-off-filters are commonly used to purify proteins, as illustrated in Section 4.2. Protein recovery is often described to be below 95 % in contrast to manufacturer specifications. Considering the given recovery rate for each centrifugation and washing step, I theoretically expect recovery rates of 95 % for Protocol I, of $0.95^4 = 81$ % for Protocol II and of $0.95^8 = 66$ % for Protocol III, for further information see Section 6.3.4.

The recovery rates for BSA via normal recovery Protocols II and III using PBS solutions were higher than expected, demonstrating the capability of cut-off-filters to support excessive centrifugation. I assume that the largest protein BSA is not lost at the filter membrane. In contrast, some losses were observed for lysozyme which is reflected by its lower recovery. This can be explained with its high basicity, resulting in high adsorption to the membrane. For all other recovery protocols, much lower recovery rates were observed, which stresses the importance of appropriate recovery protocols and especially recovery solutions, as described in Section 6.4.3.1. Differences in adsorption rates of different proteins on filtration units are discussed to be impossible to be completely suppressed^{252, 253}.

Further parameters might negatively influence protein yields: (i) precipitation of proteins due to decreasing solution volume and thus higher concentration during centrifugation, (ii) formation of a concentration gradient with highest concentration of protein close to the membrane²⁵⁴, (iii) non-specific binding interaction with the filter membrane especially in case of proteins with non-polar binding sites^{255, 256}, (iv) unfolding of protein during washing and (v) precipitation of protein due to inapt pH or ionic strength of washing solutions.

To overcome these problems, a large variety of protocols for protein recovery from filters have been discussed in the scientific community, e.g.: (i) cumbersome “washing” of the membrane via

mixing the solution with pipette between centrifugation steps to avoid concentration gradients and adsorption to the membrane surface²⁴⁰. (ii) Addition of carrier-substances such as surfactants, BSA²⁴¹ and glycerol²⁴² to overcome protein-membrane-interaction – which are, however, inapt for this study on re-establishing binding conditions. (iii) Incubation of filter-units in recovery solvent to reach re-dissolution of precipitated or adsorbed protein.

The influence of single and consecutive washing steps using water, PBS and urea-solution as well as the influence of recovery protocols on the recovery of protein sample was described in Section 6.4.3.1. Higher recovery rates for the normal recovery compared to the reversed recovery are linked to the fact that precipitated and adsorbed protein are more difficult to re-suspend without pipetting, as frequently discussed²⁴⁰. Therein, the decrease in recovery rates observed for increasing numbers of centrifugation steps and the better recovery with PBS instead of water, see Figure 37 C and E, are presumably linked to the formation of badly soluble protein aggregates. Likewise, aqueous washing solutions of low ionic strength reduced protein yields because of poor (re-)solubility of (precipitated) proteins, see Figure 37 A and E.

In general, recovery rates for lysozyme increased when applying urea-washing steps as described in literature²⁴⁹. However, this was not the case when washing steps with PBS in the normal recovery mode, see Figure 37 E, F, G and H, were used. Two interpretations are possible: (i) urea softens the meshwork of the filter unit and decreases the pore-size. Thereby, transport of lysozyme into the membrane during excessive centrifugation is decreased. I expect this influence to be minimal since the manufacturer states good compatibility of filters with 8 mol/L urea. Furthermore, hypothesis (i) can be rejected since increasing washing and centrifugation steps often led to increasing instead of decreasing recovery rates. (ii) Urea decreases protein-filter-interaction and aggregation of lysozyme and thus precipitation. My assumption is based on two observations: first, a lysozyme recovery of only 10 % was obtained using a protocol with only a single washing and centrifugation step followed by elution with water, see Figure 37 F and secondly, the recovery-rate of lysozyme for washing Protocol III (4x urea and 4x PBS, see Sections 6.4.3 and 6.4.4) was independent from the elution protocol used. Similar observations were made for BSA recovered with washing Protocol III.

6.5.2.2. Purification of HLL elution solutions from SDS and urea

None of the protocols used enables a full recovery of proteins from cut-off filters (Section 6.5.2.1). The presence of SDS in HLL eluates further complicates the purification process. Irreversible transportation of protein into the membrane and irreversible protein-membrane interaction are the most likely reasons. Leaking through the membrane is unlikely as even the sum of protein amount in all solutions (S_0 , $W_{1,x}$, $W_{2,x}$, P_3) was below 100 %, see Figure 39 C. In the presented study, this observation was made for aqueous elution solutions (P_3), similar observations are described for samples in PBS²⁵².

For the depletion of SDS from proteins using cut-off-filters, incomplete removal of SDS (elution solutions i-v, see Figure 39 E and F) is likely since recovery rates over S_0 , $W_{1,x}$, $W_{2,x}$, P_3 were below 100 % for both protein and SDS, see Section 6.4.3.2. SDS-protein-aggregates may form and impair CE-MS quantification. Loss of protein due to SDS-membrane and protein-SDS interaction during the washing and centrifugation processes might result in protein loss. From the results it is clear that the washing protocols chosen are inapt to overcome SDS-protein interaction: it seems that a fixed

amount of SDS is involved in SDS-protein aggregation given the observed differences in absolute SDS-amounts depleted from samples containing HLL elution solutions **iv** and **v** (10 % SDS, high amounts of depleted SDS observed) and those containing elution solutions **i-iii** (1 % SDS, lower amounts of depleted SDS observed).

Protein recoveries were between 12-15 % for BSA and 23-29 % for lysozyme when using HLL elution solutions **vi-viii**, see Figure 39 A. Even for these HLL elution solutions containing urea, a high extent of protein loss in cut-off-filters was observed as indicated by Figure 39 C. The recovery rates found here are much lower than those observed for washing and centrifugation of protein only, see Figure 37 A and E (BSA: 50-110 %, lysozyme 35-61 %). Despite urea being chaotropic, which is expected to prevent protein agglomeration and thereby precipitation upon centrifugation, exactly these effects seem to emerge. I assume this to be due to urea induced disruption of the tertiary structure of proteins, which can impair solubility. Depletion of urea from protein solution during centrifugation thus results in precipitation of protein.

Normal recovery of proteins from cut-off-filters using recovery-solvents such as PBS antagonizes this detrimental behavior, as was shown in Section 6.4.4. Furthermore, re-dissolving proteins via pipette-washing of the membrane in-between centrifugation steps is expected to reduce both adsorption and precipitation²⁴⁰.

Concluding everything it can be said, that few washing and centrifugation steps followed by normal elution protocol using PBS as elution solvent gave highest recovery rates and most reproducible results.

6.5.3. Performance of HLL protein equilibration

CE-MS investigations were conducted after depletion of elution solvent using cut-off-filters. As already discussed in Section 6.4.9, SDS-PAGE and SDS-CE-measurements of serum and standard protein gave unsatisfactory separation efficiency and quantification. CE-MS was chosen as primary measurement technique due to its excellent automation and high measurement speed, both described in Section 6.4.

Due to both poor depletion of SDS and poor recovery of proteins, HLL elution conditions with SDS (elution Protocols **i-v**) were not further taken into consideration.

Overall protein yields:

As presented in Section 6.4.4 **Fehler! Verweisquelle konnte nicht gefunden werden.**, the obtained overall protein yields strongly differed for the HLL elution protocols utilizing elution solutions **vi** (54 ± 11 %), **vii** (12 ± 1 %) and **viii** (25 ± 2 %). Best results were obtained for **vi**, which contained 2 % cationic surfactant CHAPS in 5 % acetic acid, followed by **viii**, which was an aqueous solution of urea and **vii**, which contained 2 % CHAPS and urea but no acetic acid. This points out that the presence of acetic acid is either necessary for the elution process using CHAPS or for the depletion of CHAPS during sample processing with cut-off-filters. Since the latter is expected to be independent from the acetic acid concentration, different yields must be discussed by the elution efficiency of the elution solution. The application of CHAPS in a non-acidic environment (elution solution **vii**) seems to impair elution performance. Slightly higher protein yields were found for experiments with 3-fold elution via Protocol **vi**. The presence of ionic binding sites on HLLs that interact with ionic amino acid residues requires pH-adjusted elution protocols. Consecutive elution with solutions at various

pH (7.2, 4.0 and 9.3) eluted mostly acidic (basic) proteins in the acidic (basic) elution fraction as described by Fasoli *et al.*²⁵⁷.

My results show that protein loss predominantly occurs during HLL elution, as lower overall protein-yields were obtained for all experiments with HLL eluates compared to the yields determined for the investigation of cut-off-filters in Section 6.4.3.1 (BSA: 90 %, lysozyme: 70 %). This is conclusive, since protein losses in cut-off-filters are only due to adsorption to the membrane and precipitation of proteins. Using HLLs, additional losses can occur: (i) HLL-binding capacity is approximately 1.00 mg, but only for highly complex protein samples such as serum. The low complexity of the model protein sample does not allow to saturate all binding sites offered by HLLs and lower overall yields of protein are expected as described by Guerrier *et al.*¹⁰. (ii) Loss of proteins occurs due to adsorption, agglomeration and precipitation in the presence of urea after elution (and later on its depletion), see Section 6.5.2.2 for a detailed discussion. It is worth noting that the recovery rates for **vi** after HLL-pre-equilibration were 2-4 times higher than those observed without HLL-pre-equilibration.

Experiments conducted at a binding ratio of 1:1 without pre-equilibration, performed in triplicate, see Section 6.4.7, gave protein yields of only 20 %. A strong increase in yields was observed for pre-equilibrated HLLs. This indicates, that irreversible binding sites exist on HLL beads, which can be pre-occupied by BSA. This is supported by the observation that no significant differences were found in both yield and inter-protein equilibration for experiments at a binding ratio of 1:50 and a binding ratio of 1:250 without pre-equilibration. At both rates maximal binding capacity is assumed to be reached for the model proteins. Thus, overloading conditions, either for one or several proteins, are necessary for efficient equilibration and elution.

Inter-protein-equilibration:

Comparing different elution protocols after the same HLL equilibration step, changes in the relative amounts of proteins after equilibration give insight into the performance of elution solvents of different composition. It was shown in Figure 40 C that depletion of BSA and enrichment of Lys was observed for all HLL elution Protocols **vi**, **vii** and **viii**. bLa was enriched 3-times more efficiently via Protocol **vi** compared to Protocol **viii**. In contrast, Protocol **vii** resulted in depletion of bLa. These observations are in good accordance with those made for the overall yield in protein. This proves that binding of bLa on HLL takes place and that elution solutions differ strongly in performance. Furthermore, this leads to the assumption that acetic acid is crucial for the elution of bLa (pI 5.1) from HLLs. Overall, 3-fold equilibration using Protocol **vi** had a beneficial impact not only on yields but also on the relative abundance of CAn.

CAn was difficult to elute by all three elution protocols when only 1-fold elution was conducted. Possible explanations are: (i) The low starting concentration of carbonic anhydrase results in binding suppressed by other proteins during HLL-incubation. Since 3-fold elution increased yields in CAn, we can neglect this assumption. (ii) The low concentration of carbonic anhydrase and the high concentration of BSA (serving as a transporter in serum) leads to preferred BSA-carbonic anhydrase interaction and thus co-depletion with BSA. Observations made in Section 6.4.6 indicate, that this is the case for bLa and BSA. Given the transport function of BSA it would be no surprise, if CAn would be impaired as well. (iii) Carbonic anhydrase is lost during cut-off-filter treatment due to adsorption and precipitation, see Section 6.5.2. (iv) The interaction between HLLs and CAn is not

reversible using the elution protocols investigated. This assumption is supported by the fact, that higher amounts of CAn were found after 3-fold elution. An explanation for low or slow elution was presented by Boschetti *et al.*²⁵⁸ and Thulasiraman *et al.*²³⁹. (v) Inaccurate quantification via CE-MS-experiments due to low protein-concentrations, as indicated by the respective R² of the calibration curve, see **Table S 1** in the SI, and by the inability to quantify CAn during pre-equilibration experiments. (vi) There are no HLL-hexapeptides which bind CAn. Similar effects were discussed by Boschetti *et al.*²⁵⁸ and Fasoli *et al.*²⁵⁷, who observed, that about 5 – 15 % of proteins found in native protein samples were lost after 1-fold equilibration.

On a molecular level, interaction between HLLs and protein needs to be considered. Fasoli *et al.* postulated, that low binding interactions comes along with high dissociation constants between proteins and HLL-surfaces (and vice versa), which leads to failure of protein adsorption during equilibration or desorption during elution. For high binding interactions, consecutive elution using a variety of solvents was suggested²⁵⁷. In this study, using 3-fold elution with Protocol **vi** proved sufficient to increase overall yields and especially recovery rates of CAn. Using different elution solutions in consecutive elution steps may be even more promising, since different elution solutions (using high ionic strengths, high amounts of surfactant, e.g. SDS, various organic ratios, e.g. acetonitrile, high salt contents, e.g. sodium chloride, various pHs, and many others) are apt to weaken different interactions between proteins and HLLs^{13, 235, 259}. In this study I demonstrated that elution via SDS (weakening of non-specific interactions between proteins and HLLS via elution Protocols **i-v**) is challenging and not compatible with subsequent CE-MS analysis. To gain access to specific proteins interacting with the HLL hexapeptides predominantly via this pathway, further adjustments prior to analysis (e.g. dialysis instead of centrifugation using cut-off-filters) and re-equilibration, have to be made.

For proteins with very low dissociation constants from the HLL beads, where no preliminary adsorption on HLLs occurs, other approaches are due. For such proteins, addition of BSA to the protein solution prior to equilibration can shift binding equilibrium of desired proteins towards higher binding if one or more of the following effects are present: (i) good binding of the desired protein to BSA with the serum transport protein BSA functioning as a mediator between HLL and protein of interest. In this research such behavior was observed for bLa. (ii) When no interaction between BSA and protein of interest occurs, only higher protein concentrations lead to a higher chemical potential and thus a shift of binding equilibrium to more protein bound to the surface.

Measures, beneficial for proteins with low dissociation constants are the blocking of irreversible binding sites with BSA. Using pre-equilibration experiments and both 3-fold and 1-fold elution, insight into the binding interaction of CAn were obtained. A pre-equilibration step is presented as a novel approach to block some HLL binding sites and simultaneously use HLLs as a carrier for “fishing proteins”, e.g. BSA or modified BSAs, to bind the desired proteins, without cumbersome preliminary immobilization of “fishing proteins”

Intra-protein-equilibration:

For intra-protein-equilibration, depletion of the most abundant CAn1 isoform and equilibration of all 4 other isoforms was observed for 1-fold and 2-fold equilibration experiments with one exception (see Section 6.4.6). Similar binding situations and elution behaviors of each isoform are assumed, which leads to successful inter-protein equilibration. I furthermore assume that HLL-

binding sites with a high specificity towards CAn and a low cross-sensitivity towards BSA, bLa and Lys are present, which is supported by the high yields and good inter-protein equilibration described above.

For BSA, especially BSA4 and BSA6 were successfully equilibrated during 1-fold equilibration experiments, whilst BSA1 and others were depleted. Binding of BSA4 and BSA6 towards well reversible binding sites is especially indicated by the results from experiments using a binding ratio of 1:1 (**P₃ none 1:1 I-III**): despite the low yields, BSA4 and BSA6 were enriched. Even 2-fold equilibration led to increasing relative concentrations of these two protein isoforms, which further supports the assumption of reversible binding sites.

For Lys, highest binding ratios to well reversible binding sites can be assumed for Lys2 and to a lower extent for Lys4 and Lys3. Lys1 either binds to less reversible binding sites or cannot compete with the other isoforms.

For bLa, interaction of bLa1 with BSA (and presumably other proteins) during equilibration is clearly demonstrated by my results: For equilibration ratios of 1:50, most abundant bLa1 is further enriched whilst other bLa isoforms become depleted so that the concentration ratio even increases upon HLL binding and elution. When binding ratios of 1:1 are used, no significant in- or decrease of any isoform is found. Even for 2-fold equilibration a strong increase in bLa1 was observed, except when a binding ratio of 1:250 was used. Here, bLa1 was presumably depleted with overly abundant BSA. Despite this strong interaction between bLa1 and BSA, HLLs pre-equilibrated with BSA did not increase relative amounts of bLa1. This is either due to (i) the degradation of HLL-bound BSA during elution and washing procedure or (ii) the necessity to have BSA in solution to have the agglomerate BSA-bLa1 becoming attached to the hexapeptides.

6.6. Summary and outlook

During this work, CE-MS with AAEE coating was shown to be a fast analysis technique to control HLL equilibration apt to indicate problems regarding reproducibility of protein yields and to provide quantitative information about inter- and even intra-protein equilibration. The latter is impossible using SDS-CE or SDS-PAGE. Internal standards, protein labeling, and digestion were avoided, resulting in a fast analytical procedure compatible with HLL eluates. To obtain both better LODs for the proteins isoforms present in this study as well as to detect further isoforms, I propose a more time-consuming approach for future research, namely peptide analysis after enzymatic digestion. Label-free analysis using “shotgun proteomics” approaches followed by data-base assisted analyses seems promising²⁶⁰⁻²⁶².

With my investigations a good foundation for successive equilibration using HLLs was laid. Challenges regarding filter units, elution conditions, working at low binding ratios and irreversible binding sites were identified and solved to a large extent. A good understanding of HLLs at equilibration rates and protein concentrations far from those suggested by the manufacturer was obtained. Besides pre-equilibration of beads, addition of BSA to samples should be tried in future research to evoke overloading conditions or use BSA as a fishing protein for proteins with weak to negligible interaction with the HLL hexapeptides. With BSA, problems regarding irreversible binding sites and low binding of proteins to HLL-surfaces due to too low overall protein concentration may be solved. Using completely different elution protocols after pre-equilibration also seems as a good approach that is worth investigating in future.

Overall, the excellent results found for 2-fold equilibration followed by analysis via both SDS-PAGE and CE-MS were promising for in-depth proteomics with low sample amounts available.

6.7. Supporting information

Table S 1: A selection of isoforms observed for BSA, lysozyme, β -lactoglobulin and carbonic anhydrase. The most abundant isoforms of are considered with their molecular masses, base-peak and relative abundance (determined from peak areas).

BSA $C_{0,BSA} = 30.5 \text{ g/L}$				
isoform	molecular mass (Da) ^a	base peak ^b (m/z)	abundance (%) ^c	R ² ^d
BSA1	66434.08	1303.6419	25.7	0.99671
BSA2	66465.52	1304.2467	22.0	0.99179
BSA3	66550.40	1359.1668	21.1	0.99700
BSA4	66818.85	1311.1241	7.2	0.98333
BSA5	66511.08	1358.3113	6.8	0.99316
BSA6	66731.86	1335.6339	6.3	0.99073
BSA7	52999.48	1128.7515	4.8	0.95543
BSA8	66699.96	1259.3270	3.7	0.99215
lysozyme $C_{0,lysozyme} = 7.62 \text{ g/L}$				
isoform	molecular mass (Da)	base peak m/z	abundance (%)	R ²
Lys1	14305.34	1431.5417	82.0	0.98533
Lys2	14287.24	1429.7350	8.4	0.99739
Lys3	14338.20	1594.1791	4.9	0.99499
Lys4	14322.25	1433.1676	4.6	0.99714
β -lactoglobulin $C_{0,\beta\text{-lactoglobulin}} = 1.91 \text{ g/L}$				
isoform	molecular mass (Da)	base peak m/z	abundance (%)	R ²
bLa1	18363.63	1225.2572	35.0	0.92702
bLa2	18277.52	1219.5164	28.7	0.92203
bLa3	18629.87	1863.9894	9.5	0.97901
bLa4	18543.82	1855.3791	7.7	0.98104
bLa5	18687.79	1246.8654	7.1	0.95841
carbonic anhydrase $C_{0,\text{carbonic anhydrase}} = 0.475 \text{ g/L}$				
isoform	molecular mass (Da)	base peak m/z	abundance (%)	R ²
CAn1	29026.04	830.3254	59.79	0.80281
CAn2	29001.54	829.631	15.86	0.68613
CAn3	29047.95	807.8771	11.66	0.83447
Can4	29067.69	831.4940	3.52	0.73381
CAn5	29089.42	832.1367	1.91	0.78972

^aMolecular mass determined after deconvolution using Agilent MassHunter Qualitative Analysis. ^bBase-peak as determined by Agilent molecular feature extractor of MassHunter Qualitative Analysis-software and used for extraction of EICs on MassHunter Quantitative Analysis-software. ^cRelative abundance calculated via Agilent MassHunter Qualitative Analysis. ^dR²-values from external calibration linear regression (in PBS using Sample B, see Section 6.4.1) using Mass Hunter Quantitative Analysis.

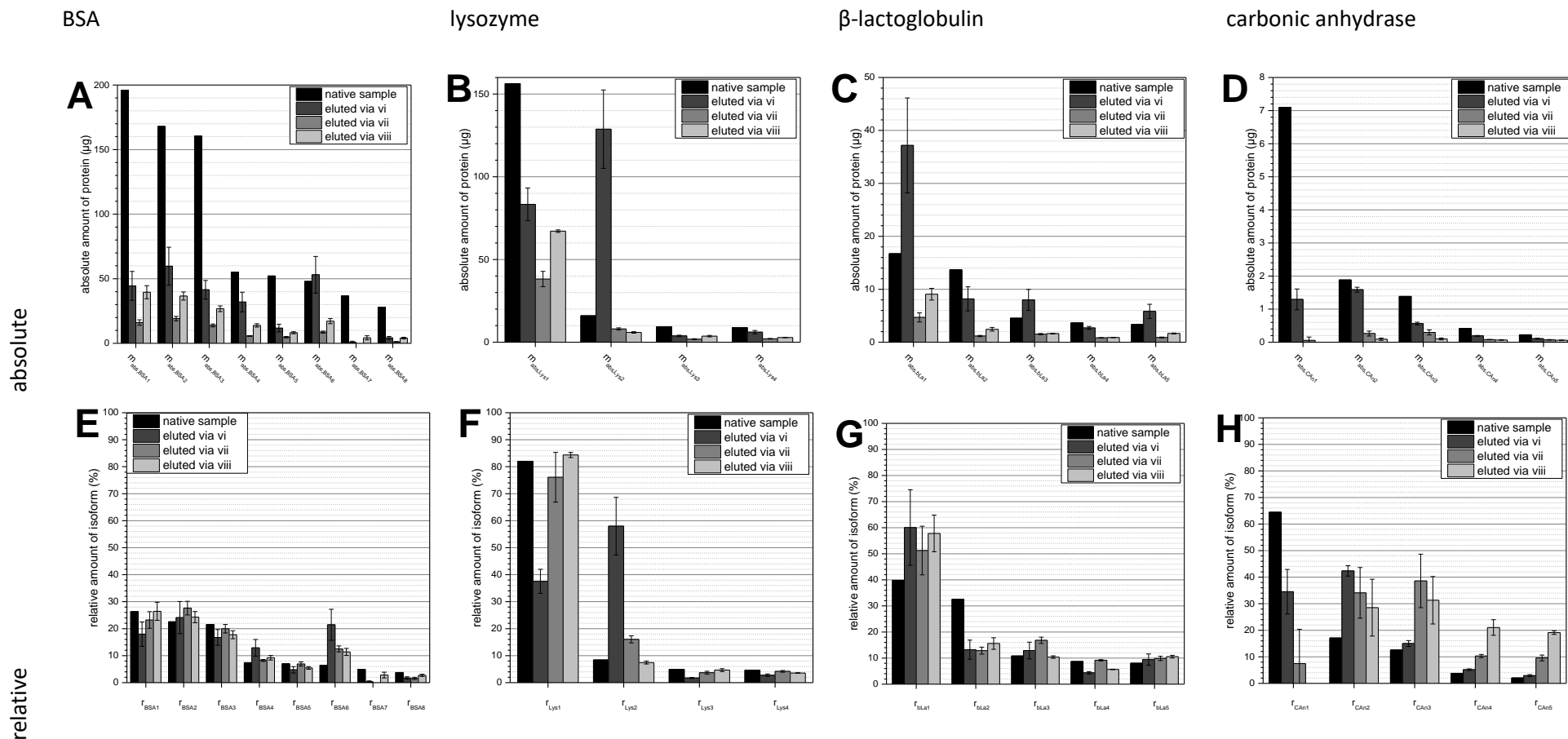


Figure S 1: CE-MS-results obtained for the one-fold-equilibration of Sample B via HLLs, see Section 6.4.4. Quantification was achieved via external calibration, see Section 6.4.1. A-D: absolute amounts calculated regarding gravimetrically determined sample volumes of each isoform of the proteins (BSA, lysozyme, β -lactoglobulin and carbonic anhydrase). A binding ratio of bound to unbound protein of 1:50 is assumed during HLL-experiments. Therein, expecting optimal binding rate, elution yield and recovery rate during sample processing, eluted samples are expected to be 100 μ L in volume with an overall protein-concentration of 10 g/L. This equals an overall amount of protein of 1.00 mg. E-H: Relative amounts of each isoform of the proteins (BSA, lysozyme, β -lactoglobulin and carbonic anhydrase). Elution protocols as given in the figure legends. Isoforms are listed in Table S 1. CE-MS analysis of intra-protein equilibration as described in Section 6.4.4.

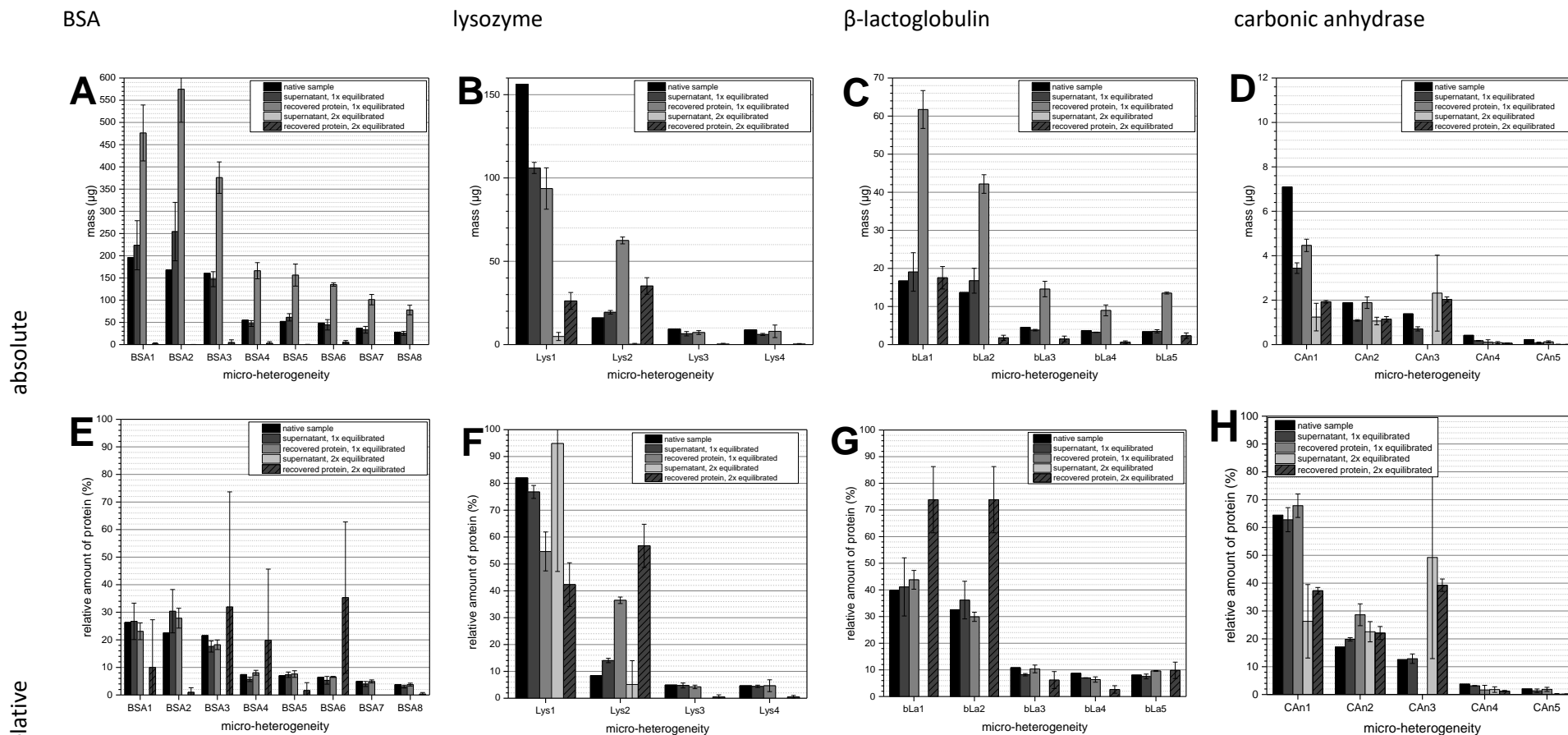


Figure S 2: CE-MS-results for supernatants and recovered protein samples obtained from one-fold and consecutive two-fold-equilibration via HLLs of Sample B, see Section 6.4.4. Quantification was achieved via external calibration, see Section 6.4.1. A-D: absolute amounts calculated regarding gravimetrically determined sample volumes of each isoform of the proteins (BSA, lysozyme, β -lactoglobulin and carbonic anhydrase). A binding ratio of bound to unbound protein of 1:50 is assumed during HLL-experiments. Therein, expecting optimal binding rate, elution yield and recovery rate during sample processing, eluted samples are expected to be 100 μ L in volume with an overall protein-concentration of 10 g/L and 8.0 g/L for 1-fold and 2-fold equilibration, respectively. This equals an overall amount of protein of 1.00 mg and 800 μ g for 1-fold and 2-fold equilibration, respectively. E-H: Relative amounts of each isoform of the proteins (BSA, lysozyme, β -lactoglobulin and carbonic anhydrase). For detailed assignment see figure legends. CE-MS analysis of intra-protein equilibration as described in Section 6.4.5.

Table S 2: Overview over changes in intra-protein profile after 1-fold equilibration, using Δr_p -values, calculated for each isoform of each protein, using Equation (8). For calculation, r_p -values of native protein sample was taken. Red values indicate $\Delta r_p < -20\%$, green $\Delta r_p > 20\%$ and gray $-20\% \leq \Delta r_p \leq 20\%$.

Experiment	BSA1	BSA2	BSA3	BSA4	BSA5	BSA6	BSA7	BSA8	Lys1	Lys2	Lys3	Lys4	bLa1	bLa2	bLa3	bLa4	bLa5	CAn1	CAn2	CAn3	CAn4	CAn5
Protocol vi	Red	Gray	Red	Green	Red	Green	Red	Red	Red	Green	Red	Red	Green	Red	Gray	Red	Gray	Red	Green	Gray	Green	Green
Protocol vii	Gray	Green	Gray	Gray	Gray	Green	Red	Red	Gray	Green	Red	Gray	Green	Red	Green	Gray	Green	Red	Green	Green	Green	Green
day 1 (binding ratio 1:50), 1-fold elution	Gray	Gray	Gray	Green	Red	Green	Red	Red	Gray	Gray	Gray	Red	Green	Red	Gray	Red	Green	Red	Green	Green	Green	Green
day 2 (binding ratio 1:50), 1-fold elution	Gray	Green	Gray	Gray	Gray	Gray	Gray	Gray	Red	Green	Gray	Gray	Gray	Gray	Gray	Red	Gray	Gray	Green	Red	Red	Gray
day 3 (binding ratio 1:50), 3-fold elution	Red	Red	Gray	Green	Gray	Green	Red	Gray	Red	Green	Red	Green	Green	Red	Gray	Red	Green	Red	Green	Green	Green	Green
day 3 (binding ratio 1:250), 3-fold elution	Red	Red	Red	Green	Red	Green	Red	Gray	Red	Green	Red	Gray	Gray	Red	Green	Green	Green	Red	Green	Green	Green	Green
P3 none 1:1 I	Gray	Gray	Gray	Green	Gray	Green	Gray	Gray	Gray	Green	Gray	Green	Gray	Gray	Gray	Gray	Gray	Red	Red	Red	Red	Red
P3 none 1:1 II	Gray	Gray	Gray	Green	Gray	Green	Red	Gray	Gray	Green	Gray	Green	Gray	Gray	Green	Gray	Gray	Red	Red	Red	Red	Red
P3 none 1:1 III	Gray	Gray	Gray	Green	Gray	Green	Gray	Gray	Gray	Green	Gray	Green	Gray	Gray	Gray	Red	Gray	Red	Red	Red	Red	Red
P3 BSA 1:1 I	Red	Red	Gray	Green	Gray	Green	Green	Green	Red	Green	Green	Green	Red	Red	Red	Gray	Green	Red	Red	Red	Red	Red
P3 BSA 1:1 II	Red	Gray	Green	Green	Gray	Red	Green	Red	Gray	Green	Green	Gray	Green	Gray	Red	Red	Gray	Red	Red	Red	Red	Red
P3 BSA 1:1 III	Red	Green	Green	Red	Red	Green	Green	Red	Red	Red	Red	Green	Red	Red	Red	Red	Red	Red	Red	Red	Red	Red
P3 F4 1:1 I	Red	Gray	Red	Green	Green	Green	Red	Green	Gray	Red	Green	Gray	Green	Gray	Red	Gray	Gray	Red	Red	Red	Red	Red
P3 F4 1:1 II	Red	Gray	Green	Red	Green	Green	Green	Gray	Gray	Green	Green	Red	Green	Gray	Red	Red	Green	Red	Red	Red	Red	Red
P3 F4 1:1 III	Red	Green	Gray	Green	Gray	Green	Green	Green	Gray	Green	Green	Red	Green	Red	Red	Gray	Gray	Red	Red	Red	Red	Red

Table S 3: Overview over changes in intra-protein profiles after 2-fold equilibration, using Δr_p -values, calculated for each isoform of each protein, using Equation (8). For calculation, r_p -values of native protein sample was taken. Red values indicate $\Delta r_p < -20\%$, green $\Delta r_p > 20\%$ and gray $-20\% \leq \Delta r_p \leq 20\%$.

Experiment	BSA1	BSA2	BSA3	BSA4	BSA5	BSA6	BSA7	BSA8	Lys1	Lys2	Lys3	Lys4	bLa1	bLa2	bLa3	bLa4	bLa5	CAn1	CAn2	CAn3	CAn4	CAn5
day 2 (binding ratio 1:50:1), 1-fold elution	Red	Red	Green	Green	Red	Green	Red	Red	Red	Green	Red	Red	Green	Red	Red	Red	Green	Red	Green	Green	Red	Red
day 3 (binding ratio 1:50:5), 3-fold elution	Red	Red	Red	Red	Red	Red	Red	Red	Gray	Green	Red	Red	Green	Red	Red	Red	Red	Red	Gray	Green	Green	Green
day 3 (binding ratio 1:250:1), 3-fold elution	Red	Red	Red	Green	Red	Green	Red	Gray	Red	Green	Red	Green	Gray	Red	Green	Green	Green	Red	Green	Green	Green	Green

STEP-WISE EQUILIBRATION OF PROTEIN SAMPLES USING HEXAPEPTIDE LIGAND LIBRARIES. OPTIMIZATION OF THE ELUTION AND PURIFICATION PROTOCOLS TO ENABLE RELOADING

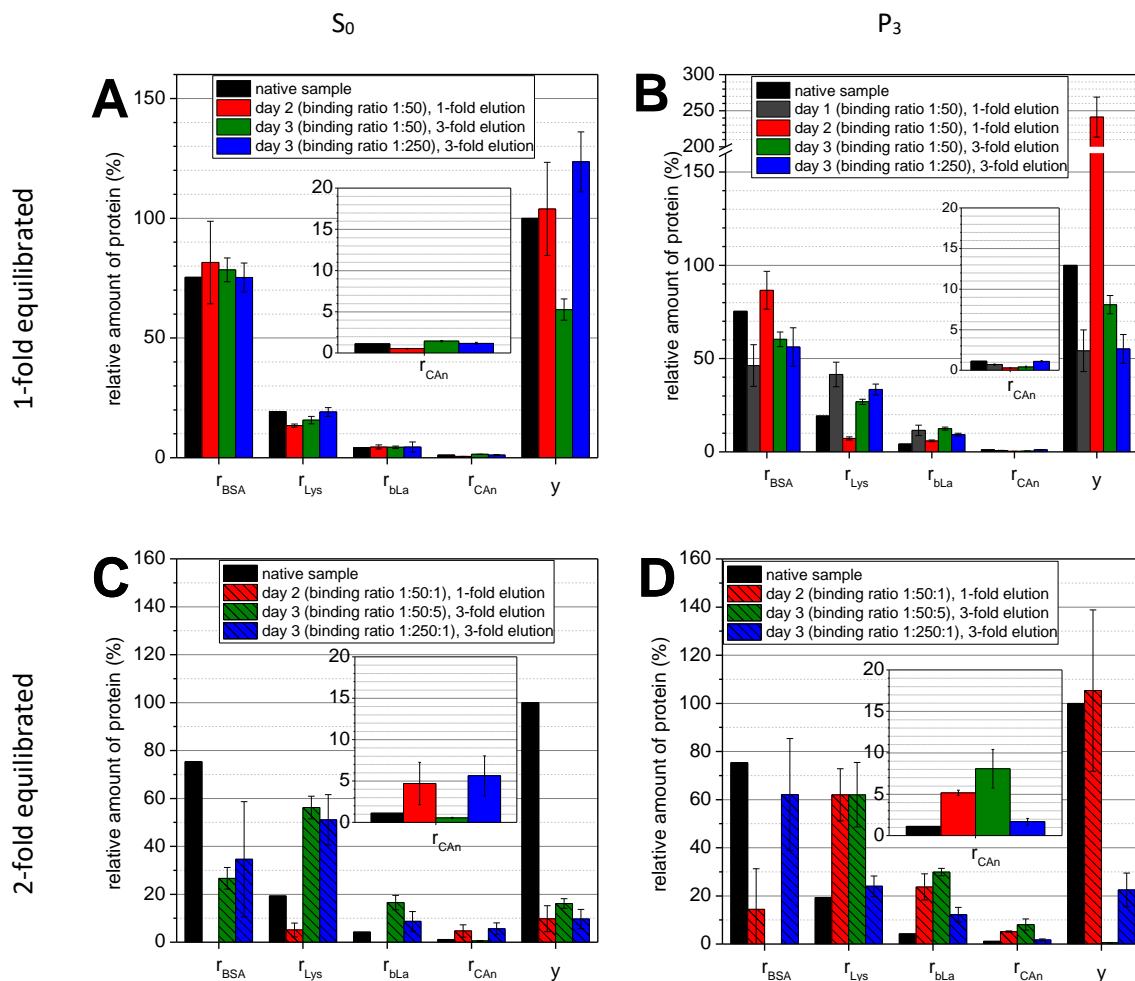


Figure S 3: Relative amount of each investigated protein, calculated according to Equation (7), and yields for 1-fold (2-fold) equilibrations on 3 (2) different days. Binding ratios of 1:50 and 1:250 followed by elution using Protocol vi either 1- or 3-fold were investigated. 2-fold equilibrations were accomplished using the previous 1-fold equilibrated sample. Color-code: 1-fold equilibration without fill-pattern, 2-fold equilibration with stripes, for details see figure legend. A & C: supernatants after 1-fold and 2-fold equilibration (S₀ 1x and S₀ 2x); B & D: recovered protein after 1-fold and 2-fold equilibration (P₃ 1x and P₃ 2x).

STEP-WISE EQUILIBRATION OF PROTEIN SAMPLES USING HEXAPEPTIDE LIGAND LIBRARIES. OPTIMIZATION OF THE ELUTION AND PURIFICATION PROTOCOLS TO ENABLE RELOADING

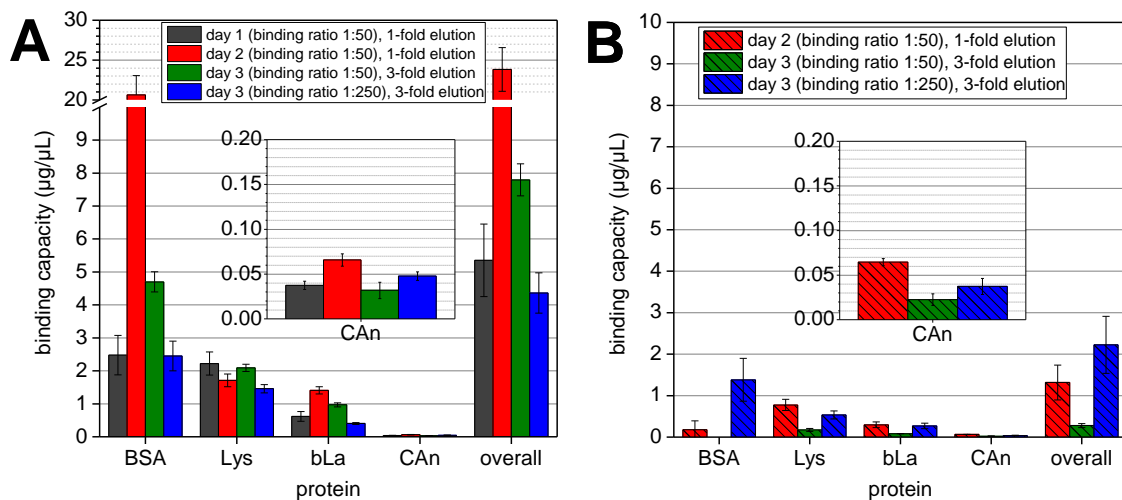


Figure S 4: Binding capacities determined for A: 1-fold and B: 2-fold equilibration, calculated using Equation (9). A binding capacity of 10 µg/µL equals 100 % yield and therefore ideal binding and recovery of proteins, see Section 6.3.4.

7. Fast CE-MS-based screening method for the determination of pI-values of cyclic peptides of very low solubility in water

7.1. Abstract

I here present a capillary electrophoresis technique with mass spectrometric detection for the determination of pI-values with simplified data evaluation. The low detection limits of CE-MS allowed applying this method to cyclic peptides of low aqueous solubility. Furthermore, the high specificity of MS enabled the parallel identification of 8 compounds and DMSO as EOF-marker. This specificity was crucial in minimizing measurement time and rendered UV-detection inapt. Accuracy was controlled using proteinogenic amino acids. Experimental pI-values deviated from literature data by only 0.1-0.5 pI units. For cyclic peptides, pI-values were determined with an accuracy of 0.3 pI units simply using migration time differences to the EOF marker. This novel technique offers high ruggedness with regard to sample impurities, speed, automation and thus throughput. Throughput was enhanced using sequential injection to simultaneously characterize multiple compounds of low solubility without sample dilution.

7.2. Introduction and motivation

Pathogenic systematic bacterial infections are caused by facultative and often antibiotic-resistant pathogens colonizing human body surfaces. For nasal infections of that type, *Styphyloloccus aurelis* is a known threat for pathogenic colonization, although the exact mechanism is unknown. This pathogenic infection is inhibited by nasal *Strapholyoloccus lugdunensis* via the production of antibiotic lugdunines, of which the cyclic peptide Lugdunin A is investigated in this work²⁶³. Lugdunins are considered to be a promising source of novel antibiotics. Therefore, their physicochemical characteristics, e.g. their pI-values, have to be investigated to understand absorption, distribution, metabolism and excretion (ADME) as a possible pharmaceutical^{264, 265}.

Besides its promising antibiotic properties, Lugdunin A-characterization provides two major challenges for pI-value determination; first, small sample amounts and second, very low solubility in water due to its low polarity. The small sample amounts are linked to the early stage of drug development within academic research. The low polarity is advantageous with regard to cell membrane permeability. Commonly, isoelectric focusing (IEF) or potentiometric and photometric titration are used²⁶⁶. Limitations of these classical methods are: For titrimetric methods, several milligrams of sample are required, hindering a fast screening of compounds from academic research and R&D. The characterization of compounds of low solubility is especially challenging as they usually require the addition of organic solvents. Then, pK_a- and pI-values can only be estimated after numerous measurements at various percentages of organic solvent, which further increases the amount of sample required for analysis²⁶⁷. Sample amounts can be minimized by microtitration methods utilizing approximately 10 µL of sample in the sub mmol/L and high µmol/L range, yet high purity of sample is required²⁶⁸. IEF conducted in a slab gel format is relatively laborious and few solutions for analytes of very low solubility in aqueous medium are available²⁶⁹: Capillary IEF with additives such as non-ionic polysaccharides, glycol or zwitterionic compounds can be used to increase solubility of analytes especially at a pH close to the pI²⁷⁰. A higher degree of automation and direct UV-detection are further advantages of capillary-based IEF, however, detection limits are often insufficient²⁷¹, if no derivatization is used. The addition of organic solvents to the separation to enhance analyte solubility would inevitably lead to changes in pI-values. Substance-specific HPLC-methods for the determination of pI- and pK_a-values are known and established in high-throughput analysis of generic assays^{265, 272}. Due to chromatographic interaction, pK_a-values are more complicated to obtain via this approach and suffer from higher inaccuracies than common titrimetric methods²⁷³. A tremendous benefit of determination of pK_a-values by separation-techniques is their high tolerance towards impurities.

In this study, pI-values were determined by CE with distinct advantages: Compounds in solution at pH-values close to their pK_a- or pI-value exhibit a strong pH-dependence of their effective electrophoretic mobility²⁷⁴. In literature, CE-UV methods for the determination of electrophoretic mobility curves in an automated approach are well-known^{274, 275}. High automation and accuracy for single compounds can be achieved, and measurement times are minimized by pressure-assisted separations²⁷⁶. High throughput is enabled by parallelizing up to 96 capillaries²⁷⁷. Another benefit of this technique is, that CO₂-absorption into buffers of high pH is minimized, increasing the accuracy in this pH-range²⁷⁵. But even with standard CE-devices, fast approaches were described²⁷⁸ based on curve fitting from 2 pH-values. However, this approach is limited to compounds of low acidity / basicity and requires reference materials with comparable pI-values.

CE-MS is an alternative for pI determination and is well applicable for the investigation of mixtures and of non-UV-active samples or such of low solubility. CE-MS hyphenation offers a solution with up to 10-fold higher sensitivities compared to conventional CE-UV, as published by Wan *et al.*²⁷⁶. Robustness was demonstrated with regard to the presence of DMSO and elevated ionic strength (25 to 150 mmol/L) in the sample with only minor changes pK_a-values by 0.06 pH-units. For calculation of pK_a-values based on the pH-dependence of the effective electrophoretic mobility in the pH-titration curve, see elsewhere^{279, 280}.

I here present a simplified approach for the determination of pI-values, taking only advantage of the fact, that the effective electrophoretic mobility of analytes is 0 at pH = pI. Simply, the difference in migration times of analyte and EOF-marker depending on pH is taken into account. At a pH higher (lower) than pI, anionic (cationic) charge evolves and thus an effective electrophoretic mobility (μ_{eff}) towards the anode (cathode). As I use mass spectrometry and thus end-column detection (that is, effective and total length of the capillary are equal), I did not calculate effective electrophoretic mobilities but chose a simplified approach just calculating the differences in detection times Δt of EOF-marker $t_{d,0}$ and of analytes $t_{d,i}$ into consideration, see Equation (10). This also facilitates calculation for measurements with additional pressure during separation. A Δt -value of 0 would indicate that the pI-value of the analyte is reached.

$$\Delta t = t_{d,i} - t_{d,0} \quad (10)$$

Negative Δt -values indicate a cationic charge on the analytes and positive Δt -values indicate anionically charged analytes.

7.3. Strategy

The analyte of interest, Lugdunin A suffers from low solubility in water, which made the development of a CE-MS method for pI-value determination pivotal. By using citric acid (pK_a = 3.13, 4.76, 6.40) and ammonium (pK_a = 9.24) at low concentrations instead of MS-incompatible “*Good buffers*”²⁸¹, MS-compatibility was granted over a pH range from 2.1 to 7.4. Based on preliminary experiments, 16 pH-steps were implemented with a fine spacing the pH region 3 to 4 after rough pI estimation for Lugdunin A in preliminary experiments.

To minimize sample amounts and work-load, on-line pH-adjustment via on-column mixing was included in the method, see Figure 48. Only 1 instead of 16 sample vials was necessary, which drastically reduced the absolute sample amount. pI values obtained for reference samples demonstrated that a pH adjustment of the samples was not necessary or, in case of Lugdunin A was futile as pH-dependent speciation of this compound occurred (see Section 7.6.2). Furthermore, with sequential injection I was able to reduce the number of analytical runs and avoid dilution of samples as well as workload: Instead of pipetting reference standards to the sample, reference standards and peptide sample were sequentially injected and analyzed in the same run. A scheme presenting the principle of both sequential-sample-injection and on-line mixing, is given in Figure 48. Further details are given in the figure legend. Comparable approaches for on-line sample processing, e.g. for enzymatic digestion²⁸², are known in literature for their simplicity in automation.

FAST CE-MS-BASED SCREENING METHOD FOR THE DETERMINATION OF PI-VALUES OF CYCLIC PEPTIDES OF VERY LOW SOLUBILITY IN WATER

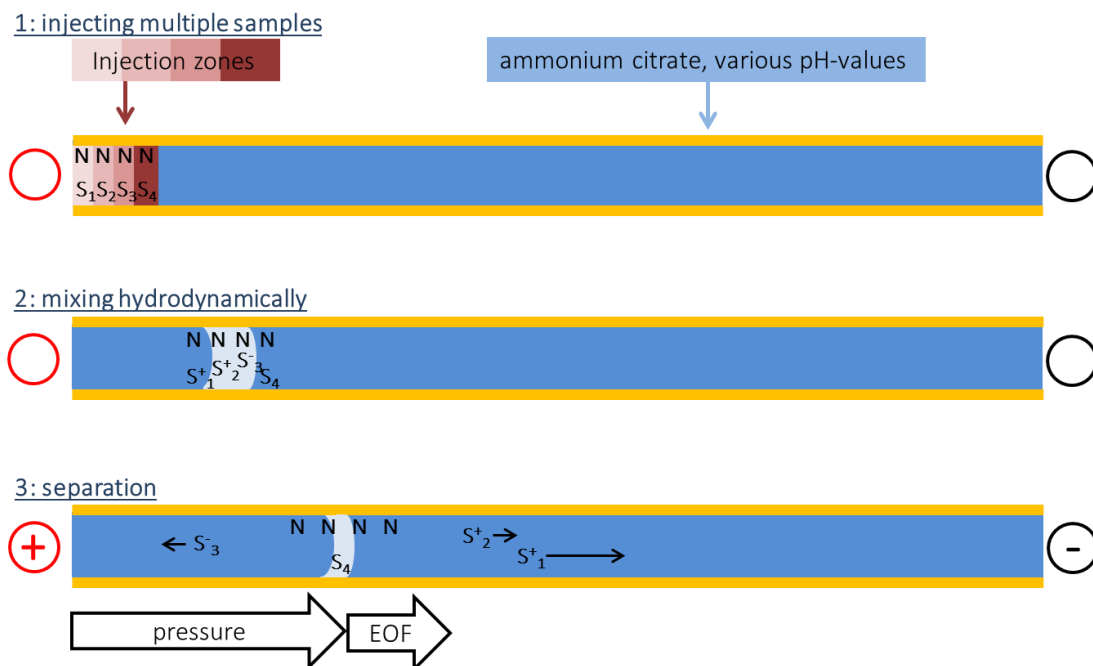


Figure 48: Scheme of sample injection and separation. N: neutral EOF-marker (*here*: DMSO). Analytes and reference substances are indicated by S_1 – S_4 . Step 1: **injection of multiple samples**; 4 consecutively injected samples and their injection zones are indicated by the 4 red squares. The samples do not need pH adjustments prior to the measurement due to fast electrophoretic mixing. Step 2: **mixing hydrodynamically**; by hydrodynamic injection of BGE after sample injection, broadening of the sample zone occurs by the laminar flow profile as indicated by the EOF-marker N. Additionally, mixing of the injection zones with BGE ions occurs, as indicated by the charges of S_1 – S_4 . Adjustment of pH-values to the level of BGE is achieved, as indicated by the charges of S_1 – S_4 . Step 3: **separation**; Further mixing of the injection zone, indicated by the diminishing light blue area, as well as broader lateral distribution of EOF-marker is indicated. Mobilization of non-charged analytes (*here*: S_4) as well as EOF-markers is due to pressure and EOF. Analytes get charged according to their pK_a - and pI -values as well as the pH-value of the BGE. Cationic analytes migrate towards the capillary outlet, *here*: S_1^+ and S_2^+ . This results in shorter migration times. The contrary holds for anionic analytes, *here*: S_3^- .

7.4. Materials and Methods

7.4.1. Instrumentation

7.4.1.1. Capillary electrophoresis

For CE analysis, an Agilent 7100 CE system (Agilent, Waldbronn, Germany) was used. Fused silica capillaries with an inner diameter of 50 μm and an outer diameter of 365 μm were purchased from Polymicro (Kehl, Germany). For CE-MS measurements running buffers according to Section 7.4.3 were used. A 100 cm bare-fused silica capillary with an internal diameter of 50 μm and an outer diameter of 360 μm was used. New capillaries were activated by consecutive rinsing with methanol, 100 mol/L sodium hydroxide solution, 50 mmol/L hydrochloric acid and water for 2 min each followed by 10 min with BGE at pH 2.5. In between runs capillaries were rinsed for 2 min with 50 mmol/L hydrochloric acid followed by 3 min with BGE. Rinsing steps were performed at 1 bar. All measurements were performed within one day using one capillary.

7.4.1.2. Mass spectrometry

A quadrupole time-of-flight mass spectrometer 6550 (QTOF 6550) from Agilent (Santa Clara, California, United States) with a sheath liquid interface from Agilent (Waldbronn, Germany) was used by implementing an Agilent isocratic pump 1260 (Agilent Technologies, Waldbronn, Germany) at a flow rate of 5 $\mu\text{L}/\text{min}$. An electrospray ionization (ESI) source was operated with a nebulizer pressure of 345 mbar, drying gas temperature of 150°C, a flow rate of 11 L/min and a fragmentor voltage of 175 V, a skimmer voltage of 65 V and an octopole voltage of 750 V. The mass range was 100-3000 m/z with a data acquisition rate of 2 spectra/s. A 50:50 (v/v) mixture of isopropanol/water was used as sheath liquid, containing 0.1% formic acid as well as a few nanogram of 3 selected calibrants for internal calibration (m/z = 121.0508, 322.0481 and 922.0097, Agilent Technologies (Waldbronn, Germany)). Hydrodynamic injection of samples was performed according to Section 7.3.

7.4.2. Chemicals

L-glutamic acid (99 %), L-glutamine (99 %) and L-phenylalanine (99 %) were purchased from Merck (Darmstadt, Germany). L-aspartic acid (100 % \pm 0.3 %) was purchased from Serva (Heidelberg, Germany). Aqueous ammonium solution (25 %), isopropanol (LC-MS-grade), citric acid (\geq 99 %), thiazolidine-4-carboxylic acid (97 %), 2-ethyl-thiazolidine-4-carboxylic acid (100 %) and L-proline (\geq 99 %) were delivered by Sigma-Aldrich (Steinheim, Germany). Water (LC-MS-grade) and dimethyl sulfoxide (DMSO, \geq 99.5 %, reagent grade) as a marker for the electroosmotic flow were obtained from Carl Roth (Karlsruhe, Germany). Potassium chloride solution (KCl, 3 mol/L, analytical grade) was delivered by Mettler Toledo (Schwarzenbach, Germany). Lugdunin and structurally related compounds T1 (Thiazolidine-4-carboxylic acid methyl ester) and T2 (2-ethyl-thiazolidine-4-carboxylic acid methyl ester) were synthesized by acid catalyzed ester-synthesis and purity was determined by NMR.

7.4.3. Preparation of samples and background electrolytes

All solutions were prepared using water (LC-MS-grade), if not stated otherwise.

Background electrolytes (BGEs) were made using a freshly prepared 250 mmol/L stock solution of citric acid in water, which was diluted with water and titrated with 10 mol/L aqueous ammonium using a WTW inoLab pH7110 pH meter (WTW, Dienslaken, Germany). 16 running buffers at

different pH levels (2.50, 2.80, 2.90, 3.00, 3.20, 3.43, 3.50, 3.60, 3.83, 4.04, 4.50, 5.00, 5.52, 6.02, 6.60 and 7.25) were used, all containing 10-25 mmol/L citric acid and 5-65 mmol/L ammonium. All BGEs were used within one week after preparation. Ionic strengths of BGEs were only roughly adjusted on the basis of preliminary conducted conductivity measurements (data not shown). This measure is sufficient, as discussed in Section 7.2.

Four samples were prepared at the following concentrations: (i) **Lugdunin A** 0.5 g/L, (ii) thiazolidin reference substance **T1** 0.5 g/L, (iii) thiazolidin reference substance **T2** 0.5 g/L, (iv) 5 amino acids **AS**, 5 mg/L each, see Section 7.4.2 for further information. The concentration of (i) is expected to be lower than described due to its low solubility. All samples were prepared using an aqueous solution containing 10 % DMSO, 2.5 mmol/L citric acid and 1.4 mmol/L ammonium. This equals a pH of approximately 3 and an ionic strength of 1/10 of the BGE at this pH to have optimal stacking conditions^{283, 284}.

7.4.4. Sequential sample injection and electrophoretic conditions

For reduction of measurement time, simultaneous measurement of analytes was achieved by multiple-sample-injection, see Figure 48 in Section 7.3. Therefore, reference samples **AS**, **T1** and **T2** as well as sample **Lugdunin A** were successively injected from their sample vials. Injections were conducted in the following order and following parameters: 5 mbar for 1 s **AS**, 100 mbar for 1 s **T1**, 100 mbar for 1 s **T2**, 100 mbar for 1 s **Lugdunin A**. Mixing of sample zones was achieved by consecutive injection of BGE at 100 mbar for 10 s and then by voltage and pressure application during separation. Measurements were performed in triplicates at each of the 16 pH levels. In total, 48 measurements were conducted. A bare-fused-silica capillary with 100 cm in length was used. Separation voltage was +30 kV. A pressure of 100 mbar was applied during runs to suppress migration of counterions from the sheath liquid into the CE capillary gradually changing the (pH-) conditions for separation²⁸⁵.

7.5. Results

7.5.1. pI-determination of amino acids and reference substances

An electropherogram illustrating how Δt -values were obtained is shown exemplarily for glutamic acid in Figure 49. Here, the extracted-ion currents (EICs) of glutamic acid and the EOF-marker DMSO are shown. The m/z -values of all EICs presented in this work are the theoretical values, which were also used for EIC-extraction. The measurement was conducted at pH 2.50, measurement conditions can be found in Section 7.4.1.1 and in the caption of Figure 49.

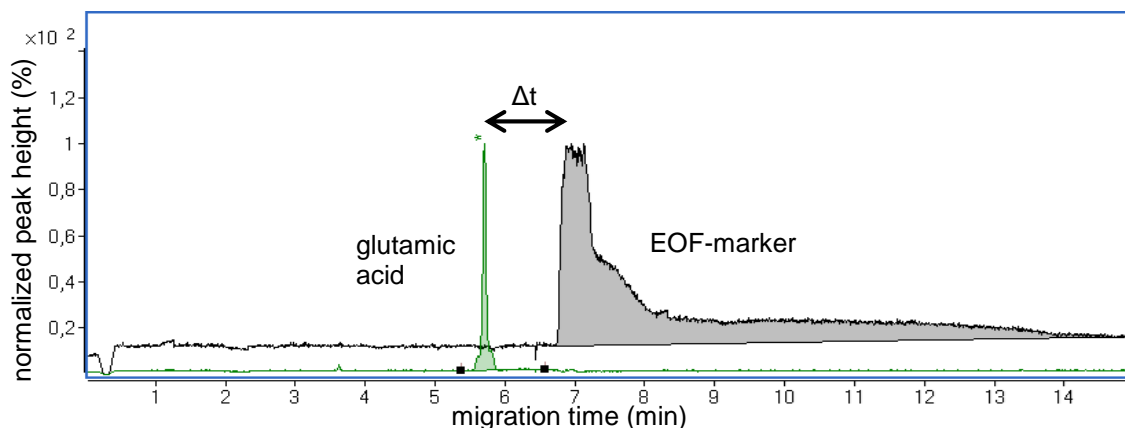


Figure 49: EICs of glutamic acid (green, $m/z = 148.0612 [M+H]^+$) and the EOF-marker DMSO (black, $m/z = 157.0349 [2M+NH_4]^+$) representatively given for the illustration of Δt -determination at pH 2.50. BGE = 25 mmol/L citric acid adjusted with 10 mmol/L ammonium to pH 2.5. Separation was performed at +30 kV and 100 mbar in a bare-fused silica capillary $L = 100$ cm, $d = 50$ μ m. Composition of samples as described in Section 7.4.3, multiple sample injection as described in Section 7.3. Peak-intensities are normalized to equal peak-heights intensity.

Δt -values were determined for each pH-value ($n = 3$) and are plotted exemplarily for glutamic acid in Figure 50. For glutamic acid, the pI-values determined with this method can be derived from extrapolation and intercept with $\Delta t = 0$ line. For glutamic acid, a pI-value of 2.9 - 3.0, is determined, which is in good accordance with the literature value of 2.98, see Table 10. Identical data evaluation was conducted for each reference compound. The results for all reference compounds are summarized in Table 10. Respective figures are found in the supporting information (SI).

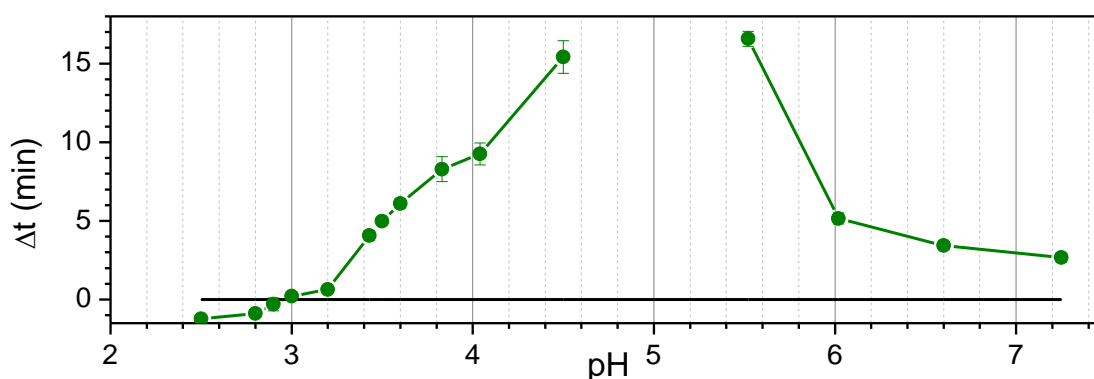


Figure 50: Δt -values determined for glutamic acid at various pH-values and a horizontal line for $\Delta t = 0$. Values below this line indicate cationic glutamic acid species, values above the black line indicate anionic glutamic acid. Crossing of the line can be observed between pH 2.9 and 3.0, the pI-value of glutamic acid is expected to be in this region, which is in good accordance with literature ($pI = 2.98$).

7.5.2. pI-determination of Lugdunin A

For Lugdunin A, 2 peaks of identical m/z were observed under almost all experimental conditions, as exemplarily indicated for pH 2.50 in Figure 51 A. From the peak shape, a fast transformation can be expected which is further accelerated at low pH, as observed previously (unpublished). Starting at pH 3.20, a peak at higher migration times than Peak 1 is observed in the injection zone depicted by the EOF-marker, as can be seen in Figure 55 in the SI. pI-values were determined for both peaks separately. In addition, an averaged Δt -value was calculated. For the averaged value, the signal of the more abundant Peak 1 was taken for pH 2.50-3.50. At higher pH values, an averaged value from Peak 1 and Peak 2 was taken into consideration due to vastly diminished peak intensity of Peak 1. Further EICs of other compounds can be found in the SI. For the thiazolidin-based reference substances T1 and T2, very low signal abundances were found. This made pI-determination for T2 troublesome, as can be seen by the respective pI-determination-plots in the SI. For T1, a pI-value above 5.5 is expected. Quenching effects made a determination at a pH close to the pI impossible as discussed in Section 7.5.1. Table 10 summarizes the results for Lugdunin A, amino acids and reference compounds.

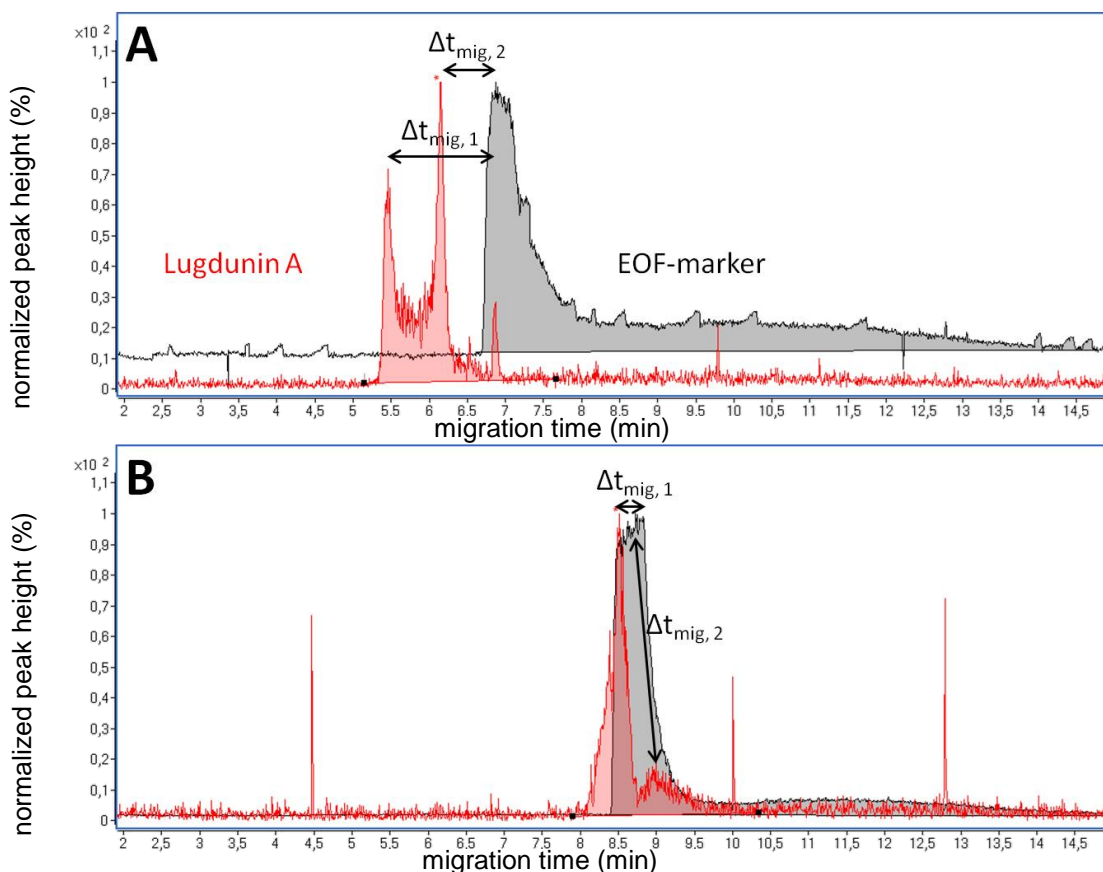


Figure 51: EICs of Lugdunin A (red) ($m/z = 783.4586 [M+H]^+$) and the EOF-marker DMSO ($m/z = 157.0349 [2M+NH_4]^+$) at A: pH 2.50 and B: pH 3.83. Lugdunin A was split into two signals, whose detection times were evaluated separately as Δt_1 and Δt_2 . Peak-intensities are normalized to equal heights.

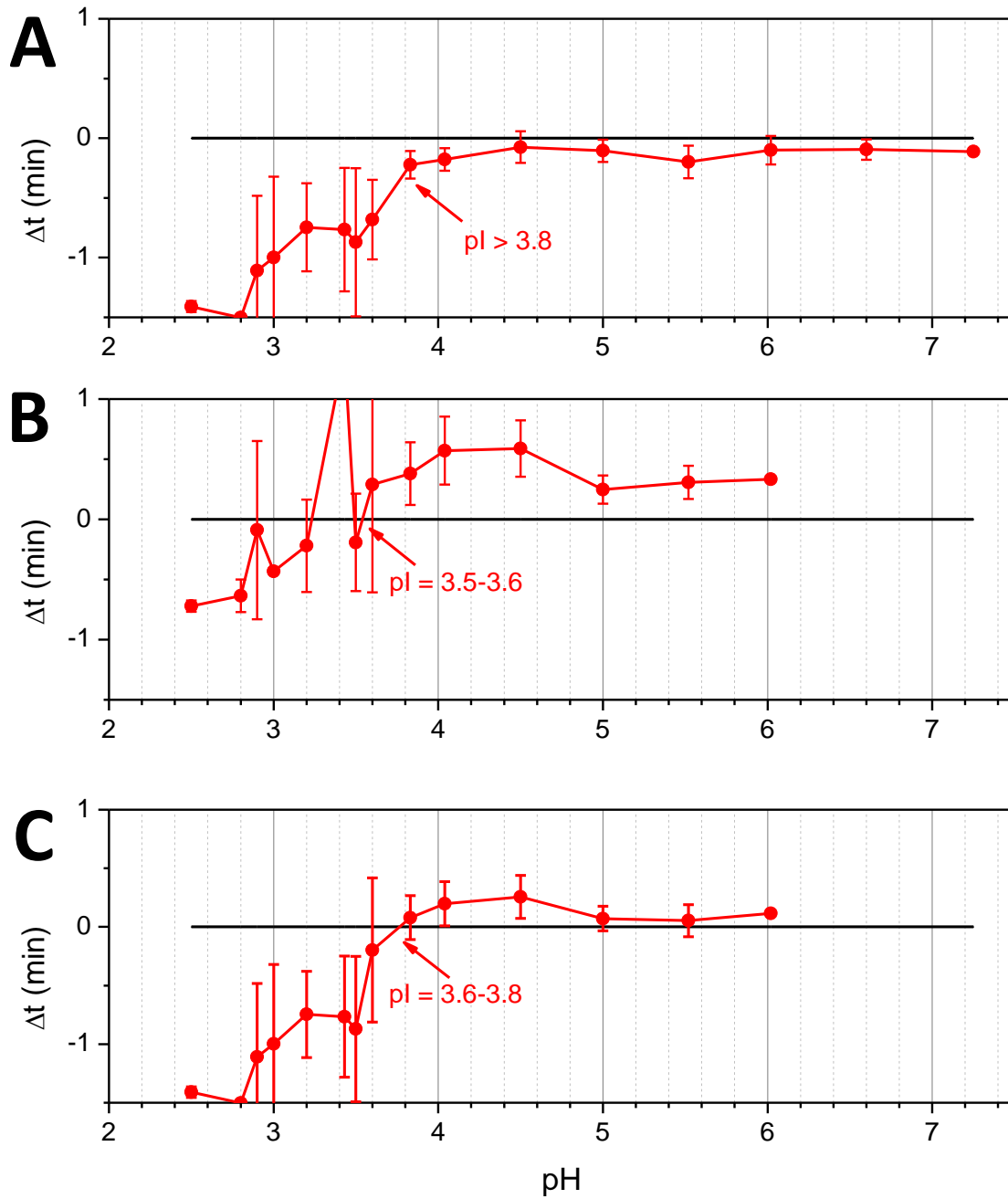


Figure 52: pI-value determination via plotting of Δt -values in dependence of the pH. By taking A: only the first peak, B: only the second peak, C: the average values of the first and the second peak into consideration. Comparable results, only differing by 0.2-0.3 pH-values were determined.

FAST CE-MS-BASED SCREENING METHOD FOR THE DETERMINATION OF pI-VALUES OF CYCLIC PEPTIDES OF VERY LOW SOLUBILITY IN WATER

Table 10: Summary of expected pI-values according to literature and determined pI-values.

Amino acid	pI expected	pI found	difference ΔpI	Ion trace extracted [M+H] ⁺
Glutamic acid	2.98	2.90-3.00	0	148.0612
Aspartic acid	3.08	2.80-2.90	0.18	134.0455
Glutamine	5.65	5.00-6.02	0	147.0771
Phenyl alanine	5.91	6.02	0.11	166.0870
Proline	6.30	<7.52	>2.22	116.0712
Thiazolidin references				
T1 ^b	6.17	≤6.02	unknown	148.0430
T2 ^c	unknown	5.00-6.02	unknown	176.0750
EOF-marker				
DMSO	-	-	-	157.0349 ^a
Lugdunin A				
Peak 1	unknown	<7.52		783.4586
Peak 2	unknown	3.50-3.60		783.4586
Average ^d	unknown	3.60-3.83		783.4586

^aThe EOF-marker DMSO is identified via its ammonium adduct [2DMSO+NH₄]⁺. ^b Thiazolidine-4-carboxylic acid methyl ester. ^c2-ethyl-thiazolidine-4-carboxylic acid methyl ester. ^dFor averaged value, the signal of the more abundant Peak 1 was taken for pH 2.50-3.50, above, an averaged value from Peak 1 and Peak 2 was taken into consideration.

7.6. Discussion

7.6.1. Suitability of the method for pI-value determination

The method presented here is apt to simultaneously measure the pI-value of multiple substance from various sample vials. pI-values for amino acids determined with CE-MS using sequential injection were comparable to literature, deviations of only 0.1-0.2 pH units were achieved. For proline, the investigated pH-range was too small to obtain reliable results. As indicated for glutamine (see SI), the Δt versus pH-curve of some compounds shows a broad plateau. This is interpreted as follows; the zwitterionic state of both glutamine and proline, is dominant over a broad pH-range, resulting in very low electrophoretic mobilities. I assume this property to derive from the high difference between the pKa-values of the two functional groups of proline (1.99 and 10.60, respectively). I expect to have proline better included when a broader pH range is investigated.

For reference substances T1 and T2, either low ionization efficiency or a necessity of further method optimization is indicated by their low signal intensities in CE-MS. Low synthesis yields cannot be neglected either, although no educt was detected by CE-MS. Especially when the compounds were estimated to comigrate with the EOF-marker no detection was possible, eventually due to additional quenching effects or formation of adducts. These effects were not observed for Lugdunin A itself.

7.6.2. Transformation of of Lugdunin A: Closed condensation- and open hydrolyzation-product of Lugdunin A

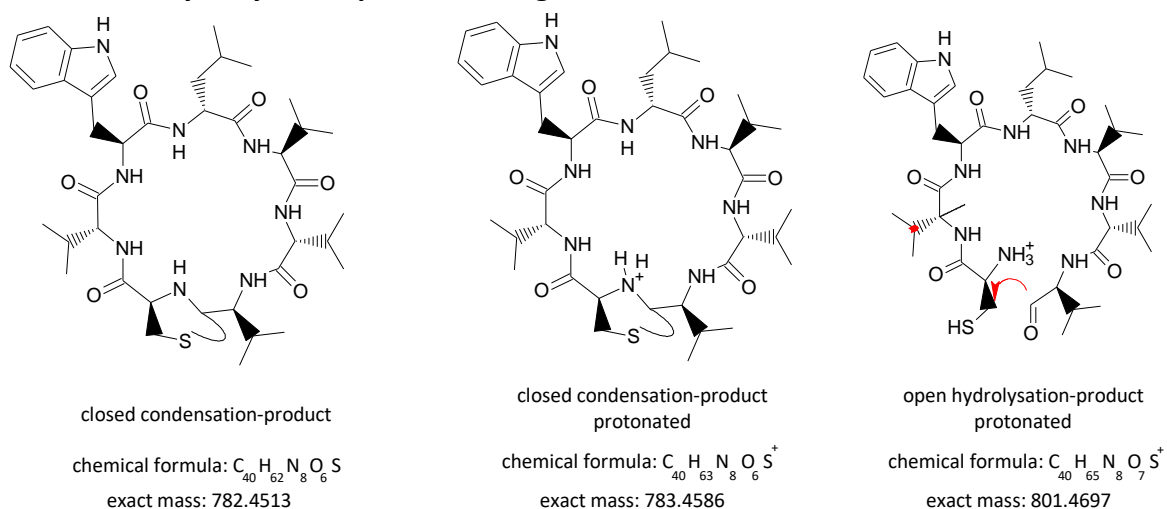


Figure 53: Illustration and chemical formula of Lugdunin A in its closed condensation-product, the respective protonated form of the closed condensation-product and the protonated open product from hydrolysis (from left to right). The respective chemical formulas as well as the exact masses are given.

In previous and LC-MS experiments (unpublished data), two forms of Lugdunin A were observed. I assume them to be the closed condensation-product and the open hydrolysis-product, see Figure 53. As shown in Figure 51 they were also detected via CE-MS. Figure 51 A shows two signals at pH 2.5 and at like m/z, connected via a plateau. It is worth noting, that in the MS-spectra signal intensities of the “dynamic & open”-form (m/z = 801.4697) were very low, see Figure 54 B. The open hydrolyzation-product comigrates with both the EOF-marker and the later-migrating peak of the closed condensation-product. The two signals at like m/z are presumably due to loss of water

during the ESI-process, a process well-known in ESI-MS for analyte-water-clusters^{251, 286} as well as water-clusters²⁸⁷. I suppose that the thiol- and amine- as well as the aldehyde-functions of the open hydrolysis-product of Lugdunin A are in close spatial proximity during the ESI process, resulting in a reaction within picoseconds, immediately after the loss of coordinated water. The observed differences in intensities of both products in Figure 54 B can thus be explained. This assumption is fostered when considering, that the primary amine-group of the open hydrolysis product exhibits a much lower pK_a -value than the thiazolidine-group of the closed condensation-product. Lower migration times are thus expected for the open hydrolysis-product as well. Therefore, the intensity ratios between the two peaks of the signal with $m/z = 783.4596$ can be taken into consideration for qualitative estimation of equilibria at various pH. A quantitative approach is difficult due to (i) co-migration with reference amino acids, (ii) different and unknown ionization efficiencies of the Lugdunin species, (iii) lack of reference compounds.

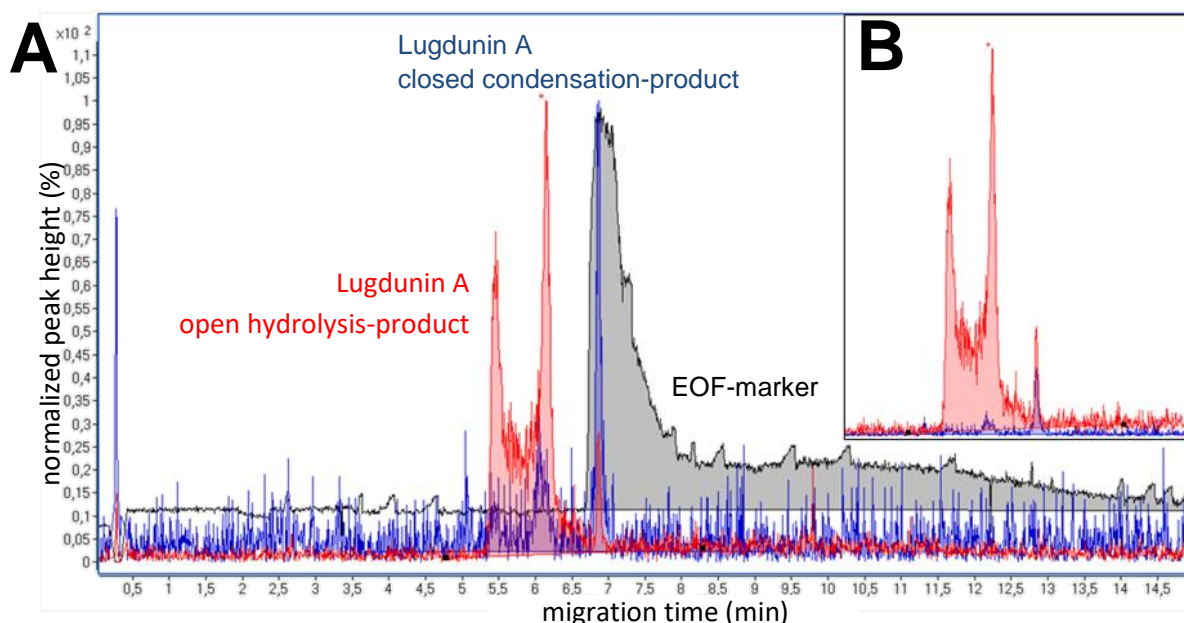


Figure 54: A: Electropherogram of a separation at pH 2.5, EICs of the EOF-marker DMSO ($m/z = 157.0349$, $[2M+NH_4]^+$, black) and for Lugdunin A as closed condensation-product ($m/z = 783.4586$, $[M+H]^+$, red) as well as open hydrolysis product ($m/z = 801.4697$, $[M+H]^+$, blue). Peak-intensities are normalized to equal heights. B: Close-up of the EICs of the two products of Lugdunin A without normalization

With increasing pH, the two peaks of the closed condensation-product begin to merge until a single peak is observed, see SI. This observation is similar to those of Schurig *et al.*^{288, 289} and others, fostering the assumption, that a dynamic equilibrium is between open hydrolysis- and closed condensation-product. In case of Lugdunin, the transformation seems acid-catalyzed. For a more detailed picture, a weighted average of signals for migration times or effective electrophoretic mobilities would have to be calculated as published by Schurig *et al.*, with the assumption that the time-scale of the observed phenomenon is much faster than the separation²⁸⁹. Similar NMR-experiments are often applied to judge dynamic equilibria^{290, 291}. Comparable investigations are yet known for capillary electrophoresis²⁸⁹.

For thiazolidine-derivates, pK_a -values of approx. 6.2 are expected, see Table 10. For primary amines, pK_a -values of approx. 3-4 are expected. Above pK_a , diminished to fading charge is expected for a monoprotic compound. The pI -value found for Lugdunin A was lower than expected for thiazolidin itself and is in the region of amines, yet is the open hydrolyzation-product the minor species

observed via MS. This observation leads to the suggestion that the weighted average between the two forms of Lugdunin A is strongly on the side of the amine and cyclization occurs during ESI process.

The method presented here offers the fast screening of compounds involved in a dynamic equilibrium such as Lugdunin A. Minor interactions between analytes and capillary surface as well as the absence of additives is promising. With regard to the small number of possible interferences and the use of reference compounds, the unexpected pI-value of 3.5-3.8 determined with CE-MS seems reliable

7.7. Supporting Information

7.7.1. Electropherograms of Lugdunin A

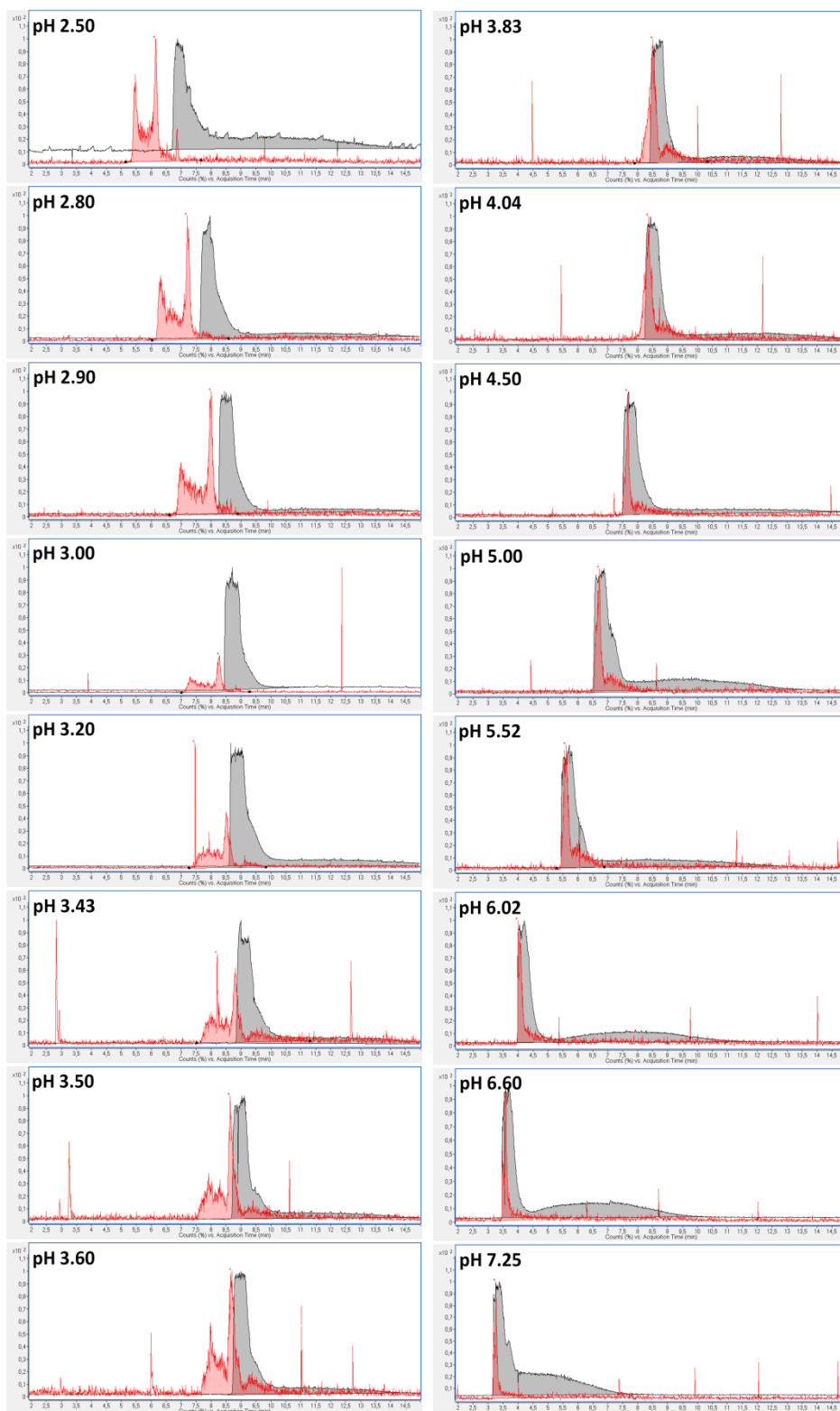
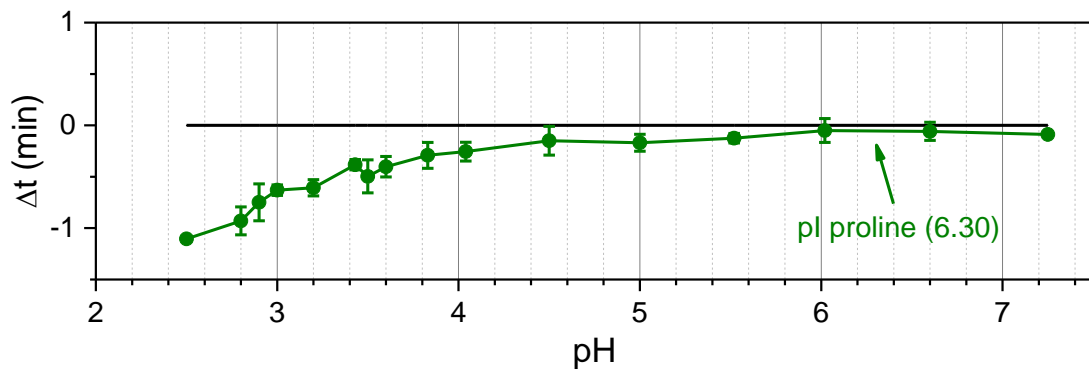
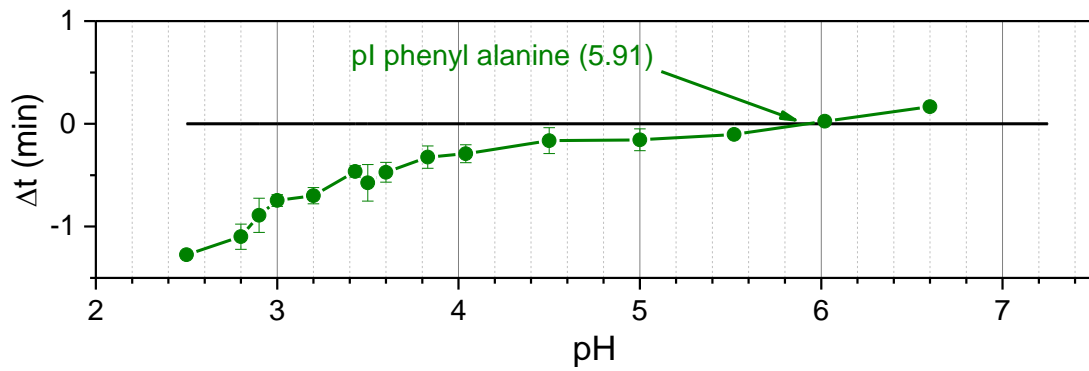
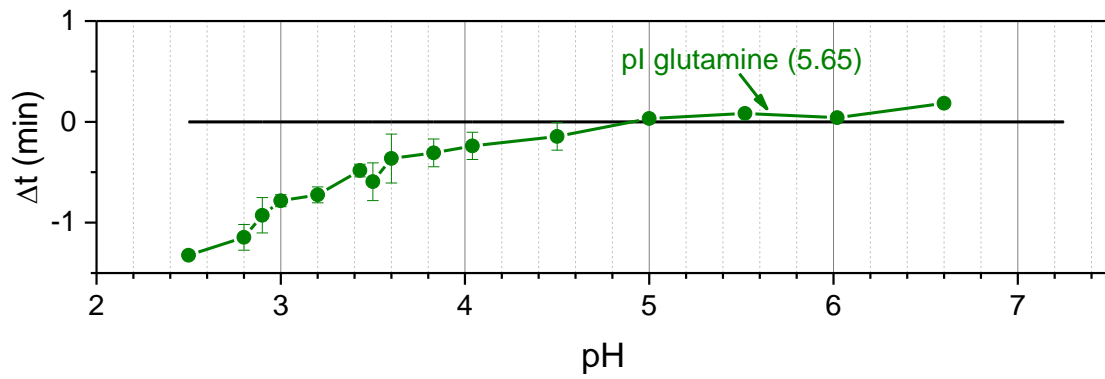
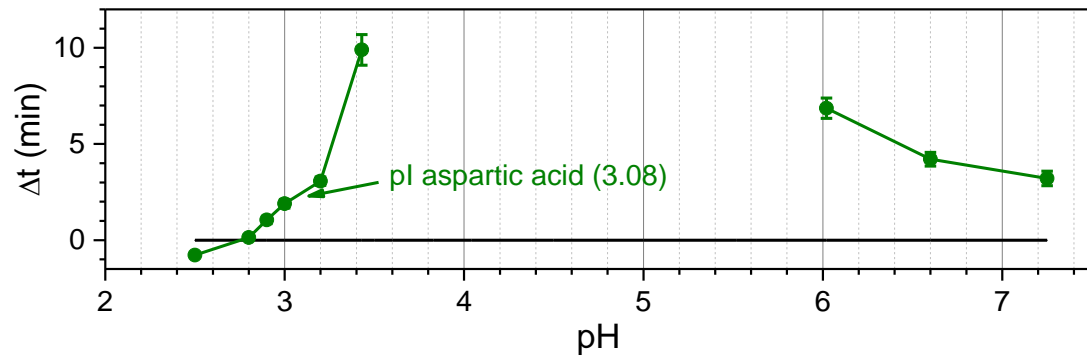


Figure 55: EICs of Lugdunin A (red) ($m/z = 783.4586 [M+H]^+$) and the EOF-marker DMSO ($m/z = 157.0349 [2M+NH_4]^+$) at all investigated pH-values. Electropherograms of representative measurements are presented. The change in peak-ratios of Lugdunin A can be observed with increasing pH. Peak-intensities are normalized to equal heights, the y-axis shows arbitrary values.

7.7.2. pI-determination for all investigated compounds



FAST CE-MS-BASED SCREENING METHOD FOR THE DETERMINATION OF pI-VALUES OF CYCLIC PEPTIDES OF VERY LOW SOLUBILITY IN WATER

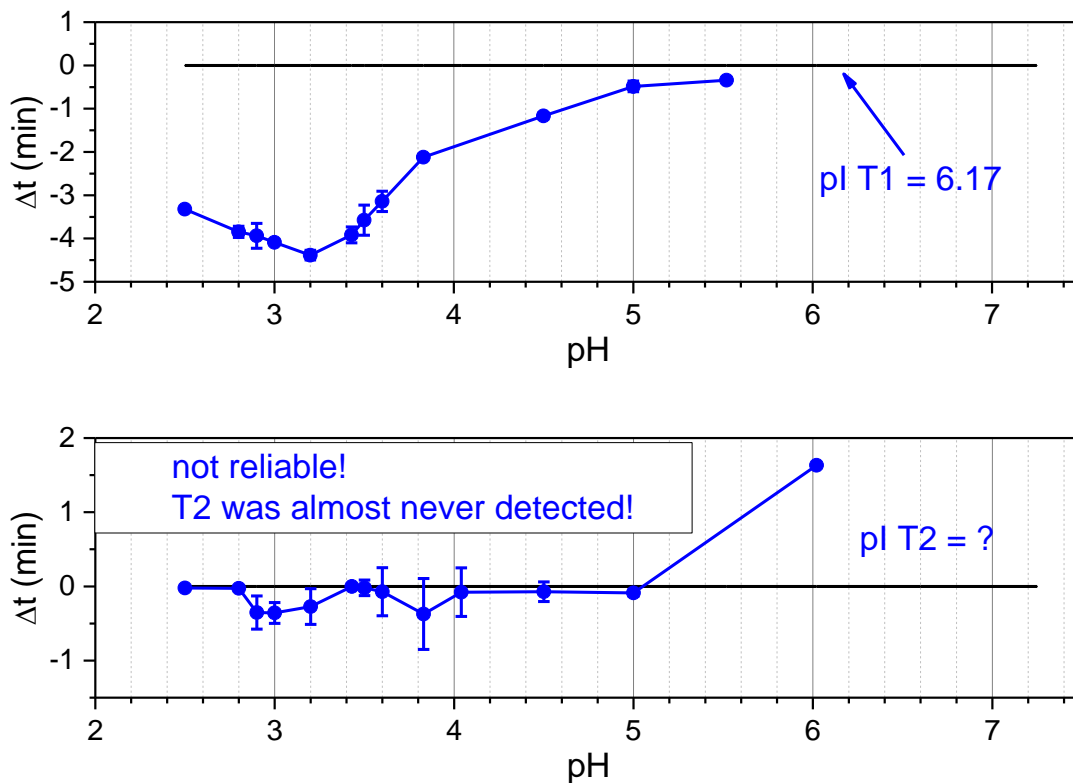


Figure 56: pI-value determination via plotting of Δt -values for all investigated amino acids and reference materials T1 and T2. The pI-values presented in the figures are the values expected according to literature.

8. Conclusion

This thesis tackled analytical challenges in proteomics regarding the separation and detection of intact proteins. Fast and reproducible capillary-based separations were aspired and successfully developed. Both techniques, cost efficient SDS-CE and high-resolution CE-MS, were optimized for a straight-forward and fast characterization of serum samples with high matrix tolerance. Especially, high compatibility with eluates from equilibration steps via hexapeptide ligand libraries was reached. Compared to SDS-CE, CE-MS revealed more detailed information on the analytes, but both techniques offered the aspired high matrix tolerance and were easily automated. A high matrix tolerance and reproducibility were achieved for both techniques.

The SDS-CE method with a new and optimized separation electrolyte proved to be easy to apply and by far cheaper than commercial kit systems. Compared to state of the art approaches, resolution was further enhanced by modifying the separation medium with the addition of 2-propanol. The underlying effects of this separation enhancement were discussed fundamentally by looking at the changes in the sieving mechanisms. The high analytical performance of the SDS-CE method was achieved by using PEO both as sieving polymer and dynamic coating, strongly reducing EOF and protein sorption to the capillary surface. In contrast, for CE-MS a covalently coupled coating made of polymerized and high protein-repelling *N*-acryloylamido ethoxyethanol was developed. This coating was remarkably stable as proved by its resistance towards flushing with organic solvent, strong base and acid. This was achieved by the successful transfer and enhancement of an approach called “direct linkage” that is, polymer linkage via stable Si-C bonds instead of hydrolytically less stable Si-O-Si-C-bonds. This synthesis procedure that was previously only known for silica particles. The development of a parallelized setup for the simultaneous preparation of up to 24 capillaries (combined length of 16 meters) coated with AAEE gave an easy access to capillaries for CE-MS-analysis. Using these capillaries, analysis of protein samples equilibrated using HLLs was possible with measuring times of 100 h of constant use and only minor interaction of both proteins and peptides, but also small polyamines, with the capillary surface. Outstanding stability, separation performance, high matrix tolerance, proven by the injection of diluted human serum, and the possibility of quantification via external calibration were demonstrated. The major drawback of the coating synthesis, the inhomogeneity of untreated bare fused silica capillaries was addressed using pre-etching with supercritical water. Scanning electron microscopy revealed that the reaction times can significantly be reduced, but also that the proposed reaction mechanism is not yet fully understood as layers formed after rinsing with LiAlH_4 . I presume that aluminum oxide species form, which may significantly contribute to the high performance of the final coating.

The results show that CE-MS is significantly better suited for the analysis of complex samples, since the higher resolving power and additional mass information give rise to a deeper insight into the sample. In addition, direct quantification is easily achieved. However, for human serum samples, a lower sensitivity for CE-MS was observed compared to 2D-PAGE. In future projects, this challenge may be addressed twofold: optimization of CE-MS separation conditions to avoid co-migration of proteins as well as development of 2D-CE-MS methods, e.g. by IEF/CE-MS, by ITP/CE-MS or even by SDS-CE/CE-MS. Therein, ITP-CE-MS is most promising regarding the enrichment of low abundant proteins which results in a larger numbers of proteins with a concentration above the LOD.

CONCLUSION

The presented CE-MS and SDS-CE-techniques were successfully applied for the characterization of protein samples equilibrated with HLLs. SDS-CE was used as a fast screening tool. It was shown that the optimized procedure is excellent for impurity profiling of technical protein products, especially after preliminary HLL-equilibration of the sample.

Two-fold equilibration via HLLs was successful and the aspired benefit of small starting volumes for the sample was achieved for standard proteins: Comparing my results with those of Guerrier *et al.*⁹ it is clear, that equilibration by a factor higher than 1000 is possible using approx. 50-fold smaller sample amounts (approx. 1 mL serum instead of 50 mL). This benefit promises, that this sample preparation technique will be investigated towards its applicability in the scope of biomarker search but also pharmaceutical analysis in future. Further investigations regarding both concentration ranges of proteins and types of proteins are necessary as irreversible binding sites at HLLs^{257, 258}, potential co-depletion of low abundant proteins with albumin²⁵² and loss of proteins via precipitation or adsorption during regeneration of samples is possible²⁴⁰⁻²⁴² are the remaining challenges to be addressed.

Overall, this thesis proof that specialized sample preparation techniques combined with electromigrative separation techniques allow an excellent interplay with high matrix tolerance and thus reduced sample preparation efforts, high separation selectivity, efficiency and robustness due to the new coatings developed and the possibility for both fast screening and in-depth analysis with only minor changes of the experimental setup.

9. Literature

1. Righetti, P. G.; Castagna, A.; Antonioli, P.; Boschetti, E., Prefractionation techniques in proteome analysis: The mining tools of the third millennium. *Electrophoresis* **2005**, *26*, (2), 297-319.
2. Dai, Z.; Zhou, J.; Qiu, S.; Liu, Y.; Fan, J., Lectin-based glycoproteomics to explore and analyze hepatocellular carcinoma-related glycoprotein markers. *Electrophoresis* **2009**, *30*, (17), 2957-2966.
3. He, Q. Y.; Chiu, J. F., Proteomics in biomarker discovery and drug development. *Journal of Cellular Biochemistry* **2003**, *89*, (5), 868-886.
4. Zamanian-Azodi, M.; Rezaei-Tavirani, M.; Mortazavian, A.; Vafaei, R.; Rezaei-Tavirani, M.; Zali, H.; Soheili-Kashani, M., Application of proteomics in cancer study. *American Journal of Cancer Science* **2013**, *2*, (2), 116-134.
5. Anderson, D.; Kodukula, K., Biomarkers in pharmacology and drug discovery. *Biochemical Pharmacology* **2014**, *87*, (1), 172-188.
6. Amiri-Dashatan, N.; Koushki, M.; Abbaszadeh, H.-A.; Rostami-Nejad, M.; Rezaei-Tavirani, M., Proteomics applications in health: biomarker and drug discovery and food industry. *Iranian Journal of Pharmaceutical Research* **2018**, *17*, (4), 1523.
7. Boschetti, E.; Righetti, P. G., The ProteoMiner in the proteomic arena: a non-depleting tool for discovering low-abundance species. *Journal of Proteomics* **2008**, *71*, (3), 255-264.
8. Guerrier, L.; Thulasiraman, V.; Castagna, A.; Fortis, F.; Lin, S.; Lomas, L.; Righetti, P. G.; Boschetti, E., Reducing protein concentration range of biological samples using solid-phase ligand libraries. *Journal of Chromatography B* **2006**, *833*, (1), 33-40.
9. Fortis, F.; Guerrier, L.; Areces, L. B.; Antonioli, P.; Hayes, T.; Carrick, K.; Hammond, D.; Boschetti, E.; Righetti, P. G., A new approach for the detection and identification of protein impurities using combinatorial solid phase ligand libraries. *Journal of Proteome Research* **2006**, *5*, (10), 2577-2585.
10. Guerrier, L.; Righetti, P. G.; Boschetti, E., Reduction of dynamic protein concentration range of biological extracts for the discovery of low-abundance proteins by means of hexapeptide ligand library. *Nature Protocols* **2008**, *3*, (5), 883.
11. Kim, E. H.; Misek, D. E., Glycoproteomics-based identification of cancer biomarkers. *International Journal of Proteomics* **2011**, *2011*.
12. Henderson, M. C.; Silver, M.; Borman, S.; Tran, Q.; Letsios, E.; Mulpuri, R.; Reese, D. E.; Wolf, J. K., A combinatorial proteomic biomarker assay to detect ovarian cancer in women. *Biomarkers in Cancer* **2018**, *10*, 1-16.
13. Righetti, P. G.; Boschetti, E., The ProteoMiner and the FortyNiners: searching for gold nuggets in the proteomic arena. *Mass Spectrometry Reviews* **2008**, *27*, (6), 596-608.
14. Clement, C. C.; Aphkhasava, D.; Nieves, E.; Callaway, M.; Olszewski, W.; Rotzschke, O.; Santambrogio, L., Protein expression profiles of human lymph and plasma mapped by 2D-DIGE and 1D SDS-PAGE coupled with nanoLC-ESI-MS/MS bottom-up proteomics. *Journal of Proteomics* **2013**, *78*, (Supplement C), 172-187.
15. Gornik, O.; Wagner, J.; Pučić, M.; Knežević, A.; Redžić, I.; Lauc, G., Stability of N-glycan profiles in human plasma. *Glycobiology* **2009**, *19*, (12), 1547-1553.
16. Knezevic, A.; Polasek, O.; Gornik, O.; Rudan, I.; Campbell, H.; Hayward, C.; Wright, A.; Kolcic, I.; O'Donoghue, N.; Bones, J., Variability, heritability and environmental determinants of human plasma N-glycome. *Journal of Proteome Research* **2008**, *8*, (2), 694-701.

17. Knežević, A.; Gornik, O.; Polašek, O.; Pučić, M.; Redžić, I.; Novokmet, M.; Rudd, P. M.; Wright, A. F.; Campbell, H.; Rudan, I., Effects of aging, body mass index, plasma lipid profiles, and smoking on human plasma N-glycans. *Glycobiology* **2010**, *20*, (8), 959-969.
18. Fang, X.; Zhang, W.-W., Affinity separation and enrichment methods in proteomic analysis. *Journal of Proteomics* **2008**, *71*, (3), 284-303.
19. Pisanu, S.; Biosa, G.; Carcangiu, L.; Uzzau, S.; Pagnozzi, D., Comparative evaluation of seven commercial products for human serum enrichment/depletion by shotgun proteomics. *Talanta* **2018**, *185*, 213-220.
20. Köhler, G.; Milstein, C., Continuous cultures of fused cells secreting antibody of predefined specificity. *Nature* **1975**, *256*, (5517), 495-497.
21. Morrison, S. L.; Johnson, M. J.; Herzenberg, L. A.; Oi, V. T., Chimeric human antibody molecules: mouse antigen-binding domains with human constant region domains. *Proceedings of the National Academy of Sciences* **1984**, *81*, (21), 6851-6855.
22. Jones, P. T.; Dear, P. H.; Foote, J.; Neuberger, M. S.; Winter, G., Replacing the complementarity-determining regions in a human antibody with those from a mouse. *Nature* **1986**, *321*, (6069), 522-525.
23. Beck, A.; Wurch, T.; Bailly, C.; Corvaia, N., Strategies and challenges for the next generation of therapeutic antibodies. *Nature Reviews Immunology* **2010**, *10*, (5), 345.
24. Craik, D. J.; Fairlie, D. P.; Liras, S.; Price, D., The future of peptide - based drugs. *Chemical Biology & Drug Design* **2013**, *81*, (1), 136-147.
25. Mitragotri, S.; Burke, P. A.; Langer, R., Overcoming the challenges in administering biopharmaceuticals: formulation and delivery strategies. *Nature Reviews Drug Discovery* **2014**, *13*, (9), 655.
26. Huhn, C.; Selman, M. H.; Ruhaak, L. R.; Deelder, A. M.; Wuhrer, M., IgG glycosylation analysis. *Proteomics* **2009**, *9*, (4), 882-913.
27. Chelius, D.; Rehder, D. S.; Bondarenko, P. V., Identification and characterization of deamidation sites in the conserved regions of human immunoglobulin gamma antibodies. *Analytical Chemistry* **2005**, *77*, (18), 6004-6011.
28. Manning, M. C.; Patel, K.; Borchardt, R. T., Stability of protein pharmaceuticals. *Pharmaceutical Research* **1989**, *6*, (11), 903-918.
29. Harris, R. J.; Kabakoff, B.; Macchi, F. D.; Shen, F. J.; Kwong, M.; Andya, J. D.; Shire, S. J.; Bjork, N.; Totpal, K.; Chen, A. B., Identification of multiple sources of charge heterogeneity in a recombinant antibody. *Journal of Chromatography B: Biomedical Sciences and Applications* **2001**, *752*, (2), 233-245.
30. Ishii, Y.; Tsukahara, M.; Wakamatsu, K., A rapid method for simultaneous evaluation of free light chain content and aggregate content in culture media of Chinese hamster ovary cells expressing monoclonal antibodies for cell line screening. *Journal of Bioscience and Bioengineering* **2016**, *121*, (4), 464-470.
31. Dubois, M.; Fenaille, F.; Clement, G.; Lechmann, M.; Tabet, J.-C.; Ezan, E.; Becher, F., Immunopurification and Mass Spectrometric Quantification of the Active Form of a Chimeric Therapeutic Antibody in Human Serum. *Analytical Chemistry* **2008**, *80*, (5), 1737-1745.

32. Yang, Z.; Hancock, W. S., Approach to the comprehensive analysis of glycoproteins isolated from human serum using a multi-lectin affinity column. *Journal of Chromatography A* **2004**, *1053*, (1-2), 79-88.
33. Kaji, H.; Yamauchi, Y.; Takahashi, N.; Isobe, T., Mass spectrometric identification of N-linked glycopeptides using lectin-mediated affinity capture and glycosylation site-specific stable isotope tagging. *Nature Protocols* **2006**, *1*, (6), 3019.
34. Caragata, M.; Shah, A. K.; Schulz, B. L.; Hill, M. M.; Punyadeera, C., Enrichment and identification of glycoproteins in human saliva using lectin magnetic bead arrays. *Analytical Biochemistry* **2016**, *497*, (Supplement C), 76-82.
35. Zhu, Z. C.; Chen, Y.; Ackerman, M. S.; Wang, B.; Wu, W.; Li, B.; Obenauer-Kutner, L.; Zhao, R.; Tao, L.; Ihnat, P. M., Investigation of monoclonal antibody fragmentation artifacts in non-reducing SDS-PAGE. *Journal of Pharmaceutical and Biomedical Analysis* **2013**, *83*, 89-95.
36. Weber, K.; Osborn, M., The reliability of molecular weight determinations by dodecyl sulfate-polyacrylamide gel electrophoresis. *Journal of Biological Chemistry* **1969**, *244*, (16), 4406-4412.
37. Towbin, H.; Staehelin, T.; Gordon, J., Electrophoretic transfer of proteins from polyacrylamide gels to nitrocellulose sheets: procedure and some applications. *Proceedings of the National Academy of Sciences* **1979**, *76*, (9), 4350-4354.
38. Burnette, W. N., "Western blotting": electrophoretic transfer of proteins from sodium dodecyl sulfate-polyacrylamide gels to unmodified nitrocellulose and radiographic detection with antibody and radioiodinated protein A. *Analytical Biochemistry* **1981**, *112*, (2), 195-203.
39. Fernandez, J.; Gharahdaghi, F.; Mische, S. M., Routine identification of proteins from sodium dodecyl sulfate - polyacrylamide gel electrophoresis (SDS - PAGE) gels or polyvinyl difluoride membranes using matrix assisted laser desorption/ionization - time of flight - mass spectrometry (MALDI - TOF - MS). *Electrophoresis* **1998**, *19*, (6), 1036-1045.
40. Patterson, S. D., Matrix-assisted laser-desorption/ionization mass spectrometric approaches for the identification of gel-separated proteins in the 5-50 pmol range. *Electrophoresis* **1995**, *16*, 1104-1114.
41. O'Farrell, P. H., High resolution two-dimensional electrophoresis of proteins. *Journal of Biological Chemistry* **1975**, *250*, (10), 4007-4021.
42. Klose, J., Protein mapping by combined isoelectric focusing and electrophoresis of mouse tissues. *Human Genetics* **1975**, *26*, (3), 231-243.
43. Sennels, L.; Salek, M.; Lomas, L.; Boschetti, E.; Righetti, P. G.; Rappsilber, J., Proteomic analysis of human blood serum using peptide library beads. *Journal of Proteome Research* **2007**, *6*, (10), 4055-4062.
44. Léger, T.; Lavigne, D.; Le Caër, J.-P.; Guerrier, L.; Boschetti, E.; Fareh, J.; Feldman, L.; Laprévotte, O.; Meilhac, O., Solid-phase hexapeptide ligand libraries open up new perspectives in the discovery of biomarkers in human plasma. *Clinica Chimica Acta* **2011**, *412*, (9), 740-747.
45. Zhang, J.; Burman, S.; Gunturi, S.; Foley, J. P., Method development and validation of capillary sodium dodecyl sulfate gel electrophoresis for the characterization of a monoclonal antibody. *Journal of Pharmaceutical and Biomedical Analysis* **2010**, *53*, (5), 1236-1243.
46. Rustandi, R. R.; Washabaugh, M. W.; Wang, Y., Applications of CE SDS gel in development of biopharmaceutical antibody - based products. *Electrophoresis* **2008**, *29*, (17), 3612-3620.

47. Shi, Y.; Li, Z.; Lin, J., Advantages of CE-SDS over SDS-PAGE in mAb purity analysis. *Analytical Methods* **2012**, *4*, (6), 1637-1642.
48. Han, M.; Phan, D.; Nightlinger, N.; Taylor, L.; Jankhah, S.; Woodruff, B.; Yates, Z.; Freeman, S.; Guo, A.; Balland, A., Optimization of CE-SDS method for antibody separation based on multi-users experimental practices. *Chromatographia* **2006**, *64*, (5), 1-8.
49. Le, M. E.; Vizel, A.; Hutterer, K. M., Automated sample preparation for CE - SDS. *Electrophoresis* **2013**, *34*, (9-10), 1369-1374.
50. Grundmann, M.; Matysik, F.-M., Analyzing small samples with high efficiency: Capillary batch injection–capillary electrophoresis–mass spectrometry. *Analytical and Bioanalytical Chemistry* **2012**, *404*, (6-7), 1713-1721.
51. Kaneta, T.; Yamamoto, D.; Imasaka, T., Postcolumn derivatization of proteins in capillary sieving electrophoresis/laser - induced fluorescence detection. *Electrophoresis* **2009**, *30*, (21), 3780-3785.
52. Sánchez - Hernández, L.; Montealegre, C.; Kiessig, S.; Moritz, B.; Neusüß, C., In - capillary approach to eliminate SDS interferences in antibody analysis by capillary electrophoresis coupled to mass spectrometry. *Electrophoresis* **2017**, *38*, (7), 1044-1052.
53. Luo, S.; Feng, J.; Pang, H.-m., High-throughput protein analysis by multiplexed sodium dodecyl sulfate capillary gel electrophoresis with UV absorption detection. *Journal of Chromatography A* **2004**, *1051*, (1), 131-134.
54. Carchon, H. A.; Chevigné, R.; Falmagne, J.-B.; Jaeken, J., Diagnosis of congenital disorders of glycosylation by capillary zone electrophoresis of serum transferrin. *Clinical Chemistry* **2004**, *50*, (1), 101-111.
55. Tsuji, K.; Little, R. J., Charge-reversed, polymer-coated capillary column for the analysis of a recombinant chimeric glycoprotein. *Journal of Chromatography A* **1992**, *594*, (1-2), 317-324.
56. Mahan, A. E.; Tedesco, J.; Dionne, K.; Baruah, K.; Cheng, H. D.; De Jager, P. L.; Barouch, D. H.; Suscovich, T.; Ackerman, M.; Crispin, M., A method for high-throughput, sensitive analysis of IgG Fc and Fab glycosylation by capillary electrophoresis. *Journal of Immunological Methods* **2015**, *417*, 34-44.
57. Gennaro, L. A.; Salas-Solano, O., On-line CE– LIF– MS technology for the direct characterization of N-linked glycans from therapeutic antibodies. *Analytical Chemistry* **2008**, *80*, (10), 3838-3845.
58. Mischak, H.; Vlahou, A.; Ioannidis, J. P., Technical aspects and inter-laboratory variability in native peptide profiling: the CE–MS experience. *Clinical Biochemistry* **2013**, *46*, (6), 432-443.
59. Herrero, M.; Ibañez, E.; Cifuentes, A., Capillary electrophoresis - electrospray - mass spectrometry in peptide analysis and peptidomics. *Electrophoresis* **2008**, *29*, (10), 2148-2160.
60. Neusüß, C.; Pelzing, M.; Macht, M., A robust approach for the analysis of peptides in the low femtomole range by capillary electrophoresis - tandem mass spectrometry. *Electrophoresis* **2002**, *23*, (18), 3149-3159.
61. Amon, S.; Zamfir, A. D.; Rizzi, A., Glycosylation analysis of glycoproteins and proteoglycans using capillary electrophoresis - mass spectrometry strategies. *Electrophoresis* **2008**, *29*, (12), 2485-2507.

62. Huhn, C.; Ruhaak, L. R.; Mannhardt, J.; Wuhrer, M.; Neusüß, C.; Deelder, A. M.; Meyer, H., Alignment of laser - induced fluorescence and mass spectrometric detection traces using electrophoretic mobility scaling in CE - LIF - MS of labeled N - glycans. *Electrophoresis* **2012**, *33*, (4), 563-566.
63. Liu, J.; Cai, Y.; Wang, J.; Zhou, Q.; Yang, B.; Lu, Z.; Jiao, L.; Zhang, D.; Sui, S.; Jiang, Y., Phosphoproteome profile of human liver Chang's cell based on 2 - DE with fluorescence staining and MALDI - TOF/TOF - MS. *Electrophoresis* **2007**, *28*, (23), 4348-4358.
64. Simò-Alfonso, E.; Conti, M.; Gelfi, C.; Righetti, P. G., Sodium dodecyl sulfate capillary electrophoresis of proteins in entangled solutions of poly (vinyl alcohol). *Journal of Chromatography A* **1995**, *689*, (1), 85-96.
65. Lausch, R.; Scheper, T.; Reif, O.-W.; Schlösser, J.; Fleischer, J.; Freitag, R., Rapid capillary gel electrophoresis of proteins. *Journal of Chromatography A* **1993**, *654*, (1), 190-195.
66. Nakatani, M.; Shibukawa, A.; Nakagawa, T., Separation mechanism of pullulan solution - filled capillary electrophoresis of sodium dodecyl sulfateproteins. *Electrophoresis* **1996**, *17*, (10), 1584-1586.
67. Nakatani, M.; Shibukawa, A.; Nakagawa, T., High-performance capillary electrophoresis of SDS-proteins using pullulan solution as separation matrix. *Journal of Chromatography A* **1994**, *672*, (1-2), 213-218.
68. Zhang, J.; Tran, N. T.; Weber, J.; Slim, C.; Viovy, J. L.; Taverna, M., Poly (N, N - dimethylacrylamide) - grafted polyacrylamide: A self - coating copolymer for sieving separation of native proteins by CE. *Electrophoresis* **2006**, *27*, (15), 3086-3092.
69. Hu, S.; Zhang, Z.; Cook, L. M.; Carpenter, E. J.; Dovichi, N. J., Separation of proteins by sodium dodecylsulfate capillary electrophoresis in hydroxypropylcellulose sieving matrix with laser-induced fluorescence detection. *Journal of Chromatography A* **2000**, *894*, (1), 291-296.
70. Chung, M.; Kim, D.; Herr, A. E., Polymer sieving matrices in microanalytical electrophoresis. *Analyst* **2014**, *139*, (22), 5635-5654.
71. Gomis, D. B.; Junco, S.; Expósito, Y.; Gutiérrez, D., Size - based separations of proteins by capillary electrophoresis using linear polyacrylamide as a sieving medium: Model studies and analysis of cider proteins. *Electrophoresis* **2003**, *24*, (9), 1391-1396.
72. Corradini, D., Buffer additives other than the surfactant sodium dodecyl sulfate for protein separations by capillary electrophoresis. *Journal of Chromatography B: Biomedical Sciences and Applications* **1997**, *699*, (1), 221-256.
73. van Tricht, E.; Geurink, L.; Pajic, B.; Nijenhuis, J.; Backus, H.; Germano, M.; Somsen, G. W.; Sängers-van de Griend, C. E., New capillary gel electrophoresis method for fast and accurate identification and quantification of multiple viral proteins in influenza vaccines. *Talanta* **2015**, *144*, 1030-1035.
74. Bietz, J. A.; Simpson, D. G., Electrophoresis and chromatography of wheat proteins: available methods, and procedures for statistical evaluation of the data. *Journal of Chromatography A* **1992**, *624*, (1-2), 53-80.

75. Werner, W. E.; Wiktorowicz, J. E.; Kasarda, D. D., Wheat varietal identification by capillary electrophoresis of gliadins and high molecular weight glutenin subunits. *Cereal Chemistry (USA)* **1994**, *71*, (5), 397-402.
76. Hjertén, S., High-performance electrophoresis: elimination of electroendosmosis and solute adsorption. *Journal of Chromatography A* **1985**, *347*, 191-198.
77. Dolnik, V.; Gurske, W. A., Capillary sieving electrophoresis with a cationic surfactant for size separation of proteins. In Google Patents US 2012/0111727 A1.
78. Van Hove, E.; Szücs, R.; Sandra, P., Alcohol modifiers in MEKC with SDS as surfactant. Study on the influence of the alcohol chain length (C1 - C12). *Journal of High Resolution Chromatography* **1996**, *19*, (12), 674-678.
79. Yu, T.; Peng, H., Quantification and deconvolution of asymmetric LC-MS peaks using the bi-Gaussian mixture model and statistical model selection. *BMC Bioinformatics* **2010**, *11*, (1), 559.
80. Buchacher, A.; Schulz, P.; Choromanski, J.; Schwinn, H.; Josic, D., High-performance capillary electrophoresis for in-process control in the production of antithrombin III and human clotting factor IX. *Journal of Chromatography A* **1998**, *802*, (2), 355-366.
81. Leo, A.; Hansch, C.; Elkins, D., Partition coefficients and their uses. *Chemical Reviews* **1971**, *71*, (6), 525-616.
82. Parodi, A. J.; Leloir, L. F., The role of lipid intermediates in the glycosylation of proteins in the eucaryotic cell. *Biochimica et Biophysica Acta (BBA)-Reviews on Biomembranes* **1979**, *559*, (1), 1-37.
83. Benedek, K.; Guttman, A., Ultra-fast high-performance capillary sodium dodecyl sulfate gel electrophoresis of proteins. *Journal of Chromatography A* **1994**, *680*, (2), 375-381.
84. Nakatani, M.; Shibukawa, A.; Nakagawa, T., Effect of temperature and viscosity of sieving medium on electrophoretic behavior of sodium dodecyl sulfate - proteins on capillary electrophoresis in presence of pullulan. *Electrophoresis* **1996**, *17*, (7), 1210-1213.
85. Lin, C. H.; Kaneta, T., On - line sample concentration techniques in capillary electrophoresis: Velocity gradient techniques and sample concentration techniques for biomolecules. *Electrophoresis* **2004**, *25*, (23 - 24), 4058-4073.
86. Law, W. S.; Zhao, J. H.; Li, S. F., On - line sample enrichment for the determination of proteins by capillary zone electrophoresis with poly (vinyl alcohol) - coated bubble cell capillaries. *Electrophoresis* **2005**, *26*, (18), 3486-3494.
87. Sumitomo, K.; Mayumi, K.; Yokoyama, H.; Sakai, Y.; Minamikawa, H.; Masuda, M.; Shimizu, T.; Ito, K.; Yamaguchi, Y., Dynamic light - scattering measurement of sieving polymer solutions for protein separation on SDS CE. *Electrophoresis* **2009**, *30*, (20), 3607-3612.
88. Monton, M. R. N.; Terabe, S., Sample enrichment techniques in capillary electrophoresis: Focus on peptides and proteins. *Journal of Chromatography B* **2006**, *841*, (1-2), 88-95.
89. Mala, Z.; Křivánková, L.; Gebauer, P.; Boček, P., Contemporary sample stacking in CE: a sophisticated tool based on simple principles. *Electrophoresis* **2007**, *28*, (1 - 2), 243-253.
90. Gebauer, P.; Boček, P., System peaks in capillary zone electrophoresis: I. Simple model of vacancy electrophoresis1. *Journal of Chromatography A* **1997**, *772*, (1-2), 73-79.

91. Quinones, I.; Ford, J. C.; Guiochon, G., High-concentration band profiles and system peaks for a ternary solute system. *Analytical Chemistry* **2000**, *72*, (7), 1495-1502.
92. Mack, S.; Cruzado - Park, I.; Chapman, J.; Ratnayake, C.; Vigh, G., A systematic study in CIEF: defining and optimizing experimental parameters critical to method reproducibility and robustness. *Electrophoresis* **2009**, *30*, (23), 4049-4058.
93. Zhu, J.; Khan, K., Separation and quantification of HMW glutenin subunits by capillary electrophoresis. *Cereal chemistry* **2001**, *78*, (6), 737-742.
94. Miralles, B.; Bartolomé, B.; Amigo, L.; Ramos, M., Comparison of Three Methods to Determine the Whey Protein to Total Protein Ratio in Milk1. *Journal of dairy science* **2000**, *83*, (12), 2759-2765.
95. Zukoski IV, C.; Saville, D., The interpretation of electrokinetic measurements using a dynamic model of the stern layer: I. The dynamic model. *Journal of Colloid and Interface Science* **1986**, *114*, (1), 32-44.
96. Zukoski IV, C.; Saville, D., The interpretation of electrokinetic measurements using a dynamic model of the stern layer: II. Comparisons between theory and experiment. *Journal of Colloid and Interface Science* **1986**, *114*, (1), 45-53.
97. Mangelsdorf, C. S.; White, L. R., Effects of stern-layer conductance on electrokinetic transport properties of colloidal particles. *Journal of the Chemical Society, Faraday Transactions* **1990**, *86*, (16), 2859-2870.
98. Kohl, F. J.; Montealegre, C.; Neusüß, C., On - line two - dimensional capillary electrophoresis with mass spectrometric detection using a fully electric isolated mechanical valve. *Electrophoresis* **2016**, *37*, (7-8), 954-958.
99. Kohl, F. J.; Sánchez - Hernández, L.; Neusüß, C., Capillary electrophoresis in two - dimensional separation systems: Techniques and applications. *Electrophoresis* **2015**, *36*, (1), 144-158.
100. Viovy, J. L.; Duke, T., DNA electrophoresis in polymer solutions: Ogston sieving, reptation and constraint release. *Electrophoresis* **1993**, *14*, (1), 322-329.
101. Leger, L.; Hervet, H.; Rondelez, F., Reptation in entangled polymer solutions by forced Rayleigh light scattering. *Macromolecules* **1981**, *14*, (6), 1732-1738.
102. Grossman, P. D.; Soane, D. S., Experimental and theoretical studies of DNA separations by capillary electrophoresis in entangled polymer solutions. *Biopolymers* **1991**, *31*, (10), 1221-1228.
103. Cottet, H.; Gareil, P.; Viovy, J. L., The effect of blob size and network dynamics on the size - based separation of polystyrenesulfonates by capillary electrophoresis in the presence of entangled polymer solutions. *Electrophoresis* **1998**, *19*, (12), 2151-2162.
104. Slater, G. W.; Noolandi, J., The biased reptation model of DNA gel electrophoresis: mobility vs molecular size and gel concentration. *Biopolymers: Original Research on Biomolecules* **1989**, *28*, (10), 1781-1791.
105. Noolandi, J., Polymer dynamics in electrophoresis of DNA. *Annual Review of Physical Chemistry* **1992**, *43*, (1), 237-256.
106. Cottet, H.; Gareil, P., Electrophoretic behaviour of fully sulfonated polystyrenes in capillaries filled with entangled polymer solutions. *Journal of Chromatography A* **1997**, *772*, (1-2), 369-384.

107. Grossman, P. D.; Soane, D. S., Capillary electrophoresis of DNA in entangled polymer solutions. *Journal of Chromatography A* **1991**, *559*, (1-2), 257-266.
108. McGregor, D. A.; Yeung, E. S., Optimization of capillary electrophoretic separation of DNA fragments based on polymer filled capillaries. *Journal of Chromatography A* **1993**, *652*, (1), 67-73.
109. Vesterberg, O., A short history of electrophoretic methods. *Electrophoresis* **1993**, *14*, (1), 1243-1249.
110. Matsudaira, P.; Matsudaira, P. T., *A practical guide to protein and peptide purification for microsequencing*. Gulf Professional Publishing: San Diego, CA, USA, 1993.
111. Westermeier, R., *Electrophoresis in practice: a guide to methods and applications of DNA and protein separations*. John Wiley & Sons: Weinheim, Germany, 2016.
112. Walker, J. M., SDS polyacrylamide gel electrophoresis of proteins. In *The protein protocols handbook*, Humana Press: Totowa, NJ, USA, 1996; pp 55-61.
113. Rath, A.; Glibowicka, M.; Nadeau, V. G.; Chen, G.; Deber, C. M., Detergent binding explains anomalous SDS-PAGE migration of membrane proteins. *Proceedings of the National Academy of Sciences* **2009**, *106*, (6), 1760-1765.
114. Fling, S. P.; Gregerson, D. S., Peptide and protein molecular weight determination by electrophoresis using a high-molarity tris buffer system without urea. *Analytical biochemistry* **1986**, *155*, (1), 83-88.
115. Lukkari, P.; Vuorela, H.; Riekkola, M.-L., Effect of buffer solution pH on the elution and separation of [beta]-blockers by micellar electrokinetic capillary chromatography. *Journal of Chromatography A* **1993**, *652*, (2), 451-457.
116. Kang, P.; Madera, M.; Alley Jr, W. R.; Goldman, R.; Mechref, Y.; Novotny, M. V., Glycomic alterations in the highly-abundant and lesser-abundant blood serum protein fractions for patients diagnosed with hepatocellular carcinoma. *International Journal of Mass Spectrometry* **2011**, *305*, (2-3), 185-198.
117. Van Hove, E.; Szücs, R.; Sandra, P., Alcohol modifiers in MEKC with SDS as surfactant. Study on the influence of the alcohol chain length (C₁-C₁₂). *Journal of High Resolution Chromatography* **1996**, *19*, 674-678.
118. De Gennes, P.-G.; Gennes, P.-G., *Scaling concepts in polymer physics*. Cornell University Press: Ithaca, NY, USA, 1979.
119. Bode, H.-J., SDS-polyethyleneglycol electrophoresis: a possible alternative to SDS-polyacrylamide gel electrophoresis. *FEBS letters* **1976**, *65*, (1), 56-58.
120. Bean, S.; Lookhart, G., Sodium dodecyl sulfate capillary electrophoresis of wheat proteins. 1. Uncoated capillaries. *Journal of Agricultural and Food Chemistry* **1999**, *47*, (10), 4246-4255.
121. Bietz, J.; Lookhart, G., Wheat varietal identification by capillary electrophoresis: An inter-laboratory comparison of methods. *LWT-Food Science and Technology* **1997**, *30*, (2), 210-213.
122. Rösch, M., Ein Versuch zu einer valenztheoretischen Begründung des feinstrukturellen Verhaltens von Polyglykoläthern. *Colloid & Polymer Science* **1957**, *150*, (2), 153-156.
123. Rösch, M., Kolloid-Z. 1956, 147, 78.(b) Rösch, M. *Fette, Seifen, Anstrichm* **1963**, *65*, 223.
124. Rösch, M., Zur Hydratbildung von Polyglykolätherlösungen anomaler Zähigkeit. *Colloid & Polymer Science* **1956**, *147*, (1), 78-79.

125. Csapo, Z.; Gerstner, A.; Sasvari-Szekely, M.; Guttman, A., Automated ultra-thin-layer SDS gel electrophoresis of proteins using noncovalent fluorescent labeling. *Analytical Chemistry* **2000**, *72*, (11), 2519-2525.
126. Kotler, L.; Miller, A. W.; Barron, A. E.; Karger, B. L., DNA sequencing with hydrophilic and hydrophobic polymers at elevated column temperatures. *Electrophoresis* **2002**, *23*, 1421-1428.
127. Barron, A. E.; Soane, D. S.; Blanch, H. W., Capillary electrophoresis of DNA in uncross-linked polymer solutions. *Journal of Chromatography A* **1993**, *652*, (1), 3-16.
128. Reynolds, J. A.; Tanford, C., Binding of dodecyl sulfate to proteins at high binding ratios. Possible implications for the state of proteins in biological membranes. *Proceedings of the National Academy of Sciences* **1970**, *66*, (3), 1002-1007.
129. Takagi, T., Capillary electrophoresis in presence of sodium dodecyl sulfate and a sieving medium. *Electrophoresis* **1997**, *18*, (12 - 13), 2239-2242.
130. Tsujii, K.; Takagi, T., Proton magnetic resonance studies of the binding of an anionic surfactant with a benzene ring to a protein polypeptide with special reference to SDS-polyacrylamide gel electrophoresis. *The Journal of Biochemistry* **1975**, *77*, (3), 511-519.
131. Oakes, J., Protein-surfactant interactions. Nuclear magnetic resonance and binding isotherm studies of interactions between bovine serum albumin and sodium dodecyl sulphate. *Journal of the Chemical Society, Faraday Transactions 1: Physical Chemistry in Condensed Phases* **1974**, *70*, 2200-2209.
132. Guo, X.; Zhao, N.; Chen, S.; Teixeira, J., Small - angle neutron scattering study of the structure of protein/detergent complexes. *Biopolymers* **1990**, *29*, (2), 335-346.
133. Werner, W. E.; Demorest, D. M.; Wiktorowicz, J. E., Automated Ferguson analysis of glycoproteins by capillary electrophoresis using a replaceable sieving matrix. *Electrophoresis* **1993**, *14*, (1), 759-763.
134. Valkó, I. E.; Sirén, H.; Riekkola, M. L., Characteristics of electroosmotic flow in capillary electrophoresis in water and in organic solvents without added ionic species. *Journal of Microcolumn Separations* **1999**, *11*, (3), 199-208.
135. Sarmini, K.; Kenndler, E., Influence of organic solvents on the separation selectivity in capillary electrophoresis. *Journal of Chromatography A* **1997**, *792*, (1-2), 3-11.
136. Sumitomo, K.; Mayumi, K.; Minamikawa, H.; Masuda, M.; Asahi, T.; Shimizu, T.; Ito, K.; Yamaguchi, Y., Buffers to suppress sodium dodecyl sulfate adsorption to polyethylene oxide for protein separation on capillary polymer electrophoresis. *Electrophoresis* **2011**, *32*, (3 - 4), 448-454.
137. Shah, S.; Jamroz, N.; Sharif, Q., Micellization parameters and electrostatic interactions in micellar solution of sodium dodecyl sulfate (SDS) at different temperatures. *Colloids and Surfaces A: Physicochemical and Engineering Aspects* **2001**, *178*, (1-3), 199-206.
138. Bailey, F.; Callard, R., Some properties of poly (ethylene oxide) 1 in aqueous solution. *Journal of applied polymer science* **1959**, *1*, (1), 56-62.
139. Bailey, F. J., *Poly (ethylene oxide)*. Academic Press Inc.: New Your, NY, USA, 2012.
140. Blandamer, M. J.; Fox, M. F.; Powell, E.; Stafford, J. W., A viscometric study of poly (ethylene oxide) in t - butyl alcohol/water mixtures. *Macromolecular Chemistry and Physics* **1969**, *124*, (1), 222-231.

141. Guttman, A.; Horvath, J.; Cooke, N., Influence of temperature on the sieving effect of different polymer matrixes in capillary SDS gel electrophoresis of proteins. *Analytical Chemistry* **1993**, *65*, (3), 199-203.
142. Devanand, K.; Selser, J., Polyethylene oxide does not necessarily aggregate in water. *Nature* **1990**, *343*, (6260), 739-741.
143. Cuniberti, C.; Ferrando, R., Electron microscope investigation of poly (ethylene oxide) supermolecular particles in solution. *Polymer* **1972**, *13*, (8), 379-384.
144. Carpenter, D. K.; Santiago, G.; Hunt, A. H. In *Aggregation of polyoxyethylene in dilute solutions*, Journal of Polymer Science: Polymer Symposia, 1974; Wiley Online Library: 1974; pp 75-92.
145. Emerson, M. F.; Holtzer, A., Hydrophobic bond in micellar systems. Effects of various additives on the stability of micelles of sodium dodecyl sulfate and of n-dodecyltrimethylammonium bromide. *The Journal of Physical Chemistry* **1967**, *71*, (10), 3320-3330.
146. Pattky, M.; Huhn, C., Advantages and limitations of a new cationic coating inducing a slow electroosmotic flow for CE-MS peptide analysis: a comparative study with commercial coatings. *Analytical and Bioanalytical Chemistry* **2013**, *405*, (1), 225-237.
147. Safarpour, M.; Rafati, A.; Gharibi, H.; Sameti, M., Rezaie, Influence of short - chain alcohols on the micellization parameters of sodium dodecyl sulfate (SDS). *Journal of the Chinese Chemical Society* **1999**, *46*, (6), 983-991.
148. Guttman, A., On the separation mechanism of capillary sodium dodecyl sulfate - gel electrophoresis of proteins. *Electrophoresis* **1995**, *16*, (1), 611-616.
149. Katayama, H.; Ishihama, Y.; Asakawa, N., Stable cationic capillary coating with successive multiple ionic polymer layers for capillary electrophoresis. *Analytical Chemistry* **1998**, *70*, (24), 5272-5277.
150. Chiari, M.; Nesi, M.; Sandoval, J. E.; Pesek, J. J., Capillary electrophoretic separation of proteins using stable, hydrophilic poly(acryloylaminoethoxyethanol)-coated columns. *Journal of Chromatography A* **1995**, *717*, (1-2), 1-13.
151. Chiu, R. W.; Jimenez, J. C.; Monnig, C. A., High molecular weight polyarginine as a capillary coating for separation of cationic proteins by capillary electrophoresis. *Analytica Chimica Acta* **1995**, *307*, 193-201.
152. Chen, F.-T. A., Rapid protein analysis by capillary electrophoresis. *Journal of Chromatography A* **1991**, *559*, (1-2), 445-453.
153. Grossman, P. D.; Colburn, J. C., *Capillary electrophoresis: Theory and practice*. Academic Press: Foster City, CA, USA, 2012.
154. Haselberg, R.; de Jong, G. J.; Somsen, G. W., Capillary electrophoresis-mass spectrometry of intact basic proteins using polybrene-dextran sulfate-polybrene-coated capillaries: System optimization and performance. *Analytica Chimica Acta* **2010**, *678*, (1), 128-134.
155. Belder, D.; Deege, A.; Husmann, H.; Kohler, F.; Ludwig, M., Cross-linked poly(vinyl alcohol) as permanent hydrophilic column coating for capillary electrophoresis. *Electrophoresis* **2001**, *22*, (17), 3813-3818.
156. Pei, L.; Lucy, C. A., Insight into the stability of poly(diallyldimethylammoniumchloride) and polybrene poly cationic coatings in capillary electrophoresis. *Journal of Chromatography A* **2014**, *1365*, 226-233.

157. Wang, Y.; Dubin, P. L., Capillary modification by noncovalent polycation adsorption: Effects of polymer molecular weight and adsorption ionic strength. *Analytical Chemistry* **1999**, *71*, (16), 3463-3468.
158. Nehmé, R.; Perrin, C.; Cottet, H.; Blanchin, M. D.; Fabre, H., Influence of polyelectrolyte coating conditions on capillary coating stability and separation efficiency in capillary electrophoresis. *Electrophoresis* **2008**, *29*, (14), 3013-3023.
159. Neusüß, C.; Demelbauer, U.; Pelzing, M., Glycoform characterization of intact erythropoietin by capillary electrophoresis-electrospray-time of flight-mass spectrometry. *Electrophoresis* **2005**, *26*, (7-8), 1442-1450.
160. Kelly, J. F.; Locke, S. J.; Ramaley, L.; Thibault, P., Development of electrophoretic conditions for the characterization of protein glycoforms by capillary electrophoresis-electrospray mass spectrometry. *Journal of Chromatography A* **1996**, *720*, (1-2), 409-427.
161. Moini, M., Metal displacement and stoichiometry of protein - metal complexes under native conditions using capillary electrophoresis/mass spectrometry. *Rapid Communications in Mass Spectrometry* **2010**, *24*, (18), 2730-2734.
162. Haselberg, R.; de Jong, G. J.; Somsen, G. W., Capillary electrophoresis–mass spectrometry for the analysis of intact proteins 2007–2010. *Electrophoresis* **2011**, *32*, (1), 66-82.
163. Haselberg, R.; Ratnayake, C. K.; de Jong, G. J.; Somsen, G. W., Performance of a sheathless porous tip sprayer for capillary electrophoresis-electrospray ionization-mass spectrometry of intact proteins. *Journal of Chromatography A* **2010**, *1217*, (48), 7605-7611.
164. Lucy, C. A.; MacDonald, A. M.; Gulcev, M. D., Non-covalent capillary coatings for protein separations in capillary electrophoresis. *Journal of Chromatography A* **2008**, *1184*, (1), 81-105.
165. Agilent Technologies, I. Polyvinyl Alcohol (PVA) Coated Capillaries. [https://www.agilent.com/en/products/capillary-electrophoresis-ce-ms/ce-ce-ms-supplies/capillaries/polyvinyl-alcohol-\(pva\)-coated-capillaries](https://www.agilent.com/en/products/capillary-electrophoresis-ce-ms/ce-ce-ms-supplies/capillaries/polyvinyl-alcohol-(pva)-coated-capillaries) (05.12.2018),
166. Ehmann, T.; Bächmann, K.; Fabry, L.; Rüfer, H.; Serwe, M.; Ross, G.; Pahlke, S.; Kotz, L., Capillary preconditioning for analysis of anions using indirect UV detection in capillary zone electrophoresis: Systematic investigation of alkaline and acid prerinsing techniques by designed experiments. *Journal of Chromatography A* **1998**, *816*, (2), 261-275.
167. Yassine, M. M.; Lucy, C. A., Factors affecting the temporal stability of semipermanent bilayer coatings in capillary electrophoresis prepared using double-chained surfactants. *Analytical Chemistry* **2004**, *76*, (11), 2983-2990.
168. Horvath, J.; Dolník, V., Polymer wall coatings for capillary electrophoresis. *Electrophoresis* **2001**, *22*, (4), 644-655.
169. Righetti, P. G.; Chiari, M.; Nesi, M.; Caglio, S., Towards new formulations for polyacrylamide matrices, as investigated by capillary zone electrophoresis. *Journal of Chromatography A* **1993**, *638*, (2), 165-178.
170. Chiari, M.; Micheletti, C.; Nesi, M.; Fazio, M.; Righetti, P. G., Towards new formulations for polyacrylamide matrices: N - acryloylaminoethoxyethanol, a novel monomer combining high hydrophilicity with extreme hydrolytic stability. *Electrophoresis* **1994**, *15*, (1), 177-186.
171. Chu, C. H.; Jonsson, E.; Auvinen, M.; Pesek, J. J.; Sandoval, J. E., A new approach for the preparation of a hydride-modified substrate used as an intermediate in the synthesis of surface-bonded materials. *Analytical Chemistry* **1993**, *65*, (6), 808-816.

172. Slinyakova, I.; Budkevich, G.; Neimark, I. E., Hydrophobic hydrosiliceous adsorbent with the Si-H bond (hydridopolysiloxane xerogel). *Kolloidnyi Zhurnal* **1965**, *27*, 758-764.
173. Morterra, C.; Low, M. J., Reactive silica. I. Formation of a reactive silica by the thermal collapse of the methoxy groups of methylated Aerosil. *The Journal of Physical Chemistry* **1969**, *73*, (2), 321-326.
174. Morterra, C.; Low, M. J., Reactive silica. II. Nature of the surface silicon hydrides produced by the chemisorption of hydrogen. *The Journal of Physical Chemistry* **1969**, *73*, (2), 327-333.
175. Zhuravlev, L., The surface chemistry of amorphous silica. Zhuravlev model. *Colloids and Surfaces A: Physicochemical and Engineering Aspects* **2000**, *173*, (1), 1-38.
176. Sandoval, J. E.; Pesek, J. J., Synthesis and characterization of a hydride-modified porous silica material as an intermediate in the preparation of chemically bonded chromatographic stationary phases. *Analytical Chemistry* **1989**, *61*, (18), 2067-2075.
177. Ashby, B. A., Addition reaction. In Google Patents: 1964.
178. Locke, D. C.; Schmermund, J. T.; Banner, B., Bonded stationary phases for chromatography. *Anal. Chem.* **1972**, *44*, (1), 90-92.
179. Pesek, J. J.; Swedberg, S. A., Allyl-bonded stationary phase as possible intermediate in the synthesis of novel high-performance liquid chromatographic phases. *Journal of Chromatography A* **1986**, *361*, 83-92.
180. Saunders, D.; Barford, R.; Magidman, P.; Olszewski, L.; Rothbart, H., Preparation and properties of a sulfobenzylsilica cation exchanger for liquid chromatography. *Anal. Chem.* **1974**, *46*, (7), 834-838.
181. Ebsworth, E.; MacDiarmid, A., Organometallic Compounds of the Group IV Elements. *The Bond to Carbon* Marcel Dekker, New York, NY **1968**.
182. Pawlenko, S., *Organosilicon chemistry*. Walter de Gruyter: New York, NY, USA, 2011.
183. Brinker, C. J.; Scherer, G. W., *Sol-gel science: the physics and chemistry of sol-gel processing*. Academic press: New York, NY, USA, 2013.
184. Sandoval, J. E.; Pesek, J. J., Hydrolytically stable bonded chromatographic phases prepared through hydrosilylation of olefins on a hydride-modified silica intermediate. *Analytical Chemistry* **1991**, *63*, (22), 2634-2641.
185. Nakatani, M.; Shibukawa, A.; Nakagawa, T., Sodium dodecyl sulfate-polyacrylamide solution-filled capillary electrophoresis of proteins using stable linear polyacrylamide-coated capillary. *Biological and Pharmaceutical Bulletin* **1993**, *16*, (12), 1185-1188.
186. Nakatani, M.; Shibukawa, A.; Nakagawa, T., Preparation and characterization of a stable polyacrylamide sieving matrix-filled capillary for high-performance capillary electrophoresis. *Journal of Chromatography A* **1994**, *661*, (1-2), 315-321.
187. Nakatani, M.; Shibukawa, A.; Nakagawa, T., Chemical stability of polyacrylamide - coating on fused silica capillary. *Electrophoresis* **1995**, *16*, (1), 1451-1456.
188. Williams, B. A.; Vigh, G., Fast, accurate mobility determination method for capillary electrophoresis. *Analytical Chemistry* **1996**, *68*, (7), 1174-1180.
189. Williams, B. A.; Vigh, G., Determination of accurate electroosmotic mobility and analyte effective mobility values in the presence of charged interacting agents in capillary electrophoresis. *Analytical chemistry* **1997**, *69*, (21), 4445-4451.

190. Righetti, P. G.; Gelfi, C.; Sebastiano, R.; Citterio, A., Surfing silica surfaces superciliously. *Journal of Chromatography A* **2004**, *1053*, (1-2), 15-26.
191. Frohnhöfer, H. G.; Geiger-Rudolph, S.; Pattky, M.; Meixner, M.; Huhn, C.; Maischein, H.-M.; Geisler, R.; Gehring, I.; Maderspacher, F.; Nüsslein-Volhard, C., Spermidine, but not spermine, is essential for pigment pattern formation in zebrafish. *Biology Open* **2016**, bio. 018721.
192. Kele, M.; Guiochon, G., Repeatability and reproducibility of retention data and band profiles on reversed-phase liquid chromatography columns: III. Results obtained with Kromasil C18 columns. *Journal of Chromatography A* **1999**, *855*, (2), 423-453.
193. Cifuentes, A.; Diez-Masa, J. C.; Fritz, J.; Anselmetti, D.; Bruno, A. E., Polyacrylamide-coated capillaries probed by atomic force microscopy: correlation between surface topography and electrophoretic performance. *Analytical Chemistry* **1998**, *70*, (16), 3458-3462.
194. De Freitas, J.; Player, M., Ultrahigh precision measurements of optical heterogeneity of high quality fused silica. *Applied Physics Letters* **1995**, *66*, (26), 3552-3554.
195. Xu, L.; Dong, X.-Y.; Sun, Y., Novel poly(vinyl alcohol)-based column coating for capillary electrophoresis of proteins. *Biochemical Engineering Journal* **2010**, *53*, (1), 137-142.
196. Belder, D.; Deege, A.; Husmann, H.; Kohler, F.; Ludwig, M., Cross - linked poly (vinyl alcohol) as permanent hydrophilic column coating for capillary electrophoresis. *Electrophoresis* **2001**, *22*, (17), 3813-3818.
197. Cobb, K. A.; Dolnik, V.; Novotny, M., Electrophoretic separations of proteins in capillaries with hydrolytically-stable surface structures. *Analytical Chemistry* **1990**, *62*, (22), 2478-2483.
198. Unger, K.; Berg, K.; Nyamah, D.; Lothe, T., Herstellung oberflächenmodifizierter Adsorbentien. *Colloid and Polymer Science* **1974**, *252*, (4), 317-321.
199. Dove, P. M.; Han, N.; Wallace, A. F.; De Yoreo, J. J., Kinetics of amorphous silica dissolution and the paradox of the silica polymorphs. *Proceedings of the National Academy of Sciences* **2008**, *105*, (29), 9903-9908.
200. Eckhardt, A.; Mikšík, I.; Deyl, Z.; Charvátová, J., Separation of low-molecular mass peptides by capillary electrophoresis with the use of alkylamines as dynamic coating agents at low pH. *Journal of Chromatography A* **2004**, *1051*, (1), 111-117.
201. Du, M.; Flanigan, V.; Ma, Y., Simultaneous determination of polyamines and catecholamines in PC-12 tumor cell extracts by capillary electrophoresis with laser-induced fluorescence detection. *Electrophoresis* **2004**, *25*, (10 - 11), 1496-1502.
202. Lange, J.; Thomas, K.; Wittmann, C., Comparison of a capillary electrophoresis method with high-performance liquid chromatography for the determination of biogenic amines in various food samples. *Journal of Chromatography B* **2002**, *779*, (2), 229-239.
203. Simo, C.; Moreno-Arribas, M. V.; Cifuentes, A., Ion-trap versus time-of-flight mass spectrometry coupled to capillary electrophoresis to analyze biogenic amines in wine. *Journal of Chromatography A* **2008**, *1195*, (1-2), 150-156.
204. Geyer, Philipp E.; Kulak, Nils A.; Pichler, G.; Holdt, Lesca M.; Teupser, D.; Mann, M., Plasma proteome profiling to assess human health and disease. *Cell Systems* **2016**, *2*, (3), 185-195.
205. Eriksson, J. H. C.; Mol, R.; Somsen, G. W.; Hinrichs, W. L. J.; Frijlink, H. W.; Jong, G. J. d., Feasibility of nonvolatile buffers in capillary electrophoresis-electrospray ionization-mass spectrometry of proteins. *Electrophoresis* **2004**, *25*, (1), 43-49.

206. Banks, J. F.; Dresch, T., Detection of Fast Capillary Electrophoresis Peptide and Protein Separations Using Electrospray Ionization With a Time-of-Flight Mass Spectrometer. *Analytical Chemistry* **1996**, *68*, (9), 1480-1485.
207. Onuska, F.; Comba, M.; Bistricki, T.; Wilkinson, R., Preparation of surface-modified wide-bore wall-coated open-tubular columns. *Journal of Chromatography A* **1977**, *142*, 117-125.
208. Pesek, J. J.; Matyska, M. T., Open tubular capillary electrokinetic chromatography in etched fused-silica tubes. *Journal of Chromatography A* **2000**, *887*, (1-2), 31-41.
209. Pesek, J. J.; Matyska, M. T., Etched chemically modified capillaries: Novel separation media for electrophoretic analyses. *Journal of Separation Science* **2004**, *27*, (15 - 16), 1285-1291.
210. Karásek, P.; Planeta, J.; Roth, M., Near-and supercritical water as a diameter manipulation and surface roughening agent in fused silica capillaries. *Analytical Chemistry* **2012**, *85*, (1), 327-333.
211. Šlais, K.; Horká, M.; Karásek, P.; Planeta, J.; Roth, M., Isoelectric focusing in continuously tapered fused silica capillary prepared by etching with supercritical water. *Analytical Chemistry* **2013**, *85*, (9), 4296-4300.
212. Yin, H. F.; Lux, J. A.; Schomburg, G., Production of polyacrylamide gel filled capillaries for capillary gel electrophoresis (CGE): Influence of capillary surface pretreatment on performance and stability. *Journal of High Resolution Chromatography* **1990**, *13*, (9), 624-627.
213. Cansell, F.; Aymonier, C.; Loppinet-Serani, A., Review on materials science and supercritical fluids. *Current Opinion in Solid State and Materials Science* **2003**, *7*, (4-5), 331-340.
214. Liebscher, A., Aqueous fluids at elevated pressure and temperature. *Geofluids* **2010**, *10*, (1 - 2), 3-19.
215. Kolodzey, J.; Chowdhury, E. A.; Adam, T. N.; Qui, G.; Rau, I.; Olowolafe, J. O.; Suehle, J. S.; Chen, Y., Electrical conduction and dielectric breakdown in aluminum oxide insulators on silicon. *IEEE Transactions on Electron Devices* **2000**, *47*, (1), 121-128.
216. Huang, T.-L. J., Durability improved colloidal silica coating. In United States Patent: 13.10.1998.
217. Moore, E., Stable positively charged alumina coated silica sols. In United States Patent Office: 10.07.1973.
218. Morikawa, H.; MIWA, S. I.; Miyake, M.; Marumo, F.; Sata, T., Structural analysis of SiO₂ - Al₂O₃ glasses. *Journal of the American Ceramic Society* **1982**, *65*, (2), 78-81.
219. Brand, J.; Haslberger, T.; Zolg, W.; Pestlin, G.; Palme, S., Depletion efficiency and recovery of trace markers from a multiparameter immunodepletion column. *Proteomics* **2006**, *6*, (11), 3236-3242.
220. Bellei, E.; Bergamini, S.; Monari, E.; Fantoni, L. I.; Cuoghi, A.; Ozben, T.; Tomasi, A., High-abundance proteins depletion for serum proteomic analysis: concomitant removal of non-targeted proteins. *Amino Acids* **2011**, *40*, (1), 145-156.
221. Granger, J.; Siddiqui, J.; Copeland, S.; Remick, D., Albumin depletion of human plasma also removes low abundance proteins including the cytokines. *Proteomics* **2005**, *5*, (18), 4713-4718.
222. Björhall, K.; Miliotis, T.; Davidsson, P., Comparison of different depletion strategies for improved resolution in proteomic analysis of human serum samples. *Proteomics* **2005**, *5*, (1), 307-317.

223. Pandey, A.; Podtelejnikov, A. V.; Blagoev, B.; Bustelo, X. R.; Mann, M.; Lodish, H. F., Analysis of receptor signaling pathways by mass spectrometry: identification of vav-2 as a substrate of the epidermal and platelet-derived growth factor receptors. *Proceedings of the National Academy of Sciences* **2000**, *97*, (1), 179-184.
224. Oda, Y.; Nagasu, T.; Chait, B. T., Enrichment analysis of phosphorylated proteins as a tool for probing the phosphoproteome. *Nature Biotechnology* **2001**, *19*, (4), 379.
225. Wolschin, F.; Wienkoop, S.; Weckwerth, W., Enrichment of phosphorylated proteins and peptides from complex mixtures using metal oxide/hydroxide affinity chromatography (MOAC). *Proteomics* **2005**, *5*, (17), 4389-4397.
226. Hwang, L.; Ayaz-Guner, S.; Gregorich, Z. R.; Cai, W.; Valeja, S. G.; Jin, S.; Ge, Y., Specific enrichment of phosphoproteins using functionalized multivalent nanoparticles. *Journal of the American Chemical Society* **2015**, *137*, (7), 2432-2435.
227. Ficarro, S. B.; Adelmant, G.; Tomar, M. N.; Zhang, Y.; Cheng, V. J.; Marto, J. A., Magnetic bead processor for rapid evaluation and optimization of parameters for phosphopeptide enrichment. *Analytical Chemistry* **2009**, *81*, (11), 4566-4575.
228. Pinkse, M. W.; Lemeer, S.; Heck, A. J., A protocol on the use of titanium dioxide chromatography for phosphoproteomics. In *Gel-Free Proteomics*, Springer Science+Business Media: New York (NY), USA, 2011; pp 215-228.
229. Kim, W.; Bennett, E. J.; Huttlin, E. L.; Guo, A.; Li, J.; Possemato, A.; Sowa, M. E.; Rad, R.; Rush, J.; Comb, M. J., Systematic and quantitative assessment of the ubiquitin-modified proteome. *Molecular Cell* **2011**, *44*, (2), 325-340.
230. Xu, G.; Paige, J. S.; Jaffrey, S. R., Global analysis of lysine ubiquitination by ubiquitin remnant immunoaffinity profiling. *Nature Biotechnology* **2010**, *28*, (8), 868.
231. Chen, C.-C.; Su, W.-C.; Huang, B.-Y.; Chen, Y.-J.; Tai, H.-C.; Obena, R. P., Interaction modes and approaches to glycopeptide and glycoprotein enrichment. *Analyst* **2014**, *139*, (4), 688-704.
232. Mechref, Y.; Madera, M.; Novotny, M. V., Glycoprotein enrichment through lectin affinity techniques. In *2D PAGE: Sample Preparation and Fractionation*, Springer: New York (NY), USA, 2008; pp 373-396.
233. Kim, S. C.; Sprung, R.; Chen, Y.; Xu, Y.; Ball, H.; Pei, J.; Cheng, T.; Kho, Y.; Xiao, H.; Xiao, L., Substrate and functional diversity of lysine acetylation revealed by a proteomics survey. *Molecular Cell* **2006**, *23*, (4), 607-618.
234. Mertins, P.; Qiao, J. W.; Patel, J.; Udeshi, N. D.; Clauser, K. R.; Mani, D.; Burgess, M. W.; Gillette, M. A.; Jaffe, J. D.; Carr, S. A., Integrated proteomic analysis of post-translational modifications by serial enrichment. *Nature Methods* **2013**, *10*, (7), 634.
235. Simó, C.; Bachi, A.; Cattaneo, A.; Guerrier, L.; Fortis, F.; Boschetti, E.; Podtelejnikov, A.; Righetti, P. G., Performance of combinatorial peptide libraries in capturing the low-abundance proteome of red blood cells. 1. Behavior of mono- to hexapeptides. *Analytical Chemistry* **2008**, *80*, (10), 3547-3556.
236. Huhn, C.; Ruhaak, L. R.; Wuhrer, M.; Deelder, A. M., Hexapeptide library as a universal tool for sample preparation in protein glycosylation analysis. *Journal of Proteomics* **2012**, *75*, (5), 1515-1528.
237. Di Girolamo, F.; Righetti, P. G.; Soste, M.; Feng, Y.; Picotti, P., Reproducibility of combinatorial peptide ligand libraries for proteome capture evaluated by selected reaction monitoring. *Journal of Proteomics* **2013**, *89*, 215-226.

238. Furka, A.; Sebestyén, F.; Asgedom, M.; Dibó, G., General method for rapid synthesis of multicomponent peptide mixtures. *International Journal of Peptide and Protein Research* **1991**, *37*, (6), 487-493.
239. Thulasiraman, V.; Lin, S.; Gheorghiu, L.; Lathrop, J.; Lomas, L.; Hammond, D.; Boschetti, E., Reduction of the concentration difference of proteins in biological liquids using a library of combinatorial ligands. *Electrophoresis* **2005**, *26*, (18), 3561-3571.
240. Albers, S.-V. A problem of "disappearing" protein during concentration of sample. https://www.researchgate.net/post/A_problem_of_disappearing_protein_during_concentration_of_the_sample (12.10.2018),
241. Olivera-Nappa, A. Protein concentration using Amicon Ultra spin column, absorption on membrane? https://www.researchgate.net/post/Protein_concentration_using_Amicon_Ultra_spin_column_a_disorption_on_membrane (12.10.2018),
242. Natrajan, G. A problem of "disappearing" protein during concentration of the sample. https://www.researchgate.net/post/A_problem_of_disappearing_protein_during_concentration_of_the_sample (12.10.2018),
243. Erde, J.; Loo, R. R. O.; Loo, J. A., Enhanced FASP (eFASP) to increase proteome coverage and sample recovery for quantitative proteomic experiments. *Journal of Proteome Research* **2014**, *13*, (4), 1885-1895.
244. Dowling, P.; Ohlndieck, K., DIGE Analysis of Immunodepleted Plasma. In *Difference Gel Electrophoresis: Methods and Protocols*, Ohlndieck, K., Ed. Springer New York: New York, NY, 2018; pp 245-257.
245. Restuccia, U.; Boschetti, E.; Fasoli, E.; Fortis, F.; Guerrier, L.; Bachi, A.; Kravchuk, A. V.; Righetti, P. G., pI-based fractionation of serum proteomes versus anion exchange after enhancement of low-abundance proteins by means of peptide libraries. *Journal of Proteomics* **2009**, *72*, (6), 1061-1070.
246. Vidova, V.; Spacil, Z., A review on mass spectrometry-based quantitative proteomics: targeted and data independent acquisition. *Analytica Chimica Acta* **2017**, *964*, 7-23.
247. Webb-Robertson, B.-J. M.; Wiberg, H. K.; Matzke, M. M.; Brown, J. N.; Wang, J.; McDermott, J. E.; Smith, R. D.; Rodland, K. D.; Metz, T. O.; Pounds, J. G., Review, evaluation, and discussion of the challenges of missing value imputation for mass spectrometry-based label-free global proteomics. *Journal of Proteome Research* **2015**, *14*, (5), 1993-2001.
248. Winiewski, J. R.; Hein, M. Y.; Cox, J.; Mann, M., A 'proteomic ruler' for protein copy number and concentration estimation without spike-in standards. *Molecular & Cellular Proteomics* **2014**, manuscript mcp. M113. 037309.
249. Wiśniewski, J. R.; Zougman, A.; Nagaraj, N.; Mann, M., Universal sample preparation method for proteome analysis. *Nature Methods* **2009**, *6*, (5), 359.
250. Simó, C.; Elvira, C.; González, N.; Román, J. S.; Barbas, C.; Cifuentes, A., Capillary electrophoresis-mass spectrometry of basic proteins using a new physically adsorbed polymer coating. Some applications in food analysis. *Electrophoresis* **2004**, *25*, (13), 2056-2064.
251. Breuker, K.; McLafferty, F. W., Stepwise evolution of protein native structure with electrospray into the gas phase, 10– 12 to 102 s. *Proceedings of the National Academy of Sciences* **2008**, *105*, (47), 18145-18152.

252. Georgiou, H. M.; Rice, G. E.; Baker, M. S., Proteomic analysis of human plasma: failure of centrifugal ultrafiltration to remove albumin and other high molecular weight proteins. *PROTEOMICS: International Edition* **2001**, *1*, (12), 1503-1506.
253. Jones, K. L.; O'Melia, C. R., Protein and humic acid adsorption onto hydrophilic membrane surfaces: effects of pH and ionic strength. *Journal of Membrane Science* **2000**, *165*, (1), 31-46.
254. Biddlecombe, R. A.; Pleasance, S., Automated protein precipitation by filtration in the 96-well format. *Journal of Chromatography B: Biomedical Sciences and Applications* **1999**, *734*, (2), 257-265.
255. Birk, H. W.; Kistner, A.; Wizemann, V.; Schütterle, G., Protein adsorption by artificial membrane materials under filtration conditions. *Artificial Organs* **1995**, *19*, (5), 411-415.
256. Martinez, F.; Martin, A.; Pradanos, P.; Calvo, J.; Palacio, L.; Hernandez, A., Protein adsorption and deposition onto microfiltration membranes: the role of solute–solid interactions. *Journal of Colloid and Interface Science* **2000**, *221*, (2), 254-261.
257. Fasoli, E.; Farinazzo, A.; Sun, C. J.; Kravchuk, A. V.; Guerrier, L.; Fortis, F.; Boschetti, E.; Righetti, P. G., Interaction among proteins and peptide libraries in proteome analysis: pH involvement for a larger capture of species. *Journal of Proteomics* **2010**, *73*, (4), 733-742.
258. Boschetti, E.; Righetti, P. G., The art of observing rare protein species in proteomes with peptide ligand libraries. *Proteomics* **2009**, *9*, (6), 1492-1510.
259. Bachi, A.; Simó, C.; Restuccia, U.; Guerrier, L.; Fortis, F.; Boschetti, E.; Masseroli, M.; Righetti, P. G., Performance of combinatorial peptide libraries in capturing the low-abundance proteome of red blood cells. 2. Behavior of resins containing individual amino acids. *Analytical Chemistry* **2008**, *80*, (10), 3557-3565.
260. Matzke, M. M.; Brown, J. N.; Gritsenko, M. A.; Metz, T. O.; Pounds, J. G.; Rodland, K. D.; Shukla, A. K.; Smith, R. D.; Waters, K. M.; McDermott, J. E., A comparative analysis of computational approaches to relative protein quantification using peptide peak intensities in label - free LC - MS proteomics experiments. *Proteomics* **2013**, *13*, (3-4), 493-503.
261. Webb - Robertson, B. J. M.; Matzke, M. M.; Jacobs, J. M.; Pounds, J. G.; Waters, K. M., A statistical selection strategy for normalization procedures in LC - MS proteomics experiments through dataset - dependent ranking of normalization scaling factors. *Proteomics* **2011**, *11*, (24), 4736-4741.
262. Mueller, L. N.; Rinner, O.; Schmidt, A.; Letarte, S.; Bodenmiller, B.; Brusniak, M. Y.; Vitek, O.; Aebersold, R.; Müller, M., SuperHirn—a novel tool for high resolution LC - MS - based peptide/protein profiling. *Proteomics* **2007**, *7*, (19), 3470-3480.
263. Zipperer, A.; Konnerth, M. C.; Laux, C.; Berscheid, A.; Janek, D.; Weidenmaier, C.; Burian, M.; Schilling, N. A.; Slavetinsky, C.; Marschal, M., Human commensals producing a novel antibiotic impair pathogen colonization. *Nature* **2016**, *535*, (7613), 511.
264. Kerns, E. H., High throughput physicochemical profiling for drug discovery. *Journal of Pharmaceutical Sciences* **2001**, *90*, (11), 1838-1858.
265. Wan, H.; Ulander, J., High-throughput p K a screening and prediction amenable for ADME profiling. *Expert Opinion on Drug Metabolism & Toxicology* **2006**, *2*, (1), 139-155.
266. Albert, A., *The Determination of Ionization Constants: a Laboratory Manual*. Springer Science & Business Media: London, 2012.

267. Avdeef, A.; Box, K.; Comer, J.; Gilges, M.; Hadley, M.; Hibbert, C.; Patterson, W.; Tam, K., PH-metric log P 11. pKa determination of water-insoluble drugs in organic solvent–water mixtures. *Journal of Pharmaceutical and Biomedical Analysis* **1999**, *20*, (4), 631-641.
268. Morgan, M. E.; Liu, K.; Anderson, B. D., Microscale titrimetric and spectrophotometric methods for determination of ionization constants and partition coefficients of new drug candidates. *Journal of Pharmaceutical Sciences* **1998**, *87*, (2), 238-245.
269. Barthelemy, M.; Guionie, M.; Labia, R., Beta-lactamases: determination of their isoelectric points. *Antimicrobial Agents and Chemotherapy* **1978**, *13*, (4), 695-698.
270. Conti, M.; Galassi, M.; Bossi, A.; Righetti, P. G., Capillary isoelectric focusing: the problem of protein solubility. *Journal of Chromatography A* **1997**, *757*, (1-2), 237-245.
271. Righetti, P. G., Determination of the isoelectric point of proteins by capillary isoelectric focusing. *Journal of Chromatography A* **2004**, *1037*, (1-2), 491-499.
272. Savić, J. S.; Dilber, S. P.; Vujić, Z. B.; Vladimirov, S. M.; Brborić, J. S., A modified RP-HPLC method for determination of pKa values of synthesized β -hydroxy- β -arylalkanoic acids. *Journal of Serbian Chemical Society* **2018**.
273. Kaliszan, R.; Wiczling, P.; Markuszewski, M. J., pH Gradient Reversed-Phase HPLC. *Analytical Chemistry* **2004**, *76*, (3), 749-760.
274. Poole, S. K.; Patel, S.; Dehring, K.; Workman, H.; Poole, C. F., Determination of acid dissociation constants by capillary electrophoresis. *Journal of Chromatography A* **2004**, *1037*, (1-2), 445-454.
275. Lowry, M.; Fakayode, S. O.; Geng, M. L.; Baker, G. A.; Wang, L.; McCarroll, M. E.; Patonay, G.; Warner, I. M., Molecular Fluorescence, Phosphorescence, and Chemiluminescence Spectrometry. *Analytical Chemistry* **2008**, *80*, (12), 4551-4574.
276. Wan, H.; Holmén, A. G.; Wang, Y.; Lindberg, W.; Englund, M.; Någård, M. B.; Thompson, R. A., High-throughput screening of pKa values of pharmaceuticals by pressure-assisted capillary electrophoresis and mass spectrometry. *Rapid Communications in Mass Spectrometry* **2003**, *17*, (23), 2639-2648.
277. McEvoy, E.; Marsh, A.; Altria, K.; Donegan, S.; Power, J., Recent advances in the development and application of microemulsion EKC. *Electrophoresis* **2007**, *28*, (1-2), 193-207.
278. Elisabet, F.; Clara, R.; Elisabeth, B.; Martí, R., A Fast Method for pKa Determination by Capillary Electrophoresis. *Chemistry & Biodiversity* **2009**, *6*, (11), 1822-1827.
279. Cleveland Jr, J.; Benko, M.; Gluck, S.; Walbroehl, Y., Automated pKa determination at low solute concentrations by capillary electrophoresis. *Journal of Chromatography A* **1993**, *652*, (2), 301-308.
280. Ishihama, Y.; Katayama, H.; Asakawa, N.; Oda, Y., Highly robust stainless steel tips as microelectrospray emitters. *Rapid Communications in Mass Spectrometry* **2002**, *16*, (10), 913-918.
281. Good, N. E.; Winget, G. D.; Winter, W.; Connolly, T. N.; Izawa, S.; Singh, R. M., Hydrogen ion buffers for biological research. *Biochemistry* **1966**, *5*, (2), 467-477.
282. Ye, M.; Hu, S.; Schoenherr, R. M.; Dovichi, N. J., On - line protein digestion and peptide mapping by capillary electrophoresis with post - column labeling for laser - induced fluorescence detection. *Electrophoresis* **2004**, *25*, (9), 1319-1326.
283. Hempel, G., Strategies to improve the sensitivity in capillary electrophoresis for the analysis of drugs in biological fluids. *Electrophoresis* **2000**, *21*, (4), 691-698.

LITERATURE

284. Huhn, C.; Neusüß, C.; Pelzing, M.; Pyell, U.; Mannhardt, J.; Pütz, M., Capillary electrophoresis-laser induced fluorescence-electrospray ionization-mass spectrometry: A case study. *Electrophoresis* **2005**, *26*, (7-8), 1389-1397.
285. Foret, F.; Thompson, T. J.; Vouros, P.; Karger, B. L.; Gebauer, P.; Bocek, P., Liquid sheath effects on the separation of proteins in capillary electrophoresis/electrospray mass spectrometry. *Analytical Chemistry* **1994**, *66*, (24), 4450-4458.
286. Schröder, D.; Roithová, J.; Schwarz, H., Electrospray ionization as a convenient new method for the generation of catalytically active iron-oxide ions in the gas phase. *International Journal of Mass Spectrometry* **2006**, *254*, (3), 197-201.
287. Lee, S.-W.; Freivogel, P.; Schindler, T.; Beauchamp, J., Freeze-dried biomolecules: FT-ICR studies of the specific solvation of functional groups and clathrate formation observed by the slow evaporation of water from hydrated peptides and model compounds in the gas phase. *Journal of the American Chemical Society* **1998**, *120*, (45), 11758-11765.
288. Wistuba, D.; Trapp, O.; Gel-Moreto, N.; Galensa, R.; Schurig, V., Stereoisomeric Separation of Flavanones and Flavanone-7-O-glycosides by Capillary Electrophoresis and Determination of Interconversion Barriers. *Analytical Chemistry* **2006**, *78*, (10), 3424-3433.
289. Trapp, O.; Trapp, G.; Schurig, V., Determination of the cis - trans isomerization barrier of enalaprilat by dynamic capillary electrophoresis and computer simulation. *Electrophoresis* **2004**, *25*, (2), 318-323.
290. STOLARSKI, R.; DUDYCZ, L.; SHUGAR, D., NMR Studies on the syn - anti Dynamic Equilibrium in Purine Nucleosides and Nucleotides. *European Journal of Biochemistry* **1980**, *108*, (1), 111-121.
291. Dyson, H. J.; Wright, P. E., Equilibrium NMR studies of unfolded and partially folded proteins. *Nature Structural and Molecular Biology* **1998**, *5*, (7s), 499.